Reactivity of Phosphaalkynes

Coordination, Cycloadditions and Subsequent Reactions

Dissertation

zur Erlangung des

DOKTORGRADES DER NATURWISSENSCHAFTEN

(Dr. rer. nat.)

der Naturwissenschaftlichen Fakultät für Chemie und Pharmazie

der Universität Regensburg

vorgelegt von

Eva-Maria Rummel

aus Regensburg

Regensburg 2016

Diese Arbeit wurde angeleitet von Prof. Dr. Manfred Scheer.

Das Promotionsgesuch wurde eingereicht am 17. März 2016
Datum des wissenschaftlichen Kolloquiums: 22. April 2016

Prüfungskommission:
Vorsitzender: Prof. Dr. Nikolaus Korber
1. Gutachter: Prof. Dr. Manfred Scheer
2. Gutachter: Prof. Dr. Henri Brunner
weitere Gutachter: Prof. Dr. Frank-Michael Matysik

Universität Regensburg

Affidavit

I hereby confirm that this thesis entitled "Reactivity of Phosphaalkynes - Coordination, Cycloadditions and Subsequent Reactions" is the result of my own work. I did not receive any help or support from third parties or commercial consultants. All sources and / or concepts applied directly or indirectly are listed and specified in the thesis stating the relevant literature.

Eidesstattliche Erklärung

Ich erkläre hiermit an Eides statt, dass ich die vorliegende Arbeit mit dem Titel „Reactivity of Phosphaalkynes - Coordination, Cycloadditions and Subsequent Reactions" ohne unzulässige Hilfe Dritter und ohne Benutzung anderer als der angegebenen Hilfsmittel angefertigt habe; die aus anderen Quellen direkt oder indirekt übernommenen Daten und Konzepte sind unter Angabe des Literaturzitats gekennzeichnet.

.....

Eva-Maria Rummel

The practical work leading to this thesis has been conducted between **October 2011 and March 2016** at the Department of Inorganic Chemistry at the University of Regensburg under the supervision of Prof. Dr. Manfred Scheer.

Results, which are not mentioned within this work, have been published during the work on this thesis:

1) U. Vogel, M. Eberl, M. Eckhardt, A. Seitz, E.-M. Rummel, A. Y. Timoshkin, E. V. Peresypkina and M. Scheer, Access to phosphorus-rich zirconium complexes, *Angew. Chem*. **2011**, *123*, 9144-9148; *Angew. Chem. Int. Ed*. **2011**, *50*, 8982-8985.

2) E.-M. Rummel, M. Eckhardt, M. Bodensteiner, E. V. Peresypkina, W. Kremer, C. Gröger and M. Scheer, Formation of 1,3-Diphosphacyclobutadiene Complexes from Phosphaalkynes and their Coordination Behavior, *Eur. J. Inorg. Chem*. **2014**, 1625-1637.

To Martin.

"Heard melodies are sweet
but those unheard are sweeter"

John Keats

Preface

A general introduction about the research topic of alkylidynephosphines (phosphaalkynes) is given in the beginning of this thesis, followed by the research objectives which could be derived from the state of literature.

As the chapters of this thesis each represent a topic on their own, a short introduction is given in the beginning of each to present the current state of research. The results of these chapters are suitable for publication in the future or are already in the process of being published. To avoid allegations of plagiarism, a list of contributions is given at the beginning of each topic, although a strict separation of results is not possible at all times.

To obtain a uniform design of this manuscript, the layout of all chapters (text settings, pictures, subchapters) is the same. However, for reasons of future publishing, the numbering of compounds, figures and tables starts anew each time. In addition, a graphical abstract has been created for each topic.

At the end of this thesis, a comprehensive summary on the topics discussed herein is given.

Table of Contents

1 Introduction

1.1 Phosphaalkynes: Discoveries

> *"Supposedly established rules have sometimes hindered the development of whole fields of chemistry; however, once breaches have been made in the generally accepted conceptions, completely novel and unexpected developments may follow rapidly."*
>
> M. Regitz, 1990[1]

P≡N (1987), C≡P (1990), and HC≡P (2007): This is the order (and years) in which the first three phosphorus containing substances in the interstellar medium have been discovered via their rotational transitions.[2] Of course, determining that the parent alkylidynephosphine or $\lambda^3\sigma^1$-phosphaalkyne[i] (containing a trivalent phosphorus atom which is coordinated once) was abundant in space has only been possible because of the seminal synthesis and meticulous characterisation of this substance by Gier[3] and further investigations by Tyler.[4] When Gier presented his findings to the Chemical Society in 1961 it should have been clear that the so called "double bond rule"[ii] was, in fact, invalid.[5] But as the (rather inconvenient) formation of HC≡P employed a technique of striking an arc between carbon electrodes in an atmosphere of PH_3 (see Figure 1-1 **I**), it took several other researchers to synthesise and characterise substances with phosphorus-carbon multiple bonds, such as the phosphabenzene,[6] to change the mind of a whole generation of chemists.[iii] In 1976, Nixon and Kroto made a range of compounds containing carbon-phosphorus double bonds and triple bonds by "conveniently" heating solutions of halogenophosphanes to 900 °C.[7] Later it was discovered that CF_3PH_2 eliminated two equivalents of HF at room temperature by simply adding it to solid pellets of sodium hydroxide.[8] The resulting FC≡P was more stable than the previously synthesised phosphaalkynes, but still not indefinitely storable (cf. Figure 1-1 **II**). Shortly after that, Appel succeeded in obtaining the silylated phosphaalkyne $(CH_3)_3SiC{\equiv}P$, which could be handled for 50 minutes at room temperature before decomposition took place.[9]

It was 20 years after the discovery of HC≡P when Becker and coworkers reported on a lab scale synthesis for the most widespread and commonly used phosphaalkyne to date, the *tert*-butyl phosphaalkyne.[10] Other than being indefinitely stable in solution and as a pure sample at -80 °C, it can easily be purified either via fractional distillation or the so-called "Becker condensation" (cf. Figure 1-1 **III**). The first step towards this compound is the

---

i Sometimes also referred to as phosphaethynes.
ii The double bond rule stated that multiple bonds between elements of the second and third or higher periods were impossible.
iii The fact that HC≡P is highly reactive, spontaneously combusts at contact with air and additionally polymerises at -130 °C did make it even more of a chemical curiosity.

formation of a phosphorus carbon double bond via salt elimination from lithium *bis*-trimethylsilyl phosphide and pivaloyl chloride with a subsequent [1,3]-silyl shift. The crucial second step is the successful elimination of hexamethyl disiloxane (HMDSO) by refluxing the C=P double bond compound over solid NaOH. This reaction sequence could be transferred to a number of other alkyl substituents over the following years.[11]

Kinetically stabilised phosphaalkynes have made a huge impact on phosphorus chemistry which can be seen in the number of reviews concerning this class of substances.[1,12] There are no limitations in respect to substituents, as phosphaalkynes can be synthesised using various protocols resulting in a wide range of substituents: alkyl and aryl substituents are possible as well as heteroatomic substituents. The rich chemistry of these compounds will be discussed in the next chapters.

The relevant question at this point was whether it was possible to synthesise the kinetically unstabilised versions of phosphaalkynes, i.e. particularly the methyl substituted substance, or whether phosphaalkynes were only stable due to the steric bulk they were subjected to. And indeed, in 1968 Denis and co-workers reported on the Flash Vacuum Thermolysis/Gas Solid Reaction (FVT/GSR) of (dichloro)alkylphosphanes[13] and again in 1991, this time using Vacuum Gas-Solid Evaporation (VGSE) of HCl from (dichloro)alkylphosphanes with the aid of K_2CO_3 to yield the desired product, MeC≡P.[14] Again ten years later, a more feasible way was published by the same group,[15] making the synthesis available in solution. Employing the strong base 1,8-Diazabicyclo[5.4.0]undec-7-ene (DBU) at low temperatures makes it possible to eliminate HCl from 1,1-(dichloro)ethylphosphane to give the unstabilised phosphaalkyne (see Figure 1-1 **IV**). Additionally, this publication describes a convenient way to obtain the precursors, halogenated alkylphosphanes, making the whole sequence readily available. To obtain a higher yield of the methyl phosphaalkyne, a slightly adjusted synthetic route regarding solvents and stoichiometry has been used in our own laboratory.[16]

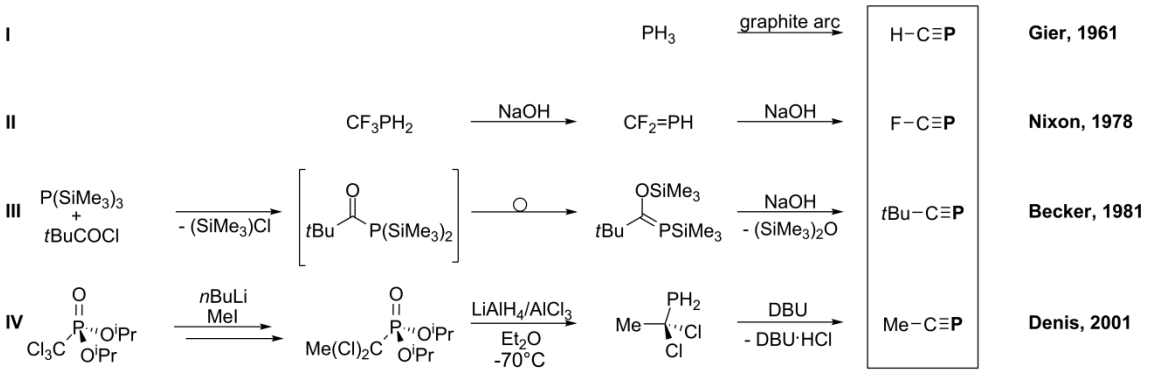

Figure 1-1 Synthetic routes towards phosphaalkynes. **I**) HC≡P formation by striking an arc in a PH_3 atmosphere; **II**) base catalysed elimination of HF to form FC≡P; **III**) formation of a C=P double bond and subsequent elimination of HMDSO to obtain the kinetically stabilised *t*BuC≡P; **IV**) synthesis of the kinetically unstabilised MeC≡P.

1.2 Phosphaalkynes: Properties

"Phosphaalkine entsprechen Alkinen in allem, Nitrilen in nichts"[iv]

M. Regitz, 1995[17]

Already the first publication by T. E. Gier on HC≡P established that indeed a threefold bond existed between the phosphorus and carbon atoms. He also determined that the hydrogen atom was located on the carbon moiety, identified by the infrared bands that showed no stretch in the characteristic region for P-H bands.[3] Tyler later corrected the reported value for the C≡P stretching band (1265 cm^{-1}) to be 1278 cm^{-1},[18] while Frost, Nixon and Kroto observed the ionisation potentials of multiple phosphaalkynes by microwave analyses.[7-8,19] However, the reactivity was presumed to be nitrile-like[20] until photoelectron spectra (PE) of *t*BuC≡P were recorded by Nixon *et al.* that showed that the π-gap between the $2p_\pi$-$3p_\pi$ electrons (e^-) was bigger than in the case of *t*BuCN. Furthermore, the first ionisation potential of 9.61 eV is corresponding to the removal of an e^- from an orbital of the π_{CP} triple bond.[21] This is one of the first indications phosphaalkynes are not as similar to nitriles as previously thought. Selected properties of the unstabilised and kinetically stabilised phosphaalkynes HC≡P, MeC≡P and *t*BuC≡P are summarised in Table 1-1.

Table 1-1 Properties of different phosphaalkynes.

	HC≡P	MeC≡P	*t*BuC≡P
$\tilde{\nu}$(C≡P) [cm^{-1}] =	1278[18]	1559[14]	1533[10]
$^{31}P\{^1H\}$ NMR: δ [ppm] =	-32[13]	-60[13]	-69.2[10]
d(C≡P) [pm][v] =	156.2[4]	154[22]	154.2[23]
IP [eV] =	10.8[19a]	9.89[24]	9.61[21]

The diagonal relationship between phosphaalkynes and alkynes can also be explained by comparison of the electronegativities of the atoms within the triple bond. The difference in electronegativity ΔE_N also has an impact on the bonding situation[vi]:

ΔE_N(alkynes) = 0 ΔE_N(nitriles) = 0.49 ΔE_N(phosphaalkynes) = 0.36

Although the absolute values for nitriles and phosphaalkynes seem to be in the same range, quite the opposite is the case: phosphorus (2.19) is smaller in electronegativity compared to carbon (2.55) and is thus the more electropositive partner in this triple bond.[25] The

iv "phosphaalkynes meet all requirements of alkynes, but none of nitriles"
v *t*BuC≡P: Bond length determined by X-Ray crystallography, while bond lengths in HC≡P and MeC≡P are determined by vibrational analyses. P=C double bonds and P-C single bonds are in the range of 170 pm and 187 pm, respectively.
vi pauling electronegativities have been used throughout this thesis

distribution of electrons in phosphaalkynes is heavily carbon sided, which contributes to the contraction of the lone pair on the heteroatom. As a result, phosphaalkynes more readily form side-on complexes with the HOMO being the triple bond, while nitriles preferentially form bonds with their lone pair on the nitrogen atom. Most likely, all those facts combined led Regitz to the statement on top of this chapter. This does not mean that phosphaalkynes will not coordinate with their lone pair; it simply means that the coordination site has to be designed to enforce η^1 coordination. This is, of course, the big difference in comparison to alkynes, which do not have the possibility to coordinate in an end-on fashion, making phosphaalkynes the more versatile building block - especially in organometallic chemistry.

1.3 Phosphaalkynes: Coordination

> *"Phosphaalkynes obviously have the very interesting potential to exhibit a duality of chemical behaviour. On the one hand they might react in a similar fashion to their better known organic counterparts the alkynes, RC≡CR, and on the other hand the phosphorus lone-pair electrons might enable them to coordinate to a variety of metal atoms, as is the case for many phosphane (R_3P) ligands. Of course, in suitable circumstances both types of behaviour might also be possible."*
>
> John F. Nixon, 1991[12f]

…and both types of behaviour had already been observed when Nixon wrote this review. The diagonal relationship to alkynes and the possibility of an end-on coordination has already been discussed in the last chapter, and deduced from these findings five major coordination forms can be proposed for phosphaalkynes as complex ligands donating 2, 4 or 6 electrons (cf. Figure 1-2).

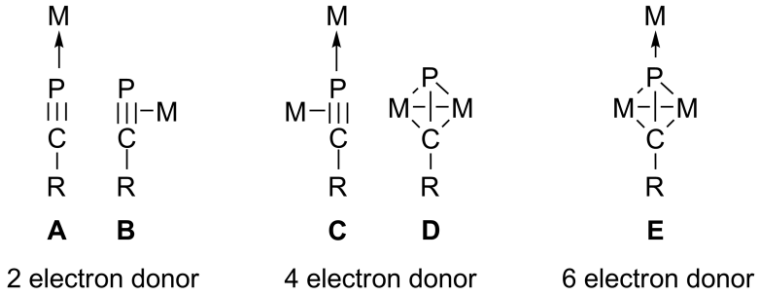

Figure 1-2 Possible coordination modes for phosphaalkynes.

The first isolated complex of a phosphaalkyne has been the side-on $2e^-$ type complex $[Pt(PPh_3)_2(t\text{BuC}{\equiv}P)]$ (Figure 1-2 **B**) in 1981 by Nixon *et al.*[26] Here, the bond between carbon and phosphorus is considerably elongated to 1.672(17) Å, and with a CCP angle of 132(2)° and the occupation of two coordination sites on the platinum metal centre it might be described best as a metallaphosphacyclopropene. The same publication also stated that the

reaction between *tert*-butyl phosphaalkyne and $Co_2(CO)_8$ led to the side-on $4e^-$ tetrahedrane complex [$Co_2(CO)_6$(*t*BuCP)] (Figure 1-2 type **D**), but the crystal structure could only be isolated one year later as an adduct complex of $W(CO)_5$(thf),[27] making the phosphaalkyne a $6e^-$ donor (Figure 1-2 type **E**) with a CP bond length of 1.695(6) Å. Only in 1987 the first example of an type **A** end-on η^1 coordinated phosphaalkyne has been isolated in form of the complex [*trans*-$Mo(AdC{\equiv}P)_2(depe)_2$] (Ad = Adamantyl, depe = 1,2-bis(diethylphosphino)ethane),[28] in which the phosphaalkyne was forced to coordinate via its lone pair in contrast to the usual coordination via its HOMO. Coordination of type **C** was also realised by Nixon *et al.* in 1988.[29] Additionally, the concept of a side-on coordinated phosphaalkyne over a metal-metal bond (Figure 1-2 type **D**) resulting in a tetrahedrane-like product can be applied to a wide range of substrates, including mixed metal complexes[30] and metal-metal multiple bonds.[31]

1.4 Phosphaalkynes: Cycloadditions

> *"The degree of cyclooligomerisation and the structure of the resulting metal complexes seem to depend mainly upon the nature of the metal used."*
>
> Binger et al., 1989[32]

As the analogy between phosphaalkynes and alkynes has already been discussed (*vide supra)*, it is of no surprise that cyclodimerisations and cyclooligomerisations are within the most reported reactions of phosphaalkynes. The groups of Nixon[33] and Binger[34] independently reported on the first cyclodimerisations of *tert*-butyl phosphaalkyne in 1986, which led to 1,3-diphosphacyclobutadiene complexes (1,3-diphosphete complexes) of the d^9 metals Co,[33-34] Rh and Ir with the general formula [$Cp^RM(\eta^4$-$P_2C_2tBu_2)$] (**1**, Figure 1-3).[33] They all have in common the essentially planar four membered ring in which all bond lengths between phosphorus and carbon are equal and between a single and double bond, making it an anti-aromatic 4π e^- ring system (cf. Figure 1-3).[33] The choice of substituents on the metal centre (and the metal centre itself) also is a crucial in determining how many diphosphete moieties are complexed: homoleptic *bis*-diphosphete complexes of nickel (**2**, cf. Figure 1-3)[35] are known as well as those of the metalate complexes of iron[36] and cobalt,[37] and co-condensation of molybdenum atoms with *t*BuC≡P leads to the formation of *tris*-diphosphacyclobutadiene molybdenum (**3**, cf Figure 1-3).[38]

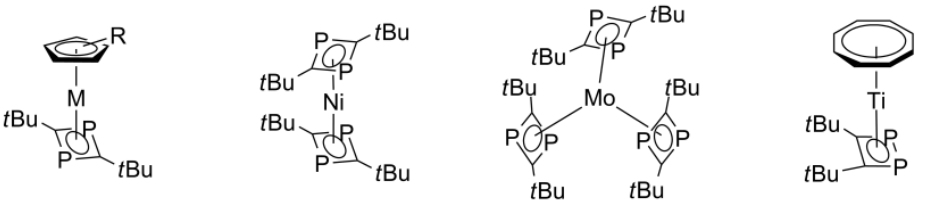

Figure 1-3 The first of their kind: **1**: first 1,3-diphosphacyclobutadiene complexes of Co, Rh and Ir published simultaneously by Regitz and Nixon; **2**: first homoleptic bis-diphosphete complex of Nickel; **3**: first homoleptic tris-diphosphete molybdenum(0) compound; **4**: first 1,2-diphosphete complex on an early transition metal.

All of those have in common the configuration of the four membered ring: the [2+2] head-to-tail cyclodimerisation of the phosphaalkyne results in the formation of the 1,3-diphosphete moiety, not of the 1,2-diphosphete moiety which would be the product of the head-to-head cyclodimerisation. Interestingly, calculations for the sterically unhindered HC≡P show clearly enough that the formation of the 1,2-diphosphete should be favoured by 37 kJ·mol^{-1}.[39] But the almost exclusive experimental observation of the 1,3-diphosphete is not happening only due to the sterically demanding *t*Bu substituent: additional calculations by Vanquickenborn *et al*. reveal that also the approach of *t*BuC≡P to transition metal centres should always be favoured in a head-to-head fashion, even if the barrier here is merely 7 kJ·mol^{-1}.[40] However, there are a few examples for 1,2-diphosphete complexes known in the literature which are obtained from phosphaalkyne dimerisation: both the titanium complex [Ti(COT)(η^4-1,2-P_2C_2tBu$_2$)][41] (COT = cyclooctatetraene; **4**, cf. Figure 1-3) and the tungsten carbonyl complex of methyl phosphaalkyne, [W(CO)$_4$(η^4-1,2-P_2C_2Me$_2$)],[42] are obtained together with their 1,3-diphosphete counterparts. Unfortunately, the 1,3- and 1,2-diphosphete complexes cannot be separated easily. In the case of the titanium complex, different phosphaalkynes have been dimerised in the coordination sphere of the transition metal and the ratio of head-to-head to head-to-tail dimer drops to zero by increasing the steric bulk on the phosphaalkyne.[41] The only reaction which leads to the selective formation of an 1,2-diphosphete is the nearly quantitative reaction from a phosphaalkyne side-on complex of tantalum with another equivalent of *t*BuC≡P to form [Cp*TaCl$_2${σ,σ,π-1,2-P_2C_2tBu$_2$}].[43] Zenneck and coworkers, however, describe a different way to 1,2-diphosphetes: via elimination of FeCl$_2$ and carbon monoxide from the diphosphetene [{Fe(CO)$_4$}$_2$σ^2-{1,2-dichloro-1,2-P_2C_2tBu$_2$)}] at elevated temperatures they obtain [Fe(CO)$_3$(η^4-1,2-P_2C_2tBu$_2$)].[44] Also not directly derived from phosphaalkynes, our own group could isolate a coordination compound of [Cp'''Fe(η^4-1,2-P_2C_2tBu$_2$)]

(Cp''' = η^5-1,2,4-$C_5H_2(t\text{Bu})_3$) dimerised by two CuBr bridges which originated from the reaction of the 1,2,4-triphosphaferrocene [Cp'''Fe(η^5-$P_3C_2t\text{Bu}_2$)] with CuBr in dichloromethane/acetonitrile.[45] Here, it was found that the stoichiometry of CuX (X = Br, I) used has an influence on the fragmentation products that could be isolated.

As has been mentioned above, a crucial step in the formation of cycloaddition products is using the right metal as well as the right ligand. Using a [Cp_2Zr] complex for the dimerisation of phosphaalkynes, instead of a diphosphete complex a diphospha-*bicyclo*[1.1.0]butane (butterfly) complex is formed with a new phosphorus-phosphorus bond. This complex is viable in the creation of different other cycloaddition products,[46] with a special focus on the tetraphosphacubane.[47] Variation of the metal can lead to six membered rings and bicyclic systems. In the reaction with the Lewis acid copper(I) iodide, even cage compounds could be isolated (cf. Figure 1-4).[48] Furthermore, the uncomplexed tetramer can be obtained by thermal treatment of *tert*-butyl phosphaalkyne in low yields[49] (or, as mentioned *vide supra*, via the zirconium butterfly mediated route). As most of these systems are not relevant to the contents of this thesis, no further description of their synthesis and properties will be given.

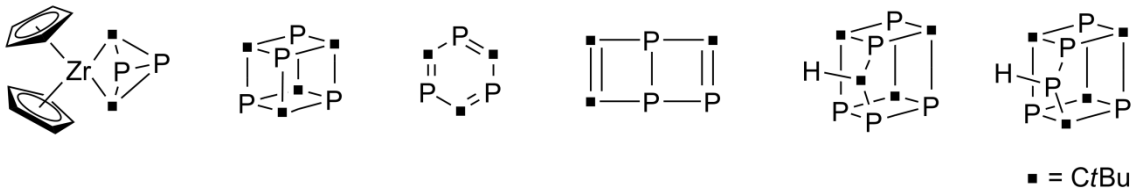

Figure 1-4 Different oligomerisation products of *t*BuC≡P: dimers, trimers and tetramers as well as cage compounds.

Not only "clean" stoichiometric reactions to form cyclic compounds with an even number of ring atoms are known in the literature, but also reactions that include fragmentation of the phosphaalkyne and subsequent cycloaddition to yield ring systems which are not easily describable in their formation mechanisms. Here, one class of compounds is of particular interest: the formation of five-membered aromatic rings containing phosphorus with the general formula $(RC)_nP_{5-n}$ (n = 1-4). These so-called (poly-) phospholyl rings can easily be compared to cyclopentadienyl ligands using the isolobal principle, which states that a phosphorus atom is interchangeable with a methine –CH fragment due to the similar frontier orbital structure. In 1989, Cowley and Hall reported on the synthesis of $NaP_2(Ct\text{Bu})_3$ and $NaP_3(Ct\text{Bu})_2$ in the reaction of $Ta(OAr)_2Cl_3$ (Ar = 2,4-*tert*-butyl-6-methylphenyl) with 3 equivalents of sodium amalgam and subsequent addition of 3 equivalents of *tert*-butyl phosphaalkyne.[50] Later that same year, Bartsch and Nixon revealed that the tantalum complex was not needed for this reaction as the fragmentation and cyclisation of the phosphaalkyne to form the 1,3-diphospholyl and 1,2,4-triphospholyl rings was due to the reducing nature of the Na/Hg mixture.[51] An easier approach to the lithium (or potassium)

salts of the (poly-)phospholyl rings is the reaction between $Li[P(SiMe_3)_2]$ (or $K[P(SiMe_3)_2]$) and *t*BuC(OSiMe$_3$)=P(SiMe$_3$), both an educt and an educt of the educt for the preparation of *t*BuC≡P.[52]

Also utilising the educts of phosphaalkyne generation, the group of Ionkin found a way to react an aryl acid chloride with $P(SiMe_3)_3$ and CsF to yield the 1,2,4-triphospholyl and 1,2,3,4-tetraphospholyl cycles.[53] This synthesis was adapted by Claudia Heinl of our group to realise the corresponding arsolyl ligands for the first time.[54] 1,2,3-triphospholyl rings have been elusive for a long time until Goicoechea *et al.* reported on the reaction of P_7^{3-} (and As_7^{3-}) zintl ions with different alkynes to yield the desired 1,2,3-triphospholyl (and 1,2,3-triarsolyl) rings.[55] Other highly reducing Zintl ions like Ge_9^{4-} can also be used to reduce *t*BuC≡P as was shown in a cooperation with Christian Benda (group of Prof. T. Fässler, TU Munich), which is part of his PhD thesis.[56]

Maybe also because of the reducing nature of the metal used, Driess and coworkers discovered that the reaction of an iron(0) arene complex and *t*BuC≡P leads to the formation of a structural isomer of pentaphosphaferrocene with one triphospholyl and one diphospholyl ligand (amongst others).[57] Similar n-phospholyl containing products could also be observed in the metal vapour co-condensation of Sc,[58] Ni[59] and Co[60] with *t*BuC≡P. Another way to form n-phosphaferrocenes involves the reaction of *tert*-butyl phosphaalkyne with the tetraphospha-*bicyclo*[1.1.0]butane (butterfly) complex $[\{Cp'''(CO)_2Fe\}_2(\mu,\eta^{1:1}\text{-}P_4)]$, from which tri-, tetra- and pentaphosphaferrocenes could be isolated.[61]

1.5 Coordination Chemistry of Phosphorus Containing Compounds

To describe all coordination chemistry of phosphorus containing compounds is of course too big an undertaking for the scope of this introduction. The focus will lie on two distinct topics which will also be approached within this thesis: the coordination of diphosphete complexes and the coordination via coinage metal salts.

1.5.1 Coordination of Diphosphete Complexes

In diphosphete complexes, the ability of the lone pairs of the phosphorus atoms to coordinate additional metals is retained as a variety of publications show. Already the first 1,3-diphosphete complex $[CpCo(\eta^4\text{-}P_2C_2tBu_2)]$ (**1a**) has been found to coordinate its own educt, $[CpCo(\eta^2\text{-}C_2H_4)_2]$, a complex which readily loses ethene. **1a** is thus able to donate the lone pairs of one or both phosphorus atoms in subsequent reactions (cf. Figure 1-5 **I**).[34] Also, metal coordination by the phosphorus moiety of different diphosphete complexes could be realised with the complexes $[PtCl_2PEt_3]$,[62] $[W(CO)_5]$,[60] $[W(CO)_4]$,[16a] $[AuPPh_3]$,[63] $[Au(PMe_3)_2]$,[64]

$[Cu(PPh_3)_2]$ and $[Ag(PMe_3)_x]$ (x = 2, 3)[65] and both $[CpNiPPh_3]$ (cf. Figure 1-5 **II**) and $[(\eta^4\text{-}cyclo\text{-}C_4Me_4)Co(CO)_2]$.[66] This successfully proves the ability of the lone pairs to coordinate a wide range of unsaturated transition metal complexes. But even more interestingly, four rhodium (**1b**) and cobalt diphosphete complexes (**1a**) could be linked via a Rh_2Cl_2 bridge, resulting in a coordination of half of the coordination sites available (see Figure 1-5 **III**).[62] Wolf and coworkers could also demonstrate the versatility of their anionic bis-(1,3-diphosphacyclobutadiene) cobalt complexes in the self-assembly with coinage metal salts to yield one-dimensional polymers[64] or a molecular square consisting of four *bis*-diphosphete complexes and four gold(I) centres (Figure 1-5 **IV**), respectively.[67] The use of copper(I) halides has additionally proven to be an interesting starting point in the synthesis of molecular (Figure 1-5 type **V**), one-dimensional (cf. Figure 1-5, **VI**) and two-dimensional polymeric assemblies (see Figure 1-5, **VII**) containing 1,3-diphosphete complexes.[16]

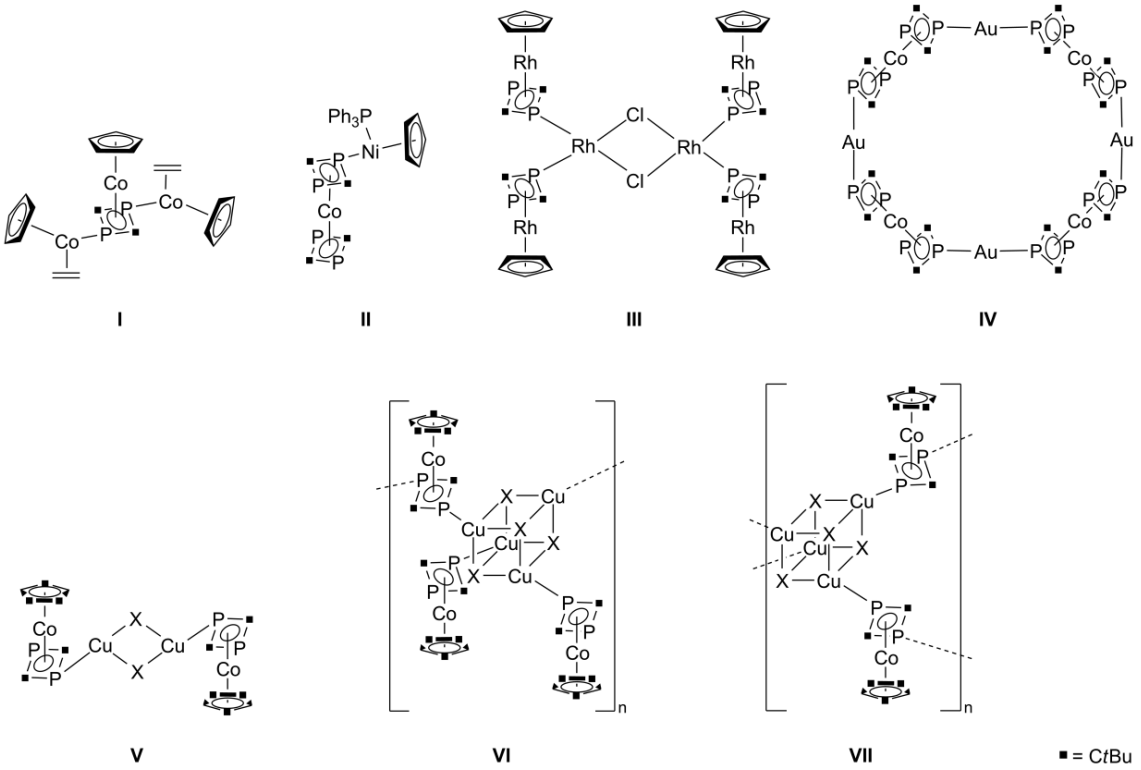

Figure 1-5 Coordination compounds derived from 1,3-diphosphete complexes.

This again shows the versatility of coinage metals in general and the versatility of Lewis acidic copper(I) halides in particular, which have been utilised especially by our group.

Short digression: Copper(I) coordination of P_n ligand complexes

P_n ligand complexes are phosphorus containing compounds that possess bonds primarily between the phosphorus atoms or towards metal centres. As this particular field is big enough to fill whole reviews,[68] only a brief overview of complexes used by our group will be given. Selected complexes can be found in Figure 1-6.

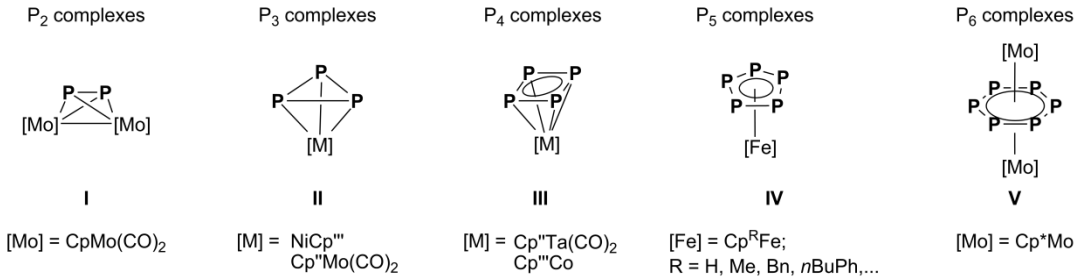

Figure 1-6 Selected examples of P_n ligand complexes. **I**) P_2 tetrahedrane complex $[\{CpMo(CO)_2\}_2(\mu,\eta^2{:}\eta^2\text{-}P_2)]$;[69] **II**) *cyclo*-$P_3$ complexes $[Cp'''Ni(\eta^3\text{-}P_3)]$[70] and $[Cp''Mo(CO)_2(\eta^3\text{-}P_3)]$;[71] **III**) *cyclo*-$P_4$ complexes $[Cp''Ta(CO)_2(\eta^4\text{-}P_4)]$[72] and $[Cp'''Co(\eta^4\text{-}P_4)]$;[73] **IV**) *cyclo*-$P_5$ pentaphosphaferrocenes with different Cp ligands;[54, 74] **V**) *cyclo*-P_6 tripledecker complex $[(Cp^*Mo)_2(\mu,\eta^6{:}\eta^6\text{-}P_6)]$.[75]

All P_n ligand complexes have been reacted with Lewis acidic Cu(I) halides and "naked" Cu(I) salts with weakly coordinating anions (WCAs) to form interesting coordination compounds in which the coinage metal takes on different coordination modes. A selection of one- or two-dimensional polymeric compounds can be found in Figure 1-7.

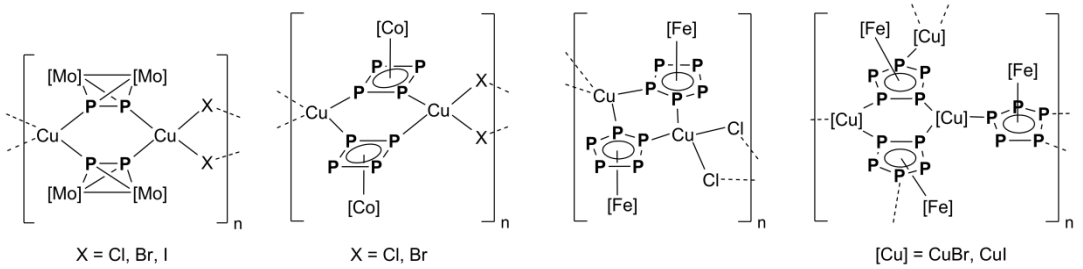

Figure 1-7 Polymers derived from P_n ligand complexes mentioned above: one-dimensional polymers $[Cu(\mu\text{-}X)\{(CpMo(CO)_2)_2(\mu,\eta^2{:}\eta^1{:}\eta^1\text{-}P_2)\}]_n$ (X = Cl, Br, I)[76] and $[Cu(\mu\text{-}X)\{Cp'''Co(\mu,\eta^4{:}\eta^1{:}\eta^1\text{-}P_4)\}]_n$ (X = Cl, Br);[73] pentaphosphaferrocene-based one-dimensional $[CuCl\{Cp^*Fe(\eta^5{:}\eta^1{:}\eta^1\text{-}P_5)\}]_n$ and two-dimensional polymers $[CuX\{Cp^*Fe(\eta^5{:}\eta^1{:}\eta^1{:}\eta^1\text{-}P_5)\}]_n$ (X = Br, I).[77]

Depending on the reaction conditions, also "zero-dimensional" spherical compounds could be obtained for P_4 and P_5 ligand complexes: $[(CuCl)_8\{Cp''Ta(CO)_2P_4\}_6]$[78] with pseudooctahedral symmetry and the icosahedral fullerene C_{80} analogue $[(CuX)_{20}(Cp^*FeP_5)_{12}]L$ (X = Cl, Br).[79] This is a demonstration on how well the copper halides can adapt to form different geometries depending on stoichiometry and solvents used.

1.5.2 Coordination via silver and gold salts

Next to copper, also group 11 silver and gold salts can be used in coordination chemistry of P_n ligand complexes and their mixed isolobal carbon containing counterparts. Here again there are two possibilities for the starting materials: either Lewis acidic M(I) salts or "naked" M(I) ions with WCAs as counterions. Both show different reactivity and are able to build molecular compounds or supramolecular networks depending on the reaction conditions. However, when using coinage metal salts in coordination chemistry one always has to bear in mind that there is a competing reaction pathway of oxidation. This can be controlled by using an appropriate solvent, which can lower the oxidation potential significantly.[80]

The P_2 tetrahedrane complex $[\{CpMo(CO)_2\}_2(\mu,\eta^2{:}\eta^2\text{-}P_2)]$ (**5**) has been subjected to naked silver and gold WCA salts, yielding a dimer compound with two tetrahedrane complexes bridging over both coinage metals and two additional tetrahedrane complexes coordinating in a side-on fashion (cf. Figure 1-9 **A**).[76,81] A similar compound with the central structural motif of an Ag_2P_4 six-membered ring could be obtained in the reaction of **5** with the Lewis acidic $AgNO_2$. Here, the remaining coordination sites on the silver cations are saturated with two NO_2 ligands.[81] The use of $AgNO_3$ leads to the formation of a one-dimensional polymer in which NO_3 acts as a bridging ligand between the silver cations.[76] The reaction with [(tht)AuCl], however, leads to the mono-coordinated $[AuCl\{Cp_2Mo_2(CO)_4(\mu_3,\eta^2{:}\eta^2{:}\eta^2\text{-}P_2)\}]$.[81] Different structural motifs can be obtained when reacting $[Cp^*Mo(CO)_2(\eta^3\text{-}P_3)]$ with Lewis acidic Cu(I) halides and silver WCA salts: the CuX (X = Cl, Br, I) salts form nearly insoluble dimeric compounds with a central Cu_2X_2 ring,[76] whereas the reaction with the silver salt of the weakly coordinating anion, $Ag[Al\{OC(CF_3)_3\}_4]$, produced three different soluble one-dimensional polymeric compounds.[82]

Short digression: The WCA $[Al\{OC(CF_3)_3\}_4]^-$

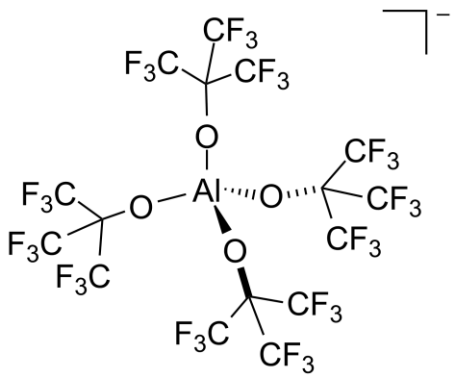

Figure 1-8 Schematic representation of the pftb anion.

Although a series of anions have been used in the reactions mentioned above, only the weakly coordinating anion $[Al\{OC(CF_3)_3\}_4]^-$ (perfluoro-*tert*-butoxyaluminate, "pftb", see Figure 1-8) leads to products with good solubility in CH_2Cl_2, THF or even toluene. The distinct properties of this anion can be attributed to its size of 1.25 nm and the resulting small coulomb interactions (which are proportional to r^{-2}) and also the highly symmetric structure where only one electron is delocalised over a very big surface.[83] This leads to postulated pseudo-gasphase conditions when using the kinetically inert anion which could be proven by isolating cations which were only postulated theoretically or have previously only been detected by mass analyses, like $[Ag(\eta^2\text{-}C_2H_4)_3][pftb]$[84] or $[Ag(\eta^2\text{-}C_2H_2)_n][pftb]$ (n = 3,4).[85]

Due to its properties, the WCA salt Ag[pftb][86] is also able to stabilise the highly reactive P_4[87] and As_4[88] tetrahedrons with the possibility of subsequent release of the reactive molecules from the coordination compound. Fabian Dielmann could prove that the *in situ* generated [Au(tht)][pftb] also could be coordinated by the cyclo-P_4 complex $[Cp''Ta(CO)_2(\eta^4\text{-}P_4)]$ ($Cp'' = \eta^5\text{-}1,3\text{-}C_5H_3tBu_2$), resulting in a supramolecular assembly of four Au centres being coordinated by eight $[Cp''Ta(CO)_2(\eta^4\text{-}P_4)]$ complexes (see Figure 1-9, **B**).[73]

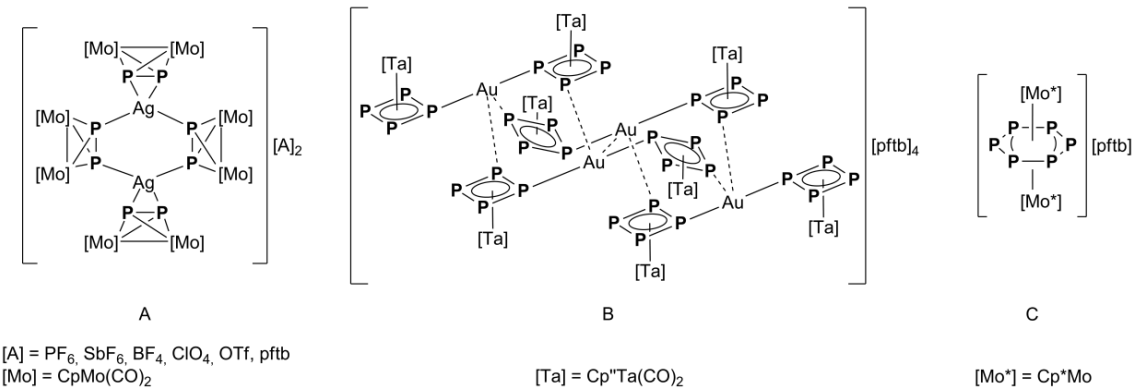

Figure 1-9 Products from the reactions of P_n ligand complexes with silver/gold salts with weakly coordinating anions.

Also E_5 complexes like pentaphosphaferrocene $[Cp^*Fe(\eta^5\text{-}P_5)]$ react with Ag[pftb] to form the one-dimensional polymer $[Ag\{Cp^*Fe(\eta^5\text{:}\eta^2\text{:}\eta^1\text{-}P_5)\}_2]_n[pftb]_n$ with a novel 1,2,3-coordination

mode for the P_5 ligand where three neighbouring P moieties are coordinating two different silver cations. The polymer thus contains two pentaphosphaferrocene complexes for every coinage metal centre.[89] Changing the steric demand on the Cp ligand by using [$Cp^{BIG}Fe(\eta^5\text{-}P_5)$] ($Cp^{BIG}$ = $\eta^5\text{-}C_5(4\text{-}n\text{Bu}C_6H_4)_5$), also a one-dimensional polymer of silver and a P_5 ligand is formed, but this time the ratio in the product is 1:1 with the P_5 ligand coordinating the silver cation in a 1,3-fashion. Additionally, the phenyl groups of the Cp^{BIG} ligand create Ag-π interactions.[90] The cyclo-P_6 triple decker complex [$(Cp^*Mo)_2(\mu,\eta^6\text{:}\eta^6\text{-}P_6)$] displays an interesting duality when reacted with Ag[pftb]: It can be oxidised (oxidation product see Figure 1-9 **C**) and coordinated likewise, depending on the reaction conditions used.[91]

1.6 References

[1] M. Regitz, *Chem. Rev.* **1990**, *90*, 191.

[2] A. Marcelino, C. José, G. Michel, *Astrophys. J. Lett.* **2007**, *662*, L91.

[3] T. E. Gier, *J. Am. Chem. Soc.* **1961**, *83*, 1769.

[4] J. K. Tyler, *J. Chem. Phys.* **1964**, *40*, 1170.

[5] a) K. S. Pitzer, *J. Am. Chem. Soc.* **1948**, *70*, 2140; b) R. S. Mulliken, *J. Am. Chem. Soc.* **1950**, *72*, 4493.

[6] G. Märkl, *Angew. Chem.* **1966**, 907.

[7] M. J. Hopkinson, H. W. Kroto, J. F. Nixon, N. P. C. Simmons, *Chem. Commun.* **1976**, 513.

[8] H. W. Kroto, J. F. Nixon, N. P. C. Simmons, N. P. C. Westwood, *J. Am. Chem. Soc.* **1978**, *100*, 446.

[9] R. Appel, A. Westerhaus, *Tetrahedron Lett.* **1981**, *22*, 2159.

[10] G. Becker, G. Gresser, W. Uhl, *Z. Naturforsch., Teil B* **1981**, *36B*, 16.

[11] a) W. Rösch, U. Vogelbacher, T. Allspach, M. Regitz, *J. Organomet. Chem.* **1986**, *306*, 39; b) T. Allspach, M. Regitz, G. Becker, W. Becker, *Synthesis* **1986**, 31.

[12] a) R. Appel, F. Knoll, I. Ruppert, *Angew. Chem. Int. Ed.* **1981**, *20*, 731; b) J. F. Nixon, *Chem. Rev.* **1988**, *88*, 1327; c) M. Regitz, P. Binger, *Angew. Chem.* **1988**, *100*, 1541; d) M. Regitz, P. Binger, *Angew. Chem. Int. Ed.* **1988**, *27*, 1484; e) M. Regitz, P. Binger, *Nachrichten aus Chemie, Technik und Laboratorium* **1989**, *37*, 896; f) J. F. Nixon, *Endeavour* **1991**, *15*, 49; g) A. C. Gaumont, J. M. Denis, *Chem. Rev.* **1994**, *94*, 1413; h) J. F. Nixon, *Coord. Chem. Rev.* **1995**, *145*, 201; i) F. Mathey, *Angew. Chem. Int. Ed.* **2003**, *42*, 1578; j) F. Mathey, *Angew. Chem.* **2003**, *115*, 1616; k) J. M. Lynam, *Organomet. Chem.* **2007**, *33*, 170; l) C. A. Russell, N. S. Townsend, in *Phosphorus(III) Ligands in Homogeneous Catalysis: Design and Synthesis*, John Wiley & Sons, Ltd, **2012**, pp. 343.

[13] B. Pellerin, J.-M. Denis, J. Perrocheau, R. Carrie, *Tetrahedron Lett.* **1986**, *27*, 5723.

[14] J. C. Guillemin, T. Janati, J. M. Denis, P. Guenot, P. Savignac, *Angew. Chem. Int. Ed.* **1991**, *30*, 196.

[15] J.-C. Guillemin, T. Janati, J.-M. Denis, *J. Org. Chem.* **2001**, 7864.

[16] a) E.-M. Rummel, M. Eckhardt, M. Bodensteiner, E. V. Peresypkina, W. Kremer, C. Gröger, M. Scheer, *Eur. J. Inorg. Chem.* **2014**, 1625; b) M. Eckhardt, PhD thesis, Regensburg **2014**.

[17] Regitz, M. GDCh-Vortrag, Hannover, **1995**, *as cited in* J. Foerstner, F. Olbrich, H. Butenschön, *Angew. Chem.* **1996**, *108*, 1323.

[18] J. W. C. Johns, H. F. Shurvell, J. K. Tyler, *Can. J. Phys.* **1969**, *47*, 893.

[19] a) D. C. Frost, S. T. Lee, C. A. McDowell, *Chem. Phys. Lett.* **1973**, *23*, 472; b) H. W. Kroto, J. F. Nixon, N. P. C. Simmons, *J. Mol. Spectrosc.* **1980**, *82*, 185; c) J. C. T. R. B. S. Laurent, T. A. Cooper, H. W. Kroto, J. F. Nixon, O. Ohashi, K. Ohno, *J. Mol. Struct.* **1982**, *79*, 215.

[20] B. Solouki, H. Bock, R. Appel, A. Westerhaus, G. Becker, G. Uhl, *Chem. Ber.* **1982**, *115*, 3747.

[21] J. C. T. R. B. S. Laurent, M. A. King, H. W. Kroto, J. F. Nixon, R. J. Suffolk, *Dalton Trans.* **1983**, 755.

[22] H. W. Kroto, J. F. Nixon, N. P. C. Simmons, *J. Mol. Spectrosc.* **1979**, *77*, 270.

[23] A. N. Chernega, M. Y. Antipin, Y. T. Struchkov, M. F. Meidine, J. F. Nixon, *Heteroat. Chem.* **1991**, *2*, 665.

[24] N. P. C. Westwood, H. W. Kroto, J. F. Nixon, N. P. C. Simmons, *Dalton Trans.* **1979**, 1405.

[25] A. F. Holleman, E. Wiberg, N. Wiberg, *Lehrbuch der Anorganischen Chemie, Vol. 102*, de Gruyter, Berlin, **2007**.

[26] J. C. T. R. B. S. Laurent, P. B. Hitchcock, H. W. Kroto, J. F. Nixon, *Chem. Commun.* **1981**, 1141.

[27] J. C. T. R. B. S. Laurent, P. B. Hitchcock, H. W. Kroto, M. F. Meidine, J. F. Nixon, *J. Organomet. Chem.* **1982**, C82.

[28] a) P. B. Hitchcock, M. J. Maah, J. F. Nixon, J. A. Zora, G. J. Leigh, M. Abu Bakar, *Angew. Chem.* **1987**, *99*, 497; b) P. B. Hitchcock, M. J. Maah, J. F. Nixon, J. A. Zora, G. J. Leigh, M. A. Bakar, *Angew. Chem. Int. Ed.* **1987**, *26*, 474.

[29] S. I. Al-Resayes, P. B. Hitchcock, M. F. Meidine, J. F. Nixon, *J. Organomet. Chem.* **1988**, *341*, 457.

[30] R. N. Bartsch, John F., N. Sarjudeen, *J. Organomet. Chem.* **1985**, 267.

[31] a) G. H. Becker, Wolfgang A; Kalcher, Willibald; Kriechbaum, Gangold W.; Pahl, Claudia; Wagner, Thomas C.; Ziegler, Manfred L., *Angew. Chem.* **1983**, *95*, 417; b) G. H. Becker, Wolfgang A; Kalcher, Willibald; Kriechbaum, Gangold W.; Pahl, Claudia; Wagner, Thomas C.; Ziegler, Manfred L., *Angew. Chem. Int. Ed.* **1983**, *22*, 413.

[32] P. Binger, B. Biedenbach, R. Schneider, M. Regitz, *Synthesis* **1989**, 960.

[33] P. B. Hitchcock, M. J. Maah, J. F. Nixon, *Chem. Commun.* **1986**, 737.

[34] a) P. Binger, R. Milczarek, R. Mynott, M. Regitz, W. Rösch, *Angew. Chem. Int. Ed.* **1986**, *25*, 644; b) P. Binger, R. Milczarek, R. Mynott, M. Regitz, W. Rösch, *Angew. Chem.* **1986**, *98*, 645.

[35] T. Wettling, G. Wolmershäuser, P. Binger, M. Regitz, *Chem. Commun.* **1990**, 1541.

[36] a) R. Wolf, J. C. Slootweg, A. W. Ehlers, F. Hartl, B. de Bruin, M. Lutz, A. L. Spek, K. Lammertsma, *Angew. Chem. Int. Ed.* **2009**, *48*, 3104; b) R. Wolf, J. C. Slootweg, A. W. Ehlers, F. Hartl, B. de Bruin, M. Lutz, A. L. Spek, K. Lammertsma, *Angew. Chem.* **2009**, *121*, 3150.

[37] a) R. Wolf, A. W. Ehlers, J. C. Slootweg, M. Lutz, D. Gudat, M. Hunger, A. L. Spek, K. Lammertsma, *Angew. Chem.* **2008**, *120*, 4660; b) R. Wolf, A. W. Ehlers, J. C. Slootweg, M. Lutz, D. Gudat, M. Hunger, A. L. Spek, K. Lammertsma, *Angew. Chem. Int. Ed.* **2008**, *47*, 4584.

[38] F. G. N. Cloke, K. R. Flower, P. B. Hitchcock, J. F. Nixon, *Chem. Commun.* **1994**, 489.

[39] M. T. Nguyen, L. Landuyt, L. G. Vanquickenborne, *J. Org. Chem.* **1993**, *58*, 2817.

[40] S. Creve, M. T. Nguyen, L. G. Vanquickenborne, *Eur. J. Inorg. Chem.* **1999**, *1999*, 1281.

[41] P. Binger, G. Glaser, S. Albus, C. Krüger, *Chem. Ber.* **1995**, 1261.

[42] C. Jones, C. Schulten, A. Stasch, *Dalton Trans.* **2006**, 3733.

[43] a) A. D. Burrows, A. Dransfeld, M. Green, J. C. Jeffery, C. Jones, J. M. Lynam, M. T. Nguyen, *Angew. Chem.* **2001**, *113*, 3321; b) A. D. Burrows, A. Dransfeld, M. Green, J. C. Jeffery, C. Jones, J. M. Lynam, M. T. Nguyen, *Angew. Chem. Int. Ed.* **2001**, *40*, 3221.

[44] F. W. Heinemann, S. Kummer, U. Seiss-Brandl, U. Zenneck, *Organometallics* **1999**, *18*, 2021.

[45] S. Deng, C. Schwarzmaier, M. Zabel, J. F. Nixon, M. Bodensteiner, E. V. Peresypkina, G. Balázs, M. Scheer, *Eur. J. Inorg. Chem.* **2011**, *2011*, 2991.

[46] a) P. Binger, T. Wettling, R. Schneider, F. Zurmühlen, U. Bergsträsser, J. Hoffmann, G.

Maas, M. Regitz, *Angew. Chem. Int. Ed.* **1991**, *30*, 207; b) P. Binger, T. Wettling, R. Schneider, F. Zurmühlen, U. Bergsträßer, J. Hoffmann, G. Maas, M. Regitz, *Angew. Chem.* **1991**, *103*, 208.

[47] a) T. Wettling, B. Geissler, R. Schneider, S. Barth, P. Binger, M. Regitz, *Angew. Chem. Int. Ed.* **1992**, *31*, 758; b) T. Wettling, B. Geissler, R. Schneider, S. Barth, P. Binger, M. Regitz, *Angew. Chem.* **1992**, *104*, 761; c) B. Geissler, T. Wettling, S. Barth, P. Binger, M. Regitz, *Synthesis* **1994**, 1337.

[48] U. Vogel, J. F. Nixon, M. Scheer, *Chem. Commun.* **2007**, 5055.

[49] a) T. Wettling, J. Schneider, O. Wagner, C. G. Kreiter, M. Regitz, *Angew. Chem. Int. Ed.* **1989**, *28*, 1013; b) T. Wettling, J. Schneider, O. Wagner, C. G. Kreiter, M. Regitz, *Angew. Chem.* **1989**, *101*, 1035.

[50] A. H. Cowley, S. W. Hall, *Polyhedron* **1989**, *8*, 849.

[51] R. Bartsch, J. F. Nixon, *Polyhedron* **1989**, *8*, 2407.

[52] a) G. Becker, W. Becker, R. Knebl, H. Schmidt, U. Weeber, M. Westerhausen, *Nova Acta Leopold.* **1985**, *59*, 55; b) R. Bartsch, P. B. Hitchcock, J. F. Nixon, *Chem. Commun.* **1987**, 1146; c) C. S. J. Callaghan, P. B. Hitchcock, J. F. Nixon, *J. Organomet. Chem.* **1999**, *584*, 87.

[53] A. S. Ionkin, W. J. Marshall, B. M. Fish, A. A. Marchione, L. A. Howe, F. Davidson, C. N. McEwen, *Eur. J. Inorg. Chem.* **2008**, *2008*, 2386.

[54] C. Heindl, PhD thesis, University of Regensburg (Regensburg), **2015**.

[55] a) R. S. P. Turbervill, J. M. Goicoechea, *Chem. Commun.* **2012**, *48*, 6100; b) R. S. P. Turbervill, A. R. Jupp, P. S. B. McCullough, D. Ergöçmen, J. M. Goicoechea, *Organometallics* **2013**, *32*, 2234; c) R. S. P. Turbervill, J. M. Goicoechea, *Inorg. Chem.* **2013**, *52*, 5527.

[56] C. Benda, PhD thesis, Technische Universität München (München), **2013**.

[57] M. Driess, D. Hu, H. Pritzkow, H. Schäufele, U. Zenneck, M. Regitz, W. Rösch, *J. Organomet. Chem.* **1987**, *334*, C35.

[58] P. L. Arnold, F. Geoffrey N. Cloke, J. F. Nixon, *Chem. Commun.* **1998**, 797.

[59] F. G. N. Cloke, P. B. Hitchcock, J. F. Nixon, D. M. Vickers, *C. R. Chim.* **2004**, *7*, 931.

[60] F. G. N. Cloke, P. B. Hitchcock, J. F. Nixon, D. M. Vickers, *J. Organomet. Chem.* **2001**, *635*, 212.

[61] a) M. Scheer, S. Deng, O. J. Scherer, M. Sierka, *Angew. Chem.* **2005**, *117*, 3821; b) M. Scheer, S. Deng, O. J. Scherer, M. Sierka, *Angew. Chem. Int. Ed.* **2005**, *44*, 3755.

[62] P. B. Hitchcock, M. J. Maah, J. F. Nixon, *Heteroat. Chem.* **1991**, *2*, 253.

[63] H. F. Dare, J. A. K. Howard, M. U. Pilotti, F. G. A. Stone, J. Szameitat, *Chem. Commun.* **1989**, 1409.

[64] J. Malberg, T. Wiegand, H. Eckert, M. Bodensteiner, R. Wolf, *Chem. Eur. J.* **2013**, *19*, 2356.

[65] J. Malberg, T. Wiegand, H. Eckert, M. Bodensteiner, R. Wolf, *Eur. J. Inorg. Chem.* **2014**, *2014*, 1638.

[66] C. Rödl, R. Wolf, *Eur. J. Inorg. Chem.* **2015**, n/a.

[67] a) J. Malberg, M. Bodensteiner, D. Paul, T. Wiegand, H. Eckert, R. Wolf, *Angew. Chem.* **2014**, *126*, 2812; b) J. Malberg, M. Bodensteiner, D. Paul, T. Wiegand, H. Eckert, R. Wolf, *Angew. Chem. Int. Ed.* **2014**, *53*, 2771.

[68] M. Scheer, *Dalton Trans.* **2008**, 4372.

[69] O. J. Scherer, H. Sitzmann, G. Wolmershäuser, *J. Organomet. Chem.* **1984**, *268*, C9.

[70] M. Eberl, PhD thesis, Regensburg (regensburg), **2011**.

[71] a) M. Scheer, G. Friedrich, K. Schuster, *Angew. Chem.* **1993**, *105*, 641; b) M. Scheer, G. Friedrich, K. Schuster, *Angew. Chem. Int. Ed.* **1993**, *32*, 593.

[72] O. J. Scherer, R. Winter, G. Wolmershäuser, *Z. Anorg. Allg. Chem.* **1993**, *619*, 827.

[73] F. Dielmann, PhD thesis, Regensburg **2011**.

[74] a) O. J. Scherer, T. Brück, *Angew. Chem.* **1987**, *99*, 59; b) F. Dielmann, R. Merkle, S. Heinl, M. Scheer, *Z. Naturforsch., Teil B* **2009**, *64*, 3.

[75] a) O. J. Scherer, H. Sitzmann, G. Wolmershäuser, *Angew. Chem.* **1985**, *97*, 358; b) O. J. Scherer, H. Sitzmann, G. Wolmershäuser, *Angew. Chem. Int. Ed.* **1985**, *24*, 351.

[76] a) J. Bai, E. Leiner, M. Scheer, *Angew. Chem.* **2002**, *114*, 820; b) J. Bai, E. Leiner, M. Scheer, *Angew. Chem. Int. Ed.* **2002**, *41*, 783.

[77] a) J. Bai, A. V. Virovets, M. Scheer, *Angew. Chem. Int. Ed.* **2002**, *41*, 1737; b) J. Bai, A. V. Virovets, M. Scheer, *Angew. Chem.* **2002**, *114*, 1808.

[78] a) B. P. Johnson, F. Dielmann, G. Balázs, M. Sierka, M. Scheer, *Angew. Chem.* **2006**, *118*, 2533; b) B. P. Johnson, F. Dielmann, G. Balázs, M. Sierka, M. Scheer, *Angew.*

Chem. Int. Ed. **2006**, *45*, 2473.

[79] a) M. Scheer, A. Schindler, C. Gröger, A. V. Virovets, E. V. Peresypkina, *Angew. Chem. Int. Ed.* **2009**, *48*, 5046; b) M. Scheer, A. Schindler, C. Gröger, A. V. Virovets, E. V. Peresypkina, *Angew. Chem.* **2009**, *121*, 5148; c) A. Schindler, C. Heindl, G. Balázs, C. Gröger, A. V. Virovets, E. V. Peresypkina, M. Scheer, *Chem. Eur. J.* **2012**, *18*, 829; d) V. Peresypkina Eugenia, C. Heindl, A. Schindler, M. Bodensteiner, V. Virovets Alexander, M. Scheer, in *Zeitschrift für Kristallographie - Crystalline Materials, Vol. 229*, **2014**, p. 735.

[80] N. G. Connelly, W. E. Geiger, *Chem. Rev.* **1996**, *96*, 877.

[81] M. Scheer, L. J. Gregoriades, M. Zabel, J. Bai, I. Krossing, G. Brunklaus, H. Eckert, *Chem. Eur. J.* **2008**, *14*, 282.

[82] L. J. Gregoriades, B. K. Wegley, M. Sierka, E. Brunner, C. Gröger, E. V. Peresypkina, A. V. Virovets, M. Zabel, M. Scheer, *Chemistry – An Asian Journal* **2009**, *4*, 1578.

[83] a) I. Krossing, I. Raabe, *Angew. Chem. Int. Ed.* **2004**, *43*, 2066; b) I. Krossing, I. Raabe, *Angew. Chem.* **2004**, *116*, 2116.

[84] a) I. Krossing, A. Reisinger, *Angew. Chem.* **2003**, *115*, 5903; b) I. Krossing, A. Reisinger, *Angew. Chem. Int. Ed.* **2003**, *42*, 5725.

[85] a) A. Reisinger, N. Trapp, I. Krossing, S. Altmannshofer, V. Herz, M. Presnitz, W. Scherer, *Angew. Chem. Int. Ed.* **2007**, *46*, 8295; b) A. Reisinger, N. Trapp, I. Krossing, S. Altmannshofer, V. Herz, M. Presnitz, W. Scherer, *Angew. Chem.* **2007**, *119*, 8445.

[86] I. Krossing, *Chem. Eur. J.* **2001**, *7*, 490.

[87] I. Krossing, *J. Am. Chem. Soc.* **2001**, *123*, 4603.

[88] a) C. Schwarzmaier, M. Sierka, M. Scheer, *Angew. Chem. Int. Ed.* **2013**, *52*, 858; b) C. Schwarzmaier, M. Sierka, M. Scheer, *Angew. Chem.* **2013**, *125*, 891.

[89] M. Scheer, L. J. Gregoriades, A. V. Virovets, W. Kunz, R. Neueder, I. Krossing, *Angew. Chem. Int. Ed.* **2006**, *45*, 5689.

[90] C. Heindl, S. Heinl, D. Lüdeker, G. Brunklaus, W. Kremer, M. Scheer, *Inorg. Chim. Acta* **2014**, *422*, 218.

[91] M. Fleischmann, F. Dielmann, L. J. Gregoriades, E. V. Peresypkina, A. V. Virovets, S. Huber, A. Y. Timoshkin, G. Balázs, M. Scheer, *Angew. Chem.* **2015**, *127*, 13303.

2 Research Objectives

Phosphaalkyne chemistry has always been an intriguing field in which many researchers have made an effort to push the limits of well-known reaction pathways with a class of substances previously belittled as a chemical curiosity. However, phosphaalkynes still remain exciting and from the state of information some major research objectives could be derived:

1 – Coordination Chemistry

As mentioned *vide supra*, the reaction of *tert*-butyl phosphaalkyne with CuI leads to the formation of a non-stoichiometric cage compound. Earlier results from our working group suggest that coordination to coinage metal salts with weakly coordinating anions typically results in different products than coordination to Lewis acids does. So, the question arose whether this could be confirmed for such a small molecule. Until now, complexes of phosphaalkynes have only been possible with stabilising ligands. Comparing the reaction of ethene and acetylene with $Ag[Al\{OC(CF_3)_3\}_4]$, we also tried to make homoleptic complexes of phosphaalkynes. In addition, the end-on coordination mode of the phosphaalkyne has been realised in the reaction with a cationic ruthenium complex.

2 – Polyphospholyl ligands

The exploration of new pathways to form polyphospholyl ligands from the reaction of *tert*-butyl phosphaalkyne with zintl ions has been a part of this thesis.

3 – Diphosphete complexes

1,3-diphosphete complexes have mostly been observed in an η^4 coordination mode with the 14 VE [CpM] fragment. As their isolobal cyclo-P_4 complexes are usually more versatile in their coordination ability, it was investigated whether reaction with suitable compounds leads to new coordination modes of the 1,3-diphosphete ligand. In another aspect, heteroleptic 1,3-diphosphete complexes have not been studied with respect to their redox activity. The competing pathways of oxidation and coordination have been explored with weakly coordinating coinage metal salts.

3 Naked Silver(I) coordinated by two Phosphaalkynes

Eva-Maria Rummel, Gábor Balázs, Alexander Virovets and Manfred Scheer

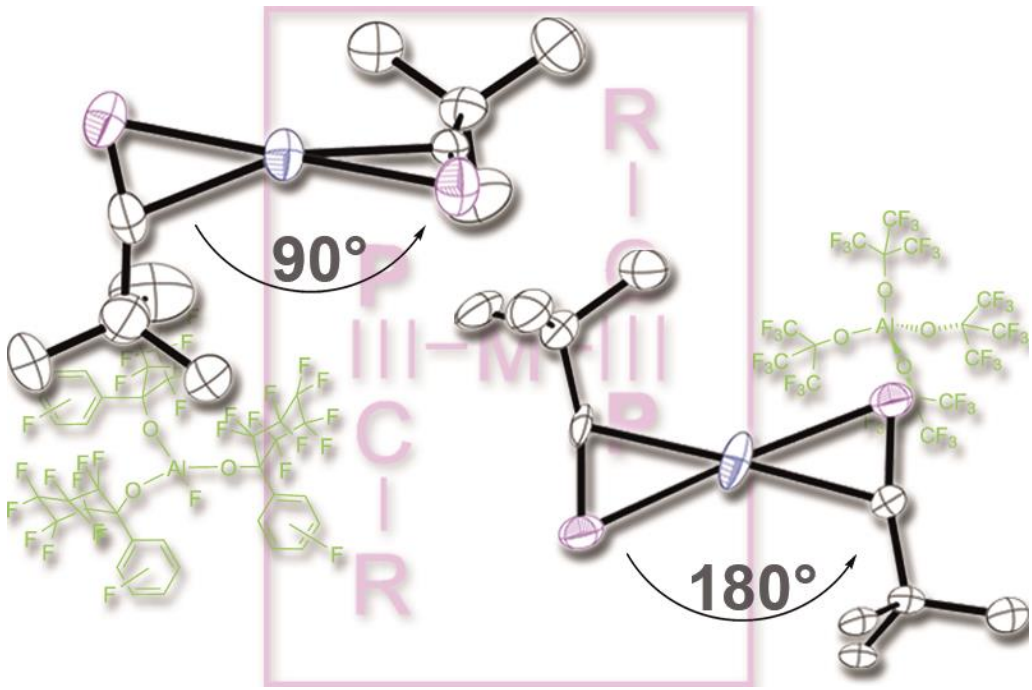

- ≡ Synthesis and characterisations of all compounds were performed by Eva-Maria Rummel
- ≡ DFT calculations were performed by Gábor Balázs
- ≡ Figures were made by Eva-Maria Rummel, except for Figure 3-21: Alexander Virovets
- ≡ X-ray measurements and calculations were done by Eva-Maria Rummel, except for final refinement of **3b**: Alexander Virovets
- ≡ Manuscript was written by Eva-Maria Rummel except DFT calculation part: Gábor Balázs and crystallographic details of **3b**: Alexander Virovets

Acknowledgement: Ag[fal] has been kindly provided by Luis Dütsch and Martin Fleischmann, University of Regensburg

3.1 Introduction

Employing the weakly coordinating anion silver salts $Ag[Al\{OC(CF_3)_3\}_4]$ and $Ag[FAl\{OC_{12}F_{15}\}_3]$, two phosphaalkynes could be coordinated to a naked silver(I) centre to form the first examples of homoleptic complexes $[Ag(\eta^2\text{-}PC\textit{t}Bu)_2][Al\{OC(CF_3)_3\}_4]$ (**1**) and $[Ag(\eta^2\text{-}PC\textit{t}Bu)_2][FAl\{OC_{12}F_{15}\}_3]$ (**2**), respectively. DFT calculations show that the perpendicular arrangement of the phosphaalkynes in **2** represents minimum energy structure of two phosphaalkynes coordinated to a silver atom, whereas for **1** a unprecedented square planar coordination mode of the phosphaalkynes was found. Reactions with additional donors lead to the trigonally planar coordinated silver salts $[((CH_3)_2CO)Ag(\eta^2\text{-}PC\textit{t}Bu)_2]^+[FAl\{OC_{12}F_{15}\}_3]^-$ (**3a**) and $[(C_7H_8)_2Ag(\eta^2\text{-}PC\textit{t}Bu)]^+[FAl\{OC_{12}F_{15}\}_3]^-$ (**3b**). All compounds have been comprehensively characterised in solution and in the solid state.

The lasting interest in alkylidenephosphane (phosphaalkyne) chemistry can be attributed to the diversity of reactions which are possible with this class of compounds. Cycloadditions[1] and formation of cage-like moieties[2] are possible as well as mere coordination to metal fragments via different coordination modes: The firstly isolated[3] and most widely used representative of this species, the *tert*-butylphosphaalkyne, has been shown to exhibit side-on coordination reactivity just as the isolobal relationship to alkynes suggests (Scheme 3-1).[4]

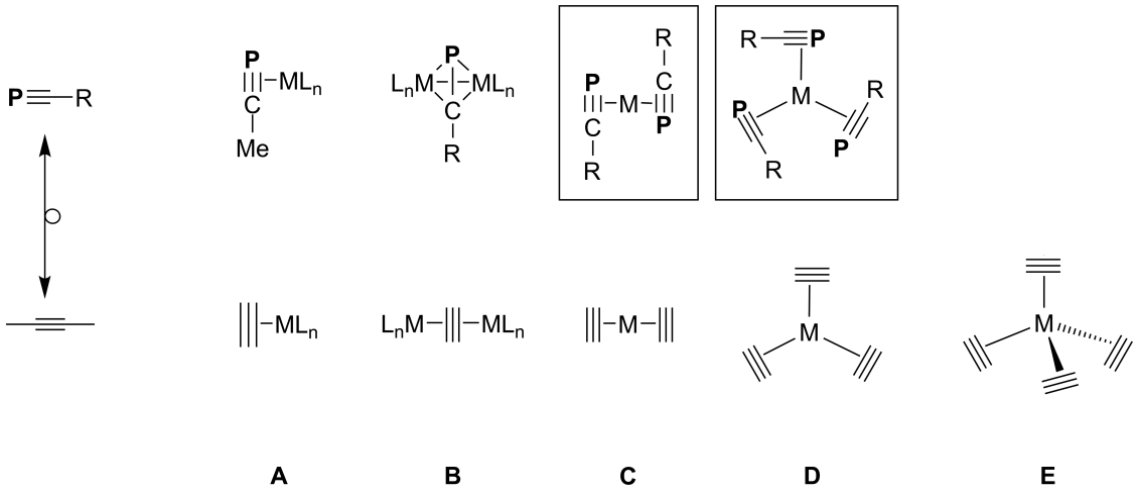

Scheme 3-1. Isolobal relationship between phosphaalkynes and alkynes. Possible side-on coordination modes for phosphaalkynes and alkynes in the coordination towards a metal atom supported by ligands (**A+B**) or side-on coordination towards naked metal atoms (**C-E**).

The side-on coordination (type **A**) of the PC-triple bond towards metal centres is one of the more common reactions[5] due to the electronic nature of the triple bond,[6] because of the HOMO which represents the π-orbital of the triple bond. However, the largest number of reported complexes shows a side-on coordination of the phosphaalkyne in bimetallic

complexes resulting in a tetrahedrane structure (type **B**).[5a, 7] All complexes of types **A** and **B** reported have in common that they are only known for ligand supported metal complexes. Homoleptic phosphaalkyne complexes of type **C** and **D** are not known so far. Since phosphaalkynes are isolobal to alkynes, it is of interest how alkynes behave in homoleptic complexes. Homoleptic silver(I) complexes of acetylene have been calculated theoretically as early as 1988,[8] but only in 2007 the group of Krossing reported on a successful synthesis of $[Ag(C_2H_2)_3]^+$ (type **D**) and $[Ag(C_2H_2)_4]^+$ (type **E**).[9] The formation of these two silver complexes has only been possible due to the use of the weakly coordinating anion (WCA) $[Al\{OC(CF_3)_3\}_4]^-$ (pftb). The same report states that the slightly more coordinating anion $[Al\{OC(CH_3)(CF_3)_2\}_4]^-$ is also able to stabilise $[Ag(C_2H_2)]^+$. These big WCAs are able to stabilise cations by considerable separation and thus create "pseudo gas-phase conditions".[10] The type **C** silver complex $[Ag(C_2H_2)_2]^+$ has been calculated and verified by high pressure mass spectrometry,[11] but no structural characterisation has been reported yet. However, computational analyses of complex $[Ag(\eta^2\text{-}C_2H_2)_2][pftb]$ predict a complexation energy of -151.5 kJ mol^{-1} (MP2/TZVPP level calculations), indicating those complexes should be accessible experimentally.[9] Therefore the question arises whether phosphaalkynes are also able to coordinate in a similar fashion and if so, how many of them can be coordinated to a WCA salt of silver (I). Here, we present the first examples of side-on coordinated homoleptic phosphaalkyne complexes.

3.2 Results and Discussion

To investigate the possible outcome of the reaction of $[Ag(P{\equiv}C\textit{t}Bu)_{n-1}]^+$ (n = 1-3) with P≡C*t*Bu, we conducted DFT calculations at the B3LYP/def2-TZVP level of theory for the gas phase. These calculations show that the coordination of one molecule of *t*BuC≡P to a hypothetical $[Ag(CH_2Cl_2)_2]^+$ ion by the substitution of a CH_2Cl_2 ligand and formation of $[Ag(P{\equiv}C\textit{t}Bu)(CH_2Cl_2)]^+$ is exothermic (–55.46 kJ·mol^{-1}). The substitution of the remaining CH_2Cl_2 ligand in $[Ag(P{\equiv}C\textit{t}Bu)(CH_2Cl_2)]^+$ by a second *t*BuC≡P is exothermic as well by –48.66 kJ·mol^{-1}. The resulting complex $[Ag(P{\equiv}C\textit{t}Bu)_2]^+$ (type **C**) should thus be accessible. For this complex, two possible arrangements of the phosphaalkyne ligands coordinating to the silver atom have been considered: a quadratic planar arrangement with *trans* geometry of the phosphaalkynes and a tetrahedral arrangement. Here, the tetrahedral coordination represents the minimum energy structure. The calculated structure with coplanar C≡P units lies higher in energy by only 4.26 kJ·mol^{-1}.The further addition of a third *t*BuC≡P ligand to $[Ag(P{\equiv}C\textit{t}Bu)_2]^+$ forming $[Ag(P{\equiv}C\textit{t}Bu)_3]^+$ is exothermic in the gas phase (–26.09 kJ·mol^{-1}) but also inhibited by entropy at room temperature: The Gibbs free energy is positive at room temperature and

becomes negative below T = 233 K (see SI), which indicates that the hypothetical complex $[Ag(P{\equiv}C\textit{t}Bu)_3]^+$ should only be stable below this temperature.

Conducting the reaction of *tert*-butylphosphaalkyne with Ag[A] (A = $[Al\{OC(CF_3)_3\}_4]$ (pftb), $[AlF\{OC_{12}F_{15}\}_3]$ (fal)] in dichloromethane at low temperatures leads to the formation of homoleptic complexes of the general formula $[Ag(P{\equiv}C\textit{t}Bu)_2]^+[A]^-$ (A = pftb (**1**); fal (**2**)) (equation (3-1)). In both complexes the phosphaalkyne ligands are coordinating in a side-on fashion to the silver cation. Interestingly, while in **1** a square planar trans-coordination is accomplished, the two phosphaalkyne ligands in **2** are coordinating the silver cation in a tetrahedral fashion.

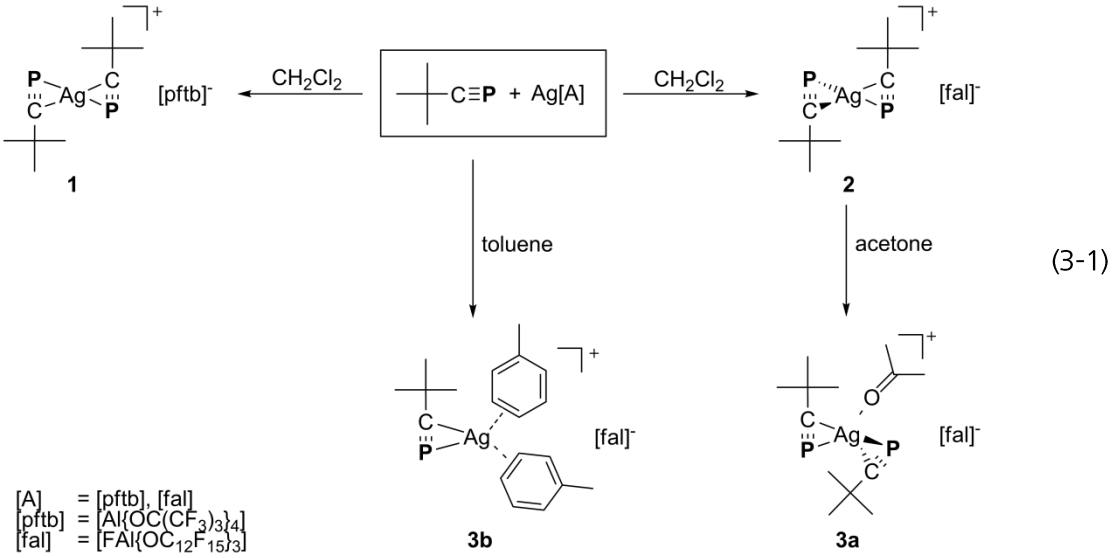

(3-1)

The presence of weakly coordinating anions are clearly crucial for this reaction, as no other silver(I) salt with other anions (like BF_4^-, PF_6^- or SbF_6^-) reacted with *t*BuC≡P in a similar fashion. Those reactions lead to the formation of a silver mirror and a mixture of (possibly) oxidation products of the phosphaalkyne which could not be separated or characterised regardless of numerous attempts.[12] Ag[pftb] on the other hand is known to stabilize reactive molecules such as white phosphorus[13] and yellow arsenic,[14] making it possible to store both over longer periods in the solid state and make them available for subsequent reactions.[15]

In a subsequent reaction (also eq. (3-1)), adding a donor to **2** leads to a change of geometry on the metal centre.[16] Here, trigonally planar heteroleptic complexes of silver(I) can be isolated. Exemplified for the donor acetone, one ligand is added to the complex forming $[((CH_3)_2CO)Ag(P{\equiv}C\textit{t}Bu)_2]^+[fal]^-$ (**3a**). Furthermore, conducting the reaction in toluene leads to the formation of the trigonal planar complex $[(C_7H_8)_2Ag(P{\equiv}C\textit{t}Bu)]^+[fal]^-$ (**3b**) and $[Ag(C_7H_8)_3]^+[fal]^-$. All compounds could be crystallized from diffusion of *n*-hexane into a dichloromethane solution.

Compound **1** and **2** form colourless crystals which also can be stored at room temperature under inert atmosphere without losing their crystallinity. Exposure to light for more than two hours, however, leads to decomposition of the silver complexes and formation of a silver mirror. X-ray structure analysis of **1** and **2** shows the two phosphaalkynes coordinated to the naked silver(I) centre in a side-on fashion. The main difference here is that while the silver atom in **1** is coordinated in a trans-fashion by the coplanar phosphaalkynes (Figure 3-1 left), in **2** the phosphaalkynes are coordinating the silver centre tetrahedrally (cf. Figure 3-1 right).

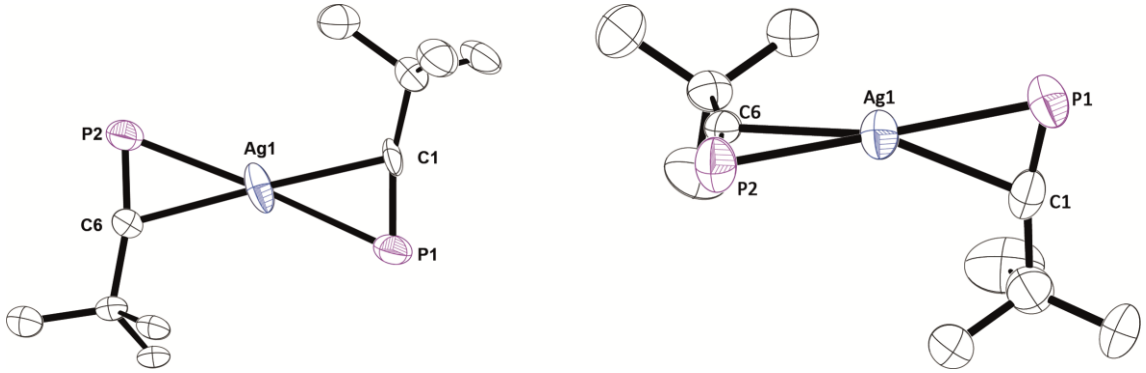

Figure 3-1 **Left**: Molecular structure of cation of **1** in the solid state. Hydrogen atoms and disorder of one *t*Bu-group (linked to C6) are omitted for clarity. Thermal ellipsoids are shown at 50% probability level. Selected bond distances [Å] and angles [°]: Ag1-P1 2.523(6), Ag1-P2 2.501(6), Ag1-C1 2.353(17), Ag1-C6 2.355(18), Ag1-(P1-C1)$_{cent}$ 2.313, Ag1-(P2-C6)$_{cent}$ 2.305, P1-C1 1.58(2), P2-C6 1.513(19); P2-Ag1-P1 175.5(2), C1-Ag1-P1 37.7(5), C1-Ag1-C6 177.3(8), C6-Ag1-P2 36.2(5), (P1-C1)$_{cent}$-Ag1-(P2-C6)$_{cent}$ 176.9. **Right:** Molecular structure of cation **A** of **2** in the solid state (66% occupation). Hydrogen atoms are omitted for clarity. Thermal ellipsoids are shown at 50% probability level. Selected bond distances [Å] and angles [°]: Ag1-P1 2.501(3), Ag1-C1 2.338(9), P1-C1 1.549(11), Ag1-P2 2.4975(18), Ag1-C6 2.333(5), P2-C6 1.561(6), P1-Ag1-P2 157.56(8), C1-Ag1-C6 144.6(3), C1-Ag1-P1 37.1(3), C6-Ag1-P2 37.18(14), C1-Ag1-P2 148.4(2), P1-C1-C2 166.9(7), P2-C6-C7 168.5(5), (P1-C1)$_{cent}$-Ag1-(P2-C6)$_{cent}$ 176.9.164.46.

In both cations, the P-C bonds are triple bonds with distances of P1-C1 and P2-C6 of **1**: 1.58(2) Å and 1.513(19) Å, **2**: 1.549(11) and 1.561(6). These are in good agreement with the triple bond distances in free *t*BuC≡P (photoelectron spectra: d = 1.536(2) Å,[5b] X-ray structure: d = 1.542(2) Å[17]). The P-C-C angles in both compounds are near 180°, also confirming a sp hybridized C atom. Slight deviations in the bond length spring from the coordination to the silver(I) centre. The cation in **2** is disordered; in Figure 3-1 (right) only molecule **A** with 66% occupation is shown. Both molecules present in the cationic part of **2** are tetrahedrally coordinating the silver centre (for a complete representation see SI). As the tetrahedrally coordinated silver cation in **2** represents the calculated minimum structure, hirshfeld surface plots have been produced[18] to receive information about possible contacts between the anions and cations in **1** and **2** (see SI). Although the nearly spherical [pftb] anions in **1** provide only enough space for the *t*BuC≡P ligand to coordinate in a square planar fashion to the silver cation, no contacts between the hirshfield surface of the [pftb] anion and the cation could be observed. In **2**, the bigger [fal] anions (which are shaped more squarely) provide a suitable

cavity for the tetrahedral arrangement of the *t*BuC≡P ligands in **2** which also displays contacts between the hydrogen atoms of the cationic part and fluorine atoms of the anionic part in the solid state. The size of the anion in compounds **1** and **2** thus has a direct influence on the geometry of the cation.

The silver cations are slightly shifted towards the more electronegative carbon atoms in the PC triple bond. In **1**, the perpendicular from silver onto the C≡P bond cuts the bond (d(PC) = 1.58(2) Å) at 0.53 Å and in **2** at 0.52 Å (d(PC) = 1.549(11) Å). Recently, Russel and coworkers reported about heteroleptic gold complexes [*t*Bu$_2$P(o-biphenyl)Au(RC≡P)][SbF$_6$] (R= *t*Bu, Ad). In these complexes, also slippage of the gold atom from the midpoint of the carbon phosphorus bond towards the negatively charged carbon atom was observed.[5h]

The reaction of **2** with donors has been exemplified in the reaction with acetone, which is added to the silver atom resulting in the trigonal planar complex **3a** (Figure 3-2 left). Conducting the reaction of Ag[fal] with *t*BuC≡P in a mixture of CH_2Cl_2 and toluene leads to the formation of trigonal planar **3b** as well as $[Ag(C_7H_8)_3]^+[fal]^-$. Being isostructural, these two complexes co-crystallise as a solid solution. The crystallographic data for the single crystal studied suggests the chemical composition $[Ag(C_7H_8)_2(P{\equiv}C\textit{t}Bu)]_{0.6}[Ag(C_7H_8)_3]_{0.4}[fal]$. Two sorts of cations statistically take the same crystallographic position resulting in the partial overlap of P≡C*t*Bu and toluene ligands. Because of this, anisotropic refinement on the phosphaalkyne moiety has not been possible (cf. Figure 3-2 right).

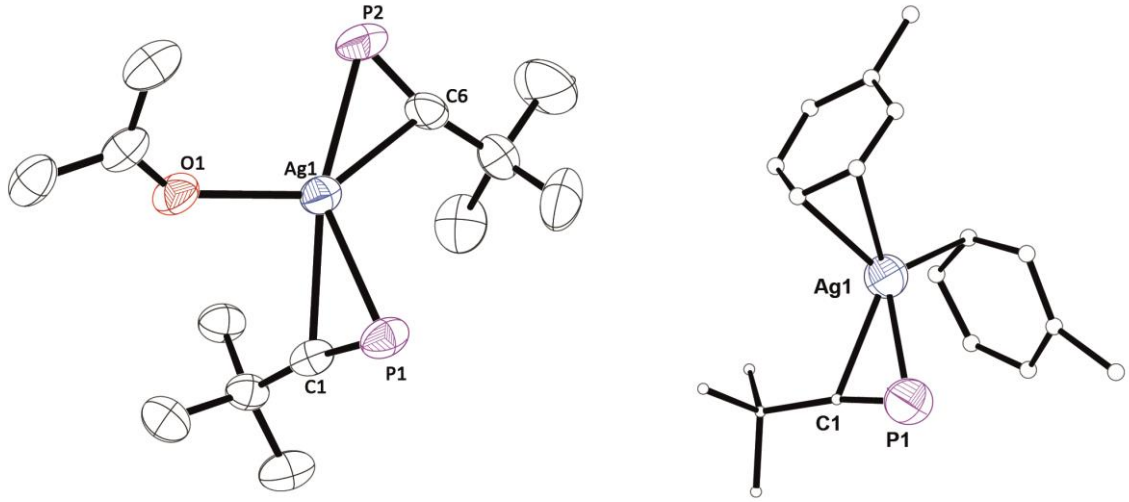

Figure 3-2 **Left:** Molecular structure of the cation of **3a** determined by X-ray crystallography. Hydrogen atoms are omitted for clarity. Thermal ellipsoids are shown at 50% probability level. Selected bond lengths [Å] and angles [°]: Ag1-P1 2.5724(12), Ag1-P2 2.4879(14), Ag1-O1 2.323(3), Ag1-C1 2.497(4), Ag1-C6 2.363(5), P1-C1 1.556(5), P2-C6 1.564(5), P1-C1-C2 170.1(3), P2-C6-C7 165.2(4). **Right:** Schematic molecular structure of the cation of **3b** in the solid state. Hydrogen atoms are omitted for clarity. Thermal ellipsoids are shown at 50% probability level, carbon atoms are shown in ball-and-stick model. Selected bond lengths [Å] and angles [°]: Ag1-C1 2.464(12)-2.498(12), Ag1-P1 2.543(3)-3.017(4), C-C1-P1 170.0(9).

The phosphorus carbon bonds in **3a** correspond to PC triple bonds with 1.556(5) and 1.564(5) Å. The silver phosphorus distances are in the same range as in **1** and **2**. These results show that indeed a trigonally planar coordination of the silver atom can be achieved and the space should be big enough for a third molecule of *t*BuC≡P.

DFT calculations show that the gas phase reaction energy of the reaction of $[Ag(P{\equiv}C\textit{t}Bu)_2]^+$ with acetone, leading to $[((CH_3)_2CO)Ag(P{\equiv}C\textit{t}Bu)_2]^+$ is negative (–48.73 kJ·mol^{-1}). Moreover, the Gibbs free energy of the reaction at room temperature is negative (ΔG^{300} = –2.66 kJ·mol^{-1}), indicating the complex should form spontaneously at room temperature. Furthermore, the substitution of a toluene ligand in $[Ag(C_7H_8)_3]^+$ by a *t*BuC≡P molecule to form $[Ag(C_7H_8)_2(P{\equiv}C\textit{t}Bu)]^+$ is exothermic (–15.37 kJ·mol^{-1}) and the Gibbs free energy is negative (see SI).

In the $^{31}P\{^1H\}$ NMR spectra of all isolated products in CD_2Cl_2, the chemical shift of the phosphaalkynes is almost the same or only slightly high field shifted in comparison to free phosphaalkyne (δ [ppm] = **1**: -66.5, **2**: -69.2, **3a**: -69.9, **3b:** -79.6, **free**: -69.2).[3] This points to a weak π-interaction between the phosphaalkyne and the silver cation in solution. Interestingly, at high concentrations of **1** in CD_2Cl_2, a broad signal is revealed slightly high field shifted, which is also present in VT NMR studies following the formation of **1** (see Figure 3) and **2** (see SI) with a slight excess of *t*BuC≡P.

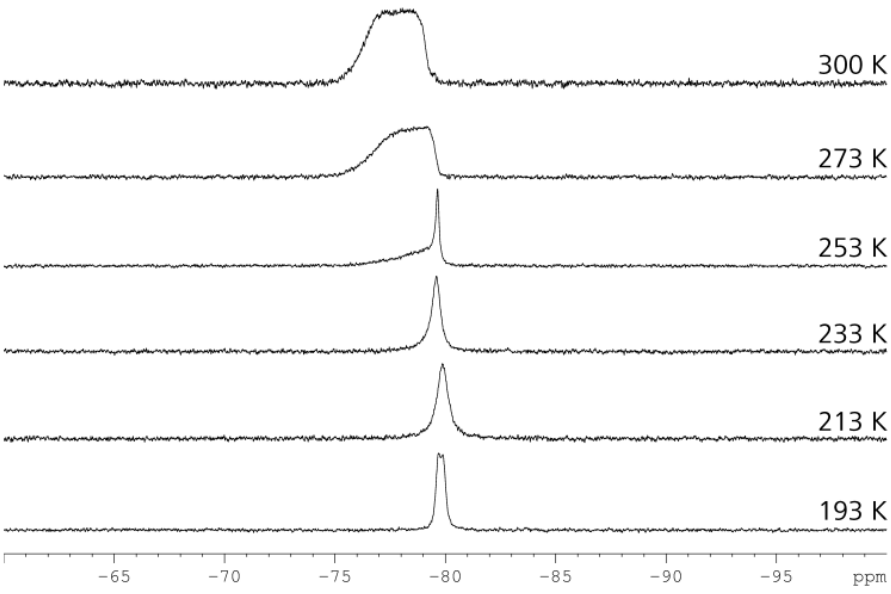

Figure 3-3 VT $^{31}P\{^1H\}$ NMR spectra of **1**, 193 K → r.t.; A broadening of the peak could be observed for a concentration of $3{\cdot}10^{-2}$ mol·l^{-1}.

The NMR spectrum of **1** at 193 K shows a signal with a very small splitting of 32.7 Hz. However, no evidence for the theoretically possible $[Ag(P{\equiv}C\textit{t}Bu)_3]^+$ cation could be found at temperatures below 233 K, where this complex should be stable according to the calculations

mentioned above. The most interesting observation, however, was a broadening of the peak starting at 253 K, leading to a r.t. signal at δ = -78 ppm with $\omega_{1/2}$ = 65.2 Hz. This indicates a strong (and fast) intermolecular exchange of the *t*BuC≡P between neighbouring complexes (see eq. (3-2)) in addition to the possible rotation of the *t*BuC≡P ligand around the $(PC)_{cent}$-Ag bond axis. To support this assumption, the same sample has been diluted to $c = 1.6 \cdot 10^{-2}$ mol·l^{-1}, where again a sharp singlet at δ = -66.5 ppm could be observed at room temperature, so obviously no intermolecular dynamics are happening in diluted solution. The high field shifted, broad peak is not only present when an excess of *t*BuC≡P is available (as is the case in the formation process), but also when the concentrated of **1** in CD_2Cl_2 is high enough.

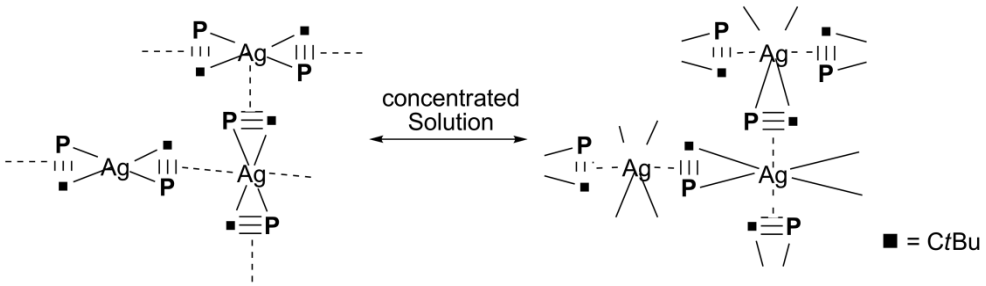

(3-2)

Adding further equivalents of phosphaalkyne to solutions of **1** at low temperatures also leads to the same ^{31}P NMR shifts both at r.t. and low temperatures. The formation of complexes with three equivalents of *t*BuC≡P thus could not be observed. Additionally, samples of **1** are synthesised using an excess of *t*BuC≡P to obtain higher yields of the product. For all stoichiometries used, X-ray crystallographic investigations only showed the formation of **1**.

As the ligands are only weakly bound to the silver(I) cation, no molecular peaks could be detected in ESI-MS spectra, due to the easy fragmentation in the gas phase. This shows the labile nature of this type of complexes. However, upon addition of acetonitrile, different MeC≡N complexes of Ag^+ could be verified in the spectra. MeC≡N as a stronger donor completely replaces the phosphaalkyne bound to the silver centre.

Additionally, IR spectra were recorded in the solid state. However, the expected C≡P absorption bands are obscured by the C-F vibrations of the anions. This is also confirmed by DFT calculations. Furthermore these calculations indicate that the ν_{CP} stretching band is considerably coupled with the δ_C vibrations of the *t*Bu group. For example, for **1** the vibrations at 1481 cm^{-1} and 1528 cm^{-1} contain the major $\nu_{P\equiv C}$ contribution (cf. SI).

3.3 Conclusions

In conclusion, we could isolate the first homoleptic complexes of phosphaalkynes bound to a "naked" metal centre without any additional ligands. Here, the two phosphaalkynes bind in a side-on coordination to the metal centre to form $[Ag(P{\equiv}C\textit{t}Bu)_2]^+[pftb]^-$ (**1**) and $[Ag(P{\equiv}C\textit{t}Bu)_2]^+[fal]^-$ (**2**). The use of the WCA [pftb] and [fal] has been crucial as no similar compounds could be isolated in the reactions of *t*BuC≡P and Ag(I) salts of smaller anions. The difference between the cations in **1** and **2** is the orientation of the phosphaalkynes in the solid state: While in **1** the silver atom is coordinated by the two phosphaalkynes in a square planar fashion, in **2** the phosphaalkynes are coordinating tetrahedrally to the silver atom, which is also the minimum energy point as disclosed by DFT calculations. NMR spectroscopic investigations for **1** show a dependency on concentration in solution. An intermolecular substitution of ligands between the silver atoms can be postulated at high concentrations, while diluted solutions do not show this exchange of ligands. By adding donor ligands to **2**, the formation of the trigonally planar complexes $[((CH_3)_2CO)Ag(P{\equiv}C\textit{t}Bu)_2]^+[fal]^-$ (**3a**) can be observed. Conducting the reaction of Ag[fal] and *t*BuC≡P in toluene another trigonally planar heteroleptic complex $[(C_7H_8)_2Ag(P{\equiv}C\textit{t}Bu)]^+[fal]^-$ (**3b**) could be obtained. All complexes could also be verified spectroscopically and by X-ray crystallography.

3.4 Supporting Information

3.4.1 Experimental

All steps were performed under an atmosphere of dry argon with standard Schlenk techniques. All solvents were freshly collected from a Solvent Purification System by M. Braun and were degassed prior to use. All NMR spectra have been recorded using deuterated Dichloromethane, which was dried over CaH_2 and distilled under inert atmosphere. *t*BuC≡P,[3] Ag[pftb][19] and Ag[fal][20] were synthesised according to literature procedures.

Synthesis of 1

A solution of $8.6 \cdot 10^{-5}$ mol Ag[pftb] in 5 ml Dichloromethane is cooled to -80 °C. To this solution, $8.6 \cdot 10^{-4}$ mol *t*BuC≡P is added at -80 °C and the reaction mixture is stirred over night to reach room temperature. The solvent and residual *t*BuC≡P are removed under reduced pressure and the residue is taken up in 3 ml fresh Dichloromethane. The solution is filtered via cannula, layered under 10 ml of hexane and stored at -30 °C. After 48h, colourless crystals of **1** can be found at the solvent boundary.

It should be noted that the product can also be obtained by reacting Ag[pftb] and *t*BuC≡P in the right stoichiometry (1:2). Some samples were crystallized by diffusion of toluene into CH_2Cl_2.

Crystalline yield: 48 mg (44 %)

Powder can be isolated in 89% yield after drying the solution in vacuo for 2 h.

^{1}H-NMR	δ [ppm] = 1.50 (s, (C<u>H</u>$_3$)$_3$CCP)
^{31}P-NMR	δ [ppm] = -66.5 (s)
^{31}P{^{1}H}-NMR	δ [ppm] = -66.5 (s)
^{19}F{^{1}H}-NMR	δ [ppm] = -75.5 (s)
^{13}C{^{1}H}-NMR	δ [ppm] = 32.6 (d, $^{2}J_{CP}$ = 5.7 Hz, (<u>C</u>H$_3$)$_3$CCP), 121.6 (q, $^{1}J_{CF}$ = 293.1 Hz, Al((OC(<u>C</u>F)$_3$)$_3$)$_4$),
Cation ESI-MS (CH_2Cl_2)	no peaks with reasonable composition detectable. Silver(I) is found upon addition of acetonitrile.
Anion ESI-MS (CH_2Cl_2)	*m/z* [%] = 967.2 (100) $[AlO_4C_{16}F_{36}]^-$
IR (KBr)	v [cm^{-1}] = 2971 (w), 2360 (w), 1626 (vw), 1475 (vw), 1354 (m), 1303 (m), 1221 (m), 974 (m), 833 (w), 728 (m)
Raman (CH_2Cl_2)	v [cm^{-1}] = 2982 (m), 2925 (m), 1482 (vs), 1445 (m), 1427 (m), 1380 (s), 817 (m), 787 (m), 736 (m), 616 (m), 529 (m), 311 (m)
Elemental analysis	calculated for $C_{26}H_{18}P_2AgAlO_4F_{36} \cdot CH_2Cl_2$ (1317.62 g·mol^{-1}): C 23.84, H 1.48; found: C 23.85, H 1.98

Synthesis of 2

A solution of $9.6 \cdot 10^{-5}$ mol Ag[fal] in 5 ml CH_2Cl_2 is cooled to -80 °C. To this solution, $4.8 \cdot 10^{-4}$ mol *t*BuC≡P is added at r.t. and the solution is stirred for an hour while the colour changes to light yellowish. The solution is layered with 10 ml of hexane and stored at -30 °C. After 12 h, colourless crystals of **2** can be found at the solvent boundary.

Yield: 65 mg (40 %) crystalline yield

^{1}H-NMR	δ [ppm] = 1.49 (s, (C$\underline{H}_3$)$_3$CCP, 18 H)
^{31}P-NMR	δ [ppm] = -69.2 (s)
^{31}P{^{1}H}-NMR	δ [ppm] = -69.2 (s)
^{19}F-NMR	δ [ppm] = -112.6 (d, $J_{F,F}$ = 284 Hz, 2F), -117.2 (d, $J_{F,F}$ = 280 Hz, 2F), -121.9 (d, $J_{F,F}$ = 280 Hz, 2F), -128 (s, 2F), -130.8 (d, $J_{F,F}$ = 280 Hz, 2F), -137.2 (d, $J_{F,F}$ = 280 Hz, 2F), -141.4 (d, $J_{F,F}$ = 280 Hz, 1F), -154.2 (t, $J_{F,F}$ = 20 Hz, 1F), -158.8 (t, $J_{F,F}$ = 18 Hz, 1F), -164.6 (t, $J_{F,F}$ = 18 Hz, 1F), -17.8 ppm (s, AlF)
^{19}F{^{1}H}-NMR	δ [ppm] = -112.6 (d, $J_{F,F}$ = 284 Hz, 2F), -117.2 (d, $J_{F,F}$ = 280 Hz, 2F), -121.9 (d, $J_{F,F}$ = 280 Hz, 2F), -128 (s, 2F), -130.8 (d, $J_{F,F}$ = 280 Hz, 2F), -137.2 (d, $J_{F,F}$ = 280 Hz, 2F), -141.4 (d, $J_{F,F}$ = 280 Hz, 1F), -154.2 (t, $J_{F,F}$ = 20 Hz, 1F), -158.8 (t, $J_{F,F}$ = 18 Hz, 1F), -164.6 (t, $J_{F,F}$ = 18 Hz, 1F), -17.8 ppm (s, AlF)
Cation ESI-MS (CH_2Cl_2)	no peaks with reasonable composition detectable. Silver(I) is found upon addition of acetonitrile: 189.1 (10) [$Ag(CH_3CN)_2$]
Anion ESI-MS (CH_2Cl_2)	*m/z* [%] = 1380.74 (100) [$AlO_3C_{36}F_{46}$]$^-$
IR (solid)	v [cm^{-1}] = 2978 (w),2919 (w), 1652 (m). 1532 (m), 1481 (s), 1367 (m), 1201 (s), 952 (s)
Elemental analysis	calculated for $C_{46}H_{18}P_2AgAlO_3F_{46}$ (1687.88 g·mol^{-1}): C 32.70, H 1.07; found: C 32.80, H 1.20

Synthesis of 3a

A solution of $9.6 \cdot 10^{-5}$ mol Ag[fal] in 5 ml CH_2Cl_2 is cooled to -80 °C. To this solution, $4.8 \cdot 10^{-4}$ mol *t*BuC≡P and $9.6 \cdot 10^{-5}$ mol acetone are added at -80 °C and the reaction mixture is stirred to reach r.t.. After this, the formation of a black precipitate can be observed. The solution is filtered via cannula, layered with 10 ml of hexane and stored at -30 °C. After 24h, colourless to light yellowish crystals of **3a** can be found at the solvent boundary.

Yield: 60 mg (36 %)

^{1}H-NMR	δ [ppm] = 1.50 (s, (C$\underline{H}_3$)$_3$CCP, 18 H), 2.26 ((CH$_3$)$_2$CO, 3H)
^{31}P-NMR	δ [ppm] = -69.9 (s)
^{31}P{^{1}H}-NMR	δ [ppm] = -69.9 (s)
^{19}F-NMR	δ [ppm] = −112.6 (d, $J_{F,F}$ = 280 Hz, 2F), −117.2 (d, $J_{F,F}$ = 279 Hz, 2F), −121.9 (d, $J_{F,F}$ = 277 Hz, 2F), −127.9 (s, 2F), −130.7 (d, $J_{F,F}$ = 275 Hz, 2F), −137.4 (d, $J_{F,F}$ = 276 Hz, 2F), −140.7 (d, $J_{F,F}$ = 277 Hz, 1F), −158.8 (dd, $J_{F,F}$ = 22 Hz, 1F), −164.9 (dd, $J_{F,F}$ = 18 Hz, 1F), −172.1 ppm (s, AlF)
^{19}F{^{1}H}-NMR	δ [ppm] = −112.6 (d, $J_{F,F}$ = 280 Hz, 2F), −117.2 (d, $J_{F,F}$ = 279 Hz, 2F), −

	121.9 (d, $J_{F,F}$ = 277 Hz, 2F), −127.9 (s, 2F), −130.7 (d, $J_{F,F}$ = 275 Hz, 2F), −137.4 (d, $J_{F,F}$ = 276 Hz, 2F), −140.7 (d, $J_{F,F}$ = 277 Hz, 1F), −158.8 (dd, $J_{F,F}$ = 22 Hz, 1F), −164.9 (dd, $J_{F,F}$ = 18 Hz, 1F), −172.1 ppm (s, AlF)
Cation ESI-MS (CH_2Cl_2)	no peaks with reasonable composition detectable. Silver(I) is found upon addition of acetonitrile: 271.4 (100)[$Ag(CH_3CN)_4$]
Anion ESI-MS (CH_2Cl_2)	*m/z* [%] = 1380.6 (100) $[AlO_3C_{36}F_{46}]^-$
IR (solid)	v [cm^{-1}] = 2984 (w),2923 (w), 1945 (m). 1844 (m) 1687 (m), 1652 (m), 1531 (m), 1482 (s), 1366 (m), 1200 (s), 952 (s)
Elemental analysis	calculated for $C_{49}H_{24}P_2AgAlO_4F_{46}$ (1745.92 g·mol^{-1}): C 33.67, H 1.38; found: C 33.58, H 1.55

Synthesis of 3b

A solution of $5 \cdot 10^{-3}$ mol (78 mg) Ag[fal] in a mixture of 1 ml CH_2Cl_2 and 4 ml toluene is stirred at r.t. To this solution, $1 \cdot 10^{-4}$ mol (V = 0.2 ml, c = 0.5 mol/L in toluene) *t*BuC≡P are added and the reaction mixture is stirred for half an hour. The solution is filtered via cannula, layered with 20 ml of hexane and stored at 5°C. After 24h, colourless to light yellowish crystals of **3b** can be found at the solvent boundary.

Yield: 50 mg (54 %)

^{1}H-NMR	δ [ppm] = 1.41 (s, $(C\underline{H}_3)_3CCP$, 18 H), 2.39 (s, $C_6H_5CH_3$, 64 H), 7.3 (m, $C_6H_5CH_3$, 88 H)
^{31}P-NMR	δ [ppm] = -79.7 (s)
^{31}P{^{1}H}-NMR	δ [ppm] = -79.7 (s)
^{19}F-NMR	δ [ppm] = -112.6 (d, $J_{F,F}$ = 276 Hz, 2F), -117.2 (d, $J_{F,F}$ = 276 Hz, 2F), -122 (d, $J_{F,F}$ = 276 Hz, 2F), -128 (s, 2F), -130.8 (d, $J_{F,F}$ = 276 Hz, 2F), -136.3 (d, $J_{F,F}$ = 280 Hz, 2F), -141.4 (d, $J_{F,F}$ = 276 Hz, 1F), -154.2 (pt, $J_{F,F}$ = 23.3 Hz, 1F), -164.8 (br, 1F), -172.1 ppm (s, AlF)
^{19}F{^{1}H}-NMR	δ [ppm] = -112.6 (d, $J_{F,F}$ = 276 Hz, 2F), -117.2 (d, $J_{F,F}$ = 276 Hz, 2F), -122 (d, $J_{F,F}$ = 276 Hz, 2F), -128 (s, 2F), -130.8 (d, $J_{F,F}$ = 276 Hz, 2F), -136.3 (d, $J_{F,F}$ = 280 Hz, 2F), -141.4 (d, $J_{F,F}$ = 276 Hz, 1F), -154.2 (pt, $J_{F,F}$ = 23.3 Hz, 1F), -164.8 (br, 1F), -172.1 ppm (s, AlF)
Cation ESI-MS (CH_2Cl_2)	no peaks with reasonable composition detectable. Silver(I) is found upon addition of acetonitrile: 147.7 (100) [$Ag(CH_3CN)$], 270.8 (40) [$Ag(CH_3CN)_4$]
Anion ESI-MS (CH_2Cl_2)	*m/z* [%] = 1381.2 (100) $[AlO_3C_{36}F_{46}]^-$

3.4.2 Spectra

3.4.2.1 NMR Spectra of 1

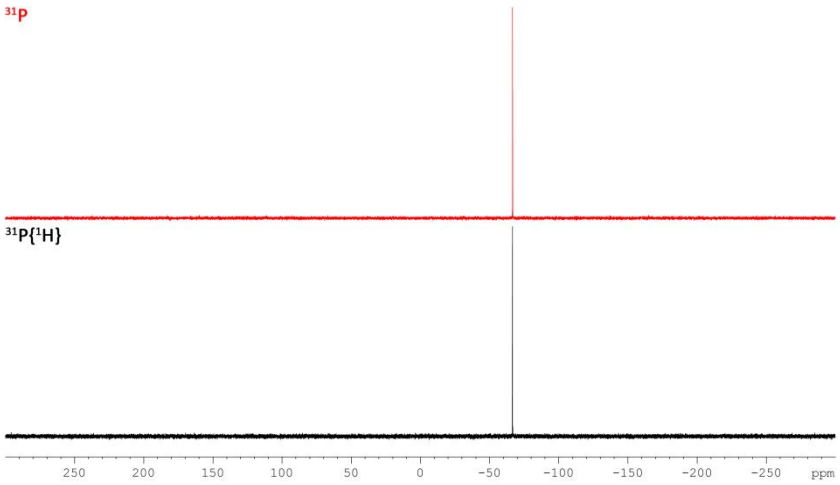

Figure 3-4 ^{31}P and $^{31}P\{^{1}H\}$ NMR spectra of complex **1** at 300K in CD_2Cl_2.

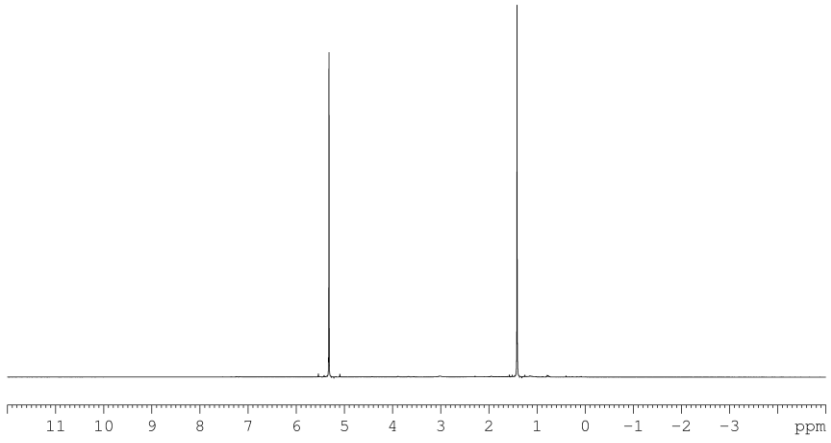

Figure 3-5 ^{1}H NMR spectrum of **1** at 300K in CD_2Cl_2.

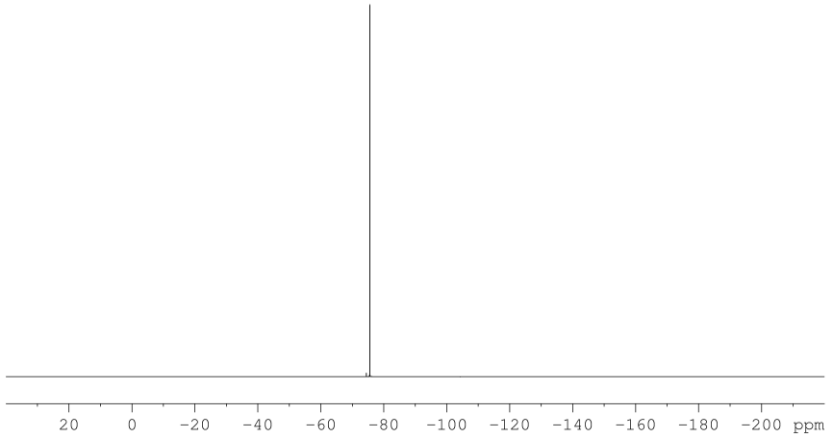

Figure 3-6 $^{19}F\{^{1}H\}$ NMR spectrum of **1** at 300K in CD_2Cl_2.

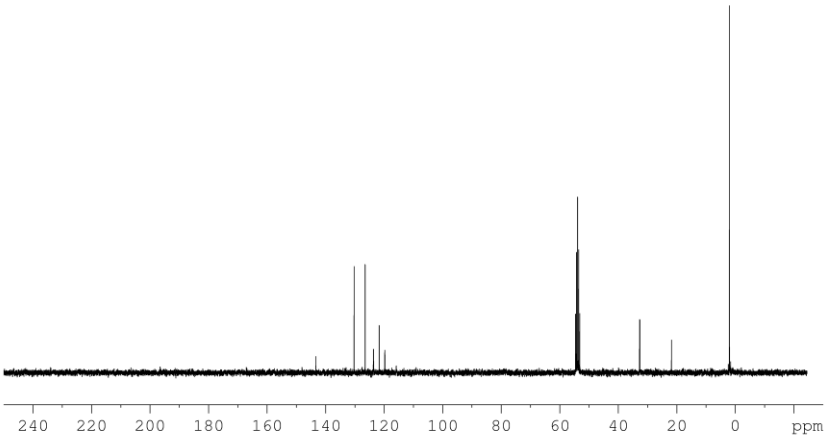

Figure 3-7 $^{13}C\{^{1}H\}$ NMR spectrum of **1** at 300K in CD_2Cl_2.

3.4.2.2 NMR Spectra of 2

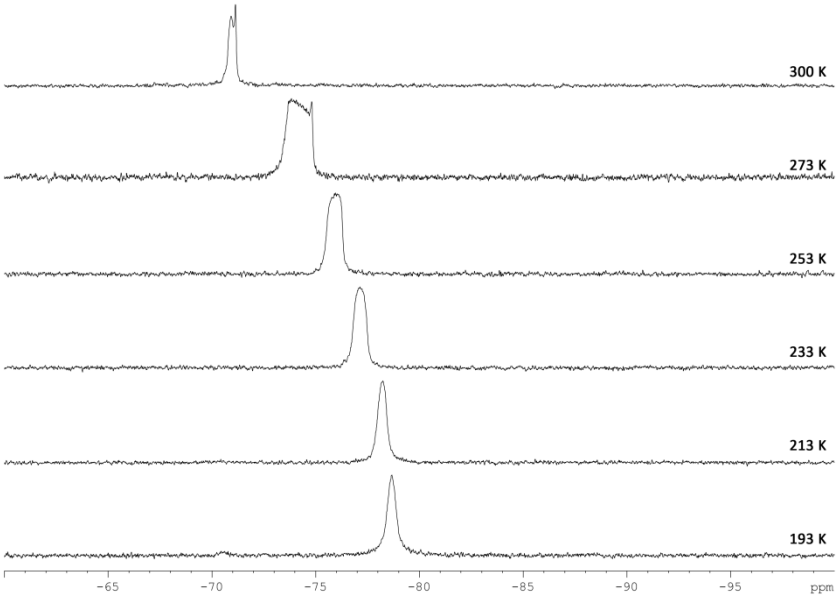

Figure 3-8 VT NMR Spectra of **2**, 193 K → r.t.

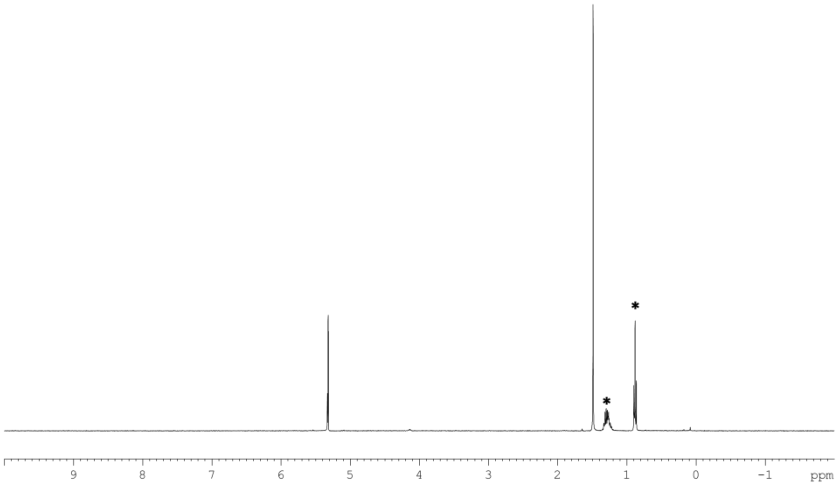

Figure 3-9 ^{1}H NMR spectrum of **2** at 300K in CD_2Cl_2. Signals marked with asterisk are residual hexane.

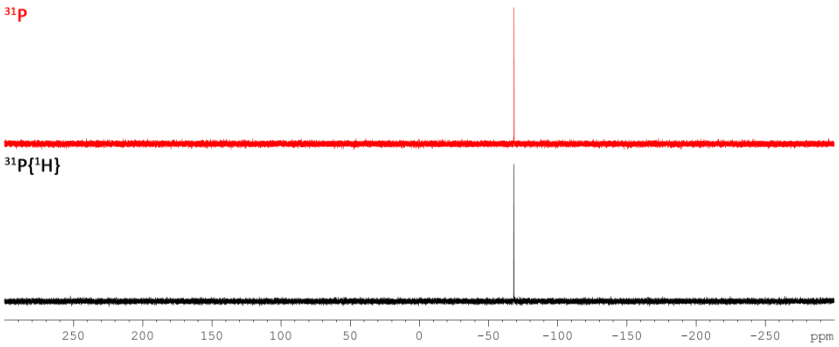

Figure 3-10 ^{31}P and $^{31}P\{^{1}H\}$ NMR spectra of **2** at 300K in CD_2Cl_2.

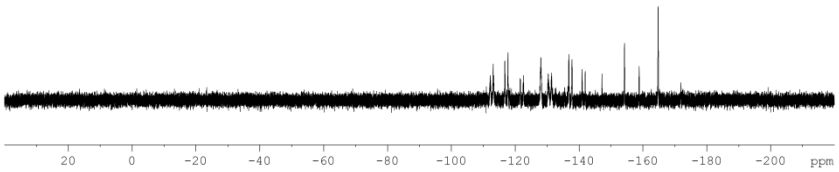

Figure 3-11 ^{19}F NMR spectrum of **2** at 300K in CD_2Cl_2.

3.4.2.3 NMR Spectra of 3a

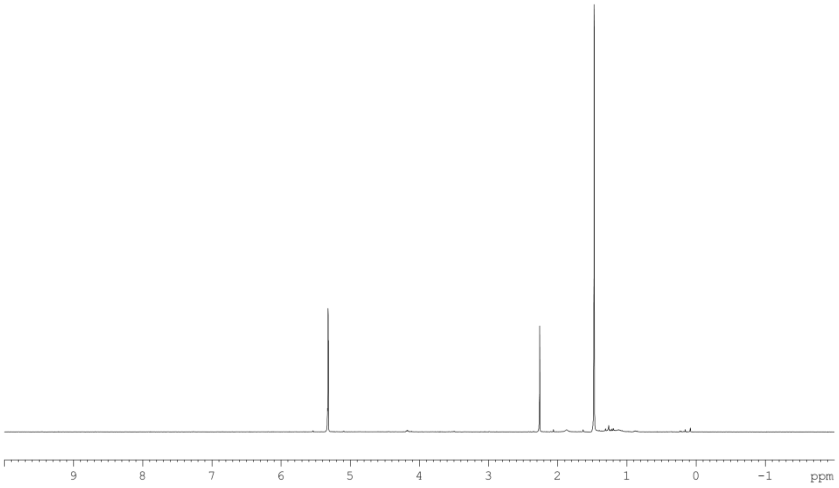

Figure 3-12 ^{1}H NMR spectrum of **3a** at 300K in CD_2Cl_2.

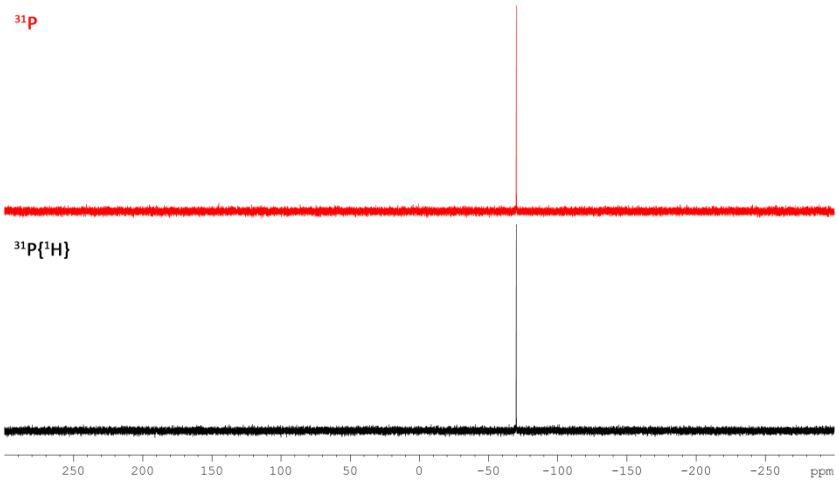

Figure 3-13 ^{31}P and $^{31}P\{^{1}H\}$ NMR spectra of **3a** at 300 K in CD_2Cl_2.

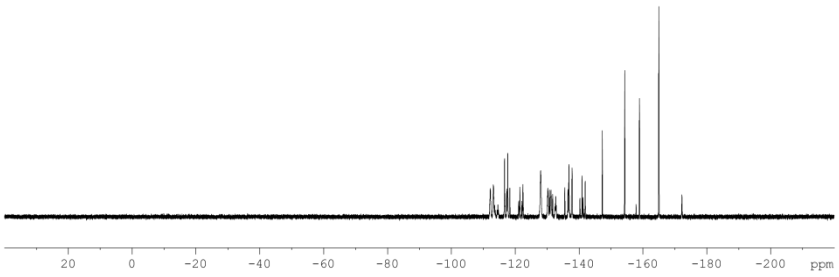

Figure 3-14 ^{19}F NMR spectrum of **3a** at 300 K in CD_2Cl_2.

3.4.2.4 NMR Spectra of 3b

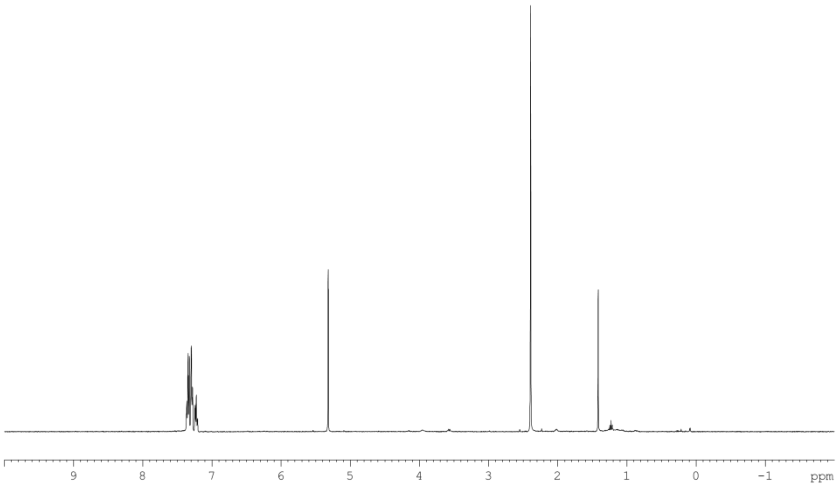

Figure 3-15 ^{1}H NMR spectrum of **3b** at 300K in CD_2Cl_2.

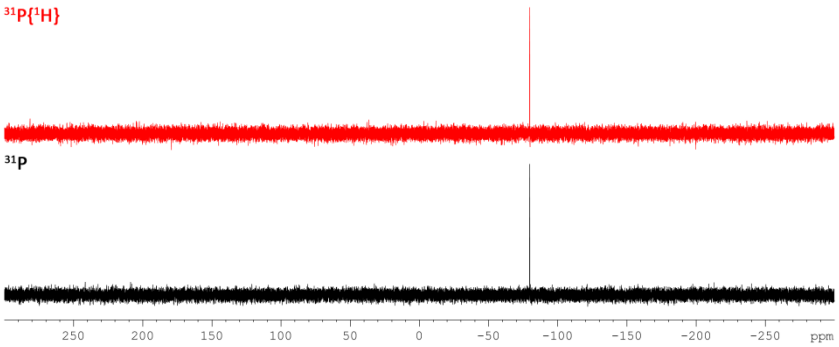

Figure 3-16 ^{31}P and $^{31}P\{^{1}H\}$ NMR spectra of **3b** at 300 K in CD_2Cl_2.

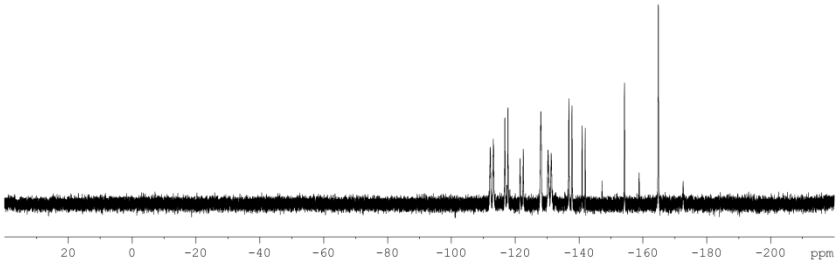

Figure 3-17 ^{19}F NMR spectrum of **3b** at 300 K in CD_2Cl_2.

3.4.3 Crystallographic Data

All compounds: Using Olex2,[21] the structures were solved with the ShelXT[22] structure solution program, using the Direct Methods solution method. The models were refined with version 2014/6 of ShelXL[22] using Least Squares minimisation.

3.4.3.1 Crystal data for 1

Single colourless block-shaped crystals of **1** were recrystallised from a mixture of CH_2Cl_2 and n-hexane by solvent layering. A suitable crystal (0.11 × 0.07 × 0.05 mm^3) was selected and mounted on a MITIGEN holder in perflourotether oil on a GV50, TitanS2 diffractometer. The crystal was kept at T = 84.9(7) K during data collection.

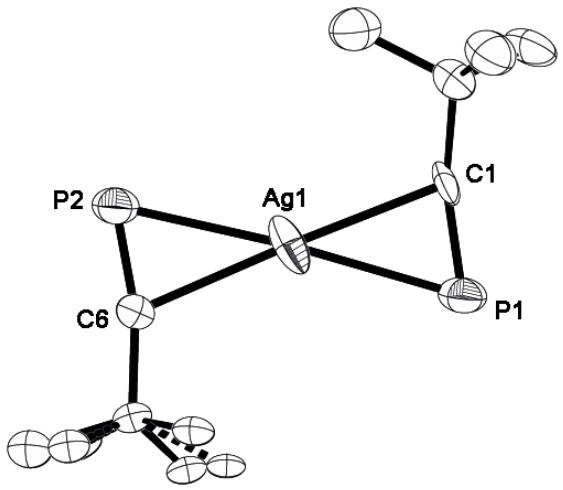

Figure 3-18 Molecular structure of **1** in the solid state. Anion, disorder and hydrogen atoms are omitted for clarity. Thermal ellipsoids are shown at 50% probability level. Selected distances [Å] and angles [°]: Ag1-P1 2.523(6), Ag1-P2 2.501(6), Ag1-C1 2.353(17), Ag1-C6 2.355(18), P1-C1 1.58(2), P2-C6 1.513(19); P2-Ag1-P1 175.5(2), C1-Ag1-P1 37.7(5), C1-Ag1-C6 177.3(8), C6-Ag1-P2 36.2(5).

Compound	**1**
Formula	$C_{26}H_{18}AgAlF_{36}O_4P_2$
$D_{calc.}$/ g cm^{-3}	2.032
μ/mm^{-1}	6.687
Formula Weight	1275.19
Colour	colourless
Shape	block
Max Size/mm	0.11
Mid Size/mm	0.07
Min Size/mm	0.05
T/K	84.9(7)
Crystal System	monoclinic
Space Group	Cc
a/Å	13.1330(5)
b/Å	16.6794(8)
c/Å	20.0329(9)
α/°	90
β/°	108.232(4)
γ/°	90
V/$Å^3$	4167.9(3)
Z	4
Z'	1
θ_{min}/°	4.426
θ_{max}/°	73.944
Measured Refl.	7059
Independent Refl.	4731
Reflections Used	4127
R_{int}	0.0869
Parameters	740
Restraints	596
Largest Peak	1.478
Deepest Hole	-2.564
GooF	1.114
wR_2 (all data)	0.3055
wR_2	0.2912
R_1 (all data)	0.1191
R_1	0.1103
Flack Parameter	0.43(3)

3.4.3.2 Crystal data for 2

Single clear colourless block-shaped crystals of **2** were obtained by recrystallisation from a mixture of CH_2Cl_2 and n-hexane by solvent layering. A suitable crystal (0.18×0.16×0.12) was selected and mounted on a mylar loop on a Xcalibur, AtlasS2, Gemini ultra diffractometer. The crystal was kept at T = 123.00(14) K during data collection.

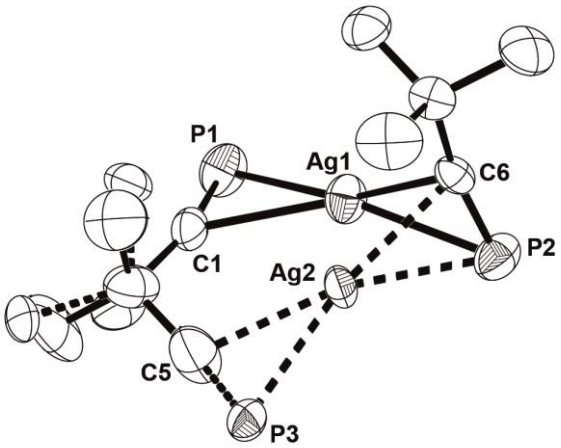

Figure 3-19 Molecular structure of the cation of **2** in the solid state. Solvent molecule and hydrogen atoms are omitted for clarity. Thermal ellipsoids are shown at 50% probability level. Disorder: Connection of atoms in part 2 is shown with dashes Selected distances [Å] and angles [°]: Ag1-P1 2.501(3), Ag1-C1 2.338(9), P1-C1 1.549(11), Ag1-P2 2.4975(18), Ag1-C6 2.333(5), P2-C6 1.561(6), P1-Ag1-P2 157.56(8), C1-Ag1-C6 144.6(3), C1-Ag1-P1 37.1(3), C6-Ag1-P2 37.18(14), C1-Ag1-P2 148.4(2).

Compound	**2**
Formula	$C_{46}H_{18}AgAlF_{46}O_3P_2(CH_2Cl_2)_{0.33}$
$D_{calc.}$/ g cm^{-3}	1.994
μ/mm^{-1}	5.600
Formula Weight	1716.51
Colour	clear colourless
Shape	block
Max Size/mm	0.18
Mid Size/mm	0.16
Min Size/mm	0.12
T/K	123.00(14)
Crystal System	orthorhombic
Flack Parameter	0.004(2)
Hooft Parameter	-0.0066(17)
Space Group	$P2_12_12_1$
a/Å	13.31482(17)
b/Å	17.4192(2)
c/Å	24.6472(3)
α/°	90
β/°	90
γ/°	90
V/Å^3	5716.54(12)
Z	4
Z'	1
Θ_{min}/°	3.587
Θ_{max}/°	66.250
Measured Refl.	40452
Independent Refl.	9968
Reflections Used	9435
R_{int}	0.0300
Parameters	973
Restraints	0
Largest Peak	0.412
Deepest Hole	-0.483
GooF	1.165
wR_2 (all data)	0.0888
wR_2	0.0879
R_1 (all data)	0.0346
R_1	0.0322

3.4.3.3 Crystal data for 3a

Single clear colourless block-shaped crystals of **3a** were obtained by recrystallisation from a mixture of CH_2Cl_2 and hexane. A suitable crystal (0.20×0.13×0.13) was selected and mounted on a mylar loop on a GV50, TitanS2 diffractometer. The crystal was kept at T = 123.01(10) K during data collection.

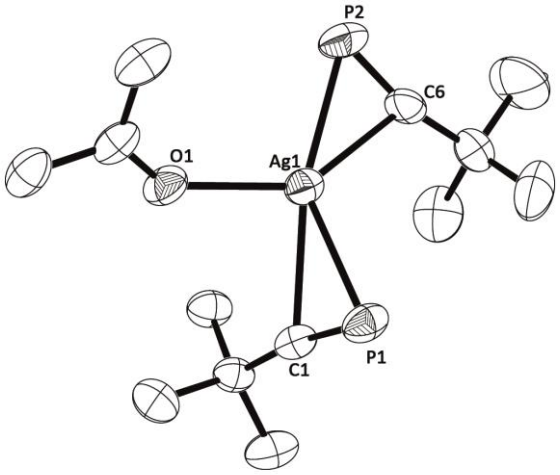

Figure 3-20 Molecular structure of the cation of **3a** in the solid state. Hydrogen atoms are omitted for clarity. Thermal ellipsoids are shown at 50% probability level. Selected bond lengths [Å] and angles [°]: Ag1-P1 2.5724(12), Ag1-P2 2.4879(14), Ag1-O1 2.323(3), Ag1-C1 2.497(4), Ag1-C6 2.363(5), P1-C1 1.556(5), P2-C6 1.564(5), P1-C1-C2 170.1(3), P2-C6-C7 165.2(4).

Compound	**3a**
Formula	$C_{49}H_{24}AgAlF_{46}O_4P_2$
$D_{calc.}$/ g cm^{-3}	1.917
μ/mm^{-1}	5.068
Formula Weight	1747.47
Colour	clear colourless
Shape	block
Max Size/mm	0.20
Mid Size/mm	0.13
Min Size/mm	0.13
T/K	123.01(10)
Crystal System	monoclinic
Space Group	$P2_1/n$
a/Å	14.1978(3)
b/Å	18.0764(3)
c/Å	24.6063(5)
α/°	90
β/°	106.496(2)
γ/°	90
V/Å^3	6055.1(2)
Z	4
Z'	1
Θ_{min}/°	3.080
Θ_{max}/°	74.268
Measured Refl.	21648
Independent Refl.	11787
Reflections Used	9301
R_{int}	0.0353
Parameters	936
Restraints	0
Largest Peak	3.852
Deepest Hole	-1.697
GooF	0.996
wR_2 (all data)	0.1504
wR_2	0.1440
R_1 (all data)	0.0628
R_1	0.0522

3.4.3.4 Crystal data for 3b

Single clear light yellow block-shaped crystals of **3b** were obtained by solvent layering a solution of **3b** in CH_2Cl_2 with toluene. A suitable crystal (0.39×0.32×0.30) was selected and mounted on a mylar loop on a Xcalibur, Ruby Gemini Ultra diffractometer. The crystal was kept at T = 123(2) K during data collection.

The crystal is the solid solution of two isostructural compounds, $[Ag(C_7H_8)_2(P{\equiv}C\textit{t}Bu)][fal]$ (**3a**) and $[Ag(C_7H_8)_3][fal]$, with a ratio of about 60%/40%. Two sorts of cations statistically take the same crystallographic position resulting in the partial overlap of P≡C*t*Bu and toluene ligands. In addition, the silver cation is disordered over two positions separated by 0.91 Å from each other. Similar mutual arrangement of three toluene ligands around disordered silver cations was found in $[Ag(C_7H_8)_3][B(C_6F_5)_4]$.[6] Due to the disorder, some SIMU restraints were applied to the close carbon atoms belonging to P≡C*t*Bu and toluene ligands during the refinement. In addition, some DFIX, FLAT and ISOR restraints were applied to the atoms belonging to the toluene ligands.

Compound	**3b**
Formula	$C_{55.80}H_{24.60}AgAlF_{46}O_3P_{0.60}$
$D_{calc.}$/ g cm^{-3}	1.902
μ/mm^{-1}	4.63
Formula Weight	1770.39
Colour	light yellow
Shape	block
Max Size/mm	0.39
Mid Size/mm	0.32
Min Size/mm	0.30
T/K	123.01(10)
Crystal System	monoclinic
Space Group	$P2_1/n$
a/Å	18.8589(2)
b/Å	16.2222(1)
c/Å	21.8623(2)
β/°	112.413(1)
V/Å^3	6183.15(10)
Z	4
Z'	1
θ_{min}/°	3.493
θ_{max}/°	66.679
Measured Refl.	65843
Independent Refl.	10888
Reflections Used	10888
R_{int}	0.0251
Parameters	976
Restraints	57
Largest Peak	2.693
Deepest Hole	-1.402
GooF	1.078
R_1	0.0659
wR_2	0.1907
wR_2 (all data)	0.1934

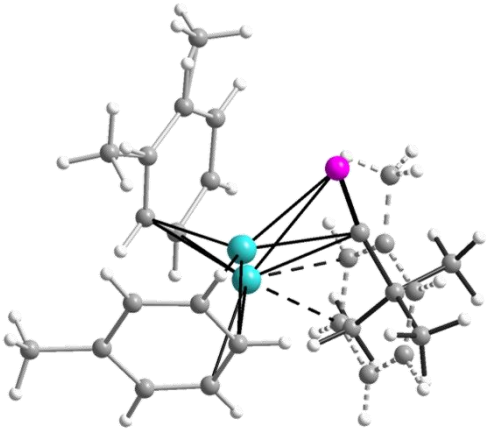

Figure 3-21 Crystallographic disorder of the cation in the crystal of **3b**. The overlapping position of the toluene ligand is shown as dashed lines.

3.4.4 Hirshfeld surfaces

Hirshfeld surface plots have been produced with the program CrystalExplorer Version 3.1.[18d]

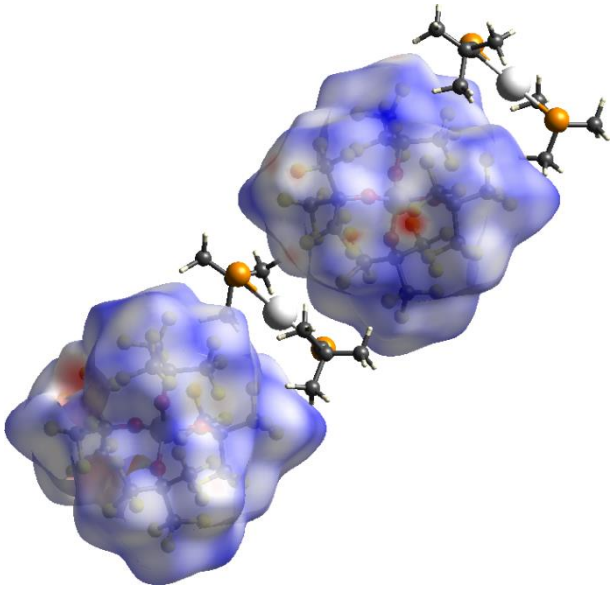

Figure 3-22 Hirshfeld plots for anions in **1**. View along crystallographic b axis. No contacts between C_s-$[Ag(t\text{BuCP})_2]^+$ and $[Al\{OC(CF_3)_3\}_4]^-$ could be observed.

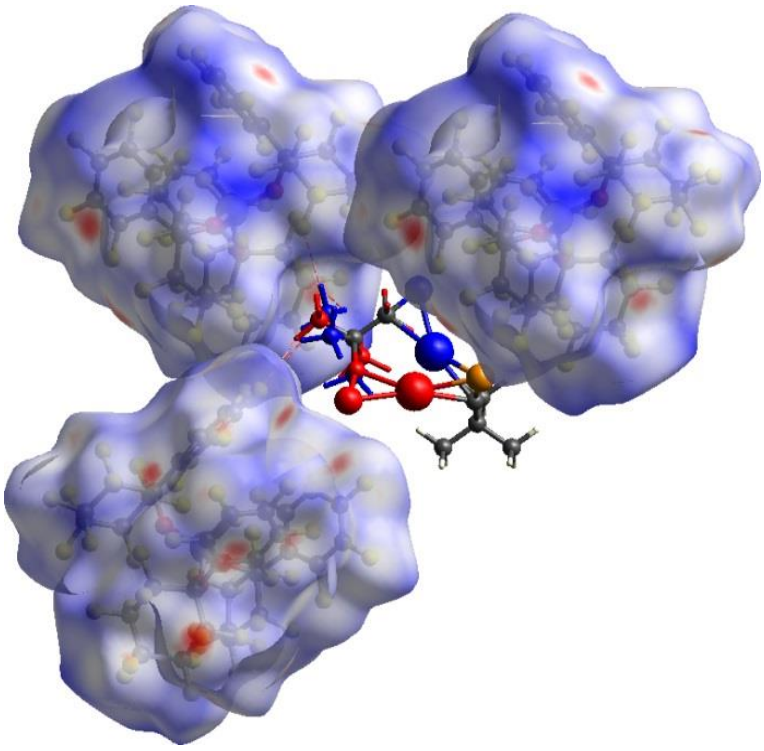

Figure 3-23 Hirshfeld plots for anions in **2**. Contacts between hydrogen atoms of T_d-$[Ag(t\text{BuCP})_2]^+$ and fluorine atoms of $[FAl\{OC_{12}F_{15}\}_3]^-$ could be observed. Shown in red: Molecule **A** in part 1 (66%), shown in blue: Molecule **B** in part 2 (33%). Contacts within the vdW radii are indicated by red dashed lines between the anions and cation.

3.4.5 DFT Calculations

All calculations have been performed with the TURBOMOLE program package[23] at the RI[24]-B3LYP[25]/def2-TZVP[24b, 26] level of theory. The Multipole Accelerated Resolution of Identity (MARI-J)[27] approximation was used in the geometry optimisation steps. The nature of the stationary points was checked by frequency calculations. For the calculation of the thermodynamic parameters the vibrational frequencies have been scaled with a factor of 0.999. For the calculation of the equilibrium constant the total SCF energy have been added to the chemical potential in order to get 'absolute' energies. The reaction energies discussed in the paper represents the total SCF energies.

The geometry of $[Ag(t\text{BuC}{\equiv}P)_2]^+$ was optimised free of symmetry restrains, leading to a geometry in which the two *t*BuC≡P units are roughly perpendicular to each other. Frequency calculations show no negative frequencies. The optimised geometry of $[Ag(t\text{BuC}{\equiv}P)_2]^+$ within the restrains of the C_s point group (parallel *t*BuC≡P units) shows one negative frequency (-12.25 cm^{-1}), indicating that this geometry is not the energy minimum structure.

Table 3-1 Calculated thermodynamic parameters (at the B3LYP/def2-TZVP level of theory) at different temperatures for the reaction: $[Ag(CH_2Cl_2)_2]^+ + t\text{BuCP} = [Ag(t\text{BuCP})(CH_2Cl_2)]^+ + CH_2Cl_2$

T (K)	ΔH (kJ·mol^{-1})	ΔS (kJ·mol^{-1}·K^{-1})	ΔG (kJ·mol^{-1})	K (l·mol^{-1})
193	-0.23	-0.0226	-51.35	7.88E+13
213	-0.24	-0.0226	-50.90	3.03E+12
233	-0.26	-0.0226	-50.44	2.03E+11
253	-0.27	-0.0227	-49.99	2.09E+10
273	-0.28	-0.0227	-49.53	2.99E+09
293	-0.28	-0.0227	-49.07	5.59E+08
300	-0.27	-0.0227	-48.93	3.30E+08

Table 3-2 Calculated thermodynamic parameters (at the B3LYP/def2-TZVP level of theory) at different temperatures for the reaction: $[Ag(t\text{BuCP})(CH_2Cl_2)]^+ + t\text{BuCP} = [Ag(t\text{BuCP})_2]^+ + CH_2Cl_2$

T (K)	ΔH (kJ·mol^{-1})	ΔS (kJ·mol^{-1}·K^{-1})	ΔG (kJ·mol^{-1})	K (l·mol^{-1})
193	-0.12	-0.0068	-47.48	7.08E+12
213	-0.12	-0.0068	-47.35	4.09E+11
233	-0.13	-0.0068	-47.21	3.83E+10
253	-0.14	-0.0068	-47.07	5.22E+09
273	-0.14	-0.0069	-46.92	9.49E+08
293	-0.15	-0.0069	-46.79	2.19E+08
300	-0.14	-0.0069	-46.74	1.37E+08

Table 3-3 Calculated thermodynamic parameters (at the B3LYP/def2-TZVP level of theory) at different temperatures for the reaction: $[Ag(t\text{BuCP})_2]^+ + t\text{BuCP} = [Ag(t\text{BuCP})_3]^+$

T (K)	ΔH (kJ·mol^{-1})	ΔS (kJ·mol^{-1}·K^{-1})	ΔG (kJ·mol^{-1})	K (l·mol^{-1})
193	3.47	-0.101	-3.14	7.07
213	3.81	-0.099	-1.14	1.90
233	4.16	-0.098	0.83	0.65
253	4.51	-0.096	2.77	0.27
273	4.85	-0.095	4.69	0.13
293	5.20	-0.094	6.57	0.07
300	5.32	-0.093	7.22	0.06

Table 3-4 Calculated thermodynamic parameters (at the B3LYP/def2-TZVP level of theory) at different temperatures for the reaction: $[Ag(t\text{BuCP})_2]^+ + Me_2CO = [Ag(t\text{BuCP})_2(Me_2CO)]^+$

T (K)	ΔH (kJ·mol^{-1})	ΔS (kJ·mol^{-1}·K^{-1})	ΔG (kJ·mol^{-1})	K (l·mol^{-1})
193	4.41	-0.14	-17.27	4.72E+04
213	4.70	-0.14	-14.48	3.56E+03
233	5.00	-0.14	-11.72	4.24E+02
253	5.31	-0.14	-8.99	7.18E+01
273	5.62	-0.13	-6.28	1.59E+01
293	5.93	-0.13	-3.59	4.37E+00
300	6.04	-0.13	-2.66	2.91E+00

Table 3-5 Calculated thermodynamic parameters (at the B3LYP/def2-TZVP level of theory) at different temperatures for the reaction: $[Ag(C_6H_5Me)_3]^+ + t\text{BuCP} = [Ag(t\text{BuCP})(C_6H_5Me)_2]^+ + C_6H_5Me$

T (K)	ΔH (kJ·mol^{-1})	ΔS (kJ·mol^{-1}·K^{-1})	ΔG (kJ·mol^{-1})	K (l·mol^{-1})
193	-1.35	0.0172	-20.04	2.66E+05
213	-1.32	0.0174	-20.38	9.96E+04
233	-1.30	0.0175	-20.73	4.44E+04
253	-1.26	0.0176	-21.09	2.26E+04
273	-1.24	0.0177	-21.43	1.26E+04
293	-1.21	0.0178	-21.79	7.67E+03
300	-1.39	0.0172	-21.29	5.10E+03

Table 3-6 Calculated thermodynamic parameters (at the B3LYP/def2-TZVP level of theory) at different temperatures for the reaction: $[Ag(t\text{BuCP})(C_6H_5Me)_2]^+ + t\text{BuCP} = [Ag(t\text{BuCP})_2]^+ + 2\ C_6H_5Me$

T (K)	ΔH (kJ·mol^{-1})	ΔS (kJ·mol^{-1}·K^{-1})	ΔG (kJ·mol^{-1})	K (l·mol^{-1})
193	-5.93	0.1406	-32.60	6.66E+08
213	-6.23	0.1390	-35.40	4.81E+08
233	-6.54	0.1377	-38.16	3.59E+08
253	-6.84	0.1364	-40.90	2.78E+08
273	-7.13	0.1353	-43.63	2.23E+08
293	-7.44	0.1343	-46.31	1.80E+08
300	-7.93	0.1326	-46.01	1.03E+08

Table 3-7 Calculated vibrational frequencies at the B3LYP/def2-TZVP level of theory (not corrected).

Compound	wave number [cm^{-1}]	vibration mode
1	1481.1	$\nu_{C\equiv P} + \delta_{CH}$
	1528.5	$\nu_{C\equiv P} + \delta_{CH}$
	1530.1	$\nu_{C\equiv P} + \delta_{CH}$
2	1476.6	$\nu_{C\equiv P} + \delta_{CH}$
	1526.5	$\nu_{C\equiv P} + \delta_{CH}$
	1527.2	$\nu_{C\equiv P} + \delta_{CH}$
3	1479.4	$\nu_{C\equiv P} + \delta_{CH}$
	1493.4	$\nu_{C\equiv P} + \delta_{CH}$
	1528.7	$\nu_{C\equiv P} + \delta_{CH}$
	1537.0	$\nu_{C\equiv P} + \delta_{CH}$
	1724.0	$\nu_{C=O}$

Table 3-8 Cartesian coordinates of the optimized geometry of $[Ag(CH_2Cl_2)_2]^+$ at the B3LYP/def2-TZVP level of theory. Total Energy: -2065.991229970 a.u.

Atom	x	y	z
Ag	0.0039375	-0.0000166	-0.0083252
Cl	2.7281090	-0.0257341	-0.3378114
Cl	1.4606613	0.2209448	2.3130133
C	3.0156211	0.1407858	1.4246687
H	3.5567861	-0.7345549	1.7642546
H	3.5527776	1.0665172	1.5946644
Cl	-2.1154949	1.3722015	-1.0841436
Cl	-2.0704454	-1.5699386	-0.8969801
C	-3.0170474	-0.1408005	-1.4216338
H	-3.1737274	-0.2108880	-2.4916417
H	-3.9411774	-0.1185165	-0.8560652

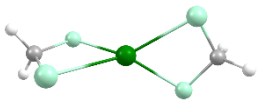

Table 3-9 Cartesian coordinates of the optimized geometry of $[Ag(t\text{BuCP})(CH_2Cl_2)]^+$ at the B3LYP/def2-TZVP level of theory. Total Energy: -1643.563516853 a.u.

Atom	x	y	z
Ag	0.0006662	-1.9095955	0.5852694
P	-1.1080537	-0.6248408	2.4148794
C	-0.6685745	0.3324030	1.2431506
C	-0.3888295	1.4551532	0.3412167
C	-0.9362720	2.7323377	1.0363658
H	-2.0110359	2.6618959	1.2022536
H	-0.7424947	3.5885577	0.3886936
H	-0.4421481	2.9045231	1.9922949
C	1.1348233	1.5948030	0.1215576
H	1.6606423	1.7374735	1.0655235
H	1.3267703	2.4605440	-0.5134136
H	1.5482603	0.7155219	-0.3769191
C	-1.1119575	1.2477103	-1.0090371
H	-0.7401665	0.3625571	-1.5294929
H	-0.9301713	2.1124365	-1.6483789
H	-2.1879768	1.1424267	-0.8710995
C	1.1783180	-4.6427661	-0.9671117
Cl	1.2388243	-2.9408282	-1.5578280
Cl	0.3856671	-4.7177063	0.6280542
H	0.5951475	-5.2178794	-1.6766734
H	2.1985610	-4.9947274	-0.8693049

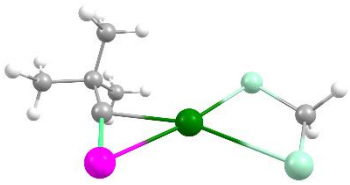

Table 3-10 Cartesian coordinates of the optimized geometry of $[Ag(t\text{BuCP})_2]^+$ (C_1 point group) at the B3LYP/def2-TZVP level of theory. Total Energy: -1221.133214907 a.u.

Atom	x	y	z
Ag	0.1350496	-0.3821835	-1.4251643
P	-1.7009733	0.9807631	-2.4962381
P	2.0655690	-2.0078797	-1.3425550
C	-2.2486019	0.1534790	-1.2762407
C	-3.0335706	-0.4951910	-0.2187204
C	-4.4888666	0.0288895	-0.3578375

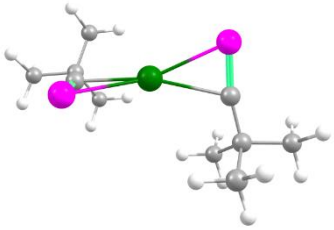

H	-4.5336964	1.1099750	-0.2274724
H	-5.1008689	-0.4377223	0.4154629
H	-4.9092095	-0.2262624	-1.3303937
C	-3.0122733	-2.0296974	-0.4061086
H	-3.3976102	-2.3150938	-1.3848884
H	-3.6390082	-2.4911980	0.3580194
H	-2.0025466	-2.4309631	-0.2986622
C	-2.4748336	-0.1165242	1.1716881
H	-1.4575121	-0.4892663	1.3075036
H	-3.1009728	-0.5669889	1.9428222
H	-2.4740974	0.9636611	1.3183795
C	2.4288520	-0.6604605	-0.6178613
C	3.0451477	0.4629743	0.0986326
C	4.4837738	0.0162673	0.4764185
H	4.4682285	-0.8597285	1.1246069
H	4.9712025	0.8327521	1.0112426
H	5.0719003	-0.2132925	-0.4118587
C	3.1095471	1.7070240	-0.8169952
H	3.6642666	1.4981288	-1.7316737
H	3.6139636	2.5152827	-0.2860080
H	2.1107482	2.0558375	-1.0870767
C	2.2451242	0.7820376	1.3820510
H	1.2327233	1.1172096	1.1476023
H	2.7456402	1.5852386	1.9242484
H	2.1829049	-0.0870682	2.0370770

Table 3-11 Cartesian coordinates of the optimized geometry of $[Ag(t\text{BuCP})_2]^+$ (Cs point group) at the B3LYP/def2-TZVP level of theory. Total Energy: -1221.131585518 a.u.

Atom	x	y	z
Ag	-0.0011068	0.0033317	0.0000000
P	-1.8229558	1.7663202	0.0000000
P	1.8182221	-1.7636510	0.0000000
C	-2.4853143	0.3425542	0.0000000
C	-3.3410335	-0.8462225	0.0000000
C	-3.0826107	-1.6894709	1.2699567
H	-2.0603165	-2.0721065	1.2938815
H	-3.7602342	-2.5441581	1.2744488
H	-3.2568439	-1.1074203	2.1747974
C	-4.8091349	-0.3364146	0.0000000
H	-5.0199982	0.2610951	0.8865708
H	-5.4740085	-1.2013905	0.0000000
H	-5.0199982	0.2610951	-0.8865708
C	-3.0826107	-1.6894709	-1.2699567
H	-3.2568439	-1.1074203	-2.1747974
H	-3.7602342	-2.5441581	-1.2744488
H	-2.0603165	-2.0721065	-1.2938815
C	2.4836627	-0.3413987	0.0000000
C	3.3410963	0.8461226	0.0000000
C	4.8085091	0.3344237	0.0000000
H	5.0185980	-0.2633662	0.8865665
H	5.4745190	1.1985237	0.0000000
H	5.0185980	-0.2633662	-0.8865665
C	3.0837158	1.6897066	-1.2699494

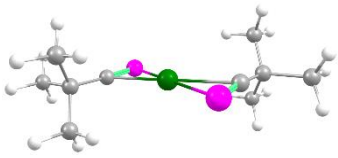

H	2.0618761	2.0735919	-1.2938681
H	3.2572221	1.1074488	-2.1747941
H	3.7623640	2.5435802	-1.2744384
C	3.0837158	1.6897066	1.2699494
H	2.0618761	2.0735919	1.2938681
H	3.7623640	2.5435802	1.2744384
H	3.2572221	1.1074488	2.1747941

Table 3-12 Cartesian coordinates of the optimized geometry of $[Ag(t\text{BuCP})_3]^+$ at the B3LYP/def2-TZVP level of theory. Total Energy: -1758.311212489 a.u.

Atom	x	y	z
Ag	0.1872984	-0.4932648	0.2206726
P	-1.8556117	-0.8450871	1.7468924
P	1.2324493	0.4846939	-1.9816864
P	2.2410643	-1.8125328	1.3170108
C	-2.2607178	0.3496267	0.8179873
C	-2.8797125	1.4761763	0.1116449
C	-1.9760291	2.7265567	0.1975178
H	-1.7798135	3.0015708	1.2341076
H	-2.4749150	3.5650947	-0.2904758
H	-1.0225489	2.5620308	-0.3068857
C	-3.1426090	1.1061305	-1.3650567
H	-2.2110207	0.9094072	-1.8960857
H	-3.6462235	1.9392871	-1.8575631
H	-3.7809351	0.2257999	-1.4424778
C	-4.2303156	1.7638211	0.8226796
H	-4.8917499	0.8989106	0.7761693
H	-4.7189933	2.6000896	0.3200945
H	-4.0765744	2.0310672	1.8680416
C	0.6790582	-0.8495804	-2.5746966
C	0.2520192	-2.0527752	-3.2855914
C	0.8161741	-3.3093800	-2.5832650
H	1.9044288	-3.2772400	-2.5291584
H	0.5261141	-4.1960591	-3.1488223
H	0.4186577	-3.4100324	-1.5719756
C	-1.2911922	-2.1202141	-3.3402969
H	-1.7210459	-2.1845952	-2.3397227
H	-1.5906709	-3.0100094	-3.8960393
H	-1.7065599	-1.2465546	-3.8426295
C	0.8232741	-1.9601117	-4.7269729
H	0.4426940	-1.0807595	-5.2462212
H	0.5164154	-2.8488644	-5.2807803
H	1.9121526	-1.9170725	-4.7173036
C	2.4174890	-0.5877761	2.2648129
C	2.7091869	0.4860378	3.2104735
C	4.0258746	0.1166267	3.9454370
H	3.9221364	-0.8212609	4.4906456
H	4.2621829	0.9076390	4.6592152
H	4.8551975	0.0234484	3.2445326
C	2.8951215	1.8191843	2.4494493
H	3.7029472	1.7482478	1.7209068
H	3.1422495	2.6083169	3.1612436
H	1.9801143	2.1072540	1.9290705

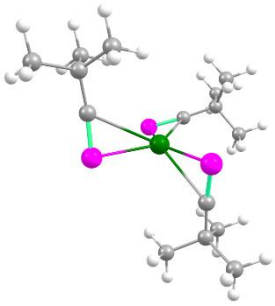

C	1.5582360	0.6119919	4.2352558
H	0.6199422	0.8763746	3.7455428
H	1.8005408	1.3978090	4.9524379
H	1.4142200	-0.3200232	4.7818649

Table 3-13 Cartesian coordinates of the optimized geometry of *t*BuC≡P at the B3LYP/def2-TZVP level of theory. Total Energy: -537.1680608182 a.u.

Atom	x	y	z
P	0.0000000	0.0000000	3.1995016
C	0.0000000	0.0000000	1.6563066
C	0.0000000	0.0000000	0.1882413
C	-0.7293067	-1.2631963	-0.3222132
H	-0.2314423	-2.1682596	0.0278437
H	-0.7339374	-1.2712169	-1.4148240
H	-1.7620467	-1.2845647	0.0278437
C	-0.7293067	1.2631963	-0.3222132
H	-1.7620467	1.2845647	0.0278437
H	-0.7339374	1.2712169	-1.4148240
H	-0.2314423	2.1682596	0.0278437
C	1.4586135	0.0000000	-0.3222132
H	1.9934891	0.8836949	0.0278437
H	1.4678748	0.0000000	-1.4148240
H	1.9934891	-0.8836949	0.0278437

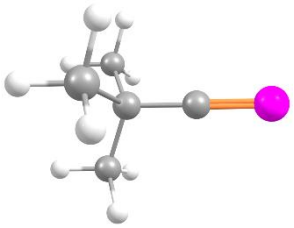

Table 3-14 Cartesian coordinates of the optimized geometry of $[Ag(t\text{BuCP})_2(Me_2CO)]^+$ at the B3LYP/def2-TZVP level of theory. Total Energy: -1414.272538237 a.u.

Atom	x	y	z
Ag	-0.1872884	0.3804070	0.6594503
P	-0.7551610	-2.1516991	0.7114232
P	1.0636331	2.3914570	1.5504707
O	-2.1507270	1.5430850	-0.1195511
C	-0.7216592	-1.7589814	-0.8023742
C	-0.7407052	-1.6229493	-2.2616304
C	-2.0801644	-0.9940025	-2.7112887
H	-2.9249226	-1.6068435	-2.3958565
H	-2.0928982	-0.9266061	-3.8003674
H	-2.2018564	0.0078903	-2.3000539
C	-0.6051706	-3.0504753	-2.8554290
H	0.3356284	-3.5143226	-2.5592024
H	-0.6291873	-2.9801352	-3.9441009
H	-1.4267906	-3.6903735	-2.5339518
C	0.4417308	-0.7492930	-2.7374909
H	0.3624773	0.2694506	-2.3524229
H	0.4314452	-0.6954964	-3.8270319
H	1.3977656	-1.1703918	-2.4255383
C	1.9745458	1.1205116	1.7008381
C	3.0546103	0.1639012	1.9810115
C	3.4591493	-0.5905877	0.6956957
H	2.6362354	-1.1997637	0.3196188
H	4.2971164	-1.2528168	0.9179795

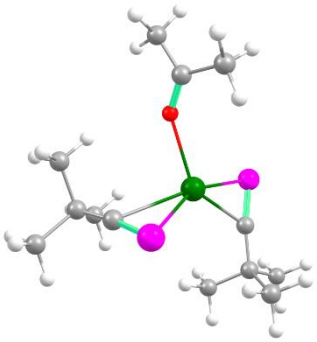

H	3.7684068	0.1017409	-0.0877791
C	4.2618898	0.9929158	2.4968030
H	4.5991557	1.7068594	1.7454901
H	5.0847738	0.3122403	2.7206648
H	4.0067702	1.5358605	3.4067790
C	2.6121601	-0.8358807	3.0728224
H	2.3239927	-0.3190316	3.9883669
H	3.4425429	-1.5049467	3.3030913
H	1.7707576	-1.4432737	2.7376254
C	-3.1701929	2.0466720	0.3355423
C	-4.1374947	2.7521590	-0.5701715
H	-3.7078275	2.8964077	-1.5583978
H	-4.4395468	3.7108896	-0.1434263
H	-5.0467760	2.1489588	-0.6563761
C	-3.5060249	1.9885230	1.7982717
H	-2.8419928	1.3112617	2.3316020
H	-4.5446764	1.6846490	1.9440046
H	-3.4137243	2.9920303	2.2248897

Table 3-15 Cartesian coordinates of the optimized geometry of Me_2CO at the B3LYP/def2-TZVP level of theory. Total Energy: -193.1207625528 a.u.

Atom	x	y	z
C	0.0000000	0.0000000	-0.6413001
O	0.0000000	0.0000000	-1.8504631
C	0.0000000	1.2886407	0.1546812
C	0.0000000	-1.2886407	0.1546812
H	0.0000000	2.1428288	-0.5189059
H	0.0000000	-2.1428288	-0.5189059
H	0.8779295	1.3321851	0.8050531
H	-0.8779295	1.3321851	0.8050531
H	-0.8779295	-1.3321851	0.8050531
H	0.8779295	-1.3321851	0.8050531

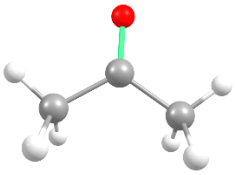

Table 3-16 Cartesian coordinates of the optimized geometry of $[Ag(tBuCP)(C_6H_5Me)_2]^+$ at the B3LYP/def2-TZVP level of theory. Total Energy: -1226.936491546 a.u.

Atom	x	y	z
Ag	0.3470457	0.1420647	-0.5002360
P	0.6101824	-2.2747030	0.2230454
C	-0.7459500	-1.8191664	0.8607741
C	-2.0351865	-1.6542407	1.5385665
C	-3.0721456	-1.0295136	0.5788986
H	-2.7737967	-0.0239842	0.2763450
H	-4.0352431	-0.9575039	1.0863348
H	-3.2006465	-1.6391429	-0.3156282
C	-2.5073537	-3.0721062	1.9610900
H	-2.6406430	-3.7179938	1.0934650
H	-3.4648968	-2.9827358	2.4766658
H	-1.7933361	-3.5393461	2.6390665
C	-1.8646543	-0.7691497	2.7933600
H	-1.1415468	-1.2030415	3.4841704

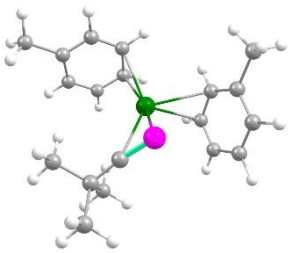

H	-2.8237504	-0.6856120	3.3070136
H	-1.5309074	0.2335858	2.5246186
C	0.3658730	2.6193040	-0.3455348
C	-0.7162527	2.8830842	0.5094282
C	1.6397611	2.4154051	0.2120889
H	-1.6954817	3.0813432	0.0921590
H	2.4998420	2.2839133	-0.4330208
C	-0.5188808	2.9528434	1.8798073
C	1.8169050	2.4752438	1.5936856
H	-1.3566760	3.1885792	2.5254527
H	2.8078460	2.3351220	2.0076463
C	0.7485803	2.7563727	2.4458761
H	0.2483418	2.7304641	-1.4169898
C	0.0568996	0.0336609	-3.2915831
C	-0.5541105	-1.1921123	-3.5496002
C	1.4465621	0.1040067	-3.1190746
H	-1.6232767	-1.2458471	-3.7077534
H	1.9234792	1.0703538	-2.9971635
C	0.2296945	-2.3372053	-3.6352401
C	2.2442241	-1.0438564	-3.2094829
H	-0.2316933	-3.2928807	-3.8497134
C	1.6084748	-2.2614299	-3.4650186
H	2.2049756	-3.1623125	-3.5508218
H	-0.5330832	0.9427632	-3.3005435
C	0.9433615	2.8492833	3.9335367
H	0.5151683	1.9778727	4.4366836
H	1.9990801	2.8999146	4.1968545
H	0.4458523	3.7314186	4.3400241
C	3.7429630	-0.9638792	-3.0966222
H	4.1442557	-1.7877054	-2.5041908
H	4.2051825	-1.0248235	-4.0854695
H	4.0649610	-0.0263074	-2.6429701

Table 3-17 Cartesian coordinates of the optimized geometry of $[Ag(C_6H_5Me)_3]^+$ at the B3LYP/def2-TZVP level of theory. Total Energy: -961.2481592796 a.u.

Atom	x	y	z
Ag	-0.1181741	0.4219823	-0.5486211
C	-0.3149639	2.7388258	0.2409143
C	-1.2312473	2.2273271	1.1754132
C	1.0072412	2.9876331	0.6491031
H	-2.2694666	2.0928934	0.8973964
H	1.7156634	3.4139457	-0.0499639
C	-0.8271204	1.9834868	2.4879648
C	1.3885482	2.7430902	1.9578739
H	-1.5489836	1.6102055	3.2035619
H	2.4050904	2.9597914	2.2643660
C	0.4769652	2.2490726	2.9024354
H	-0.6597058	3.0876024	-0.7256132
C	-0.5722791	0.8158490	-3.2214081
C	-1.2258051	-0.3056414	-3.7320132
C	0.8223610	0.8078988	-3.0670985
H	-2.2985331	-0.2933319	-3.8737746
H	1.3323089	1.7124185	-2.7536006

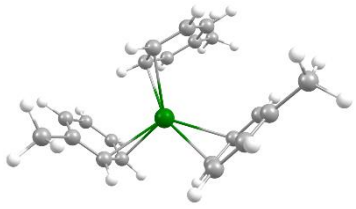

C	-0.4792251	-1.4209292	-4.0920602
C	1.5828915	-0.3134948	-3.4322768
H	-0.9730435	-2.2904554	-4.5074155
C	0.9054924	-1.4227473	-3.9416115
H	1.4715248	-2.2960867	-4.2441341
H	-1.1322913	1.7219295	-3.0224857
C	0.9016828	2.0374088	4.3291214
H	1.7852097	1.3978922	4.3879319
H	1.1656996	2.9887710	4.7974359
H	0.1088951	1.5821089	4.9212926
C	3.0853825	-0.2935756	-3.3455305
H	3.4860424	-1.2796975	-3.1080827
H	3.5182147	0.0078530	-4.3034400
H	3.4384805	0.4128047	-2.5935366
C	-0.2676014	-2.0125272	-0.2743947
C	-1.5599092	-2.2238575	0.2318226
C	0.7973293	-1.7681498	0.6093210
H	-2.3691243	-2.4324752	-0.4574805
H	1.8099696	-1.6850374	0.2343510
C	-1.8046578	-2.2260771	1.6024552
C	0.5522946	-1.7557163	1.9859568
H	1.3698408	-1.5930964	2.6762659
C	-0.7248975	-1.9917447	2.4671884
H	-0.8940780	-2.0074811	3.5376753
H	-0.0752108	-2.1642999	-1.3310018
C	-3.1777253	-2.5002294	2.1524767
H	-3.9112354	-2.6250667	1.3568331
H	-3.1779352	-3.4111983	2.7555945
H	-3.5139146	-1.6878737	2.8007926

3.5 References

[1] A. Chirila, R. Wolf, J. C. Slootweg, K. Lammertsma, *Coord. Chem. Rev.* **2014**, *57*, 270.

[2] a) U. Vogel, J. F. Nixon, M. Scheer, *Chem. Commun.* **2007**, 5055; b) R. Streubel, *Angew Chem Int Ed Engl* **1995**, *34*, 436; c) R. Streubel, *Angew. Chem. Int. Ed.* **1995**, *34*, 436; d) E. P. O. Fuchs, W. Rösch, M. Regitz, *Angew. Chem.* **1987**, *99*, 1058; e) T. Wettling, J. Schneider, O. Wagner, C. G. Kreiter, M. Regitz, *Angew. Chem. Int. Ed.* **1989**, *28*, 1013; f) T. Wettling, J. Schneider, O. Wagner, C. G. Kreiter, M. Regitz, *Angew. Chem.* **1989**, *101*, 1035; g) M. D. Francis, P. B. Hitchcock, J. F. Nixon, L. Nyulászi, *Eur. J. Inorg. Chem.* **2008**, *2008*, 1761; h) A. Hoffmann, A. Mack, R. Goddard, P. Binger, M. Regitz, *Eur. J. Inorg. Chem.* **1998**, *1998*, 1597; i) J. Renner, U. Bergsträßer, P. Binger, M. Regitz, *Eur. J. Inorg. Chem.* **2000**, *2000*, 2337; j) N. M. West, P. S. White, J. L. Templeton, J. F. Nixon, *Organometallics* **2009**, 1425; k) M. Regitz, T. Weitling, R. Fässler, B. Breit, B. Geissler, M. Julino, A. Hoffmann, U. Bergsträsser, *Phosphorus, Sulfur, and Silicon and the Related Elements* **1996**, *109*, 425.

[3] G. Becker, G. Gresser, W. Uhl, *Z. Naturforsch., Teil B* **1981**, *36B*, 16.

[4] a) J. F. Nixon, *Chem. Rev.* **1988**, *88*, 1327; b) M. Regitz, P. Binger, *Angew. Chem. Int. Ed.* **1988**, *27*, 1484; c) L. N. R. Markovski, Vadim D., *Tetrahedron* **1989**, *45*, 6019; d) M. Regitz, *Chem. Rev.* **1990**, *90*, 191; e) J. F. Nixon, *Endeavour* **1991**, *15*, 49; f) M. Regitz, *J. Heterocycl. Chem.* **1994**, *31*, 663; g) A. C. Gaumont, J. M. Denis, *Chem. Rev.* **1994**, *94*, 1413; h) J. F. Nixon, *Coord. Chem. Rev.* **1995**, *145*, 201; i) F. Mathey, *Angew. Chem. Int. Ed.* **2003**, *42*, 1578; j) F. Mathey, *Angew. Chem.* **2003**, *115*, 1616; k) C. A. Russell, N. S. Townsend, in *Phosphorus(III) Ligands in Homogeneous Catalysis: Design and Synthesis*, John Wiley & Sons, Ltd, **2012**, pp. 343.

[5] a) J. C. T. R. B. S. Laurent, P. B. Hitchcock, H. W. Kroto, J. F. Nixon, *Chem. Commun.* **1981**, 1141; b) J. C. T. R. B. S. Laurent, M. A. King, H. W. Kroto, J. F. Nixon, R. J. Suffolk, *Dalton Trans.* **1983**, 755; c) S. I. Al-Resayes, P. B. Hitchcock, M. F. Meidine, J. F. Nixon, *J. Organomet. Chem.* **1988**, *341*, 457; d) P. Binger, B. Biedenbach, A. T. Herrmann, F. Langhauser, P. Betz, R. Goddard, C. Krüger, *Chem. Ber.* **1990**, 1617; e) D. Carmichael, S. I. Al-Resayes, J. F. Nixon, *J. Organomet. Chem.* **1993**, *453*, 207; f) C. Jones, C. Schulten, A. Stasch, *Dalton Trans.* **2006**, 3733; g) T. Schaub, U. Radius, *Z. Anorg. Allg. Chem.* **2006**, *632*, 981; h) R. A. Sanguramath, N. S. Townsend, J. M. Lynam, C. A. Russell, *Eur. J. Inorg. Chem.* **2014**, *2014*, 1783.

[6] H. Oberhammer, G. Becker, G. Gresser, *J. Mol. Struct.* **1981**, *75*, 283.

[7] a) G. Becker, W. A. Herrmann, W. Kalcher, G. W. Kriechbaum, C. Pahl, T. C. Wagner, M. L. Ziegler, *Angew. Chem.* **1983**, *95*, 417; b) G. Becker, W. A. Herrmann, W. Kalcher, G. W. Kriechbaum, C. Pahl, T. C. Wagner, M. L. Ziegler, *Angew. Chem. Int. Ed.* **1983**, *22*, 413; c) S. I. Al-Resayes, P. B. Hitchcock, M. F. Meidine, J. F. Nixon, *Chem. Commun.* **1984**, 1080; d) R. Bartsch, J. F. Nixon, N. Sarjudeen, *Journal of Organometallic Chemistry* **1985**, 267; e) P. B. Hitchcock, M. F. Meidine, J. F. Nixon, *J. Organomet. Chem.* **1987**, 337; f) P. B. Hitchcock, M. J. Maah, J. F. Nixon, *Heteroat. Chem.* **1991**, *2*; g) J. C. T. R. B. S. Laurent, P. B. Hitchcock, H. W. Kroto, M. F. Meidine, J. F. Nixon, *J. Organomet. Chem.* **1982**, C82.

[8] J. Miralles-Sabater, M. Merchan, I. Nebot-Gil, P. M. Viruela-Martin, *The Journal of Physical Chemistry* **1988**, *92*, 4853.

[9] a) A. Reisinger, N. Trapp, I. Krossing, S. Altmannshofer, V. Herz, M. Presnitz, W. Scherer, *Angew. Chem. Int. Ed.* **2007**, *46*, 8295; b) A. Reisinger, N. Trapp, I. Krossing, S. Altmannshofer, V. Herz, M. Presnitz, W. Scherer, *Angew. Chem.* **2007**, *119*, 8445.

[10] a) I. Krossing, I. Raabe, *Angew. Chem. Int. Ed.* **2004**, *43*, 2066; b) I. Krossing, I. Raabe, *Angew. Chem.* **2004**, *116*, 2116.

[11] B. C. Guo, A. W. Castleman Jr, *Chem. Phys. Lett.* **1991**, *181*, 16.

[12] As chemical oxidation through silver(I) could be observed, we have conducted CV measurements in dichloromethane. Unfortunately, every attempt to oxidize *t*BuCP electrochemically has led to decomposition of the molecule and thus no oxidation potential could be derived from the measurements.

[13] I. Krossing, *J. Am. Chem. Soc.* **2001**, *123*, 4603.

[14] a) C. Schwarzmaier, M. Sierka, M. Scheer, *Angew. Chem. Int. Ed.* **2013**, *52*, 858; b) C. Schwarzmaier, M. Sierka, M. Scheer, *Angew. Chem.* **2013**, *125*, 891.

[15] a) C. Schwarzmaier, A. Y. Timoshkin, M. Scheer, *Angew. Chem.* **2013**, *125*, 7751; b) C. Schwarzmaier, A. Schindler, C. Heindl, S. Scheuermayer, E. V. Peresypkina, A. V. Virovets, M. Neumeier, R. Gschwind, M. Scheer, *Angew. Chem.* **2013**, *125*, 11097; c) C. Schwarzmaier, A. Y. Timoshkin, M. Scheer, *Angew. Chem. Int. Ed.* **2013**, *52*, 7600; d) C. Schwarzmaier, A. Schindler, C. Heindl, S. Scheuermayer, E. V. Peresypkina, A. V. Virovets, M. Neumeier, R. Gschwind, M. Scheer, *Angew. Chem. Int. Ed.* **2013**, *52*, 10896; e) I. Krossing, I. Raabe, *Angew. Chem.* **2001**, *113*, 4544; f) I. Krossing, I. Raabe, *Angew. Chem. Int. Ed.* **2001**, *40*, 4406; g) I. Krossing, *Dalton Trans.* **2002**, *0*, 500.

[16] Subsequent investigations have been conducted with **2** as crystallographic problems

arise from the use of the pftb$^-$ anion present in **1**.

[17] A. N. Chernega, M. Y. Antipin, Y. T. Struchkov, M. F. Meidine, J. F. Nixon, *Heteroat. Chem.* **1991**, *2*, 665.

[18] a) J. J. McKinnon, D. Jayatilaka, M. A. Spackman, *Chem. Commun.* **2007**, 3814; b) M. A. Spackman, D. Jayatilaka, *CrystEngComm* **2009**, *11*, 19; c) M. A. Spackman, J. J. McKinnon, *CrystEngComm* **2002**, *4*, 378; d) S. K. Wolff, D. J. Grimwood, J. J. McKinnon, M. J. Turner, D. Jayatilaka, M. A. Spackman, University of Western Australia, **2012**.

[19] I. Krossing, *Chem. Eur. J.* **2001**, *7*, 490.

[20] T. Köchner, N. Trapp, T. A. Engesser, A. J. Lehner, C. Röhr, S. Riedel, C. Knapp, H. Scherer, I. Krossing, *Angew. Chem.* **2011**, *123*, 11449.

[21] O. V. Dolomanov, L. J. Bourhis, R. J. Gildea, J. A. K. Howard, H. Puschmann, *J. Appl. Crystallogr.* **2009**, *42*, 339.

[22] G. M. Sheldrick, *Acta Cryst.* **2008**, *A64*, 112.

[23] a) F. Furche, R. Ahlrichs, C. Hättig, W. Klopper, M. Sierka, F. Weigend, *WIREs Comput. Mol. Sci.* **2014**, *4*, 91; b) R. Ahlrichs, M. Bär, M. Häser, H. Horn, C. Kölmel, *Chem. Phys. Lett.* **1989**, *162*, 165; c) O. Treutler, R. Ahlrichs, *J. Chem. Phys.* **1995**, *102*, 346

[24] a) K. Eichkorn, O. Treutler, H. Öhm, M. Häser, R. Ahlrichs, *Chem. Phys. Lett.* **1995**, *242*, 652; b) K. Eichkorn, F. Weigend, O. Treutler, R. Ahlrichs, *Theor. Chem. Acc.* **1997**, *97*, 119.

[25] a) P. A. M. Dirac, *Proc. Royal Soc. A* **1929**, 714; b) J. C. Slater, *Phys. Rev.* **1951**, 385; c) S. H. Vosko, L. Wilk, M. Nusair, *Can. J. Phys.* **1980**, 1200; d) A. D. Becke, *Phys. Rev. A* **1988**, 3098; e) C. Lee, W. Yang, R. G. Parr, *Phys. Rev. B* **1988**, 785; f) A. D. Becke, *J. Chem. Phys.* **1993**, 5648.

[26] A. Schäfer, C. Huber, R. Ahlrichs, *J. Chem. Phys. Lett.* **1994**, 5829.

[27] M. Sierka, A. Hogekamp, R. Ahlrichs, *J. Chem. Phys.* **2003**, *118*, 9136.

4 End-on complexes of Phosphaalkynes and Nitriles: a Comparison

Eva-Maria Rummel, Marcella Desat, Manfred Scheer

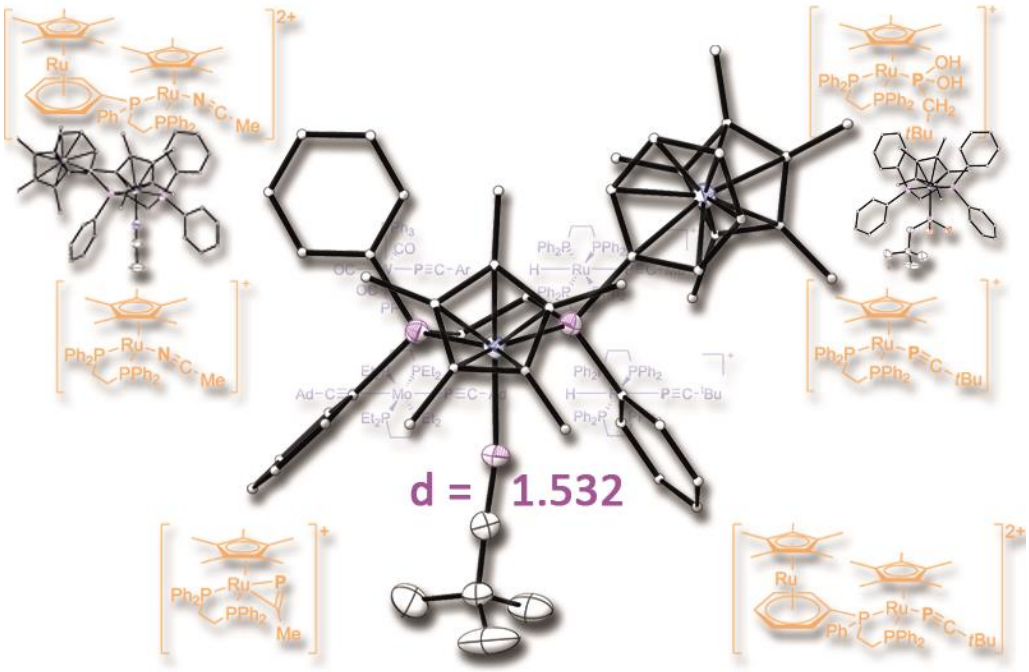

≡ All syntheses and characterisations were performed by Eva-Maria Rummel

≡ Some syntheses and characterisations were repeated by Marcella Desat in the course of her bachelor thesis

≡ Figures were made by Eva-Maria Rummel

≡ X-ray measurements and calculations were done by Eva-Maria Rummel

≡ Manuscript was written by Eva-Maria Rummel

4.1 Introduction

Different coordination complexes of phosphaalkynes and nitriles have been prepared from the reaction of [Cp*Ru(dppe)]$^{+}$[A]$^{-}$ (A = pftb: **1a**; A = PF_6: **1b**) with *t*BuC≡P, MeC≡P and MeC≡N. The end-on complexes of [Cp*Ru(dppe)(η^1-*t*BuC≡P)]$^{+}$[A]$^{-}$ (A = pftb: **2a**; A = PF_6: **2b**) and [{Cp*Ru(dppe)}{Cp*Ru}(η^1-*t*BuC≡P)]$^{2+}$·2[pftb]$^{-}$ (**3**) could be realised for the kinetically stabilised *tert*-butyl phosphaalkyne. The phosphaalkyne complex **2a** can be reacted with water to form the phosphine product [Cp*Ru(dppe)(η^1-P(OH)$_2$CH$_2$*t*Bu)][pftb] (**4**). In the reaction of **1a/b** with MeC≡P, complexes of the general formula [Cp*Ru(dppe)(MeC≡P)]$^{+}$[A]$^{-}$ (A = pftb: **5a**; A = PF_6: **5b**) were obtained. Reactions of **1a/b** with MeC≡N lead to the end-on complexes [Cp*Ru(dppe)(η^1-MeC≡N)]$^{+}$[A]$^{-}$ (A = pftb: **6a**; A = PF_6: **6b**).

In coordination chemistry, phosphaalkynes usually behave more like alkynes than their lighter homologues nitriles. This is due to their electronegativity differences: as the phosphorus atom is partially positively charged, the lone pair contracts and the HOMO is thus located on the C-P triple bond.[1] Because of this, out of the five possible coordination forms that can be observed for phosphaalkynes, type **B** and **D** are more easily realised than type **A**, **C** and **E** (cf. Figure 4-1).

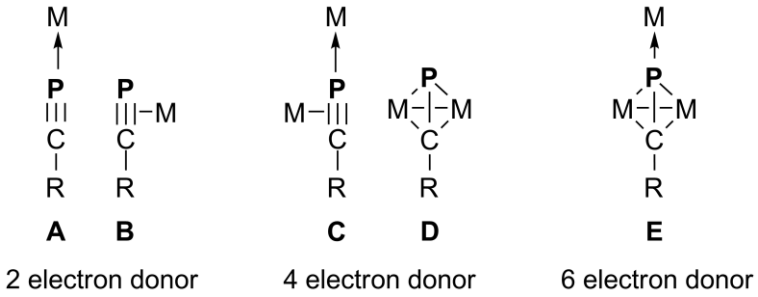

Figure 4-1 Possible coordination modes for phosphaalkynes as 2, 4 and 6 electron donors.

However, with a suitable environment available on the metal complex, end-non complexes can be realised for phosphaalkynes. The first example was characterised by Nixon et al. who were able to coordinate adamantyl phosphaalkyne AdC≡P on a molybdenum complex to form *trans*-[Mo(η^1-P≡CAd)$_2$(depe)$_2$] (depe = $Et_2PCH_2CH_2PEt_2$) in 1987 (see Figure 4-1 **I**).[2] This coordination mode could also be realised over time for other metal complexes of ruthenium, iron, cobalt and tungsten.

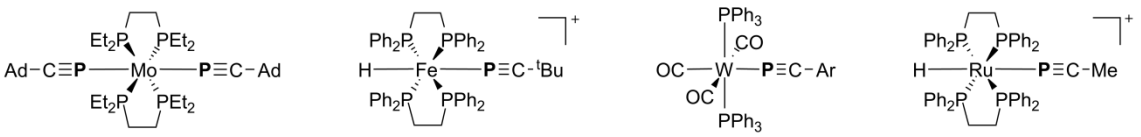

I, Nixon 1987 **II**, Nixon 1998 **III**, Scheer 1998 **IV**, Jones 2008

Ar = 2,4,6-$C_6H_2tBu_3$

Figure 4-2 Examples of end-on coordination of phosphaalkynes on metal centres. **I**: First structurally characterised η^1-complex of AdC≡P.[2] **II**: First structurally characterised complex of *t*BuC≡P.[3] **III**: First structurally characterised end-on complex of MesCP (Mes = 2,4,5-$C_6H_2tBu_3$).[4] **IV**: First end-on complex of MeC≡P.[5]

However, the reasons for this are the Lewis acidity and the sterical properties of the metal complexes used. Only if the side-on coordination is impossible due to steric strain on the metal centre an end-on coordination mode will ensue. For *t*BuC≡P , the bond length of the coordinated phosphaalkyne will decrease from 1.542(2) Å in the uncoordinated form[6] to 1.512(5) Å in the end-on complex *trans*-[FeH(η^1-P≡C*t*Bu)(dppe)$_2$][BPh_4] (dppe = $Ph_2PCH_2CH_2PPh_2$, cf. Figure 4-2 **II**).[3] Also aromatic substituents on a phosphaalkyne could be coordinated end-on to a sterically shielded tungsten centre (Figure 4-2 **III**).[4] In the last years, the end-on coordination could also be observed for the kinetically not stabilised methyl phosphaalkyne (Figure 4-2 **IV**).[5]

Interestingly, hydrometalation processes (which are well-known for alkynes) have only been investigated in the late 90s of the last century.[7] Here, the phosphaalkyne (typically *t*BuC≡P) is inserted into a metal-hydride bond and thus reduced to form the corresponding σ-phosphaalkenyl complex. Subsequent reaction with oxygen leads to the formation of a λ^5-phosphaalkenylmetallacycle. Additionally, the groups of Nixon and Pombeiro obtained a rare phosphinidene oxide complex upon hydrolysis of their rhenium complex [ReCl(dppe)$_2$(η^1-P≡C*t*Bu)].[8] The complex *trans*-[FeH(η^1-*t*BuC≡P)(dppe)$_2$][BF_4] can undergo a stepwise reduction of the phosphaalkyne with HBF_4 to form a fluorophosphine complex *trans*-[FeH(η^1-PF_2CH_2*t*Bu)(dppe)$_2$][BF_4].[3] This leads to the conclusion that end-on phosphaalkyne coordination complexes are excellent starting materials for further investigations concerning the properties of "naked" phosphaalkynes.

The cationic ruthenium complex [Cp*Ru(dppe)]$^+$ has been known to stabilise highly reactive E_4 tetrahedrons end-on (E = P,[9] As[10]). As this complex proves to have an excellent steric environment for end-on coordination, we wanted to coordinate phosphaalkynes and nitriles onto this tetrahedral complex to compare their features. Herein we report on end-on coordination of *tert*-butyl phosphaalkyne and subsequent hydrolysis of the complex. Moreover, complexes of the smaller phosphaalkyne MeC≡P have been prepared and compared to complexes of MeC≡N.

4.2 Results and Discussion

In a salt metathesis reaction between [Cp*Ru(dppe)Cl] and Tl[A] (A = pftb, PF_6), the reactive $[Cp^*Ru(dppe)]^+[A]^-$ (**1a**: A = pftb; **1b**: A = PF_6) with a vacant coordination site is generated in situ and used as is in all following reactions.[10] The thus generated complexes **1a** and **1b** have been reacted with *t*BuC≡P, MeC≡P and MeC≡N to compare the influence of the different sterical demands as well as electronics in these reactions.

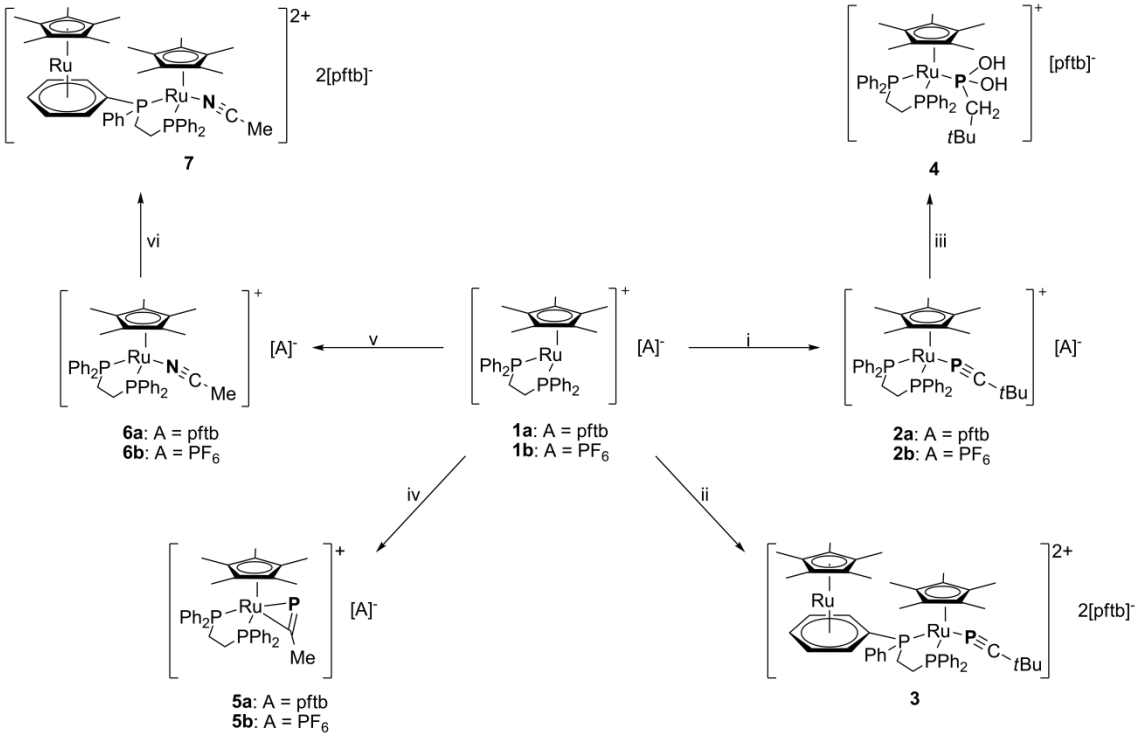

Scheme 4-1 Reaction pathways of **1a** and **1b**: i) *t*BuC≡P in CH_2Cl_2, -80 °C → r.t.; ii) *t*BuC≡P in CH_2Cl_2 at r.t., iii) subsequent hydrolysis of **2a**; iv) $CH_3C{\equiv}P$ in CH_2Cl_2, -80 °C → r.t.; v) $CH_3C{\equiv}N$ in CH_2Cl_2, -80 °C → r.t.; v) subsequent product after crystallisation.

When **1a** was reacted with *t*BuC≡P at -80°C, the $^{31}P\{^1H\}$ NMR spectrum was monitored at different temperatures. At -80 °C, there is no sign of reaction of the two compounds. Starting at -60 °C, the reaction starts: Both the phosphaalkyne and the dppe singlet of the educt complex **1a** decrease and give rise to a triplet at δ = 35 ppm (P≡C*t*Bu) and a doublet at δ = 70 ppm (dppe) which are coupling with each other ($^2J_{PP}$ = 53 Hz; cf. Figure 4-3).

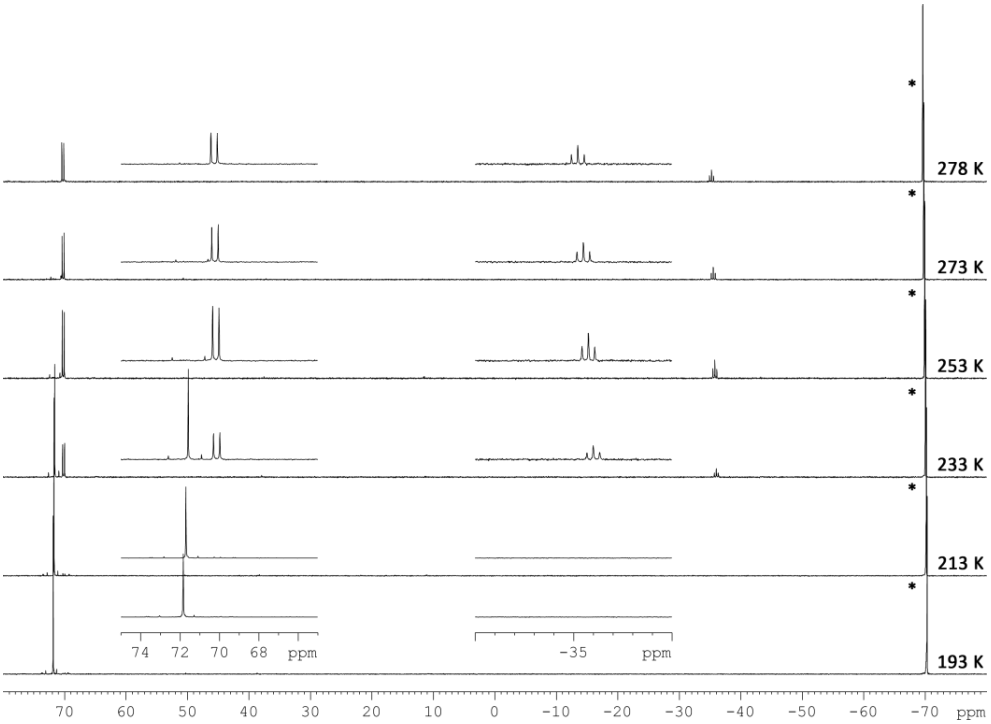

Figure 4-3 Reaction control $^{31}P\{^{1}H\}$ NMR spectra of **3** from -80 °C to room temperature in CD_2Cl_2. Signal marked with an asterisk is excess *t*BuC≡P.

As no other signals (except the signal for excess *t*BuC≡P) could be observed, a clean reaction is assumed to form [Cp*Ru(dppe)(η^1-*t*BuC≡P)] (**2a**) (cf. Scheme 4-1 **i**). Mass analysis of the reaction mixture and elemental analysis of the yellow powder obtained upon removal of the solvent support the suggestion that **2a** indeed is formed exclusively under these conditions. Crystallisation from diffusion of hexane into a layer of the substance in CH_2Cl_2 however yields only yellow crystals of the different product [{Cp*Ru(dppe)}{Cp*Ru}(η^1-*t*BuC≡P)]$^{2+}$·2[pftb]$^-$ (**3**) which could be structurally characterised by x-ray crystallography. Here, an additional [Cp*Ru] fragment is coordinated to one phenyl group of the dppe ligand. This product could also be obtained by conducting the reaction at room temperature. Yellow needles of **3** crystallise in the monoclinic space group *Cc*; the molecular structure is depicted in Figure 4-4.

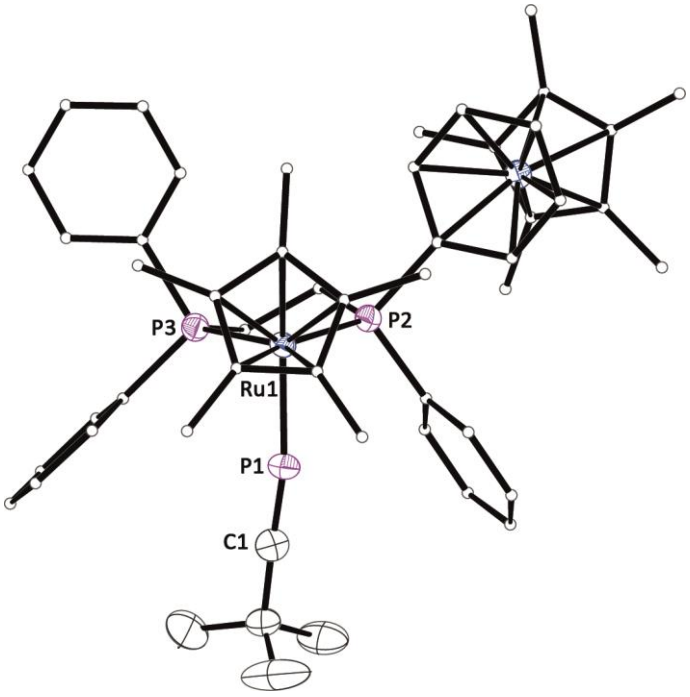

Figure 4-4 Molecular structure of the cation of **3** in the solid state. Hydrogen atoms are omitted for clarity, carbon framework of the ligands is shown in ball-and-stick representation. Thermal ellipsoids are shown at 50% probability level. Selected bond lengths [Å] and angles [°]: C1-P1 1.532(7), P1-Ru1 2.2508(15), P2-Ru 2.3150(14), P3-Ru1 2.3262(15), C1-P1-Ru1 168.6(3), P1-Ru1-P2 90.35(6), P1-Ru1-P3 87.29(5).

In the coordinated η^1-phosphaalkyne, the phosphorus-carbon bond length is 1.536(5) Å and therefore close to free phosphaalkyne (1.542(2) Å).[6] This, in combination with the nearly linear P1-C1-C2 angle of 176.1(5)°, leads to the conclusion of an intact phosphaalkyne moiety coordinated with the phosphorus lone pair towards the ruthenium atom. The execution of the reaction at room temperature to form **3** could be the reason why an additional {Cp*Ru} fragment is eliminated from a second molecule of **1a** and coordinates to a phenyl group of the dppe ligand. As reaction mixtures of **2a** are dried *in vacuo* and washed with hexane before uptake in CH_2Cl_2 and subsequent crystallisation by layering with an apolar solvent, the dppe ligand is likely removed from the mixture. Also direct crystallisation from the crude reaction mixture (with or without layering of hexane) failed. Because crystallographic problems arise from the use of the pftb anion, the reaction has also been conducted with **1b** to circumvent these obstacles. Although NMR and mass spectrometry as well as elemental analyses show the formation of **2b** in a similar fashion as **2a**, no crystals could be grown from concentrated solutions or layering solutions of **2b** with hexane or pentane. This shows that the choice of anion does not affect the product which is formed but unfortunately does not improve the crystallisation process either.

Interestingly, compound **2a** can be reacted with two equivalents of H_2O in CH_2Cl_2 to form [Cp*Ru(dppe)(η^1-P(OH)$_2$CH$_2$*t*Bu)] (**4**, see Scheme 4-1 **ii**). X-Ray structure analysis of yellow **4**

confirms the molecular structure. The compound crystallises in monoclinic space group $P2_1/c$ (cf. Figure 4-5).

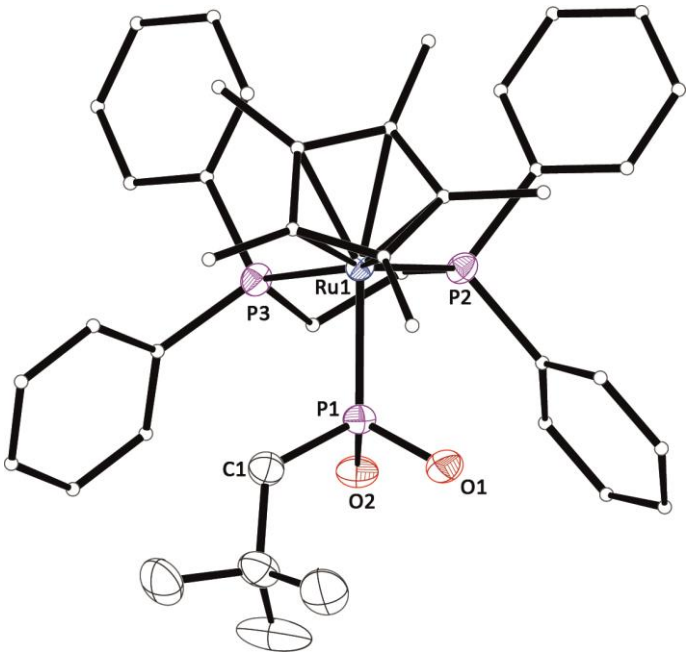

Figure 4-5 Molecular structure of the cation of **4** in the solid state. Hydrogen atoms are omitted for clarity, carbon framework of the ligands is shown in ball-and-stick representation. Thermal ellipsoids are shown at 50% probability level. Selected bond lengths [Å] and angles [°]: Ru1-P1 2.2587(10), P1-O1 1.615(3), P1-O2 1.619(3), P1-C1 1.820(4), P1-Ru1-P2 88.51(3), P1-Ru1-P3 93.17(4), C1-P1-Ru1 116.34(14), O1-P1-Ru1 114.23(12), O1-P1-O2 102.35(17).

The bond length between the carbon and phosphorus atoms (1.822 Å) and the angles on both the carbon and the phosphorus atom lead to the conclusion that a sp^3 hybridised carbon atom and a sp^3 hybridised phosphorus atom are present in **4**. The phosphorus oxygen bond lengths are equally long and resemble single bonds, so definitely two hydroxyl groups are present in compound **4**. The Ru-P bond is of similar length as in **3**. The ^{31}P and $^{31}P\{^1H\}$ NMR spectra of the reaction mixture show the formation of different products with corresponding peaks for the dppe ligands as well as for the phosphorus atom in different phosphine oxides, phosphinidenes and the phosphaalkyne. Signals corresponding to each other are a triplet at $\delta = 231$ ppm which couples with a dublet at 77.2 ppm ($^2J_{PP}$ = 54 Hz) and a triplet at $\delta = 185$ ppm which couples with a dublet at 79 ppm ($^2J_{PP}$ = 47 Hz). The signals are in a ratio of 1:4 with additional signals for complex **2a** and small residues of **1a**. A comparison of compound **4** can be made with the complex *trans*-[ReCl(dppe)$_2$(P≡C*t*Bu)] of the groups of Pombeiro and Nixon who report on the nucleophilic attack of one equivalent of water on this compound (see Scheme 4-2).[8]

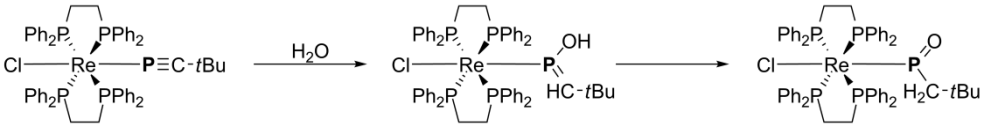

Scheme 4-2 Reaction of *trans*-[ReCl(dppe)(P≡C*t*Bu)] with one equivalent of water and subsequent hydrogen shift to form the phosphinidene-oxide.

To see whether also the kinetically unstabilised methyl phosphaalkyne could be coordinated end-on, similar reactions were carried out to get complexes of the general formula [Cp*Ru(dppe)(P≡CMe)][pftb] (**5a**) and [Cp*Ru(dppe)(P≡CMe)][PF_6] (**5b**) (Scheme 4-1 **iv**). Unfortunately, neither the low temperature nor the room temperature route led to the desired products. The ^{31}P NMR spectra of the reaction mixtures only reveal that the dppe ligands are chemically not equivalent and that another phosphorus atom, arguably of the former phosphaalkyne, was found lowfield shifted at $\delta = 176$ ppm (**5a**) or 250 ppm (**5b**) respectively. Crystals suitable for X-ray analysis could not yet be obtained, so it was impossible to gain an insight into the nature of the obtained products. However, the shifts are in the region for P=C double bonds which could suggest that the smaller phosphaalkyne rather prefers a side-on coordination. As to emphasise the differences not only between methyl phosphaalkyne and *tert*-butyl phosphaalkyne but methyl phosphaalkyne and acetonitrile, respectively, the acetonitrile complexes [Cp*Ru(dppe)(η^1-N≡CMe)][pftb] (**6a**) and [Cp*Ru(dppe)(η^1-N≡CMe)][pftb] (**6b**) have been prepared as well (see Scheme 4-1 **v**). Here, in agreement with the available lone pair on the group 15 element, the end-on complexes could be obtained in good yields of about 60%. ^{31}P and ^{31}P{^{1}H} NMR spectra only show a singlet for the chemically equivalent phosphorus atoms on the dppe ligand and mass spectra and elemental analysis support the suggestion of end-on complexes of acetonitrile. However, again only crystals of [{Cp*Ru(dppe)}{Cp*Ru}(η^1-N≡CMe)]$^{2+}$·2[pftb]$^-$ (**7**) suitable for X-ray structure analysis are formed (Figure 4-6).

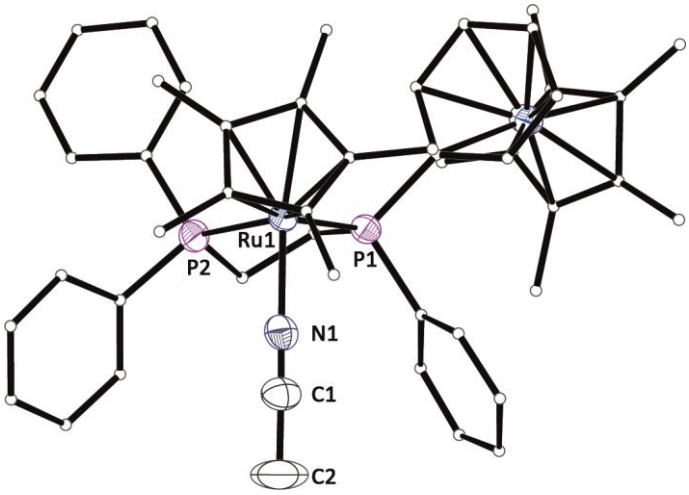

Figure 4-6 Molecular structure of the cation of **7** in the solid state. Hydrogen atoms are omitted for clarity, carbon framework of the ligands is shown in ball-and-stick representation. Thermal ellipsoids are shown at 50% probability level. Selected bond lengths [Å] and angles [°]: Ru1-N1 2.068(6), N1-C1 1.103(10), C1-C2 1.464(12), C1-N1-Ru1 172.1(6).

The smooth elimination of the dppe ligand from **1a** in this case could be caused by an associative substitution of dppe by acetonitrile which leads to the formation of a $[(CH_3CN)_3RuCp^*][pftb]$ complex. This complex could subsequently exchange CH_3CN for the phenyl group of another dppe ligand at room temperature. Acetonitrile to arene ligand exchange has been thoroughly studied for cationic ruthenium complexes and is favoured by ΔH = 3.4 kcal/mol in pure benzene, and up to 7.5 kcal/mol for substituted benzene aromats like dimethylaniline.[11]

4.3 Conclusions

The comparison between the reactivity of phosphaalkynes and nitriles shows that although the Lewis acidic compound $[Cp^*Ru(dppe)]^+[A]^-$ (A = pftb: **1a**; A = PF_6: **1b**) is suitable for an end-on coordination of the sterically hindered *t*BuC≡P, the smaller phosphaalkyne MeC≡P rather reacts in a side-on fashion as can be determined by ^{31}P NMR spectroscopy. $^{31}P\{^1H\}$ VT studies suggest that the reaction of **1a** and *t*BuC≡P leads to the formation of $[Cp^*Ru(dppe)(\eta^1\text{-}t\text{BuC}\equiv P)]^+[A]^-$ (A = pftb: **2a**; A = PF_6: **2b**) exclusively, however only crystals of $[\{Cp^*Ru(dppe)\}\{Cp^*Ru\}(\eta^1\text{-}t\text{BuC}\equiv P)]^{2+}$ $2[pftb]^-$ (**3**) containing an additional [Cp*Ru] fragment could be obtained. This product is also formed exclusively when the reaction is conducted at r.t. To take the size effect into consideration we also conducted the reactions of **1a**/**1b** with MeC≡P. As the space demand of this phosphaalkyne is considerably smaller, instead of the end-on coordination complexes like **2a**/**2b** the side-on complexes $[Cp^*Ru(dppe)(\eta^2\text{-MeC}=P)]^+[A]^-$ (A = pftb: **5a**; A = PF_6: **5b**) are formed which can be determined by phosphorus NMR spectroscopy of the products. With a nitrile of a similar size however,

complexes [Cp*Ru(dppe)(η^1-MeC≡N)]$^+$[A]$^-$ (A = pftb: **6a**; A = PF_6: **6b**) have been synthesised. This is due to the lone pair of nitriles being the HOMO of the molecule. Here, also only the complex with an additional {Cp*Ru} fragment [{Cp*Ru(dppe)}{Cp*Ru}(η^1-MeC≡N)]$^+$[pftb]$^-$ (**7**) could be structurally characterised. Another interesting starting point to further research is the formation of the phosphine product [Cp*Ru(dppe)(η^1-P(OH)$_2$CH$_2$*t*Bu)][pftb] (**4**), which is formed after hydrolysis of **2a**.

4.4 Supporting Information

4.4.1 Experimental

All steps were performed under an atmosphere of dry nitrogen with standard Schlenk techniques. All solvents were freshly collected from a Solvent Purification System (SPS) by M. Braun and were degassed prior to use. All NMR spectra have been recorded using deuterated dichloromethane or chloroform, which were dried over CaH_2, refluxed for three hours and then distilled under inert atmosphere. [Cp*Ru(dppe)Cl],[12] Tl[pftb],[13] *t*BuC≡P[14] and MeC≡P[15] were synthesised according to literature procedures. $TlPF_6$ was purchased and handled as received in a dry glove box.

Synthesis of 1a

A solution of 178 mg Tl[pftb] (0.15 mmol) in 3 ml CH_2Cl_2 is added to a solution of [Cp*Ru(dppe)Cl] (100 mg, 0.15 mmol) in CH_2Cl_2 (3 mL) at room temperature. The solution is stirred for 15-30 minutes until a thick colourless precipitate of TlCl is formed. The solution is filtered via cannula and used without crystallisation.

Synthesis of 1b

A solution of 52 mg $TlPF_6$ (0.15 mmol) in 3 ml CH_2Cl_2 is added to a solution of [Cp*Ru(dppe)Cl] (100 mg, 0.15 mmol) in CH_2Cl_2 (3 mL) at room temperature. The solution is stirred for 15-30 minutes until a thick colourless precipitate of TlCl is formed. The solution is filtered via cannula and used without crystallisation.

Synthesis of [Cp*Ru(dppe)(η¹-*t*BuC≡P)]⁺[A]⁻ (A = pftb: 2a; A = PF_6: 2b)

A solution of **1a** or **1b** in CH_2Cl_2 is cooled to -80 °C. To this solution, 0.15 mmol *t*BuC≡P are added at once and the mixture is stirred until it reaches room temperature. The next day, the solution is layered under 10 ml of pure hexane and left to crystallise. If no crystals were obtained, the solutions were dried *in vacuo* and the resulting powder was washed with hexane and analysed. From the crude mixture of **2a**, upon recrystallisation only crystals of **3** could be obtained.

Analytical data for 2a:

Yield 122 mg, 48%

^{1}H-NMR (CD_2Cl_2)	δ [ppm] = 0.88 (d, $^4J_{PH}$ = 1.5 Hz, 9H, *t*BuC≡P), 1.61 (pq, $^4J_{PH}$ = 1.8 Hz, $^4J_{PH}$ = 3.6 Hz, 15H, Cp*), 2.53-2.69 (m, 4H, dppe), 7.19-7.58 (m, 20H, dppe)
^{31}P-NMR (CD_2Cl_2)	δ [ppm] = -35.7 (t, $^2J_{PP}$ = 54.4 Hz, *t*BuC≡P), 70.1 (d, $^2J_{PP}$ = 54.4 Hz, dppe)

$^{31}P\{^1H\}$-NMR (CD_2Cl_2)	δ [ppm] = -35.7 (t, $^2J_{PP}$ = 54.4 Hz, *t*BuC≡P), 70.1 (d, $^2J_{PP}$ = 54.4 Hz, dppe)
$^{19}F\{^1H\}$-NMR (CD_2Cl_2)	δ [ppm] = -75.8 (s, pftb)
Cation ESI-MS (CH_2Cl_2)	*m/z* [%] = 735.2 (100) $[M]^+$, 635.1 (83) $[M\text{-}t\text{BuC}{\equiv}P]^+$
Anion ESI-MS (CH_2Cl_2)	*m/z* [%] = 967.1 (100) $[pftb]^-$
Elemental analysis	calculated for $C_{57}H_{48}AlF_{36}O_4P_3Ru{\cdot}CH_2Cl_2$ (1786.05 g/mol): C 38.96, H 2.82 found: C 39.18, H 3.63

Analytical data for 2b:

Yield 43 mg, 33%

$^{31}P\{^1H\}$-NMR (CD_2Cl_2)	δ [ppm] = -143.7 (s, $^1J_{PF}$ = 710 Hz, PF_6), -34.3 (t, *t*BuC≡P, $^2J_{PP}$ = 54 Hz, dppe), 70.1 (d, $^2J_{PP}$ = 54 Hz, dppe), 76.9 (d, $^2J_{PP}$ = 54 Hz, dppe)
$^{19}F\{^1H\}$-NMR (CD_2Cl_2)	δ [ppm] = -73.3 (d, $^1J_{PF}$ = 710 Hz, PF_6)
Cation ESI-MS (CH_2Cl_2)	m/z [%] = 735.3 (47) $[M]^+$, 635.2 (100) $[M\text{-}t\text{BuC}{\equiv}P]^+$
Anion ESI-MS (CH_2Cl_2)	m/z [%] = 144.8 (100) $[PF_6]^-$
Elemental analysis	calculated for $C_{41}H_{48}F_6P_4Ru{\cdot}C_6H_{14}$ (966.27 g/mol): C 58.44, H 6.47 found: C 60.82, H 5.99

Analytical data for (3):

Cation ESI-MS (CH_2Cl_2)	*m/z* [%] = 771.3 (53) $[M+2H_2O]^+$, 669.2 (34) $[M+Cl\text{-}t\text{BuC}{\equiv}P]^+$, 635.2 (100) $[M\text{-}t\text{BuC}{\equiv}P]^+$
Anion ESI-MS (CH_2Cl_2)	*m/z* [%] = 967.0 (100) $[pftb]^-$

Synthesis of [Cp*Ru(dppe)(η¹-P(OH)₂CH₂*t*Bu)]·[pftb]⁻ (4)

To a solution of 0.1 mmol **2a** in 5 ml CH_2Cl_2 0.1 mmol H_2O in 3 ml CH_2Cl_2 are added at room temperature and the mixture is stirred for twelve hours. The solution is layered under 10 ml of pure hexane and left to crystallise at -30 °C. Although NMR studies only suggest that **2a** is present in solution, few crystals of **4** suitable for X-ray analysis could be obtained.

$^{31}P\{^1H\}$ NMR (CD_2Cl_2)	δ [ppm] = 231 (t, $^2J_{PP}$ = 54 Hz), 77.2 (d, $^2J_{PP}$ = 54 Hz), 185 (t, $^2J_{PP}$ = 47 Hz), 79 (d, $^2J_{PP}$ = 47 Hz)
Cation ESI-MS (CH_2Cl_2)	*m/z* [%] = 771.3 (100) $[M]^+$, 485 (5) $[M+(Cp^*Ru)]^{2+}$,
Anion ESI-MS (CH_2Cl_2)	*m/z* [%] = 967.1 (100) $[pftb]^-$

Reaction of [Cp*Ru(dppe)]⁺[A]⁻ with MeC≡P (A = pftb: 5a; A = PF_6: 5b)

To a solution of **1a** or **1b** in 5 ml CH_2Cl_2 at -80 °C are added 0.15 mmol MeC≡P and the mixture is stirred for twelve hours. The solutions are dried *in vacuo* and taken up in 5 ml fresh CH_2Cl_2. The mixture is then layered under 10 ml of pure hexane and left at 5 °C. As no crystals

were obtained, the crude mixture was dried *in vacuo* and the resulting powder was washed with hexane and analysed subsequently.

Analytical data for 5a:

Yield: brown-orange powder, 142 mg, 54%.

$^{31}P\{^{1}H\}$-NMR (CD_2Cl_2)	δ [ppm] = 70.3 (s, educt), 78.7 (d, 2P, $^{2}J_{PP}$ = 50 Hz, P(C_6H_5)$_2$), 177 (t, 1P, $^{2}J_{PP}$ = 50 Hz, MeC=P)
$^{19}F\{^{1}H\}$-NMR (CD_2Cl_2)	δ [ppm] = -75.8 (s, pftb)
Cation ESI-MS (CH_2Cl_2)	*m/z* [%] = 771.2 (18) [MH+$C_5(CH_3)_5$-MeCP]$^+$, 729.2 (100) [M+Cl]$^+$, 635.2 (82) [M-MeC≡P]$^+$
Anion ESI-MS (CH_2Cl_2)	*m/z* [%] = 967.1 (100) [pftb]$^-$
Elemental analysis	calculated for $C_{54}H_{42}AlF_{36}O_4P_3Ru \cdot CH_2Cl_2$ (1744.01 g/mol): C 37.84, H 2.54 found: C 37.65, H 3.09

Analytical data for 5b:

Yield: brown-orange powder, 51 mg, 39%.

$^{31}P\{^{1}H\}$-NMR ($CDCl_3$)	δ [ppm] = -143.9 (s, $^{1}J_{PF}$ = 713.1 Hz, PF_6), 76.3 (d, 2P, $^{2}J_{PP}$ = 50 Hz, dppe), 250 (t, 1P, $^{2}J_{PP}$ = 50 Hz, C=P)
$^{19}F\{^{1}H\}$-NMR ($CDCl_3$)	δ [ppm] = -73.3 (d, $^{1}J_{PF}$ = 712.6 Hz, PF_6)
Cation ESI-MS (CH_2Cl_2)	*m/z* [%] = 729.2 (34) [M+Cl]$^+$, 692.8.2 (8) [M]$^+$, 635.2 (100) [M-MeC≡P]$^+$
Anion ESI-MS (CH_2Cl_2)	*m/z* [%] = 144.8 (100) [PF_6]$^-$
Elemental analysis	calculated for $C_{38}H_{42}F_6P_4Ru \cdot 0.5C_6H_{14}$ (881.17 g/mol): C 55.83, H 5.60 found: C 56.04, H 5.77

Synthesis of [Cp*Ru(dppe)(η^1-MeC≡N)]$^+$[A]$^-$ (A = pftb: 6a; A = PF_6: 6b)

A solution of **1a** or **1b** in CH_2Cl_2 is cooled to -80 °C. To this solution, 1 ml (exc.) MeC≡N are added at once and the mixture is stirred until it reaches room temperature. The next day, the solution is dried *in vacuo*, taken up in 5ml CH_2Cl_2 and layered under 10 ml of pure hexane and left to crystallise at -30 °C. If no crystals were obtained, the solutions were dried *in vacuo* and the resulting powder was washed with hexane and analysed. From the crude mixture of **6a**, upon recrystallisation only crystals of **7** could be obtained.

Analytical data for 6a:

Yield: dark yellow solid, 162 mg, 66%.

^{1}H-NMR ($CDCl_3$)	δ [ppm] = 1.44 (s, 15H, Cp*], 1.66 (s, 3H, MeCN, br), 2.35-2.46 (m, 4H, dppe), 7.43-7.53 (m, 20H. dppe)
^{31}P-NMR ($CDCl_3$)	δ [ppm] = 76.1 (s, dppe)
$^{31}P\{^{1}H\}$-NMR ($CDCl_3$)	δ [ppm] = 76.3 (s, dppe)
$^{19}F\{^{1}H\}$-NMR ($CDCl_3$)	δ [ppm] = -75.7 (s, pftb)

Cation ESI-MS (CH_2Cl_2)	*m/z* [%] = 676.2 (15) $[M]^+$, 635.2 (100) $[M\text{-}MeCN]^+$
Anion ESI-MS (CH_2Cl_2)	*m/z* [%] = 967.1 (100) $[pftb]^-$
Elemental analysis	calculated for $C_{54}H_{42}AlF_{36}NO_4P_2Ru \cdot CH_2Cl_2$ (1727.04 g/mol): C 38.21, H 2.56, N 0.81 found: C 38.91, H 2.63, N 0.69

Analytical data for 6b:

Yield: dark yellow powder, 75 mg, 61%.

^{1}H-NMR ($CDCl_3$)	δ [ppm] = 1.44 (t, $^4J_{PH}$ = 1.6 Hz, 15H, Cp*), 1.64 (s, 3H, MeCN), 2.28-2.51 (m, 4H, dppe), 7.42-7.55 (m, 20H, dppe)
^{31}P-NMR ($CDCl_3$)	δ [ppm] = -143.7 (s, $^1J_{PF}$ = 710.3 Hz, PF_6), 75.8 (s, dppe)
$^{31}P\{^1H\}$-NMR ($CDCl_3$)	δ [ppm] = -143.7 (s, $^1J_{PF}$ = 711.0 Hz, PF_6), 75.8 (s, dppe)
$^{19}F\{^1H\}$-NMR ($CDCl_3$)	δ [ppm] = -73.6 (d, $^1J_{PF}$ = 710.4 Hz, PF_6)
Cation ESI-MS (CH_2Cl_2)	*m/z* [%] = 676.2 (11) $[M]^+$, 667.1 (43) $[M\text{-}MeCN\text{+}O_2]^+$, 635.2 (100) $[M\text{-}MeCN]^+$
Anion ESI-MS (CH_2Cl_2)	*m/z* [%] = 144.8 (100) $[PF_6]^-$
Elemental analysis	calculated for $C_{38}H_{42}F_6NP_3Ru \cdot 0.5C_6H_{14}$ (864.20 g/mol): C 56.93, H 5.71, N 1.62 found: C 57.06, H. 5.49, N 1.24

Analytical data for 7:

light yellow needles, few crystals.

Cation ESI-MS (CH_2Cl_2)	*m/z* [%] = 676.2 (20) $[M\text{-}Cp^*Ru]^+$, 635.1 (15) $[M\text{-}Cp^*Ru\text{-}CH_3CN]^+$, 456.3 (100) $[M]^{2+}$
Anion ESI-MS (CH_2Cl_2)	*m/z* [%] = 967.0 (100) $[pftb]^-$

4.4.2 Crystallographic Data

All structures have been processed using Olex2,[16] the structures were solved with the SIR92[17] or ShelXT[18] structure solution program, using the Direct Methods solution method. The models were refined with version 2014/6 of ShelXL[19] using Least Squares minimisation. Experimental and crystal data created by ReportPlus in Olex2.

4.4.2.1 Compound 3

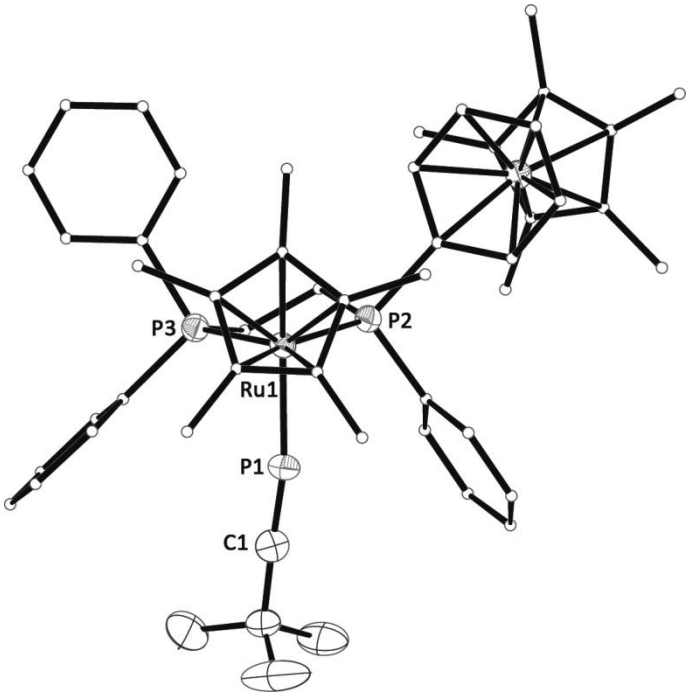

Figure 4-7 Molecular structure of the cation of **3** in the solid state. Hydrogen atoms are omitted for clarity, carbon framework of the ligands is shown in ball-and-stick representation. Thermal ellipsoids are shown at 50% probability level. Selected bond lengths [Å] and angles [°]: C1-P1 1.532(7), P1-Ru1 2.2508(15), P2-Ru 2.3150(14), P3-Ru1 2.3262(15), C1-P1-Ru1 168.6(3), P1-Ru1-P2 90.35(6), P1-Ru1-P3 87.29(5).

Single yellow needle shaped crystals of **3** were obtained by recrystallisation from diffusion of hexane into a solution of **3** in CH_2Cl_2. A suitable crystal (0.16x0.13x0.08) was selected and mounted on a mylar loop on a Xcalibur, AtlasS2, Gemini ultra diffractometer.. The crystal was kept at T = 123(1) K during data collection.

Crystal Data for **3**. $C_{84}H_{65}O_8F_{72}Al_2P_3Ru_2Cl_2$, M_r = 2990.27, monoclinic, *Cc* (No. 9), a = 16.5571(2) Å, b = 29.6151(3) Å, c = 22.3331(3) Å, β = 101.8700(10)°, V = 10716.6(2) Å^3, T = 293(2) K, Z = 4, Z' = 1, μ(CuK$_\alpha$) = 4.981 mm^{-1}, 42707 reflections measured, 16079 unique (R_{int} = 0.0267) which were used in all calculations. The final wR_2 was 0.0958 (all data) and R_1 was 0.0355 (I > 2σ(I)).

4.4.2.2 Compound 4

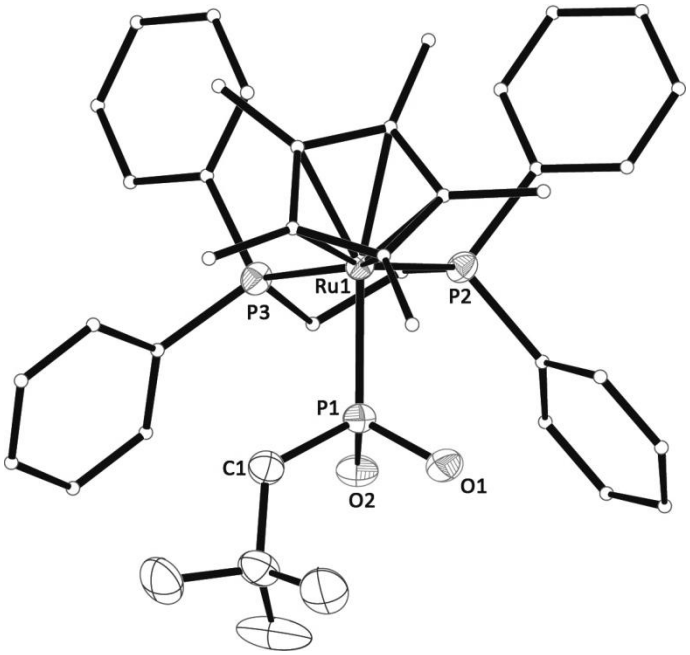

Figure 4-8 Molecular structure of the cation of **4** in the solid state. Hydrogen atoms are omitted for clarity, carbon framework of the ligands is shown in ball-and-stick representation. Thermal ellipsoids are shown at 50% probability level. Selected bond lengths [Å] and angles [°]: Ru1-P1 2.2587(10), P1-O1 1.615(3), P1-O2 1.619(3), P1-C1 1.820(4), P1-Ru1-P2 88.51(3), P1-Ru1-P3 93.17(4), C1-P1-Ru1 116.34(14), O1-P1-Ru1 114.23(12), O1-P1-O2 102.35(17).

Single clear yellow needle shaped crystals of **4** were obtained by recrystallisation from diffusion of hexane into a solution of **4** in CH_2Cl_2. A suitable crystal (0.46×0.26×0.17) was selected and mounted on a mylar loop on a SuperNova, Single source at offset, Atlas diffractometer. The crystal was kept at T = 122.99(18) K during data collection.

Crystal Data for **4**. $C_{58}H_{52}AlCl_2F_{36}O_6P_3Ru$, M_r = 1820.85, monoclinic, $P2_1/c$ (No. 14), a = 13.08840(10) Å, b = 20.88160(10) Å, c = 25.57720(10) Å, β = 90.44°, V = 6990.21(7) Å^3, T = 122.99(18) K, Z = 4, Z' = 1, μ(CuK$_\alpha$) = 4.626 mm^{-1}, 45325 reflections measured, 13858 unique (R_{int} = 0.0227) which were used in all calculations. The final wR_2 was 0.1872 (all data) and R_1 was 0.0642 (I > 2σ(I)).

4.4.2.3 Compound 7

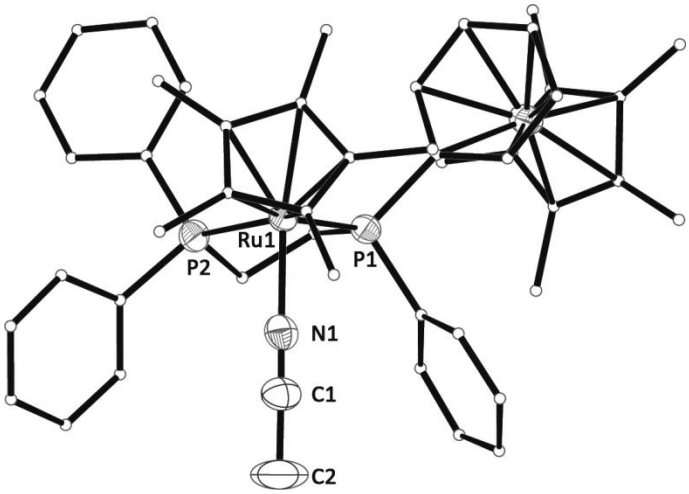

Figure 4-9 Molecular structure of the cation of **7** in the solid state. Hydrogen atoms are omitted for clarity, carbon framework of the ligands is shown in ball-and-stick representation. Thermal ellipsoids are shown at 50% probability level. Selected bond lengths [Å] and angles [°]: Ru1-N1 2.068(6), N1-C1 1.103(10), C1-C2 1.464(12), C1-N1-Ru1 172.1(6).

Single clear light yellow block-shaped crystals of **7** were obtained by recrystallisation from diffusion of hexane into a solution of **7** in CH_2Cl_2. A suitable crystal (0.18×0.07×0.06) was selected and mounted on a mylar loop on a SuperNova, Single source at offset, Atlas diffractometer. The crystal was kept at T = 122.97(19) K during data collection.

Crystal Data for **7**. $C_{81}H_{59}Al_2Cl_2F_{72}NO_8P_2Ru_2$, M_r = 2931.23, triclinic, P-1 (No. 2), a = 16.1015(4) Å, b = 16.4043(4) Å, c = 24.8006(7) Å, α = 100.768(2)°, β = 90.325(2)°, γ = 118.377(2)°, V = 5628.1(3) Å^3, T = 122.97(19) K, Z = 2, Z' = 1, μ(CuK$_\alpha$) = 4.601 mm^{-1}, 18115 reflections measured, 18115 unique, which were used in all calculations. The final wR_2 was 0.2786 (all data) and R_1 was 0.0954 (I > 2σ(I)).

4.5 References

[1] J. C. T. R. B. S. Laurent, M. A. King, H. W. Kroto, J. F. Nixon, R. J. Suffolk, *Dalton Trans.* **1983**, 755.

[2] a) P. B. Hitchcock, M. J. Maah, J. F. Nixon, J. A. Zora, G. J. Leigh, M. Abu Bakar, *Angew. Chem.* **1987**, *99*, 497; b) P. B. Hitchcock, M. J. Maah, J. F. Nixon, J. A. Zora, G. J. Leigh, M. A. Bakar, *Angew. Chem. Int. Ed.* **1987**, *26*, 474.

[3] M. F. Meidine, M. Amélia N. D. A.Lemos, A. J. L. Pombeiro, J. F. Nixon, P. B. Hitchcock, *Dalton Trans.* **1998**, *0*, 3319.

[4] T. Gröer, G. Baum, M. Scheer, *Organometallics* **1998**, *17*, 5916.

[5] C. Jones, C. Schulten, A. Stasch, *Eur. J. Inorg. Chem.* **2008**, *2008*, 1555.

[6] A. N. Chernega, M. Y. Antipin, Y. T. Struchkov, M. F. Meidine, J. F. Nixon, *Heteroat. Chem.* **1991**, *2*, 665.

[7] a) R. B. Bedford, A. F. Hill, C. Jones, *Angew. Chem.* **1996**, *108*, 587; b) R. B. Bedford, A. F. Hill, C. Jones, *Angew. Chem. Int. Ed.* **1996**, *35*, 547; c) R. B. Bedford, A. F. Hill, C. Jones, A. J. P. White, D. J. Williams, J. D. E. T. Wilton-Ely, *Organometallics* **1998**, *17*, 4744.

[8] P. B. Hitchcock, J. A. Johnson, M. A. N. D. A. Lemos, M. F. Meidine, J. F. Nixon, A. J. L. Pombeiro, *Chem. Commun.* **1992**, 645.

[9] a) I. de los Rios, J.-R. Hamon, P. Hamon, C. Lapinte, L. Toupet, A. Romerosa, M. Peruzzini, *Angew. Chem.* **2001**, *113*, 4028; b) I. de los Rios, J.-R. Hamon, P. Hamon, C. Lapinte, L. Toupet, A. Romerosa, M. Peruzzini, *Angew. Chem. Int. Ed.* **2001**, *40*, 3910.

[10] a) C. Schwarzmaier, A. Y. Timoshkin, M. Scheer, *Angew. Chem.* **2013**, *125*, 7751; b) C. Schwarzmaier, A. Y. Timoshkin, M. Scheer, *Angew. Chem. Int. Ed.* **2013**, *52*, 7600.

[11] S. P. Nolan, K. L. Martin, E. D. Stevens, P. J. Fagan, *Organometallics* **1992**, *11*, 3947.

[12] M. I. E. Bruce, Benjamin G.; Low, Paul J.; Skelton, Brian W.; White, Allan H., *Organometallics* **2003**, 3184.

[13] M. Gonsior, I. Krossing, N. Mitzel, *Z. Anorg. Allg. Chem.* **2002**, *628*, 1821.

[14] G. Becker, G. Gresser, W. Uhl, *Z. Naturforsch., Teil B* **1981**, *36B*, 16.

[15] J.-C. Guillemin, T. Janati, J.-M. Denis, *J. Org. Chem.* **2001**, 7864.

[16] O. V. Dolomanov, L. J. Bourhis, R. J. Gildea, J. A. K. Howard, H. Puschmann, *J. Appl.*

Crystallogr. **2009**, *42*, 339.

[17] A. Altomare, G. Cascarano, C. Giacovazzo, A. Guagliardi, *J. Appl. Crystallogr.* **1993**, *26*, 343.

[18] G. M. Sheldrick, *Acta Cryst.* **2015**, *A71*, 3.

[19] G. M. Sheldrick, *Acta Cryst.* **2015**, *C71*, 3.

5 Zintl ions and phosphaalkynes: Ways to prepare Polyphospholyl ligands

Eva-Maria Rummel, Christian Benda, Thomas Fässler, Manfred Scheer*

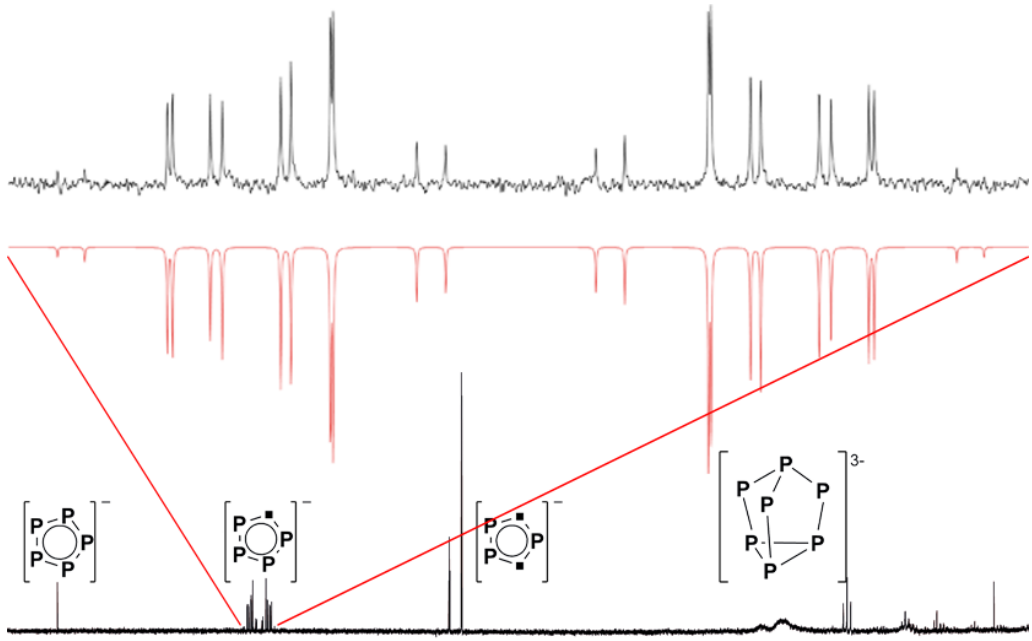

≡ All syntheses and characterisations were performed by Eva-Maria Rummel

≡ Reactions of K_4Ge_9 with *tert*-butyl phosphaalkyne have been conducted within the scope of a cooperation with Christian Benda from the working group of Prof. Dr. Thomas Fässler. The results are also part of his doctoral thesis. K_4Ge_9 was produced and provided by Christian Benda (TU München).

≡ Figures were made by Eva-Maria Rummel

≡ Manuscript was written by Eva-Maria Rummel

5.1 Introduction

For several years now, click chemistry has been an intensive research topic.[1] If one is asked for a typical "click reaction" most will mention the [2+3] cycloaddition of alkynes with azides to form 1,2,3-triazoles. According to the diagonal relationship between alkynes and phosphaalkynes, phosphaalkynes react in the same way with azides resulting in 1,2,3,4-triazaphospholes (Figure 5-1 **V**).[2] But also other cycloaddition reactions are known for different 1,3-dipolar substrates (cf. Figure 5-1 **I-IV**). Interestingly, reduction of *tert*-butyl phosphaalkyne with Na/Hg also leads to a 1,2,4-triphospholyl ring[3] which is also obtained by from the reaction of $LiP(SiMe_3)_2$ and *t*BuC≡P (Figure 5-1 **VI**).[4] The latter two reactions, however, do not belong to click chemistry as they are not atom efficient.

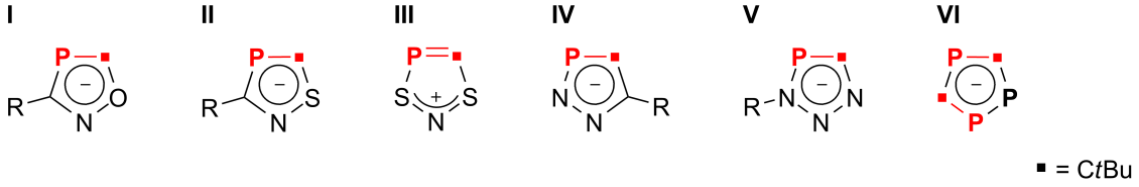

Figure 5-1 Heteroatomic rings derived from *tert*-butyl phosphaalkyne.

The 6π aromatic five membered rings with one to five carbon atoms exchanged for phosphorus atoms belong to the class of (poly-)phospholyl (or (poly-)phospholide) rings and are well known in the literature.[5] This is easily understandable due to the isolobal relationship between phosphorus and methine fragments. Up to date, all possible parent n-phospholyl systems (n = 1-5, Figure 5-2) as well as a wide range of symmetrical and asymmetrical n-phosphametallocenes ($[(P_n(CR)_{5-n})Fe(P_m(CR)_{5-m})]$, n= 1-3, m= 0-3) have been synthesised.

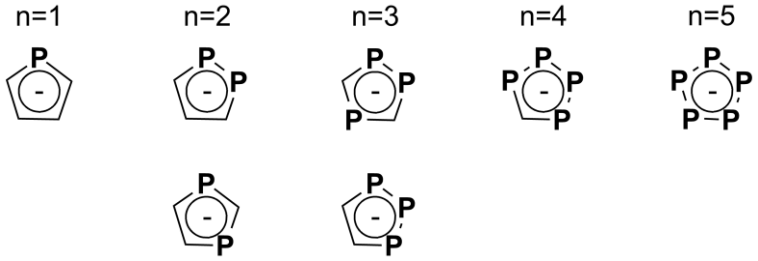

Figure 5-2 All possible n-phospholyl $P_n(CR)_{5-n}$ (n=1-5) rings.

The successful synthesis of the 1,2,4-triphospholyl ring and its complexes has also led to a series of coordination compounds which have been thoroughly characterised and show interesting properties and coordination modes.[6] The structural isomer 1,2,3-triphospholyl cycle and its ferrocene complex has recently made a new impact in two different syntheses: Our own group performed the reaction of the butterfly complex $[\{Cp'''(CO)_2Fe\}_2(\mu,\eta^1{:}\eta^1\text{-}P_4)]$ with monophenylacetylene which led to the ferrocene analogon

[Cp'''Fe(η^5-1,2,3-P_3(C*t*Bu)$_2$)].[6e, 7] Another approach used the reaction of the zintl type ion P_7^{3-} with symmetrical and asymmetrical alkynes yielding a variety of substituted 1,2,3-triphospholides in moderate yields.[8]

Only in recent years also the tetraphospholyl cycles have been targeted and syntheses aimed especially to create these compounds and their tetraphosphaferrocene sandwich complexes have been published.[9] Now the question arises whether also phosphaalkynes are capable of forming analogous cycles in addition to those already known.

5.2 Results and Discussion

5.2.1 Reactions with K_4Ge_9

As the zintl type ions K_4Ge_9 has already been successfully reacted with acetylenes like bis(trimethylsilyl)acetylene in ethylenediamine (will be shortened "en" in the following) to yield $[Ge_9(CHCH_2)_n]^{(4-n)-}$ (n = 1 - 3),[10] the question arose whether similar results could be obtained using *tert*-butyl phosphaalkyne. From first test reactions between the zintl ion K_4Ge_9 and *t*BuC≡P however only a non-evaluable product mixture could be obtained. Stoichiometry and conditions have been tested, and finally it was discovered that the first complications of these reactions arose from the solvent. The solvent used first, en, is the suitable solvent for zintl ions, but not for the phosphaalkyne as NMR measurements confirmed. Only 37% of the phosphaalkyne remain in solution while 63% are reacting with the solvent to form a product mixture (cf. Figure 5-3).

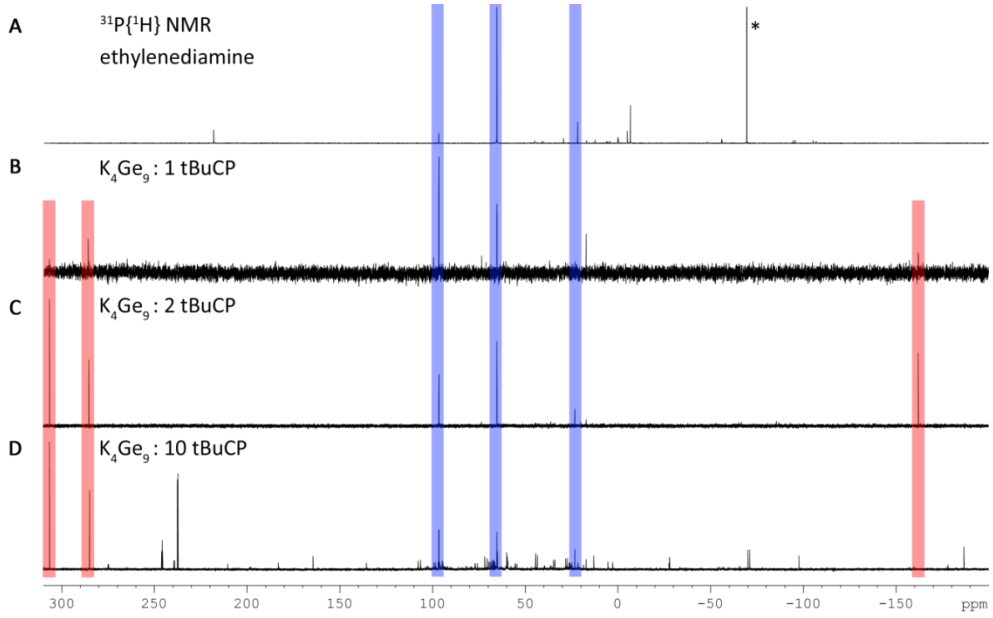

Figure 5-3 $^{31}P\{^1H\}$ NMR spectra of reaction mixtures of K_4Ge_9 and *t*BuC≡P in different stoichiometries in en (measured with C_6D_6 capillary). **A**) *t*BuC≡P in en; signal marked with asterisk is free *t*BuCP; **B**) 1:1; **C**) 1:2; **D**) 1:10 stoichiometry. Blue underlay depicts signals present which are coming from reaction of *t*BuCP and en, red underlay depicts signals present only in the presence of K_4Ge_9. **D**) Signals at 240 ppm are K[P_3(C*t*Bu)$_2$].

From the reactions in en, which have been filtered and subsequently layered with toluene, two known oxidation products of Ge_9^{4-} could be isolated and identified as $[K(18\text{-crown-6})]_6[Ge_9{=}Ge_9{=}Ge_9]\cdot(en)_3\cdot(tol)$[11] and $^1_\infty[K(18\text{-crown-6})]_2[Ge_9]\cdot(en)$.[12] This leads to the conclusion that similarly to the reduction of phosphaalkynes with Na/Hg[3] also the highly reductive germanium clusters are able to reduce phosphaalkynes to yield the known $[K][P_3(C\textit{t}Bu)_2]$ five-membered ring. Other phosphorus containing compounds could not be isolated by washing with aliphatic solvents or fractionalised crystallisation. Mass spectrometric analysis of reaction mixtures (electron spray ionisation, anion mode) has been used to identify several five membered rings with different numbers of *tert*-butyl groups.

Because of the side reaction of the solvent with the phosphaalkyne, all further reactions had to be conducted in acetonitrile. This solvent will solve K_4Ge_9 only poorly but will not react with the phosphaalkyne. Additionally, every reaction mixture has been layered with [18-crown-6] in hexane for an improved crystallisation. From reactions with varying stoichiometric ratios always a mixture of products was formed with different main products: From a 1:4 stoichiometry between K_4Ge_9 and phosphaalkyne a singlet at $\delta = -21$ ppm represents the main product with 55% conversion, and in a 1:10 stoichiometry the $K[(C\textit{t}Bu)_2P_3]$ triphospholyl ring with typical chemical shifts at $\delta = 249$ ppm (t) and 242.7 ppm (d) can be found in 38% conversion. The signal at -21 ppm, however, decreases to 18%. In the 1:4 ratio, several signals are found in the range between 11 and 39 ppm which are not present when using an excess of phosphaalkyne. Here, also two new doublets at ca. 85 ppm can be found (cf. Figure 5-4).

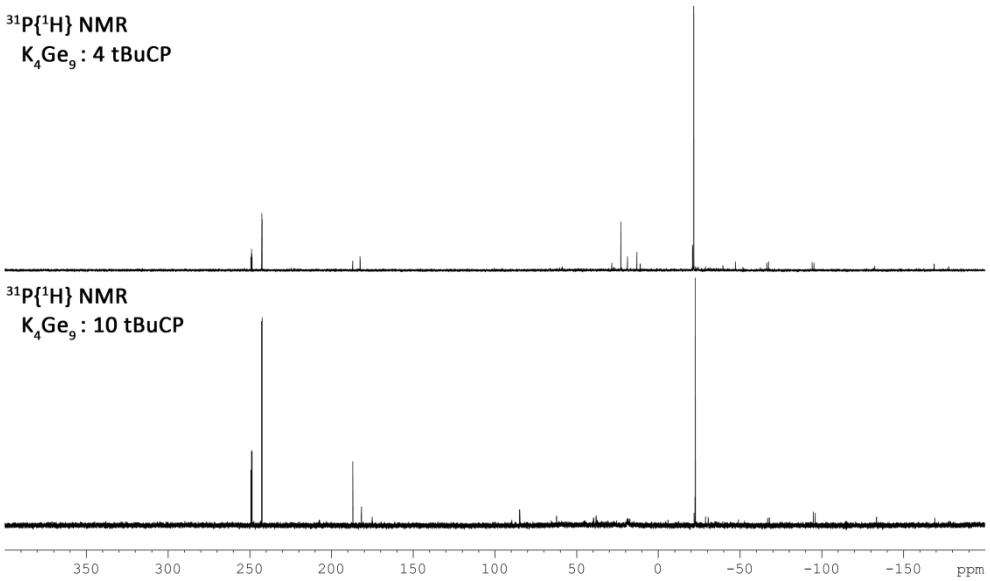

Figure 5-4 $^{31}P\{^1H\}$ NMR spectra of a 1:4 (upper spectrum) or 1:10 stoichiometry (lower spectrum) in acetonitrile. Main signals are the $[K][P_3(C\textit{t}Bu)_2]$ phospholyl ring at $\delta = 240$-250 ppm and a singlet at -21 ppm.

As acetonitrile is not a very suitable solvent for the zintl ion and a residue of K_4Ge_9 is always present in the reaction vessels, the residual has been dried and weighed to determine the correct stoichiometric ratios. For the first reaction a 1:10 and for the second a 1:16 ratio is thus determined. Unfortunately, no crystallisation attempt has been successful so no further statement about phosphorus containing products of the reaction can be made.

5.2.2 Reactions with Li_3P_7

In the reaction of *tert*-butyl phosphaalkyne with another zintl ion, P_7^{3-}, a much cleaner outcome was determined by NMR spectroscopy. The reaction between Li_3P_7 and *t*BuC≡P in THF leads to a series of five membered ring systems (see eq. (5-1)). In contrast to Goicoecheas work, which focuses on the K_3P_7 compound or its protonated species K_2HP_7, we decided to use the lithiated compound due to its solubility in THF.

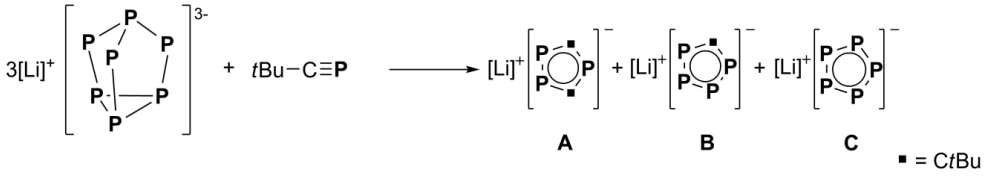

(5-1)

After washing with hexane and Et_2O, the $^{31}P\{^1H\}$ NMR spectrum at 300 K reveals that all three ring species **A**, **B** and **C** have been formed in addition to some minor products. Also, about 50% of the mixture is the educt complex Li_3P_7. Some of the *t*BuC≡P is reduced by the zintl ion to form the 1,2,4-triphospholide ring **A**, and the pentaphospholide **C** (δ = 471.7 ppm). We were explicitly interested in generating the tetraphospholide ring **B**, and it can be found in the $^{31}P\{^1H\}$ NMR spectrum in the range between δ = 348.9-366.5 ppm (see Figure 5-5).

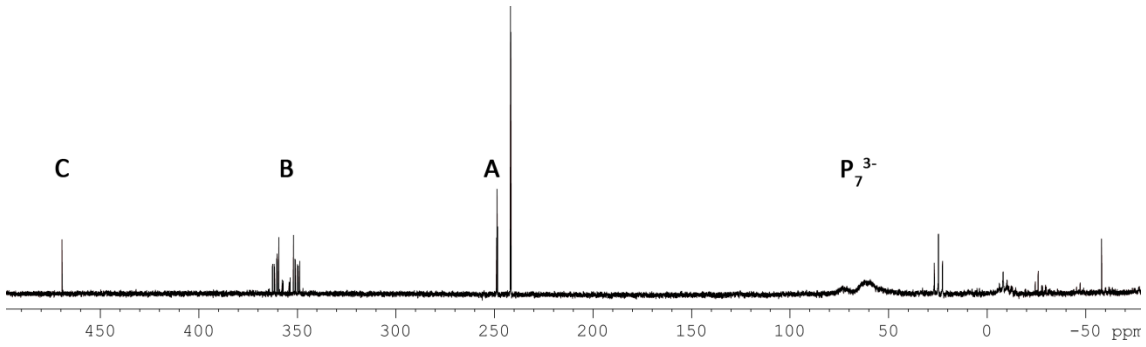

Figure 5-5 $^{31}P\{^1H\}$ NMR spectrum of Li_3P_7 and *t*BuC-P in THF-d_8 at r.t. Educt signal can be seen at around 60 ppm, and the three phospholide rings **A**, **B** and **C** (cf. equation (5-1)) are found in the known ranges.

The AA'MM' spin system for the tetraphospholide ion B has been simulated to receive information about the coupling constants (cf. Figure 5-6). They resemble the known coupling

constants for this five membered ring determined by our group (albeit for the iron sandwich complex [Cp'''Fe(η^5-P_4C*t*Bu)])[9a, 9b] and the similar compound with a supermesityl substituent by the group of Ionkin.[9c] Coupling constants for the simulated spectrum can be found in the Supporting Information.

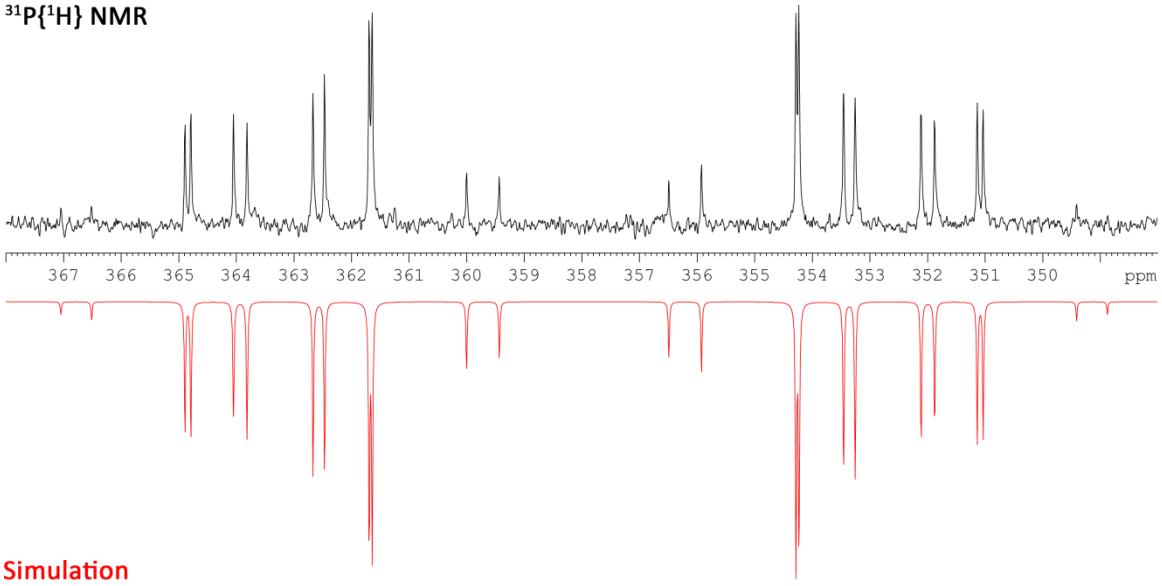

Figure 5-6 Section of the $^{31}P\{^1H\}$ NMR spectrum showing the multiplet for **B** (above, black) and simulation for this signal (below, red).[13]

Due to the presence of a mixture of products formed, crystallisation was a problem. Layering experiments with different solvents as well as using different crown ethers have not been successful. In addition, trials to trap the formed phospholide rings in a reaction with [$FeBr_2$(dme)] or [Cp*Fe(tmeda)Cl] were not successful.

5.3 Conclusions

In agreement with the findings of Becker *et al.* on the reduction of phosphaalkynes it was possible to obtain the 1,2,4-triphospholide ring K[(C*t*Bu)$_2P_3$] from reactions of *tert*-butylphosphaalkyne with K_4Ge_9. Due to the highly reducing nature of the zintl ion further phosphorus containing products could be observed in the NMR spectra but could not be separated to determine their composition. In another series of reactions between the zintl ion P_7^{3-} and *t*BuC≡P, different phospholide rings [P_n(C*t*Bu)$_{5-n}$]$^-$ (n = 3-5) are found in the NMR spectra of the reaction mixtures. The separation of those phospholyl rings proved difficult due to the similar solubility of the compounds. Further investigations concerning follow up reactions to separate the different species are ongoing.

5.4 Supporting Information

5.4.1 Experimental

All steps were performed under an atmosphere of dry argon with standard Schlenk techniques. Schlenk tubes were equipped with stirring bars, heated, evacuated and subsequently transferred into a glovebox while still hot. All solvents were distilled using standard procedures and were degassed prior to use. NMR spectra have been recorded using deuterated benzene, pyridine, acetonitrile or THF, which were dried over Na/K alloy (C_6D_6, THF-d_8) or NaH (CD_3CN, pyr-d_5) and distilled under an inert atmosphere. *t*BuC≡P[14] and $[Li_3P_7{\cdot}(dme)_3]$[15] have been prepared according to literature procedures. $[K_4Ge_9]$ has been synthesised by Christian Benda and was used as received after transfer into a glovebox.

5.4.2 Reactions of K_4Ge_9 with tBuC≡P

Reactions in ethylenediamine (en):

4ml of en are added to 194 mg ($2.4{\cdot}10^{-5}$ mol) K_4Ge_9 via cannula and the mixture is stirred at room temperature for an hour. Within 10 minutes, the orange-red solution exhibits a colour change to green. To this mixture, different ratios of *t*BuCP in 1 ml en are added at once (see Table 5-1). At the spot of entrance, sometimes a change of colour to blue can be observed which is not sustained. After twelve hours, the dark green solution is filtered via cannula and layered with a solution of 240 mg ($9.6{\cdot}10^{-5}$ mol) 18-crown-6 in 6 ml toluene.

Table 5-1 Stoichiometric ratios of phosphaalkyne added to K_4Ge_9.

Ratio	V(*t*BuC≡P) / ml	Residue K_4Ge_9
1:1	0.03	-
1:2	0.06	-
1:10	0.30	-

NMR reaction in en

1ml of en are added to 49 mg ($6.0{\cdot}10^{-6}$ mol) K_4Ge_9 via cannula and to this mixture, 0.075 ml *t*BuCP are added at once. After three hours stirring at room temperature, the solvent is removed *in vacuo* and resolved in 0.5 ml deuterated pyridine. A ^{1}H NMR spectrum is obtained.

Reactions in acetonitrile

4ml of acetonitrile are added to 194 mg ($2.4{\cdot}10^{-5}$ mol) K_4Ge_9 via cannula and the mixture is stirred at room temperature for one hours. To this mixture, different ratios of *t*BuCP are added directly at once (see Table 5-2). After sixteen hours, the orange-red solution is filtered

via cannula and layered with a solution of 240 mg (9.6·10-5 mol) 18-crown-6 in 8 ml hexane. The residue K4Ge9 after filtration is dried under reduced pressure and weighed to determine the true ratio of the reaction partners.

Table 5-2 Stoichiometric ratios of phosphaalkyne added to K_4Ge_9 in acetonitrile.

Ratio	V(tBuC≡P) / ml	m(residue K_4Ge_9) / mg	true ratio
1:3.5	0.10	130	1:10
1:10	0.30	70	1:16

NMR reaction in CD_3CN

1ml of deuterated acetonitrile are added to 49 mg ($6.0\cdot10^{-6}$ mol) K_4Ge_9 via cannula and to this mixture, 0.075 ml *t*BuCP are added at once. After three hours stirring at room temperature, the solution is put into a NMR tube for measurements.

5.4.3 Reactions of $Li_3P_7(dme)_3$ with *t*BuC≡P

10 ml of THF are added to 100 mg ($1.97\cdot10^{-4}$ mol) $Li_3P_7(dme)_3$, 7/3 equivalents of *t*BuC≡P (0.05 ml, $4.59\cdot10^{-4}$ mol) are added directly and the mixture is stirred at room temperature for three days. During this time, the orange-red solution exhibits a colour change to dark red. The solvent is removed *in vacuo*, washed with hexane and Et_2O and parts of the orange-red residue are taken up in THF-d_8 to obtain NMR data. 69 mg of 12-crown-4 are added to the solution which is subsequently layered with hexane. Unfortunately, only oil could be isolated from the mixtures.

$^{31}P\{^1H\}$-NMR	δ [ppm] = 471.7 (s, LiP_5), 363.2 (m, LiP_4C*t*Bu, MM') and 352.7 (m, LiP_4C*t*Bu, AA') AA'MM' spin system: $^1J_{AM}$ = 502.7 Hz, $^2J_{AM'}$ = -1.2 Hz, $^3J_{AA'}$ = 64.9 Hz, $^1J_{MM'}$ = 483.8 Hz), 250.9 (t, $^2J_{PP}$ = 47.3, $LiP_3(C$*t*$Bu)_2$), 244.0 (d, $^2J_{PP}$ = 47.3, $LiP_3(C$*t*$Bu)_2$),
Anion ESI-MS (DME)	*m/z* [%] = 967.1 (100) $[pftb]^-$

5.5 References

[1] a) H. C. Kolb, M. G. Finn, K. B. Sharpless, *Angew. Chem. Int. Ed.* **2001**, *40*, 2004; b) H. C. Kolb, M. G. Finn, K. B. Sharpless, *Angew. Chem.* **2001**, *113*, 2056.

[2] T. Allspach, M. Regitz, G. Becker, W. Becker, *Synthesis* **1986**, 31.

[3] R. Bartsch, J. F. Nixon, *Polyhedron* **1989**, *8*, 2407.

[4] G. Becker, W. Becker, R. Knebl, H. Schmidt, U. Weeber, M. Westerhausen, *Nova Acta Leopold.* **1985**, *59*, 55.

[5] a) F. Mathey, *Chem. Rev.* **1988**, *88*, 429; b) P. L. Floch, *Coord. Chem. Rev.* **2006**, *250*, 627.

[6] a) M. Driess, D. Hu, H. Pritzkow, H. Schäufele, U. Zenneck, M. Regitz, W. Rösch, *J. Organomet. Chem.* **1987**, *334*, C35; b) M. Scheer, J. Krug, *Z. Anorg. Allg. Chem.* **1998**, *624*, 399; c) A. Elvers, F. Heinemann, S. Kummer, B. Wrackmeyer, M. Zeller, U. Zenneck, *Phosphorus, Sulfur, and Silicon and the Related Elements* **1999**, *144*, 725; d) S. Deng, C. Schwarzmaier, U. Vogel, M. Zabel, J. F. Nixon, M. Scheer, *Eur. J. Inorg. Chem.* **2008**, *2008*, 4870; e) S. Deng, C. Schwarzmaier, C. Eichhorn, O. Scherer, G. Wolmershauser, M. Zabel, M. Scheer, *Chem. Commun.* **2008**, 4064; f) A. Schindler, G. Balazs, M. Zabel, C. Groeger, R. Kalbitzer, M. Scheer, *C. R. Chim.* **2010**, *13*, 1241; g) S. Deng, C. Schwarzmaier, M. Zabel, J. F. Nixon, M. Bodensteiner, E. V. Peresypkina, G. Balázs, M. Scheer, *Eur. J. Inorg. Chem.* **2011**, *2011*, 2991; h) C. Heindl, A. Schindler, M. Bodensteiner, E. V. Peresypkina, A. V. Virovets, M. Scheer, *Phosphorus, Sulfur, and Silicon and the Related Elements* **2014**, *190*, 397; i) C. Heindl, E. V. Peresypkina, A. V. Virovets, V. Y. Komarov, M. Scheer, *Dalton Trans.* **2015**, *44*, 10245; j) C. Heindl, A. Kuntz, E. V. Peresypkina, A. V. Virovets, M. Zabel, D. Ludeker, G. Brunklaus, M. Scheer, *Dalton Trans.* **2015**, *44*, 6502.

[7] S. Deng, C. Schwarzmaier, M. Zabel, J. F. Nixon, A. Y. Timoshkin, M. Scheer, *Organometallics* **2009**, *28*, 1075.

[8] a) R. S. P. Turbervill, J. M. Goicoechea, *Chem. Commun.* **2012**, *48*, 6100; b) R. S. P. Turbervill, J. M. Goicoechea, *Eur. J. Inorg. Chem.* **2013**, n/a; c) R. S. P. Turbervill, A. R. Jupp, P. S. B. McCullough, D. Ergöçmen, J. M. Goicoechea, *Organometallics* **2013**, *32*, 2234; d) R. S. P. Turbervill, J. M. Goicoechea, *Inorg. Chem.* **2013**, *52*, 5527; e) R. S. P. Turbervill, J. M. Goicoechea, *Eur. J. Inorg. Chem.* **2014**, *2014*, 1660; f) R. S. P. Turbervill, J. M. Goicoechea, *Chem. Rev.* **2014**, *114*, 10807; g) T. P. Robinson, M. J. Cowley, D. Scheschkewitz, J. M. Goicoechea, *Angew. Chem. Int. Ed.* **2015**, *54*, 683.

[9] a) M. Scheer, S. Deng, O. J. Scherer, M. Sierka, *Angew. Chem.* **2005**, *117*, 3821; b) M. Scheer, S. Deng, O. J. Scherer, M. Sierka, *Angew. Chem. Int. Ed.* **2005**, *44*, 3755; c) A. S. Ionkin, W. J. Marshall, B. M. Fish, A. A. Marchione, L. A. Howe, F. Davidson, C. N. McEwen, *Eur. J. Inorg. Chem.* **2008**, *2008*, 2386.

[10] C. B. Benda, J.-Q. Wang, B. Wahl, T. F. Fässler, *Eur. J. Inorg. Chem.* **2011**, *2011*, 4262.

[11] L. Yong, S. D. Hoffmann, T. F. Fässler, *Z. Anorg. Allg. Chem.* **2005**, *631*, 1149.

[12] a) C. Downie, Z. Tang, A. M. Guloy, *Angew. Chem.* **2000**, *112*, 346; b) C. Downie, Z. Tang, A. M. Guloy, *Angew. Chem. Int. Ed.* **2000**, *39*, 337.

[13] Simulation performed using WIN-DAISY module in Topspin 2.1 processing software by Bruker.

[14] G. Becker, G. Gresser, W. Uhl, *Z. Naturforsch., Teil B* **1981**, *36B*, 16.

[15] V. Manriquez, W. Hönle, H. G. von Schnering, *Z. Anorg. Allg. Chem.* **1986**, *539*, 95.

6 A Novel Coordination mode for 1,3-Diphosphete ligands

Eva-Maria Rummel, Awal Noor, Rhett Kempe and Manfred Scheer*

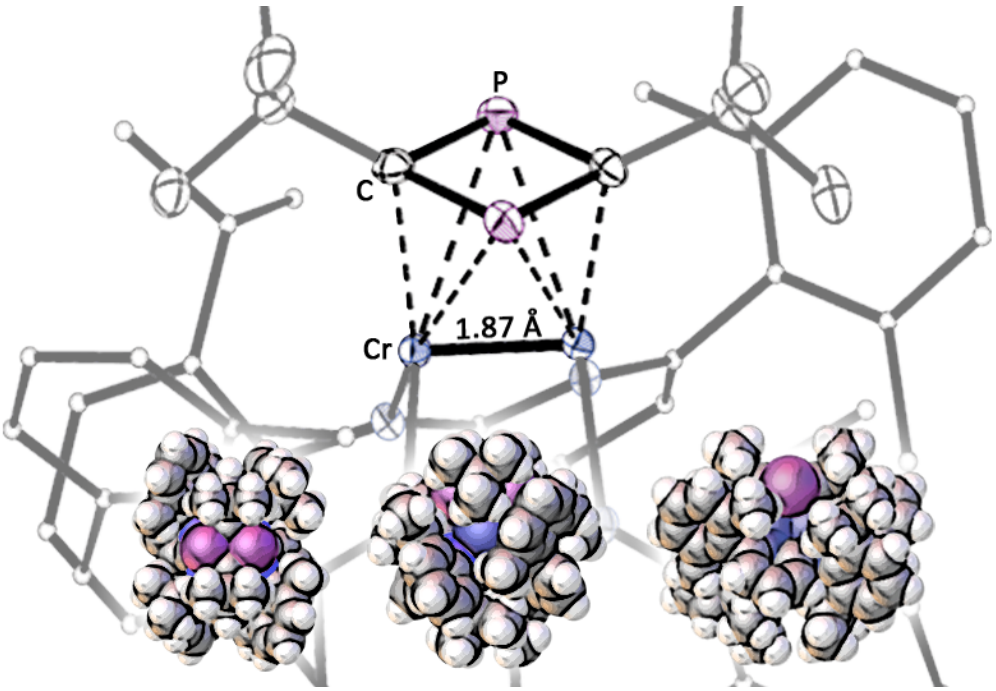

≡ All syntheses and characterisations were performed by Eva-Maria Rummel

≡ Educt ArCr^{5}CrAr provided by Awal Noor and Rhett Kempe

≡ X-ray measurements and calculations were done by Eva-Maria Rummel

≡ Figures were made by Eva-Maria Rummel

≡ Manuscript was written by Eva-Maria Rummel

6.1 Introduction

The reaction of LCr≡CrL (L=Ar=$N_2C_{25}H_{29}$, **1**) with R-C≡P (R = *t*Bu, Me, Ad) yields the neutral dimerisation compounds [$L_2Cr_2(\mu,\eta^1{:}\eta^1{:}\eta^2{:}\eta^2\text{-}P_2C_2R_2)$] (R = *t*Bu (**2**), Me (**3**)) or the tetrahedrane complex [$L_2Cr_2(\mu,\eta^2{:}\eta^2\text{-}P{=}CAd)$] (**4**), respectively. The 1,3-diphosphete complexes **2** and **3** are the first ones having this structural feature spanned over a metal-metal multiple bond, while **4** shows a side-on coordination mode for the slightly bigger adamantyl phosphaalkyne.

All six possible coordination modes for phosphaalkynes as $2e^-$, $4e^-$ and $6e^-$ donors (cf. Figure 6-1) have been discovered immediately in the years after the isolation of the kinetically stabilised phosphaalkyne *t*BuC≡P.[1] The first complex of a phosphaalkyne side-on coordinated on a metal centre, [$Pt(PPh_3)_2$(*t*BuC≡P)] by Nixon *et al.*[2] (type **B**), has already been isolated 1981 and showed the excellent coordinating ability of the carbon phosphorus triple bond, which represents the HOMO of the molecule.[3] Although the contracted lone pair at the phosphorus atom is quite passive, reaction products of type **A** and **C** as in Figure 6-1 can be observed with the right geometry imposed on the metal centre.[4]

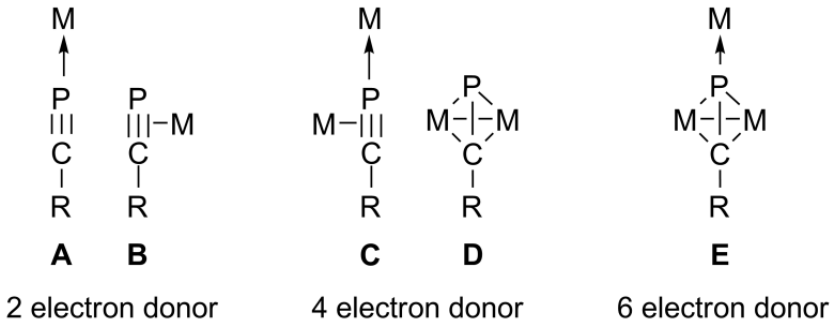

Figure 6-1 Possible coordination modes for phosphaalkynes.

The reaction between *t*BuC≡P and $Co_2(CO)_8$, however, leads to a $4e^-$ side-on coordination to form a tetrahedrane structured complex [$Co_2(CO)_6$(*t*BuCP)] (Figure 6-1 type **D**),[2] which could later be isolated and structurally characterised as an adduct complex of [$W(CO)_5$(thf)],[5] making the phosphaalkyne a $6e^-$ donor (Figure 6-1 type **E**). The tetrahedrane coordination over metal-metal bonds is a concept well established in phosphaalkyne chemistry and can be applied to a variety of complexes including mixed metal complexes[6] and metal-metal multiple bonds.[7] As a rule of thumb, phosphaalkynes will usually coordinate in a side-on fashion as soon as a metal-metal bond is present in a molecule. However, the more common products of the reaction of phosphaalkynes with a variety of isolated metal fragments are the diphosphacyclobutadiene (diphosphete) complexes. The [2+2] cycloaddition product of two phosphaalkynes in the coordination sphere of a transition metal fragment was first observed

by Regitz and Nixon in 1986 when they discovered the 1,3-diphosphete complex [$Cp^RCo(\eta^4\text{-}P_2C_2tBu_2)$] (R = H, Me) simultaneously (Figure 6-2, **I**).[4a,8] Since then, also homoleptic 1,3-diphosphete complexes have been discovered (cf. Figure 6-2, **II**).[9] However, the head-to-tail dimers (1,3-diphosphetes) are not the thermodynamically stable isomer of this reaction. The head-to-head cyclodimerised 1,2-diphosphetes should be the thermodynamically and kinetically favoured product.[10] Nevertheless, for the 1,2-derivative only three examples derived from phosphaalkynes are known in the literature so far (Figure 6-2, **III**).[11]

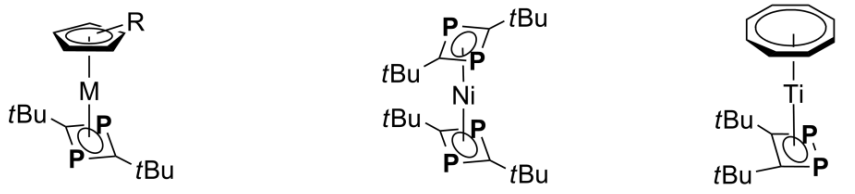

I **II** **III**

Regitz, 1986
M = Co; R = H

Nixon, 1986
M = Co, Rh, Ir; R= H, Me

Regitz, 1990

Binger, 1995

Figure 6-2 **I**) The first 1,3-diphosphacyclobutadiene complexes;[4a, 8] **II**) The first homoleptic diphosphete complex;[9a] **III**) the first 1,2-diphosphete complex.[11a]

All known diphosphete complexes have in common the η^4-coordination to a sole metal centre. Herein, we now want to report on the first example of a 1,3-diphosphete ligand over a metal-metal multiple bond. In addition, the sterical demand of the phosphaalkynes used in this reaction and the resulting change of coordination will be discussed.

6.2 Results and Discussion

The complex ArCr^{5}CrAr (Ar = Aryl, **1**) with a quintuple bond has been reacted with phosphaalkynes RC≡P (R = Me, *t*Bu, Ad) in hexane at r.t. (Scheme 6-1) and stirred for 16 h. The conversion is indicated by a change of colour from dark violet to crimson red for all three compounds. As is evident by NMR spectroscopy (*vide infra*), the smaller phosphaalkynes *t*BuC≡P and MeC≡P react in a 2:1 stoichiometry with **1** to yield the 1,3-diphosphete complexes [$L_2Cr_2(\mu,\eta^1\text{:}\eta^1\text{:}\eta^2\text{:}\eta^2\text{-}P_2C_2R_2)$] (R = *t*Bu (**2**), R = Me (**3**)), while the bigger AdC≡P reacts with compound **1** to form the side-on complex [$L_2Cr_2(\mu,\eta^2\text{:}\eta^2\text{-}P{=}CAd)$] (**4**).

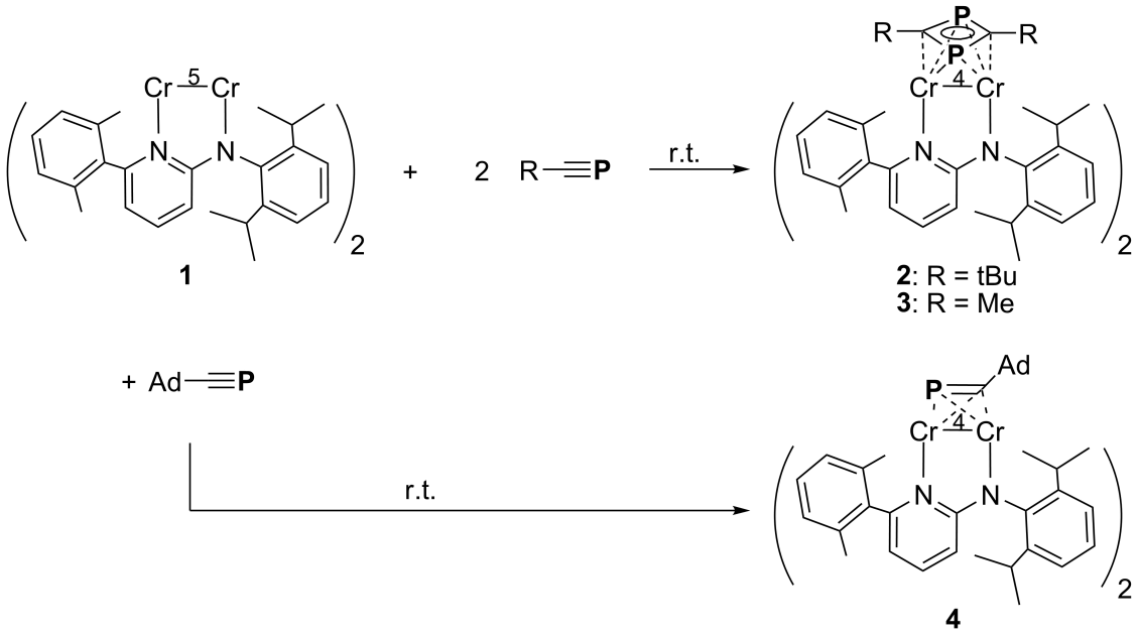

Scheme 6-1 Reaction of **1** with RC≡P (R = Me, *t*Bu, Ad).

Crystal structure analyses could be carried out for **2** and **4** which show that in the course of this reaction, the $Cr^{5}Cr$ quintuple bond (bond length 1.749 Å)[12] is reduced to a $Cr^{4}Cr$ quadruple bond of 1.8698(4) Å (**2**) or 1.8054(13) Å (**4**), respectively. The bond lengths vary because of the geometry of the ligand (cf Figure 6-3): in **2**, the *tert*-butyl groups are small enough to access the open space above the arylligands and are able to dimerise forming a $\mu,\eta^{1:1:2:2}$ coordinated 1,3-diphosphete ligand. This structural motif has not been observed over a metal-metal multiple bond so far (Figure 6-3 left).

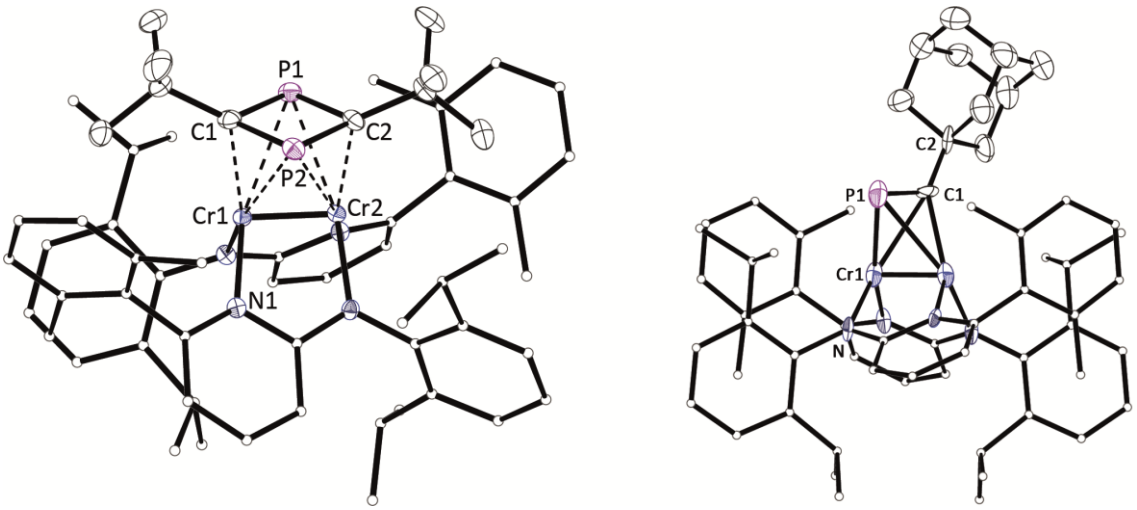

Figure 6-3 **Left**: Molecular structure of **2** in the solid state. Hydrogen atoms are omitted, carbon atoms of the ligand are shown in a ball-and-stick representation for clarity. Thermal ellipsoids are shown at 50% probability level. Selected bond lengths [Å] and angles [°]: Cr1-Cr2 1.8698(4), P1-P2 2.6711(7), P1-C1 1.802(2), P1-C2 1.822(2), P2-C1 1.8175(19), P2-C2 1.803(2), C1-P1-C2 84.92(9), C2-P2-C1 85.02(9), P1-C1-P2 95.10(9), P2-C2-P1 94.94(9). **Right**: Molecular structure of **4** in the solid state. Hydrogen atoms are omitted, carbon atoms of the ligand are shown in a ball-and-stick representation for clarity. Thermal ellipsoids are shown at 50% probability level. Selected bond lengths [Å] and angles [°]: Cr1-Cr1' 1.8054(13), Cr1-P1 2.674(3), Cr1-C1 2.117(8), Cr1-C1' 2.388(9), C1-P1 1.730(16), Cr1'-Cr1-C1 74.5(3), Cr1'-Cr1-P1 58.42(6), C2-C1-P1 121.9(7).

In contrast, the steric demand of the adamantyl group in **4** is too distinct for this and thus a side-on phosphaalkyne complex is formed (Figure 6-3 right).

In **2**, the nearly perfectly planar C_2P_2 diphosphete ring (dihedral angle of 1.1°) is located over the Cr-Cr quadruple bond, with the bond lengths in the four membered ring being essentially equal (1.802(2)–1.822(2) Å). In contrast to diphosphete moieties which are η^4 coordinated to one metal fragment, the *tert*-butyl groups in **2** are considerably angled out of the plane by 27° (Figure 6-4 **A**). Although the phosphorus lone pairs are pointing to the direction perpendicular to the Cr-Cr-bond (Figure 6-4 **B**), the calotte model (Figure 6-4 **C**) shows they are shielded by the ligand and *tert*-butyl groups of the diphosphete moiety and cannot be accessed easily. Even small molecules like [(tht)AuCl] are not coordinated by the phosphorus lone pairs in **2**. This is in contrast to the known cyclo-E_4 (E_4 = P_4, As_4, AsP_3) ligands on top of this Cr-Cr complex, which have been studied earlier by our group.[13] As the *cyclo*-E_4-ligands are isolobal to the diphosphete moiety in **2**, a comparison can be made: here, lewis acids like $[W(CO)_5(thf)]$ could be coordinated to the P/As atoms which are taking the place of the *t*BuC- fragment in **2**. As this space is obviously occupied by the organic groups, coordination has not been possible.

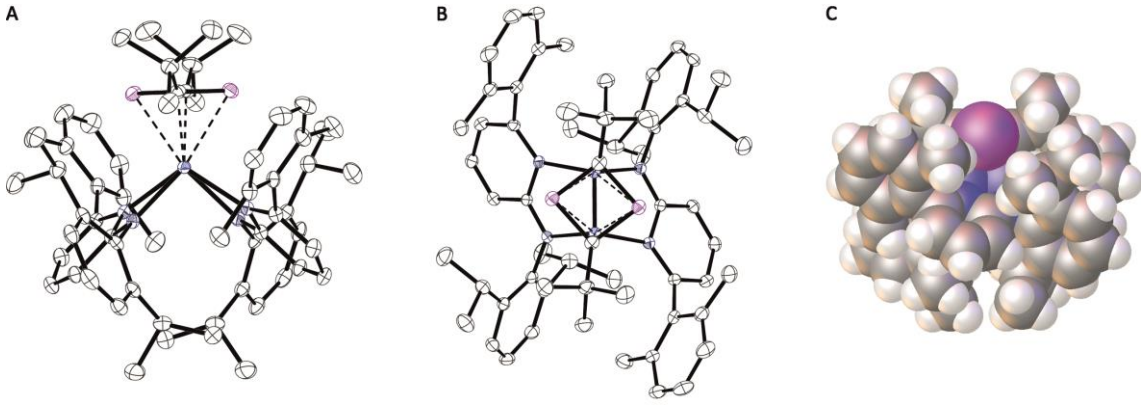

Figure 6-4 Representations of **2**. **A**) View along the Cr-Cr bond axis. The planarity of the 1,3-diphosphete ligand is an important structural feature. **B**) View from top. The *t*Bu-groups from the diphosphete ligand are pointing into the open space above the arylligands. **C**) View along the P-P axis in space filling model. The phosphorus lone pairs (which should be in the diphosphete plane) are shielded and cannot approach further substituents.

In contrast to the novel 1,3-diphosphete ligand in **2**, a side-on coordination is realised in **4**. Here, the chromium-chromium distance of 1.8054(13) Å is elongated in comparison to **1** (1.749(2) Å)[12] but still shorter than in the diphosphete complex **2** (1.8698(4) Å). Accordingly, the triple bond between the phosphorus and carbon atom of the former phosphaalkyne is elongated to 1.730(16) Å and thus in the range of a double bond. This is also confirmed by the angle on the C2 atom of 121.9(7)° which confirms a sp^2 hybridisation (Figure 6-5 **A**). Both chromium atoms and the P-C bond form a distorted tetrahedron with the adamantyl ligand filling the space over one of the ligands stabilizing the Cr-Cr multiple bond (Figure 6-5 **B**). In

comparison with **2**, the planar arrangement of an adamantyl diphosphete ligand would not fit into the cavity opened by the phenyl substituents on the ligand. Whether the phosphorus lone pair is available for further coordination (Figure 6-5) has to be determined yet.

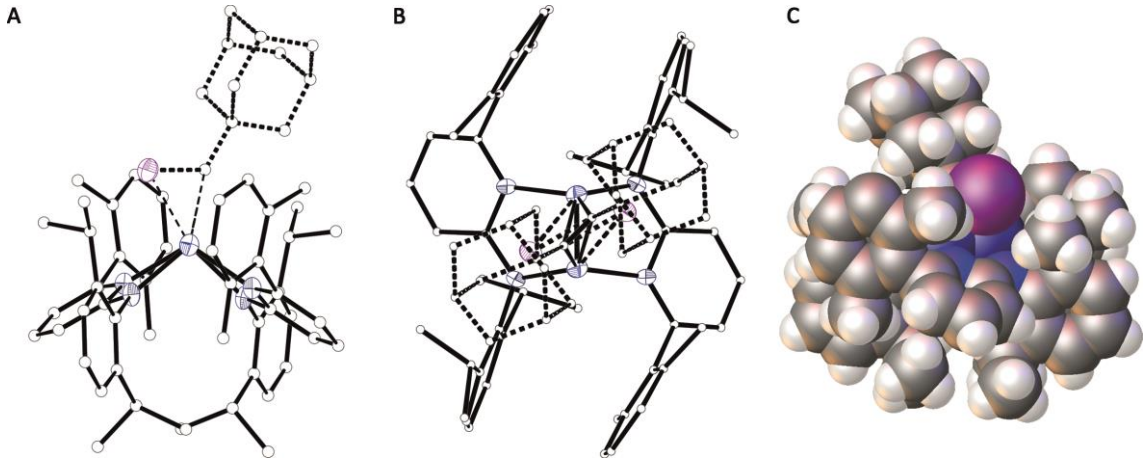

Figure 6-5 Representations of **4**. **A**) View along the Cr-Cr bond axis. Only one possible orientation of the adamantyl phosphaalkyne is shown in dashed lines. The adamantyl substituent is pointing upwards over the aryl ligands. **B**) View from top. The Ad-substituent from both possible orientations of the phosphaalkyne are shown. **C**) View along the P-P axis in space filling model. The phosphorus lone pairs could be able to approach further substituents.

Reactions have been carried out in different stoichiometries; however both phosphaalkynes prefer the coordination mode they have taken on. The coordination form present can easily be distinguished by their NMR shifts: The 1,3-diphosphete exhibits a shift in the range of δ ~ 100 ppm while the side-on coordinated phosphaalkyne is shifted to low field at δ ~ 460 ppm. As can be seen in NMR spectra of crude **2** and **4**, about 95-97% of the solution will be the preferred coordination mode as shown above while the remaining 3-5% of the solution is the other one. While conversion is not completed for **2** when the reaction is carried out in a 1:1 stoichiometry, and for **4** a 1:2 stoichiometry will only result in the observation of free adamantyl phosphaalkyne in the phosphorus NMR spectra.

The distinct NMR shifts also lead to the conclusion that the reaction of **1** with the sterically unhindered and kinetically unstabilised MeC≡P in the stoichiometric ratio of 1:1 or 1:2 also leads to the [2+2] cycloaddition product $[L_2Cr_2(\mu,\eta^1{:}\eta^1{:}\eta^2{:}\eta^2\text{-}P_2C_2Me_2)]$ (**3**). Here, the ^{31}P and $^{31}P\{^1H\}$ NMR spectra show a singlet at a shift of δ = 114.4 ppm (while no signal at > 450 ppm could be detected) and LIFDI mass analysis of the red solution also ascertains a mass peak at 934.34 Da (**3**$^+$). However, as the solubility again is given in every common solvent, up to this date no crystals could be grown from concentrated solutions. Drying solutions *in vacuo* leads to the formation of an oily residue, so no elemental analysis could be conducted. In addition, solutions of **3** are also extremely air-sensitive and show signs of decay upon opening of the Schlenk containing the product. Due to the delicate handling that is required when working

with this compound, no further analysis could be obtained for **3** so far. It can be concluded that the size of the phosphaalkyne has a direct influence on the product formed.

6.3 Conclusions

A novel coordination mode for 1,3-diphosphete ligands has been realised in the reaction between *t*BuC≡P and a LCr^{5}CrL (L=Ar=$N_2C_{25}H_{29}$, **1**) complex with a quintuple bond. Although a side on coordination is more common over metal-metal multiple bonds for phosphaalkynes, here a [2+2] cycloaddition could be observed in the case of *t*BuC≡P to form [$L_2Cr_2(\mu,\eta^1{:}\eta^1{:}\eta^2{:}\eta^2\text{-}P_2C_2t\text{Bu}_2)$] (**2**). Because of the shielding of the aryl ligands, the phosphorus lone pairs are not available for further coordination. The same result can be obtained in the reaction of the kinetically not stabilised MeC≡P with **1**, as spectroscopic data suggests, to form [$L_2Cr_2(\mu,\eta^1{:}\eta^1{:}\eta^2{:}\eta^2\text{-}P_2C_2\text{Me}_2)$] (**3**). Unfortunately, no crystals could be obtained for this compound. Enhancing the steric bulk on the phosphaalkyne leads to a side-on coordination of the P≡C triple bond which can be found in compound [$L_2Cr_2(\mu,\eta^2{:}\eta^2\text{-}P{=}CAd)$] (**4**) with an adamantyl substituent. Thus, the kind of complex formed is directly dependent on the substituent on the phosphaalkyne.

6.4 Supporting Information

6.4.1 Experimental

All steps were performed under an atmosphere of dry argon with standard Schlenk techniques. All solvents were freshly collected from a Solvent Purification System by M. Braun and were degassed prior to use. All NMR spectra have been recorded using deuterated benzene, which was dried over a Na/K alloy, refluxed for three hours and then distilled under inert atmosphere. *t*BuC≡P,[1] MeC≡P[14] and AdC≡P[15] have been synthesised according to literature procedure. The quintuple bond compound [L_2Cr_2] (**1**) has been kindly provided by Awal Noor and Rhett Kempe.[12]

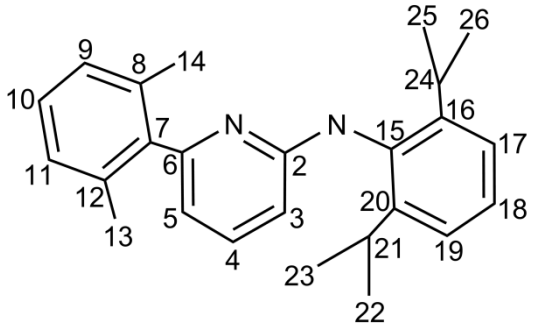

Figure 6-6 Ligand numbering scheme.

Synthesis of 2

To a solution of $1.22 \cdot 10^{-4}$ mol (100 mg) **1** in 10 ml hexane is added $2.5 \cdot 10^{-4}$ mol *t*BuC≡P. The colour of the solution instantly changes from dark violet to crimson red. After stirring overnight, the solution is filtered over silica and the solvent is removed under reduced pressure. The residue is taken up in 2 ml fresh hexane or pentane and stored at +5 °C. After some time, red crystals of **2** are forming on the solvent front.

Yield: 53 mg (43 %)

^{1}H-NMR	δ [ppm] = 0.69 (d, 3H, J = 6.6 Hz, $H^{22,23/25,26}$), 0.95 (pt, 6H, J = 7.4 Hz, $H^{22,23/25,26}$), 1.05 (s, 6H, $H^{13,14}$), 1.06 (s, 18H, $(tBuC)_2P_2$), 1.12 (d, 6H, J = 6.6 Hz, $H^{22,23/25,26}$), 1.28 (d, 6H, J = 6.6 Hz, $H^{22,23/25,26}$), 1.38 (s, 6H, $H^{13,14}$), 3.5 (dsept, 2H, J = 6.6 Hz, $H^{21/24}$), 4.12 (sept, 2H, J = 6.6 Hz, $H^{21,24}$), 5.54 (d, 2H, J = 6.6 Hz, H^3), 5.6 (d, 2H, J = 7.5 Hz, $H^{9,11/17,19}$), 6.24 (d, 2H, J =7.4 Hz, H^5), 6.37 (d, 2H, J = 7.8 Hz, H^4), 6.70 (q, 4H, J = 7.4 Hz, $H^{9,11/17,19}$), 7.02 (m, 2H, $H^{9,11/17,19}$), 7.19 (m, 2H, $H^{10/18}$), 7.26 (m, 2H, $H^{10/18}$)
^{31}P-NMR	δ [ppm] = 106.7 (s)
^{31}P{^{1}H}-NMR	δ [ppm] = 106.7 (s)
Elemental analysis	calculated for $C_{60}H_{76}Cr_2N_4P_2$ (1018.4 g/mol): C 70.69, H 7.52, N 5.49; found: C 69.55, H 7.81, N 5.06.
FD MS (toluene)	*m/z* [%] = 1019 (100) [M^+]

Synthesis of 3

To a solution of $1.22 \cdot 10^{-4}$ mol (100 mg) **1** in 10 ml THF is added $2.5 \cdot 10^{-4}$ mol MeC≡P. The colour of the solution instantly changes from dark violet to crimson red. After stirring overnight, the solution is filtered over silica and the solvent is removed under reduced pressure. The residue is taken up in 2 ml fresh hexane and stored at +5 °C.

^{31}P-NMR	δ [ppm] = 114.4 (s)
^{31}P{^{1}H}-NMR	δ [ppm] = 114.4 (s)
FD MS (toluene)	*m/z* [%] = 934.4 (10) [M^+]; 876.4 (100) [M^+-MeCP] in a scaled version from 800-1200 Da; *m/z* [%] = 876.4 (20) [M^+-MeCP], 358.4 (100) [L]

Synthesis of 4

To a solution of $4.88 \cdot 10^{-5}$ mol (40 mg) **1** in 10 ml hexane is added $9.76 \cdot 10^{-5}$ mol (17.4 mg) AdC≡P in 10 ml hexane. The colour of the solution instantly changes from dark violet to crimson red. After stirring overnight, the solution is filtered over silica and the solvent is removed under reduced pressure. The residue is taken up in 15 ml fresh pentane and stored at +5 °C.

Fractionised crystallisation leads to a total yield of 32 mg (67%)

^{1}H-NMR	δ [ppm] = 0.75 (d, 6H, J = 6.9 Hz, $H^{22,23/25,26}$), 0.91 (d, 6H, J = 7.4 Hz, $H^{22,23/25,26}$), 1.07 (s, 6H, $H^{13,14}$), 1.12 (d, 6H, J = 6.7 Hz, $H^{22,23/25,26}$), 1.37 (d, 6H, J = 6.9 Hz, $H^{22,23/25,26}$), 1.70 (t, 2.6 Hz, 3H, AdCP), 1.38 (s, 6H, $H^{13,14}$), 1.94 (br, 6H, AdCP), 2.5 (br, 6H, AdCP), 3.45 (sept, 2H, J = 6.7 Hz, $H^{21/24}$), 3.98 (sept, 2H, J = 6.7 Hz, $H^{21,24}$), 5.54 (d, 2H, J = 6.7 Hz, H^{3}), 5.66 (d, 2H, J = 7.2 Hz, $H^{9,11/17,19}$), 6.24 (m, 2H, H^{5}), 6.37 (m, 2H, H^{4}), 6.70 (m, 4H, $H^{9,11/17,19}$), 7.02 (m, 2H, $H^{9,11/17,19}$), 7.19 (m, 2H, $H^{10/18}$), 7.26 (m, 2H, $H^{10/18}$)
^{31}P-NMR	δ [ppm] = 460.6 (s)
^{31}P{^{1}H}-NMR	δ [ppm] = 460.6 (s)
FD MS (toluene)	*m/z* [%] = 996.4 (100) [M^+], 818.3 (20) [**1**$^+$], 714.4 (35) [L_2^+]

6.4.2 NMR Spectra

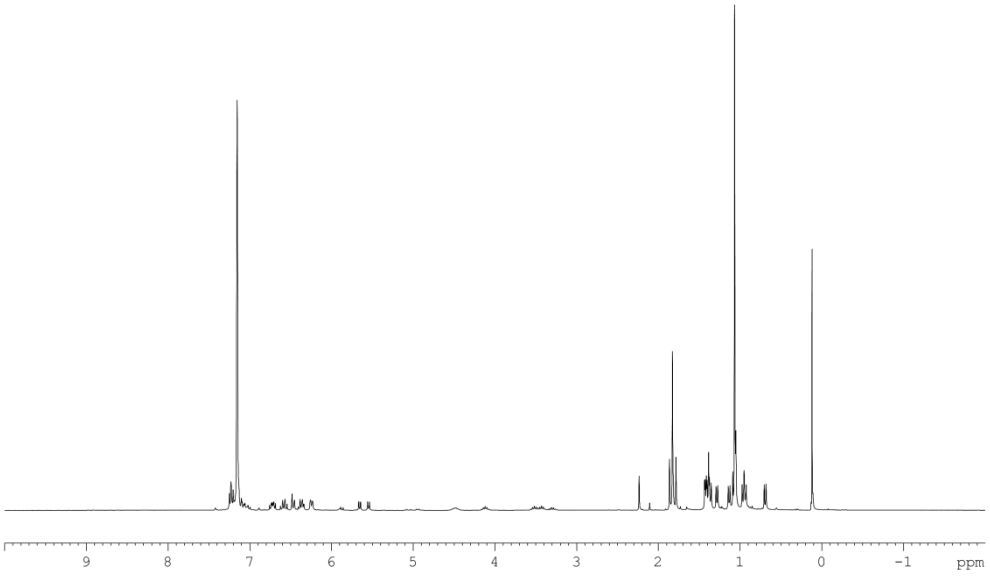

Figure 6-7 ^{1}H NMR spectrum of **2** in C_6D_6 at r.t.

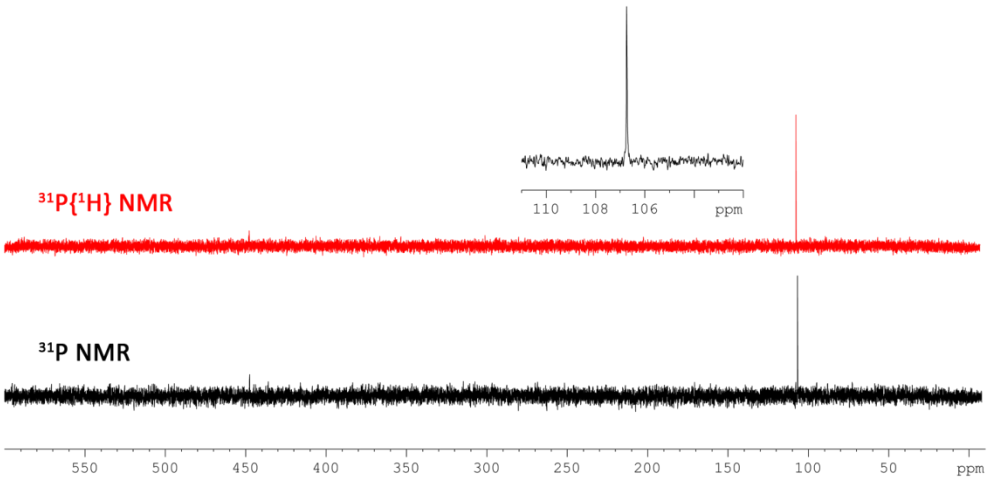

Figure 6-8 ^{31}P (black) and $^{31}P\{^{1}H\}$ (red) NMR spectra of **2** in C_6D_6 at r.t. Main signal is the [2+2] cycloaddition product at δ = 106 ppm, with minor impurities from the side-on product (3%) at δ = 450 ppm.

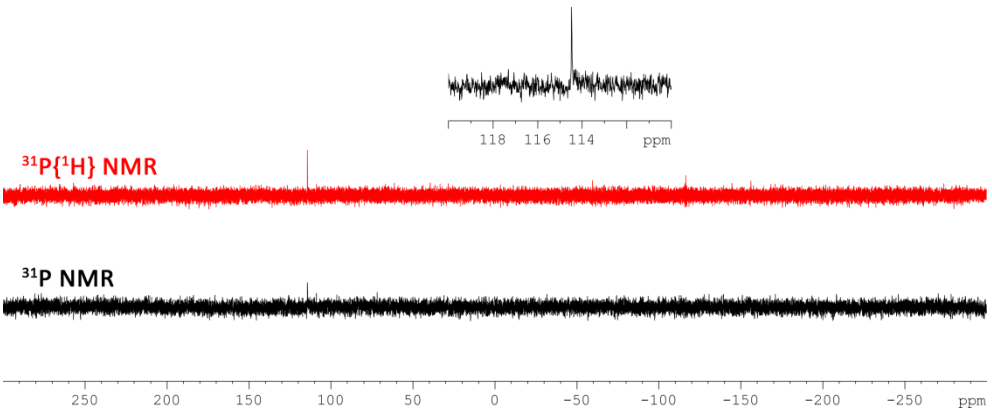

Figure 6-9 ^{31}P (black) and $^{31}P\{^{1}H\}$ (red) NMR spectra of **3** in C_6D_6 at r.t.

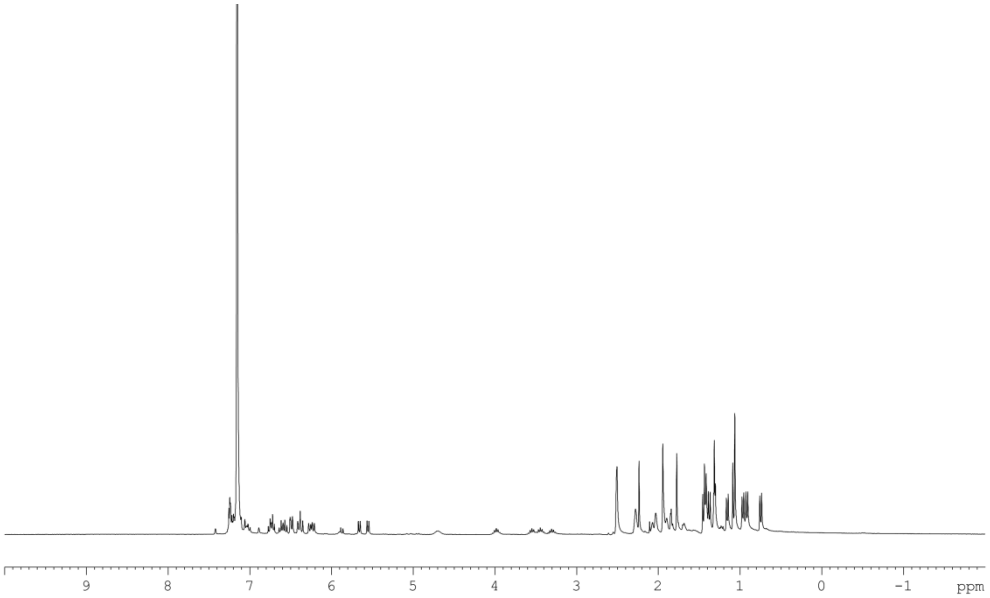

Figure 6-10 ^{1}H NMR spectra of **4** in C_6D_6 at r.t.

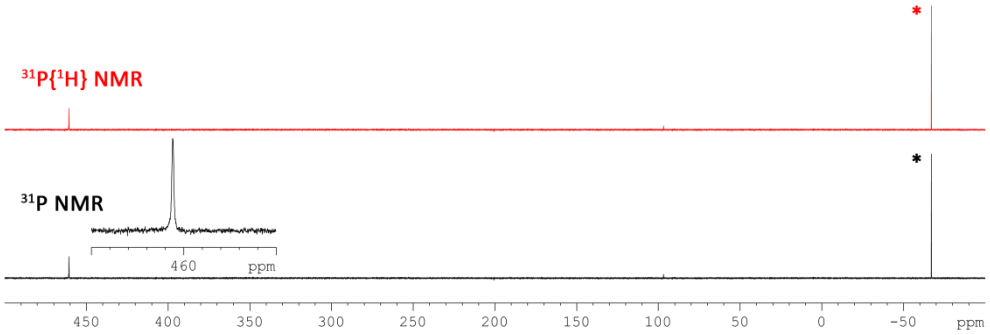

Figure 6-11 ^{31}P (black) and ^{31}P{^{1}H} (red) NMR spectra of reaction mixtures of **4** in C_6D_6 at r.t. Signal marked with an asterisk is residual AdC≡P. Main product of the reaction is the side-on complex **4** at δ = 460 ppm with minor impurities from the cycloaddition product at δ = 100 ppm (5%).

6.4.3 Crystallographic Data

Using Olex2,[16] all structures were solved with the ShelXT structure solution program,[17] using the Direct Methods solution method. The model was refined with version 2014/6 of ShelXL using Least Squares minimisation.[18] Experimental and crystal data created by ReportPlus in Olex2.

6.4.3.1 Compound 2

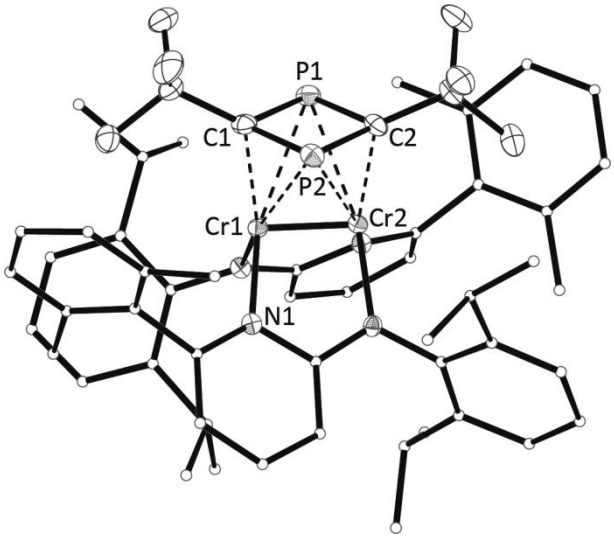

Figure 6-12 Molecular structure of **2** in the solid state. Hydrogen atoms are omitted, carbon atoms of the ligand are shown in a ball-and-stick representation for clarity. Thermal ellipsoids are shown at 50% probability level. Selected bond lengths [Å] and angles [°]: Cr1-Cr2 1.8698(4), P1-P2 2.6711(7), P1-C1 1.802(2), P1-C6 1.822(2), P2-C1 1.8175(19), P2-C6 1.803(2), C1-P1-C6 84.92(9), C6-P2-C1 85.02(9), P1-C1-P2 95.10(9), P2-C6-P1 94.94(9).

Single red block-shaped crystals of **2** were obtained by recrystallisation from hexane. A suitable crystal (0.21×0.12×0.09) was selected and mounted on a mylar loop on a SuperNova, Single source at offset, Atlas diffractometer. The crystal was kept at T = 123.01(10) K during data collection.

Crystal Data for **2**. $C_{66}H_{90}Cr_2N_4P_2$, M_r = 1105.35, triclinic, P-1 (No. 2), a = 12.8677(2) Å, b = 13.10453(19) Å, c = 18.2132(3) Å, α = 99.9375(13)°, β = 90.7104(13)°, γ = 92.7071(12)°, V = 3021.09(8) Å^3, T = 123.01(10) K, Z = 2, Z' = 1, μ(CuK$_\alpha$) = 3.776 mm^{-1}, 43906 reflections measured, 11933 unique (R_{int} = 0.0237) which were used in all calculations. The final wR_2 was 0.1142 (all data) and R_1 was 0.0339 (I > 2(I)).

6.4.3.2 Compound 4

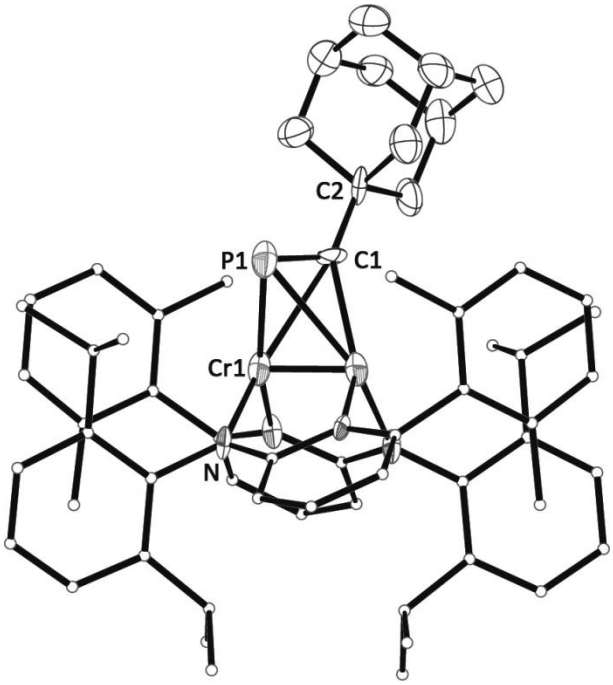

Figure 6-13 Molecular structure of **4** in the solid state. Hydrogen atoms are omitted, carbon atoms of the ligand are shown in a ball-and-stick representation for clarity. Thermal ellipsoids are shown at 50% probability level. Selected bond lengths [Å] and angles [°]: Cr1-Cr1' 1.8054(13), Cr1-P1 2.674(3), Cr1-C1 2.117(8), Cr1-C1' 2.388(9), C1-P1 1.730(16), Cr1'-Cr1-C1 74.5(3), Cr1'-Cr1-P1 58.42(6), C2-C1-P1 121.9(7).

Single clear red plate-shaped crystals of **4** were obtained by recrystallisation from hexane. A suitable crystal (0.10×0.07×0.02) was selected and mounted on a mitogen holder on a GV50, TitanS2 diffractometer. The crystal was kept at T = 123.1(3) K during data collection.

Crystal Data for **4**. $C_{61}H_{73}N_4PCr_2$, M_r = 997.20, monoclinic, $P2/c$ (No. 13), a = 10.2784(6) Å, b = 22.2038(13) Å, c = 12.5344(5) Å, β = 105.268(5)°, V = 2759.6(3) Å^3, T = 123.1(3) K, Z = 2, Z' = 0.5, μ(CuK$_\alpha$) = 3.820 mm^{-1}, 9569 reflections measured, 5342 unique (R_{int} = 0.0442) which were used in all calculations. The final wR_2 was 0.2464 (all data) and R_1 was 0.0834 (I > 2σ(I)).

6.5 References

[1] G. Becker, G. Gresser, W. Uhl, *Z. Naturforsch., Teil B* **1981**, *36B*, 16.

[2] J. C. T. R. B. S. Laurent, P. B. Hitchcock, H. W. Kroto, J. F. Nixon, *Chem. Commun.* **1981**, 1141.

[3] J. C. T. R. B. S. Laurent, M. A. King, H. W. Kroto, J. F. Nixon, R. J. Suffolk, *Dalton Trans.* **1983**, 755.

[4] a) P. B. Hitchcock, M. J. Maah, J. F. Nixon, *Chem. Commun.* **1986**, 737; b) P. B. Hitchcock, M. J. Maah, J. F. Nixon, J. A. Zora, G. J. Leigh, M. Abu Bakar, *Angew. Chem.* **1987**, *99*, 497; c) S. I. Al-Resayes, P. B. Hitchcock, M. F. Meidine, J. F. Nixon, *J. Organomet. Chem.* **1988**, *341*, 457.

[5] J. C. T. R. B. S. Laurent, P. B. Hitchcock, H. W. Kroto, M. F. Meidine, J. F. Nixon, *J. Organomet. Chem.* **1982**, C82.

[6] R. N. Bartsch, John F., N. Sarjudeen, *J. Organomet. Chem.* **1985**, 267.

[7] a) G. Becker, W. A. Herrmann, W. Kalcher, G. W. Kriechbaum, C. Pahl, T. C. Wagner, M. L. Ziegler, *Angew. Chem.* **1983**, *95*, 417; b) G. Becker, W. A. Herrmann, W. Kalcher, G. W. Kriechbaum, C. Pahl, T. C. Wagner, M. L. Ziegler, *Angew. Chem. Int. Ed.* **1983**, *22*, 413.

[8] a) P. Binger, R. Milczarek, R. Mynott, M. Regitz, W. Rösch, *Angew. Chem. Int. Ed.* **1986**, *25*, 644; b) P. Binger, R. Milczarek, R. Mynott, M. Regitz, W. Rösch, *Angew. Chem.* **1986**, *98*, 645.

[9] a) T. Wettling, G. Wolmershäuser, P. Binger, M. Regitz, *Chem. Commun.* **1990**, 1541; b) F. G. N. Cloke, K. R. Flower, P. B. Hitchcock, J. F. Nixon, *Chem. Commun.* **1994**, 489; c) R. Wolf, A. W. Ehlers, J. C. Slootweg, M. Lutz, D. Gudat, M. Hunger, A. L. Spek, K. Lammertsma, *Angew. Chem.* **2008**, *120*, 4660; d) R. Wolf, A. W. Ehlers, J. C. Slootweg, M. Lutz, D. Gudat, M. Hunger, A. L. Spek, K. Lammertsma, *Angew. Chem. Int. Ed.* **2008**, *47*, 4584; e) R. Wolf, J. C. Slootweg, A. W. Ehlers, F. Hartl, B. de Bruin, M. Lutz, A. L. Spek, K. Lammertsma, *Angew. Chem. Int. Ed.* **2009**, *48*, 3104; f) R. Wolf, J. C. Slootweg, A. W. Ehlers, F. Hartl, B. de Bruin, M. Lutz, A. L. Spek, K. Lammertsma, *Angew. Chem.* **2009**, *121*, 3150; g) R. Wolf, A. W. Ehlers, M. M. Khusniyarov, F. Hartl, B. de Bruin, G. J. Long, F. Grandjean, F. M. Schappacher, R. Pöttgen, J. C. Slootweg, M. Lutz, A. L. Spek, K. Lammertsma, *Chem. Eur. J.* **2010**, *16*, 14322.

[10] a) M. T. Nguyen, L. Landuyt, L. G. Vanquickenborne, *J. Org. Chem.* **1993**, *58*, 2817; b)

S. Creve, M. T. Nguyen, L. G. Vanquickenborne, *Eur. J. Inorg. Chem.* **1999**, *1999*, 1281.

[11] a) P. Binger, G. Glaser, S. Albus, C. Krüger, *Chem. Ber.* **1995**, 1261; b) A. D. Burrows, A. Dransfeld, M. Green, J. C. Jeffery, C. Jones, J. M. Lynam, M. T. Nguyen, *Angew. Chem.* **2001**, *113*, 3321; c) A. D. Burrows, A. Dransfeld, M. Green, J. C. Jeffery, C. Jones, J. M. Lynam, M. T. Nguyen, *Angew. Chem. Int. Ed.* **2001**, *40*, 3221; d) C. Jones, C. Schulten, A. Stasch, *Dalton Trans.* **2006**, 3733.

[12] a) A. Noor, F. R. Wagner, R. Kempe, *Angew. Chem. Int. Ed.* **2008**, *47*, 7246; b) A. Noor, F. R. Wagner, R. Kempe, *Angew. Chem.* **2008**, *120*, 7356.

[13] a) C. Schwarzmaier, A. Noor, G. Glatz, M. Zabel, A. Y. Timoshkin, B. M. Cossairt, C. C. Cummins, R. Kempe, M. Scheer, *Angew. Chem.* **2011**, *123*, 7421; b) C. Schwarzmaier, A. Noor, G. Glatz, M. Zabel, A. Y. Timoshkin, B. M. Cossairt, C. C. Cummins, R. Kempe, M. Scheer, *Angew. Chem. Int. Ed.* **2011**, *50*, 7283.

[14] J.-C. Guillemin, T. Janati, J.-M. Denis, *J. Org. Chem.* **2001**, 7864.

[15] T. Allspach, M. Regitz, G. Becker, W. Becker, *Synthesis* **1986**, 31.

[16] O. V. Dolomanov, L. J. Bourhis, R. J. Gildea, J. A. K. Howard, H. Puschmann, *J. Appl. Crystallogr.* **2009**, *42*, 339.

[17] G. M. Sheldrick, *Acta Cryst.* **2015**, *A71*, 3.

[18] G. M. Sheldrick, *Acta Cryst.* **2015**, *C71*, 3.

7 Synthesis of two 1,3-Diphosphacyclobutadiene complexes of MeC≡P and their redox behavior

Eva-Maria Rummel, Maria Eckhardt, Felix Riedelberger and Manfred Scheer*

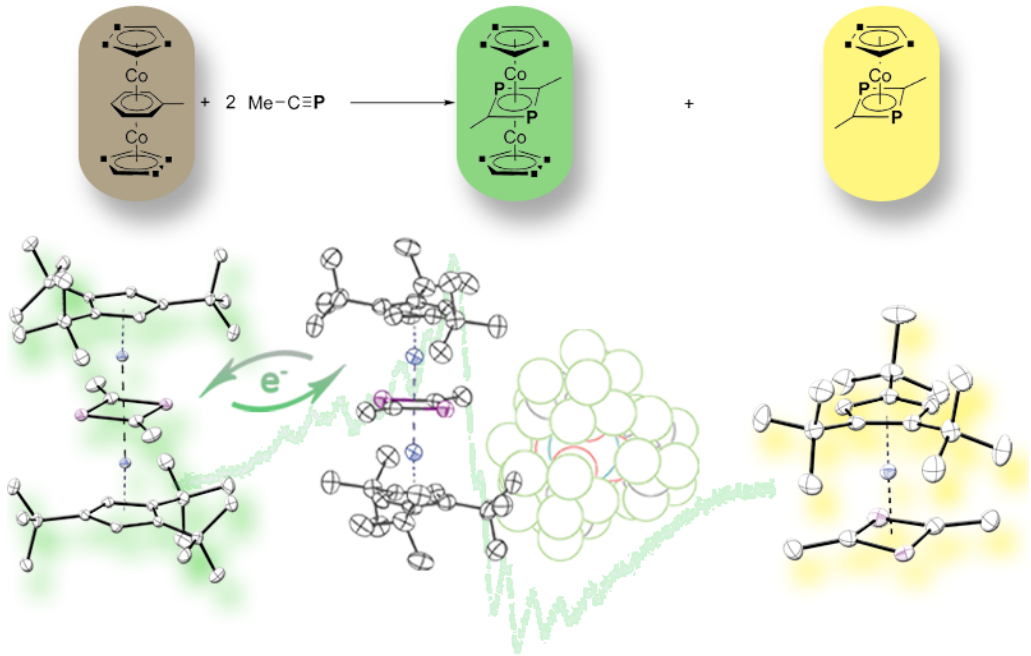

≡ All syntheses and characterisations were performed by Eva-Maria Rummel, except first synthesis of compound **1** (Maria Eckhardt)

≡ Figures were made by Eva-Maria Rummel

≡ CV measurements and evaluations were conducted by Felix Riedlberger

≡ All X-Ray measurements and refinements were done by Eva-Maria Rummel except for compound **1** (Maria Eckhardt)

≡ Manuscript was written by Eva-Maria Rummel

Acknowledgement: Moritz Modl acquired the EPR spectrum of compound **[1][pftb]**

7.1 Introduction

A novel triple decker complex [{Cp'''Co}$_2$(μ,η^4:η^4-$P_2C_2Me_2$)] (**1**) and a 1,3-diphosphete sandwich complex from ethynylphosphane (methyl phosphaalkyne) [Cp'''Co(η^4-$P_2C_2Me_2$)] (**2**) were isolated from the reaction of [Cp'''Co$_2$(μ,η^4:η^4-C_7H_8)] and methyl phosphaalkyne. Both complexes have been characterised and studied in their electrochemical behaviour. Complex **1** could be oxidised using the silver(I) salt of the weakly coordinating anion Ag[Al{OC(CF$_3$)$_3$}$_4$] (= Ag[pftb]) to form [{Cp'''Co}$_2$(μ,η^4:η^4-$P_2C_2Me_2$)][pftb] (**[1][pftb]**). A second (irreversible) oxidation could not be employed, however the fragmentation and subsequent oxidation/hydrolysis of **1** to form [{Cp'''Co}$_2$(μ-CCH_3)(μ-POOH)][pftb] (**3**) was found. Oxidation of the triple decker complex [Cp'''Co$_2$(μ,η^4:η^4-C_7H_8)] yielded [Cp'''Co$_2$(η^6-C_7H_8)][pftb] (**4**), which could also be produced by a salt metathesis reaction from Tl[pftb] and [Cp'''Co(μ-Cl)]$_2$.

Since the first isolation of the parent compound of alkylidynephosphanes (phosphaalkynes), HC≡P, by T. Gier in 1961,[1] the chemistry of phosphaalkynes has developed into an active research area. However, it took another forty years until a successful laboratory synthesis for the kinetically unstabilised ethynylphosphane (methyl phosphaalkyne) has been reported.[2] MeC≡P has since been employed in synthetic routes which have previously only been known for the kinetically stabilised *t*BuC≡P.[3]

Formed from a head-to-tail cyclodimerisation of phosphaalkynes within the coordination sphere of cyclopentadienyl cobalt fragments, the fully unsaturated 1,3-diphosphacyclobutadiene (1,3-diphosphete) $P_2C_2R_2$ cycles have been among the first to be isolated.[4] This is a result of the reactivity of the HOMO of phosphaalkynes, which is the π-orbital of the P≡C triple bond. In agreement with this, phosphaalkynes share a similar reaction behaviour with alkynes, while the lone pair reactivity (similar to nitriles) can only be observed in special cases.[5] The first to isolate a diphosphete complex of MeC≡P have been Jones and coworkers, who reported on 1,2- and 1,3-diphosphete tungsten complexes from the reaction of [W(CO)$_5$(thf)] and MeC≡P with a 80:20 ratio in favour of the 1,2-isomer.[6] In regards to the redox properties of diphosphete complexes, to the best of our knowledge only the 1,3-diphosphete complex [(η^6-C_7H_8)Fe(η^4-P_2C_2*t*Bu$_2$)] has been subjected to CV measurements which reveal a reversible oxidation of the iron core.[7] Additionally, the anionic bis-1,3-diphosphete complexes of Fe and Co could be electrochemically and chemically oxidised to form their respective neutral compounds.[8] As the redox chemistry of phosphorus containing complexes like Cp*FeP_5 have been of interest for inorganic chemists for over a decade,[9] we are naturally interested in the electrochemical properties of phosphorus

containing cycles like the unsaturated diphosphete moieties. We herein report on the formation of novel 1,3-diphosphete complexes of methyl phosphaalkyne and their oxidation chemistry employing silver salts of the weakly coordinating anion (WCA) $[Al\{OC(CF_3)_3\}_4]^-$ which is known to stabilise intermediates, compounds only known in mass spectrometry and highly reactive compounds.[10]

7.2 Results and Discussion

From the reaction of $[\{Cp'''Co\}_2(\mu,\eta^4{:}\eta^4\text{-}C_7H_8)]$ (which forms 14 VE (Cp'''Co) fragments in solution)[11] with MeC≡P, two new diphosphete complexes of methyl phosphaalkyne could be isolated after column chromatographic workup: the triple decker complex $[\{Cp'''Co\}_2(\mu,\eta^4{:}\eta^4\text{-}P_2C_2Me_2)]$ (**1**) and the sandwich complex $[Cp'''Co(\eta^4\text{-}P_2C_2Me_2)]$ (**2**) (eq. (7-1)). While sandwich complexes like **2** are well known, triple decker complexes like **1** are an unusual case.

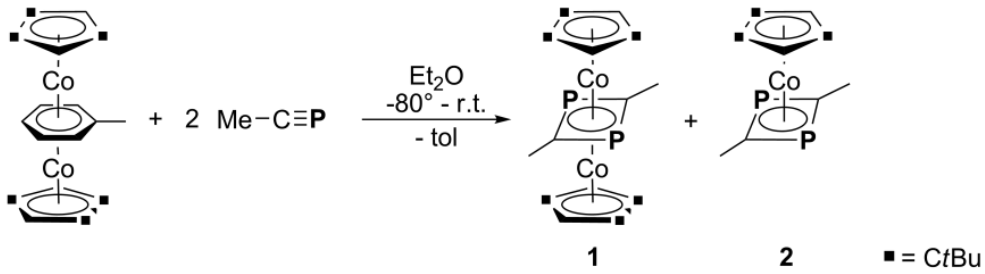

(7-1)

Compound **1** crystallises as green needles. The molecular structure is shown in Figure 7-1 and reveals a 1,3-diphosphete ligand as the middle deck in a triple decker sandwich complex. The bond distances between phosphorus and carbon in the four membered ring are essentially equal (1.839(2) Å and 1.838(3) Å) and angles within the 1,3-diphosphete moiety can be compared to complexes containing the same (Cp'''Co) fragment.[12] The Co-Co distance (3.55 Å) is outside the covalent bond with the diphosphete ring coordinating symmetrically between the two metal fragments. The only other complex bearing a 1,3-diphosphete middle deck is the uranium compound $[\{U(Ts^{tol})\}_2(\mu{:}\eta^4{:}\eta^4\text{-}C_2P_2tBu_2)]$ (Ts^{tol} = tris(N-(4-MeC_6H_4)amidodimethylsilyl)methane) obtained by Liddle *et al.*[13] Although the steric demand of the used *t*BuC≡P is slightly larger, the diphosphete ring is also distributed symmetrically between the metal fragments like in **1**.

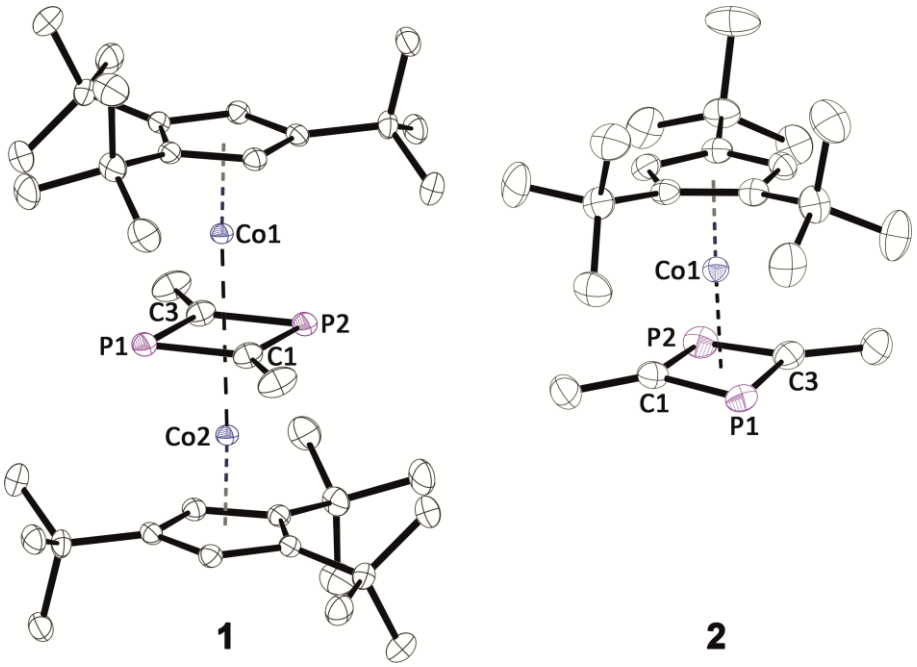

Figure 7-1 **Left:** Molecular structure of **1** in the solid state. Hydrogen atoms are omitted for clarity. Thermal ellipsoids are shown at 50% probability level. Selected bond lengths [Å] and angles [°]: P1-C1 1.839(2), C1-P1' 1.838(3), C1-C2 1.498(4), C1'-P1-C1 79.20(11), P1-C1-C2 129.93(19); **Right**: Molecular structure of **2** in the solid state. Hydrogen atoms are omitted for clarity. Thermal ellipsoids are shown at 50% probability level. Selected bond lengths [Å] and angles [°]: P1-C3 1.7925(16), P1-C1 1.7910(16), P2-C3 1.7857(16), P2-C1 1.7904(17), C1-P1-C3 81.00(7), C3-P2-C1 81.21(7), P2-C3-P1 98.66(8), P2-C1-P1 98.54(8).

Dark yellow blocks of **2** crystallise in the space group *P*-1 (cf. Figure 7-1). The crystals underwent first order phase transition below 183 K accompanied by an increase in volume and loss of crystallinity. The final measurement had to be conducted at 183 K. The bond distances and angles are within the range of the corresponding values for **1** and the isotypical complexes [Cp‘‘‘Co(η^4-P_2C_2tBu$_2$)] (**A**) and [Cp‘‘‘Co(η^4-P_2C_2iPr$_2$)] (**B**).[12]

While **2** shows a peak at $\delta = 65$ ppm in C_6D_6, which is slightly low-field shifted in comparison to the isotypical complexes **A** and **B**. The shift of **1** cannot be determined without uncertainties: Dissolving **1** in C_6D_6 leads to the same NMR shift as for **2**. As the values however should at least be slightly different, some considerations have been made in regard to the stability of the products. DFT calculations show that the {Cp‘‘‘Co} fragment from [{Cp‘‘‘Co}$_2$($\mu,\eta^4{:}\eta^4$-C_7H_8)] can be stabilised by aromatic solvents[11] which should also be true for **1**. As solubility experiments show, decomposition of **1** takes place in $CHCl_3$ and CH_2Cl_2 after ca. 5 minutes which is shown by a change of colour from dark green to dark brown. Until now, no solvent could be found in which **1** was adequately soluble but did not dissociate which makes it impossible to discuss NMR values for **1** without speculation. In the FD mass spectrum, both compounds could be characterised by their molecular peak.

As only little electrochemical analysis has been carried out for diphosphete complexes so far, we recorded CV spectra for both compounds (for spectra see supporting information). Compound **2** shows an irreversible oxidation at $E_{1/2}$ = 0.45 V and no reductions. As complex **1** decomposes in CH_2Cl_2, CV experiments had to be carried out in THF, where **1** only shows two reversible and one irreversible reduction compared to ferrocene. Unfortunately, reduction by K or KH could not be employed during the scope of this thesis. As we wanted to compare the oxidation behaviour of **1** and **2** with the oxidation behaviour of the *t*Bu-analogue compound **A** (*vide infra*), we chose to use a Ag(I) salt with the weakly coordinating anion (WCA) $[Al\{OC(CF_3)_3\}_4]^-$ ($[pftb]^-$) as an oxidising agent. Oxidation by silver(I) is strongly dependent on the solvent used[14] but carrying out the reaction in different solvents we always found that there was an one-electron oxidation process happening which led to the formation of **[1][pftb]** (see eq. (7-2)). If the same reaction is carried out with **2**, no product could be isolated. Only the formation of an insoluble black precipitate in a colourless solution could be observed independent on the reaction conditions applied.

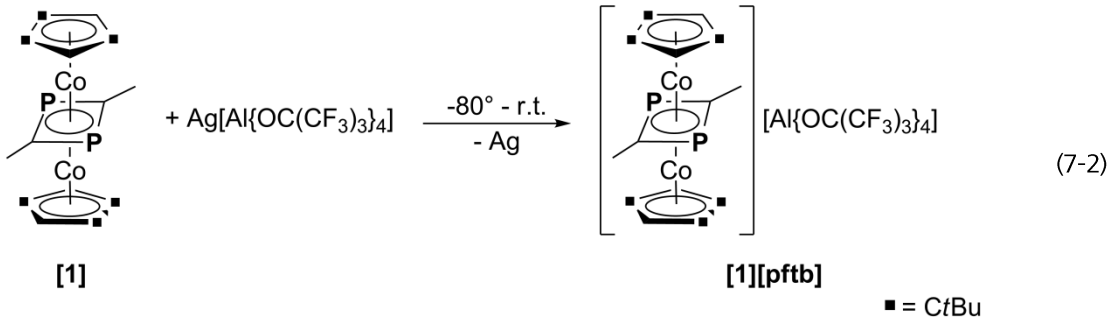

(7-2)

The solid solid state structure of dark green **[1][pftb]** is shown in Figure 7-2. The distances and angles within the diphosphete ring did not change essentially in comparison to **1** (the bond distances are with 1.839(7)-1.864(7) Å still in the range between single and double bonds), but the distance between the two cobalt centres decreased from 3.55 Å to 3.45 Å.

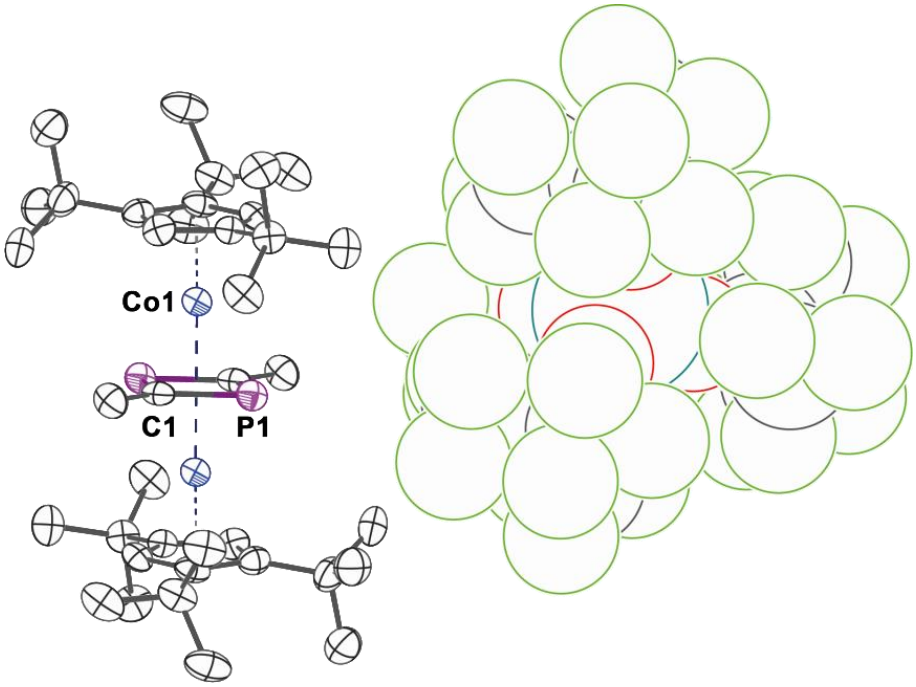

Figure 7-2 Molecular structure of Molecule A in **[1][pftb]** in the solid state. Hydrogen atoms and molecule B omitted for clarity. Anion shown in space-filling spheres. Thermal ellipsoids are shown at 50% probability level. Selected Bond lengths [Å] and angles [°]: P1-C1 1.839(7), P1-C1' 1.864(7), C1-P1-C1' 78.5(3), P1-C1-P1' 101.5(3), Co1-Co1' 3.4522(19).

The paramagnetic **[1][pftb]** has been analysed *via* ESI mass spectrometry, where the molecular peak could be found at 700.4 Da. Interestingly, at room temperature no EPR signal could be detected for the 31 VE triple decker complex. The EPR spectrum at 77.4 K (for baseline corrected spectrum see supporting information) shows an isotropic g value of 1.995, which points to one unpaired electron. The hyperfine structure of the anisotropic multiplet leads to the conclusion that the electron is centred on the 7/2 spin core ^{59}Co atoms. The spectrum could be fitted by considering coupling with the two Co nuclei (I = 7/2). The g-values and A-values are given in Figure 7-3.

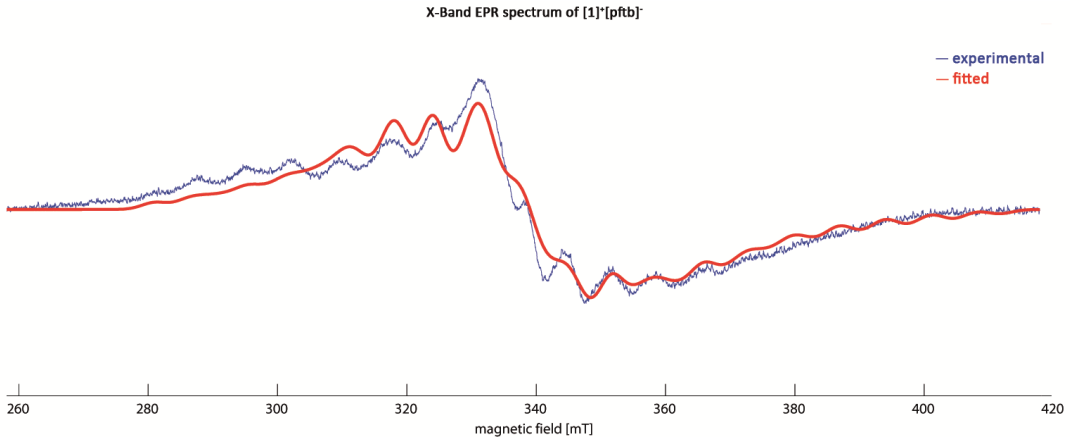

Figure 7-3 Experimental (blue) and simulated (red) X-band EPR spectrum of **[1][pftb]** in CH_2Cl_2 at 77K. Parameters used for fitting: g_x = 1.858, g_y = 1.995, g_z = 2.079; A_{1x} = 170.58, A_{1y} = 34.56, A_{1z} = 145.29, A_{2x} = 191.95, A_{2y} = 14.18, A_{2z} = 213.82.

Theoretically, as the first oxidation is centred on one of the cobalt atoms, we should be able to oxidise compound **[1][pftb]** even further. However, this could not be realised with any oxidation agent. This could point to a possible decomposition of the complex, and it was once possible to isolate a decomposition product after prolonged storage of the solution. Here, possible oxidation and hydrolysis of the phosphorus atom led to a fragmentation of the 1,3-diphosphete middle deck to form [{Cp'''Co}$_2$(μ-CCH$_3$)(μ-POOH)][pftb] (**3**), which lost one MeCP unit. The green compound crystallises in space group *P*-1 with two molecules in the unit cell. Both molecules are facing each other forming hydrogen bridges between the P=O and P-OH moieties (cf Figure 7-4).

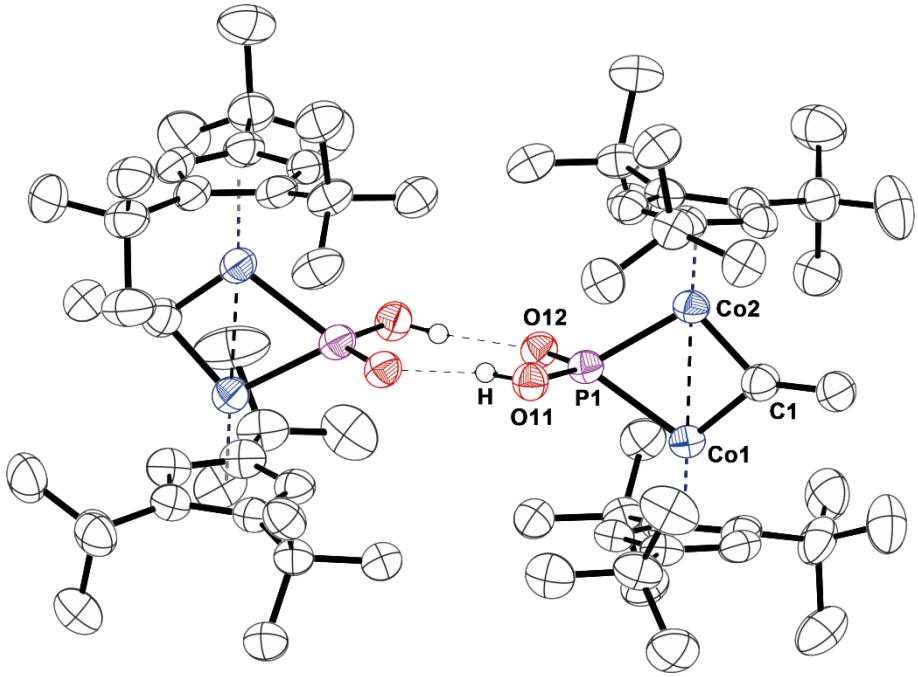

Figure 7-4 Molecular structure of two cations of **3** in the solid state. Hydrogen atoms are omitted for clarity. Thermal ellipsoids are shown at 50% probability level. Selected bond distances (Å) and angles (°): Co1-Co2 2.3853(11), Co1-C1 1.788(5), Co1-P1 2.1778(14), Co2-C1 1.802(6), Co2-P1 2.1697(13), O11-P1 1.488(3), P1-O11 1.570(3), Co2-P1-Co1 66.55(4), Co1-C1-Co2 83.3(2), C1-Co1-P1 104.68(19), C1-Co2-P1 104.50(17).

Interestingly, the ·CCH$_3$ fragment as well as the ·P=O(OH) moieties are bridging over two Cobalt atoms with a drastically reduced Co-Co distance (d(Co-Co) = 2.83 Å) in comparison to **1** and **[1][pftb]**. The distance between both carbon atoms of the former diphosphete is 1.477(9) Å with a trigonally planar coordinated, sp^2 hybridised C1. The distance between C1 and the Cobalt atoms is 1.788(5)-1.802(6) Å, and the distance between P1 and Co1/Co2 is 2.1778(14) and 2.1697(13) Å, respectively. The angular sum is 359.05°, which essentially points to a planar cyclodimetallaphosphabutane. Only few crystals could be collected for the compound, so no ^{31}P NMR characterisation was possible.

To see whether compound **[1][pftb]** can also be obtained by reacting an oxidised version of [{Cp'''Co}$_2$(μ,η^4:η^4-C$_7$H$_8$)] with methyl phosphaalkyne, we tried to form

[{Cp'''Co}$_2$(μ,η^4:η^4-C_7H_8)][pftb] via oxidation of [{Cp'''Co}$_2$(μ,η^4:η^4-C_7H_8)] with Ag[pftb]. The product, however, was not the targeted oxidised species, but the sandwich complex [Cp'''Co(η^6-C_7H_8)][pftb] (**4**). Only a preliminary model can be shown here as crystals of compound **4** show incommensurable modulation. The q-Vector is 0.0345 and X-ray structure analysis gives an average structure as shown below. The red paramagnetic 19 VE product and crystallises in the orthorhombic space group *Pbca* with one independent molecule in the asymmetric unit (see Figure 7-5).

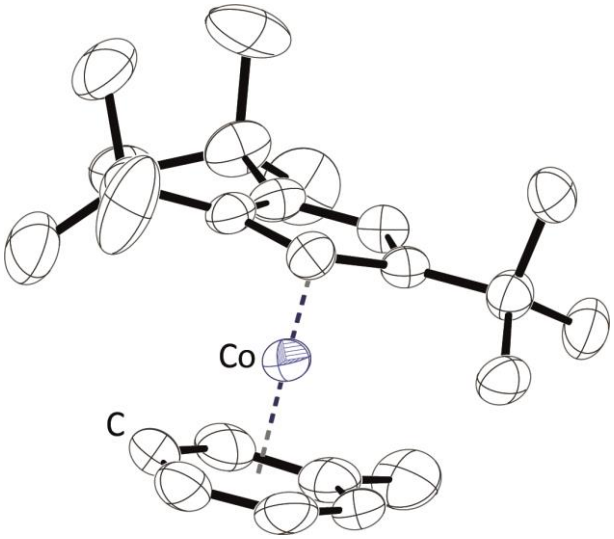

Figure 7-5 Molecular structure of the cation of **4** in the solid state. Hydrogen atoms are omitted for clarity. Thermal ellipsoids are shown at 50% probability level. Distance between cobalt centre and plane of rings: 1.65 Å (Co-tol$_{cent}$) and 1.76 Å (Co-Cp'''$_{cent}$).

Compound **4** could also be synthesised quantitatively from [{Cp'''Co}(μ-Cl)]$_2$ and Tl[pftb] via salt elimination in CH_2Cl_2. Unfortunately, **4** does not react with the phosphaalkyne since in the $^{31}P\{^1H\}$-NMR spectrum of the reaction mixture only a signal for unconverted MeC≡P can be detected after several hours reaction time even at elevated temperatures. In addition, no change of the colour of the solution could be detected.

7.3 Conclusions

We could show that the reaction of MeC≡P with the 14 VE fragment (Cp'''Co) leads to two different heteroleptic 1,3-diphosphete complexes, the triple decker complex [{Cp'''Co}$_2$(μ,η^4:η^4-$P_2C_2Me_2$)] (**1**) and the sandwich complex [Cp'''Co(η^4-$P_2C_2Me_2$)] (**2**). Compound **2** shows an irreversible oxidation in CH_2Cl_2, while complex **1** shows two reversible and one irreversible reductions in THF. However, for **1** an oxidation by the WCA silver(I) salt Ag[Al{OC(CF$_3$)$_3$}$_4$] could be carried out and yielded the paramagnetic [{Cp'''Co}$_2$(μ,η^4:η^4-$P_2C_2Me_2$)][pftb] (**[1][pftb]**). Compound **[1][pftb]** shows an unpaired electron in the EPR spectrum at 77 K which couples with two cobalt centres (^{59}Co: *I* = 7/2).

Although a second oxidation could not be chemically observed, a product of oxidation and subsequent hydrolysis ([{Cp'''Co}$_2$(μ-CCH$_3$)(μ-POOH)][pftb], **3**) could be isolated. In this compound, the 1,3-diphosphete moiety underwent fragmentation, which can be viewed as an indicator for a possible change of structure upon further oxidation. To check whether **[1][pftb]** could be created by reacting MeC≡P with an already oxidised {Cp'''Co} fragment, [Cp'''Co$_2$(η^6-C$_7$H$_8$)][pftb] (**4**) was prepared. However, no reaction was observed between methylphosphaalkyne and the 19 VE sandwich complex **4**.

7.4 Supporting Information

7.4.1 Experimental

All steps were performed under an atmosphere of dry argon with standard Schlenk techniques. All solvents were freshly collected from a Solvent Purification System by M. Braun and were degassed prior to use. NMR spectra have been recorded using deuterated benzene or dichloromethane, which were dried over Na/K alloy (C_6D_6) or CaH_2 (CD_2Cl_2) and distilled under inert atmosphere. $CH_3C{\equiv}P$,[2] [{Cp'''Co}$_2$(μ,η^4:η^4-C_7H_8)][15], [{Cp'''Co}(μ-Cl)]$_2$,[16] Tl[Al{OC(CF_3)$_3$}$_4$][17] and Ag[Al{OC(CF_3)$_3$}$_4$][18] (will be shortened Tl[pftb] and Ag[pftb]) have been prepared according to literature procedures.

Synthesis of 1

A solution of $CH_3C{\equiv}P$ in Et_2O (10 mL, $1.18{\cdot}10^{-3}$ mol) is cooled to -80 °C. To this solution, [{Cp'''Co}$_2$(μ,η^4:η^4-C_7H_8)] (200 mg, $2.9{\cdot}10^{-4}$ mol) in 5mL Et_2O is added dropwise while stirring. An instant colour change from dark brown to dark green can be observed. The solution is left to warm up to room temperature. After five hours of additional stirring, crystals of **1** are forming on the solvent border and can be isolated. The residual solution is filtered over silica gel and the solvent removed *in vacuo*. The residue is subjected to column chromatography over dried silica gel (length 15 cm, diameter 3 cm).

	Fraction 1	**Fraction 2**
Colour	dark green	yellow
Eluted with	pentane	*n*-hexane
Compound	**1**	**2**

The solvents were removed *in vacuo* and the residues (mostly oil) subsequently taken up in small amounts of *n*-hexane.

Fraction 1 contained dark green **1**,

Analytical data:[i]

Elemental analysis	calculated for $C_{38}H_{64}Co_2P_2$ (700.7 g·mol^{-1}): C 65.13, H 9.21; found: C 65.14, H 9.23
EI-MS (hexane, 70eV)	*m/z* [%] =700.2 (1) [M^+]

[i] Elemental analysis and EI-MS have been collected by Maria Eckhardt.

Fraction 2 contained yellow **2**, Yield: 23 mg

Analytical data:

^{1}H-NMR (C_6D_6)	δ [ppm] = 1.26 (d, 6H, $^{3}J_{PH}$ = 9.28 Hz, $C_2P_2(C\underline{H}_3)_2$), 1.39 (s, 18H, $C_5H_2(C_4\underline{H}_9)_3$), 1.41 (s, 9H, $C_5H_2(C_4\underline{H}_9)_3$), 4.36 (s, 2H, $C_5\underline{H}_2(C_4H_9)_3$)
^{31}P-NMR (C_6D_6)	δ [ppm] = 65.5 (s, $\omega_{1/2}$ = 21.3 Hz)
^{31}P{^{1}H}-NMR (C_6D_6)	δ [ppm] = 65.5 (s, $\omega_{1/2}$ = 21.3 Hz)
Elemental analysis	calculated for $C_{21}H_{35}CoP_2$ (408.15 g·mol^{-1}): C 61.74, H 8.64; found: C 57.25, H 8.25
EI-MS (toluene, 70eV)	*m/z* [%] = 408.2 (60) [M^{+}]

Synthesis of [1][pftb]

A solution of 7.13·10^{-5} mol **1** in 20 mL Et_2O is layered over a solution of 1.42·10^{-4} mol Ag[pftb] in CH_2Cl_2 and stored at -30 °C until complete diffusion took place. The resulting green solution with dark precipitate is dried *in vacuo*, taken up in 3mL CH_2Cl_2 and filtered over silica gel. The green solution is layered under 15 mL of hexane and stored at -30 °C to yield dark green crystals of **[1][pftb]** suitable for X-ray analysis. The residual solution can be subsequently layered with additional hexane to yield microcrystalline powder of **[1][pftb]**.

Yield: 92 mg (77%)

Analytical data:

Elemental analysis	calculated for $C_{54}H_{64}Co_2P_2AlO_4F_{36}\cdot CH_2Cl_2$ (1752.7 g·mol^{-1}): C 37.68, H 3.79; found: C 37.51, H 3.95
Cation ESI-MS (CH_2Cl_2)	*m/z* [%] = 700.4 (100) [M^{+}], 384.2 (15) [Cp'''Co(tol)$^{+}$]
Anion ESI-MS (CH_2Cl_2)	*m/z* [%] = 967.1 (100) [pftb^{-}]
EPR (CH_2Cl_2, 77K)	g_{iso} = 2.009823, g_x = 1.858, g_y = 1.995, g_z = 2.079; A_{1x} = 170.58, A_{1y} = 34.56, A_{1z} = 145.29, A_{2x} = 191.95, A_{2y} = 14.18, A_{2z} = 213.82.

After prolonged storage oxidation took place to form compound **3**:

Cation ESI-MS (CH_2Cl_2)	*m/z* [%] = 700.4 (100) [**[1]**$^{+}$], 677.4 (27) [(Cp'''Co)$_2$MeCP(OH)$_2$]
Anion ESI-MS (CH_2Cl_2)	*m/z* [%] = 967.1 (100) [pftb^{-}]

Synthesis of 4

A solution of $3.05 \cdot 10^{-4}$ molL^{-1} [{Cp'''Co}(μ-Cl)]$_2$ in 10 mL toluene is added to a solution of Tl[pftb] in a mixture of 15 mL toluene and 3 mL CH_2Cl_2 and stirred for 24 hours. The resulting red solution with a white precipitate of TlCl is filtered over silica and dried *in vacuo.* The red foaming residue is isolated and ca. 50 mg are taken up in 3 mL CH_2Cl_2, layered under 10 mL of hexane and stored at -30 °C to yield dark red crystals of **4** suitable for X-ray analysis.

Yield: 778 mg (94%)

Analytical data:

^{19}F-NMR (C_6D_6)	δ [ppm] = -75.4 (s)
^{19}F{^{1}H}-NMR (C_6D_6)	δ [ppm] = -75.4 (s)
Elemental analysis	calculated for $C_{40}H_{37}CoAlF_{36}O_4 \cdot CH_2Cl_2$ (1435.1 g·mol^{-1}): C 33.18, H 2.72; found: C 32.36, H 2.70
Cation ESI-MS (CH_2Cl_2)	*m/z* [%] = 384.1 (100) [M$^+$]
Anion ESI-MS (CH_2Cl_2)	*m/z* [%] = 967.1 (100) [pftb$^-$]

7.4.2 Cyclovoltammograms

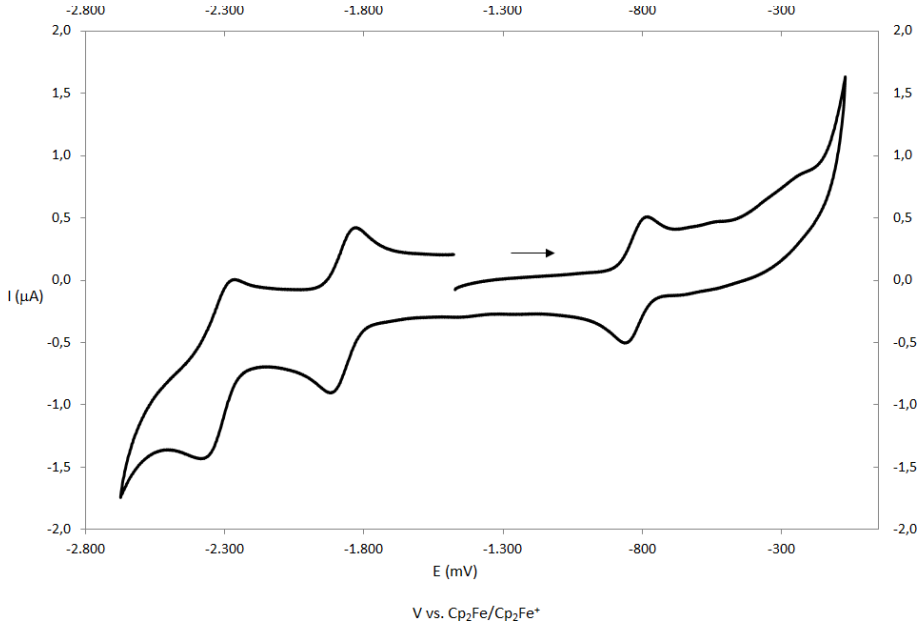

Figure 7-6 Cyclovoltammogram of **1** recorded at a platinum disc electrode in THF at 200 mV/s, referenced against Cp_2Fe/Cp_2Fe^+. Supporting electrolyte $[Bu_4N][PF_6]$ (0.1 mol/L). Two reversible reductions at $E_{1/2}$ = -0.8 V and $E_{1/2}$ = -1.85 V an irreversible reduction at $E_{1/2}$ = -2.3 V can be observed in the solvent window.

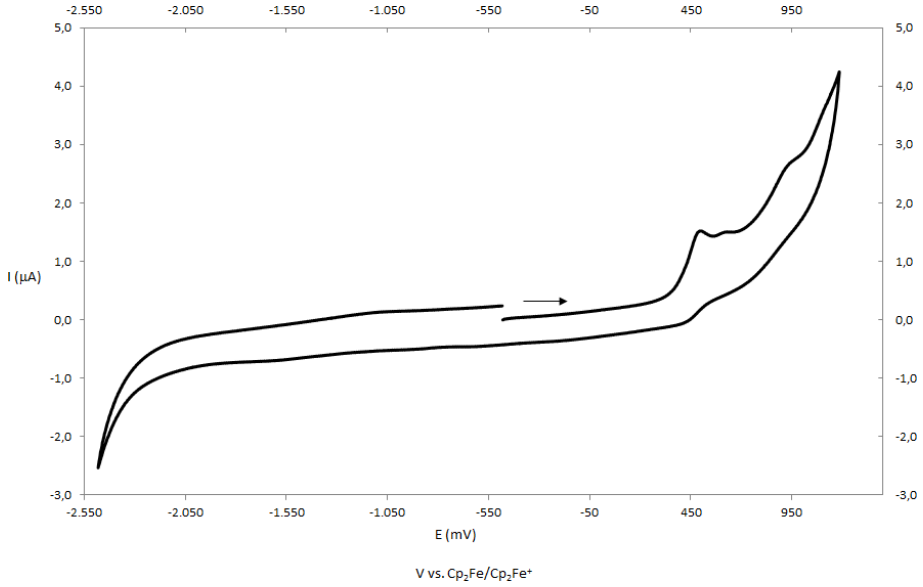

Figure 7-7 Cyclovoltammogram of **2** recorded at a platinum disc electrode in CH_2Cl_2, referenced against Cp_2Fe/Cp_2Fe^+. Supporting electrolyte $[Bu_4N][PF_6]$ (0.1 mol/L). Regardless of potential rates, only an irreversible oxidation could be observed in the solvent window.

7.4.3 EPR Spectrum

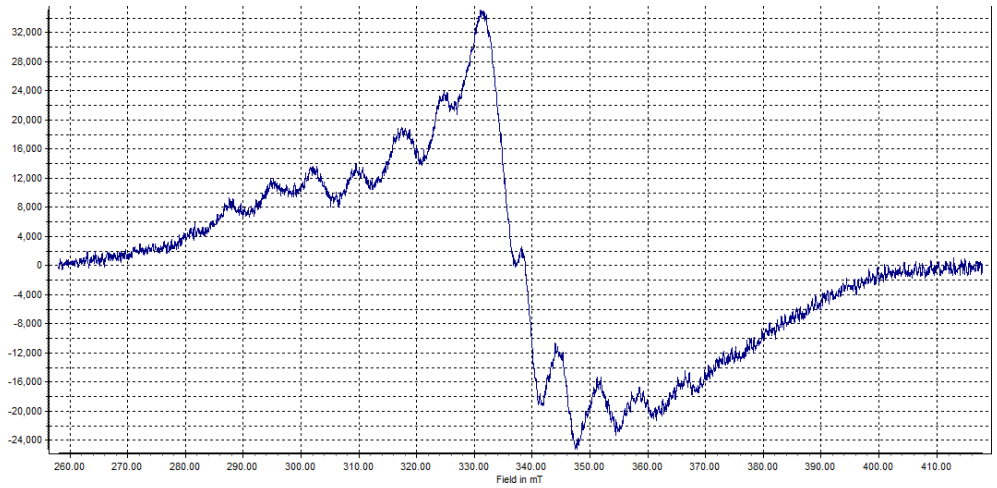

Figure 7-8 Baseline corrected EPR spectrum of **[1][pftb]**. A g value of 2 could be determined, indicating one unpaired electron. Hyperfine structure indicates the electron is ^{59}Co centred. Spectrum recorded at 77.4 K in CH_2Cl_2.

7.4.4 NMR spectra

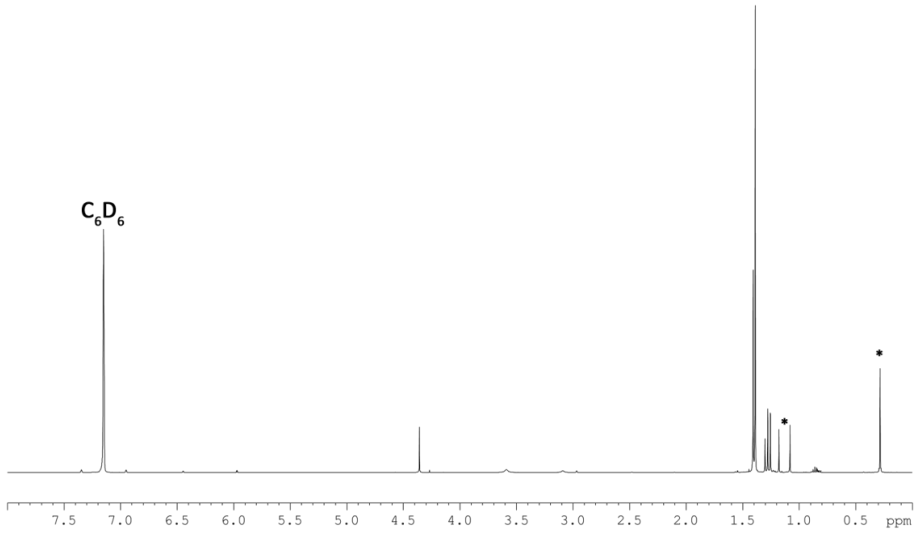

Figure 7-9 ^{1}H NMR spectrum of **2** in C_6D_6 at 300 K. Signals marked with an asterisk are silicon grease and minor impurities.

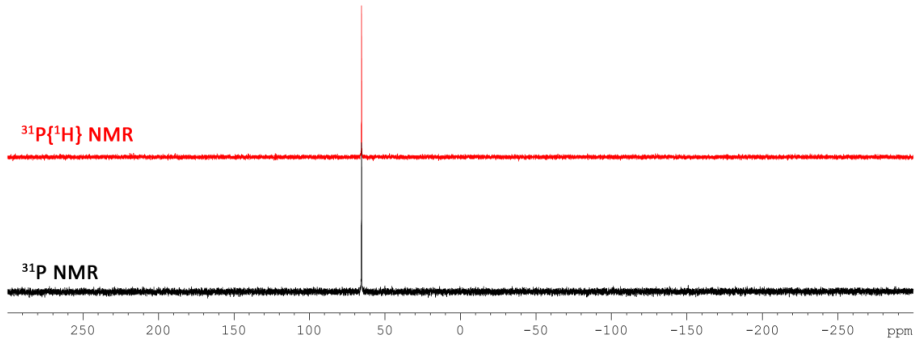

Figure 7-10 ^{31}P (black) and ^{31}P{^{1}H} (red) NMR spectra of **2** in C_6D_6 at 300 K.

7.4.5 Crystallographic data

As structural details for compound **1** are already included in the dissertation of Maria Eckhardt, no further data will be given here.

Using Olex2,[19] all structures were solved with the ShelXT structure solution program,[20] using the Direct methods solution method. The models were refined with version 2014/6 of ShelXL[21] using Least Squares minimisation.

7.4.5.1 Compound 2

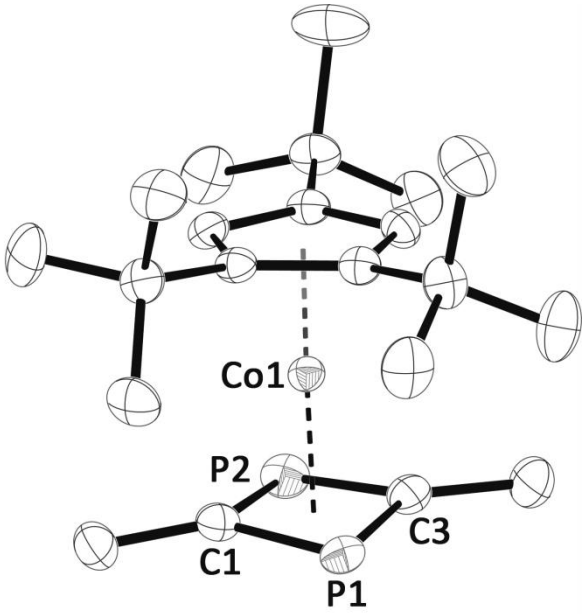

Figure 7-11 Molecular structure of **2** in the solid state. Hydrogen atoms are omitted for clarity. Thermal ellipsoids are shown at 50% probability level. Selected bond lengths [Å] and angles [°]: P1-C3 1.7925(16), P1-C1 1.7910(16), P2-C3 1.7857(16), P2-C1 1.7904(17), C1-P1-C3 81.00(7), C3-P2-C1 81.21(7), P2-C3-P1 98.66(8), P2-C1-P1 98.54(8).

Single clear light orange block-shaped crystals of **2** were obtained by crystallisation from hexane at r.t. A suitable crystal (0.21×0.12×0.04) was selected and mounted on a mitigen holder on a Xcalibur, Atlas^{S2}, Gemini ultra diffractometer. The crystal was kept at T = 182.9(6) K during data collection as first order phase transition accompanied by an increase in volume of and loss of crystallinity took place below this temperature.

Crystal Data for **2**. $C_{21}H_{35}CoP_2$, M_r = 408.36, triclinic, P-1 (No. 2), a = 9.25753(14) Å, b = 9.93611(13) Å, c = 11.86967(16) Å, α = 82.9524(11)°, β = 89.1001(12)°, γ = 83.3831(12)°, V = 1076.35(3) Å^3, T = 182.9(6) K, Z = 2, Z' = 1, μ(CuK$_\alpha$) = 7.632 mm^{-1}, 11361 reflections measured, 3768 unique (R_{int} = 0.0220) which were used in all calculations. The final wR_2 was 0.0599 (all data) and R_1 was 0.0240 (I > 2σ(I)).

7.4.5.2 Compound [1][pftb]

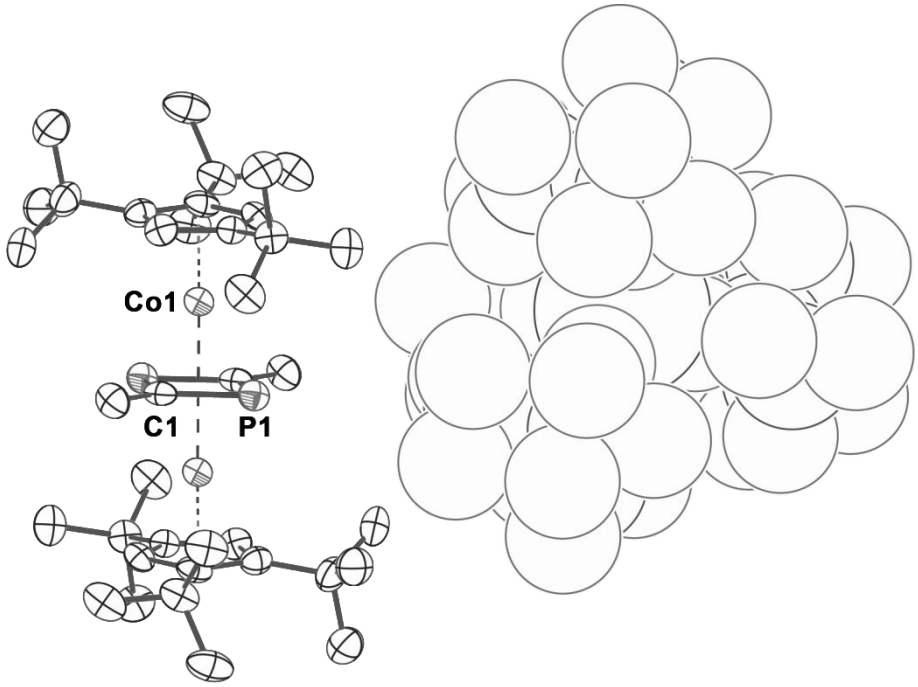

Figure 7-12 Molecular structure of Molecule A in **[1][pftb]** in the solid state. Hydrogen atoms and molecule B omitted for clarity. Anion shown in space-filling spheres. Thermal ellipsoids are shown at 50% probability level. Selected Bond lengths [Å] and angles [°]: P1-C1 1.839(7), P1-C1′ 1.864(7), C1-P1-C1′ 78.5(3), P1-C1-P1′ 101.5(3), Co1-Co1′ 3.4522(19).

Single clear dark green block-shaped crystals of (**[1][pftb]**) were obtained by diffusion of hexane into a solution of **[1][pftb]** in CH_2Cl_2 A suitable crystal (0.38×0.22×0.08) was selected and mounted on a mitigen holder on a GV50, TitanS2 diffractometer. The crystal was kept at T = 123.5(9) K during data collection.

Crystal data for **[1][pftb]**: $C_{54}H_{64}AlCo_2F_{36}O_4P_2$, M_r = 1667.83, triclinic, P-1 (No. 2), a = 10.4962(3) Å, b = 12.6761(4) Å, c = 25.5265(5) Å, α = 83.317(2)°, β = 89.0423(18)°, γ = 89.363(2)°, V = 3372.64(16) Å^3, T = 123.5(9) K, Z = 2, Z' = 1, μ(CuK$_\alpha$) = 5.742 mm^{-1}, 26034 reflections measured, 11168 unique (R_{int} = 0.0531) which were used in all calculations. The final wR_2 was 0.3328 (all data) and R_1 was 0.1126 (I > 2σ(I)).

7.4.5.3 Compound 3

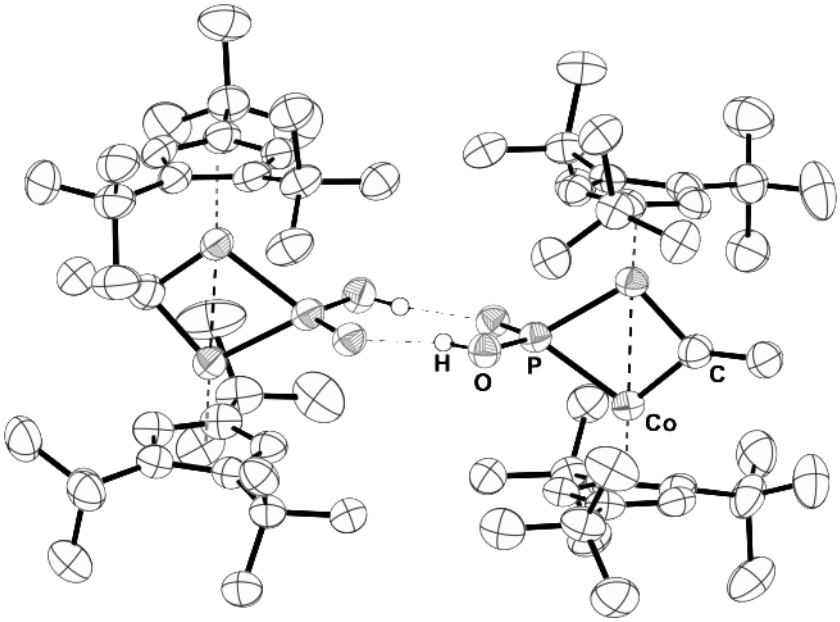

Figure 7-13 Molecular structure of two cations of **3** in the solid state. Hydrogen atoms are omitted for clarity. Thermal ellipsoids are shown at 50% probability level. Selected bond distances (Å) and angles (°):Co1-Co2 2.3853(11), Co1-C1 1.788(5), Co1-P1 2.1778(14), Co2-C1 1.802(6), Co2-P1 2.1697(13), Co2-P1-Co1 66.55(4), Co1-C1-Co2 83.3(2), C1-Co1-P1 104.68(19), C1-Co2-P1 104.50(17).

Single green rod-shaped crystals of (**3**) were obtained by crystallisation from diffusion of hexane into a solution of **3** in CH_2Cl_2. A suitable crystal was selected and mounted on a mylar loop on a Xcalibur, Atlas, Gemini ultra diffractometer. The crystal was kept at T = 123.00(14) K during data collection.

Crystal Data for **3**. $C_{105}H_{126}Al_2Cl_2Co_4F_{72}O_{12}P_2$, M_r = 3370.57, triclinic, P-1 (No. 2), a = 15.6948(4) Å, b = 20.5290(7) Å, c = 22.3059(7) Å, a = 76.935(3)°, b = 80.111(3)°, g = 81.106(3)°, V = 6846.5(4) Å^3, T = 123.00(14) K, Z = 2, Z' = 1, $\mu(CuK_a)$ = 5.822 mm^{-1}, 41916 reflections measured, 23556 unique (R_{int} = 0.0270) which were used in all calculations. The final wR_2 was 0.2350 (all data) and R_1 was 0.0774 (I > 2σ(I)).

7.4.5.4 Compound 4

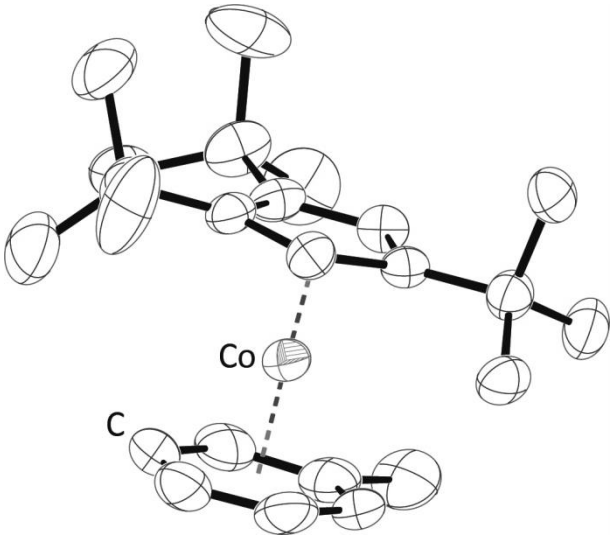

Figure 7-14 Molecular structure of the cation of **4** in the solid state. Hydrogen atoms are omitted for clarity. Thermal ellipsoids are shown at 50% probability level. Distance between cobalt centre and plane of rings: 1.65 Å (Co-tol_{cent}) and 1.76 Å (Co-Cp'''_{cent}).

Single red block-shaped crystals of **4** were obtained by recrystallisation from diffusion of hexane into a solution of **4** in CH_2Cl_2 A suitable crystal (0.20×0.20×0.08) was selected and mounted on a mylar loop on a SuperNova, Single source at offset, AtlasS2 diffractometer. The crystal was kept at T = 123.01(10) K during data collection.

Crystal Data for **4**. $C_{40}H_{37}AlCoF_{36}O_4$, M_r = 1351.60, orthorhombic, Pbca (No. 61), a = 16.3870(3) Å, b = 20.5562(4) Å, c = 29.8780(5) Å, V = 10064.5(3) Å^3, T = 123.01(10) K, Z = 8, Z' = 1, $\mu(CuK_\alpha)$ = 4.482 mm^{-1}, 58466 reflections measured, 10110 unique (R_{int} = 0.0799) which were used in all calculations. The final wR_2 was 0.3080 (all data) and R_1 was 0.1008 (I > 2σ(I)).

7.5 References

[1] T. E. Gier, *J. Am. Chem. Soc.* **1961**, *83*, 1769.

[2] J.-C. Guillemin, T. Janati, J.-M. Denis, *J. Org. Chem.* **2001**, 7864.

[3] G. Becker, G. Gresser, W. Uhl, *Z. Naturforsch., Teil B* **1981**, *36B*, 16.

[4] a) P. Binger, R. Milczarek, R. Mynott, M. Regitz, W. Rösch, *Angew. Chem. Int. Ed.* **1986**, *25*, 644; b) P. Binger, R. Milczarek, R. Mynott, M. Regitz, W. Rösch, *Angew. Chem.* **1986**, *98*, 645; c) P. B. Hitchcock, M. J. Maah, J. F. Nixon, *Chem. Commun.* **1986**, 737.

[5] J. C. T. R. B. S. Laurent, M. A. King, H. W. Kroto, J. F. Nixon, R. J. Suffolk, *Dalton Trans.* **1983**, 755.

[6] C. Jones, C. Schulten, A. Stasch, *Dalton Trans.* **2006**, 3733.

[7] M. Driess, D. Hu, H. Pritzkow, H. Schäufele, U. Zenneck, M. Regitz, W. Rösch, *J. Organomet. Chem.* **1987**, *334*, C35.

[8] a) R. Wolf, A. W. Ehlers, J. C. Slootweg, M. Lutz, D. Gudat, M. Hunger, A. L. Spek, K. Lammertsma, *Angew. Chem.* **2008**, *120*, 4660; b) R. Wolf, A. W. Ehlers, J. C. Slootweg, M. Lutz, D. Gudat, M. Hunger, A. L. Spek, K. Lammertsma, *Angew. Chem. Int. Ed.* **2008**, *47*, 4584; c) R. Wolf, J. C. Slootweg, A. W. Ehlers, F. Hartl, B. de Bruin, M. Lutz, A. L. Spek, K. Lammertsma, *Angew. Chem. Int. Ed.* **2009**, *48*, 3104; d) R. Wolf, J. C. Slootweg, A. W. Ehlers, F. Hartl, B. de Bruin, M. Lutz, A. L. Spek, K. Lammertsma, *Angew. Chem.* **2009**, *121*, 3150.

[9] R. G. Winter, W.E., *Organometallics* **1999**, *18*, 1827.

[10] a) I. Krossing, I. Raabe, *Angew. Chem. Int. Ed.* **2004**, *43*, 2066; b) I. Krossing, I. Raabe, *Angew. Chem.* **2004**, *116*, 2116.

[11] F. Dielmann, PhD thesis, Regensburg **2011**.

[12] E.-M. Rummel, M. Eckhardt, M. Bodensteiner, E. V. Peresypkina, W. Kremer, C. Gröger, M. Scheer, *Eur. J. Inorg. Chem.* **2014**, 1625.

[13] D. Patel, J. McMaster, W. Lewis, A. J. Blake, S. T. Liddle, *Nat Commun* **2013**, *4*.

[14] N. G. Connelly, W. E. Geiger, *Chem. Rev.* **1996**, *96*, 877.

[15] J. J. Schneider, D. Wolf, C. Janiak, O. Heinemann, J. Rust, C. Krüger, *Chem. Eur. J.* **1998**, *4*, 1982.

[16] F. D. Baumann, Elmar; Ehleiter, Yvonne; Kaim, Wolfgang; Kärcher, Jörg; Kelemen, Marc; Krammer, Ralf; Saurenz, Dirk; Stalke, Dietmar; Wachter, Christoph; Wolmershäuser, Gotthelf; Sitzmann, Helmut, *J. Organomet. Chem.* **1999**, 267.

[17] M. Gonsior, I. Krossing, N. Mitzel, *Z. Anorg. Allg. Chem.* **2002**, *628*, 1821.

[18] I. Krossing, *Chem. Eur. J.* **2001**, *7*, 490.

[19] O. V. Dolomanov, L. J. Bourhis, R. J. Gildea, J. A. K. Howard, H. Puschmann, *J. Appl. Crystallogr.* **2009**, *42*, 339.

[20] G. M. Sheldrick, *Acta Cryst.* **2015**, *A71*, 3.

[21] G. M. Sheldrick, *Acta Cryst.* **2015**, *C71*, 3.

8 Oxidation driven structural changes: From 1,3-Diphosphete to 1,2-Diphosphete complexes

Eva-Maria Rummel, Gábor Balázs, Veronika Heinl, Felix Riedelberger and Manfred Scheer*

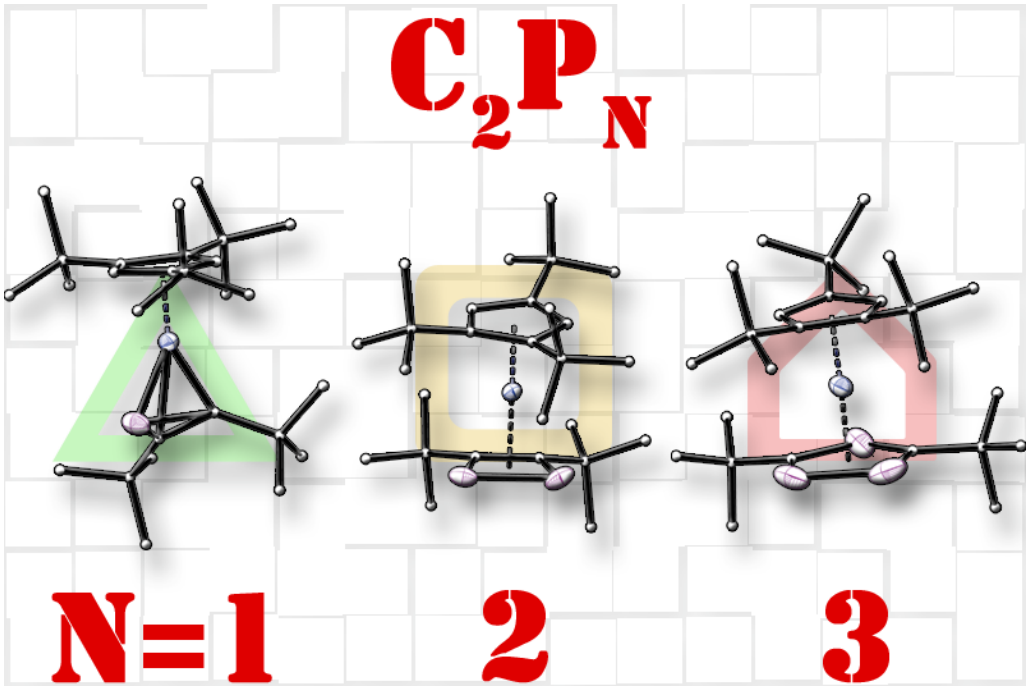

≡ Syntheses and characterisations were performed by Eva-Maria Rummel

≡ Some syntheses and characterisations were repeated by Veronika Heinl during a laboratory course

≡ DFT calculations were performed by Gábor Balázs

≡ CV measurements and evaluations were conducted by Felix Riedlberger

≡ Figures and schemes were made by Eva-Maria Rummel

≡ X-ray measurements, structure solution and refinement were done by Eva-Maria Rummel

≡ Manuscript was written by Eva-Maria Rummel except DFT calculation part: Gábor Balázs

8.1 Introduction

Reaction of the 1,3-diphosphete complex [Cp'''Co(η^4-P_2C_2tBu$_2$)] (**1**) with Ag[Al{OC(CF_3)$_3$}$_4$] (Ag[pftb]) was carried out using different reaction conditions to employ the competitive coordination and oxidation pathways. Depending on the stoichiometry and the solvent, a one dimensional polymer [Ag{Cp'''Co(η^4:η^1:η^1-P_2C_2tBu$_2$)}]$_n$·n[pftb] (**2**), different addition products [(Et_2O)$_{2n}$Ag$_n$Cp'''Co(μ,η^4:η^1:η^1-P_2C_2tBu$_2$)}]·n[pftb] (n=1: **3a**; n=2: **3b**), and a novel coordination compound [Ag$_2$Cp'''Co(μ,η^4:η^1:η^1-1,2-P_2C_2tBu$_2$)}$_2$Cp'''Co(μ,η^4:η^1-1,2-P_2C_2tBu$_2$)}$_2$]·2[pftb] (**4**) could be isolated. In **4**, the initial 1,3-diphosphete surprisingly isomerised to form a coordination compound of a 1,2-diphosphete complex [Cp'''Co(η^4-1,2-P_2C_2tBu$_2$)] (**I-1**). The release of **I-1** out of its coordination compound **4** has been successfully achieved. In addition, an alternative synthesis for the 1,2-diphosphete complex **I-1** has been developed. Furthermore, a ring expansion product [Cp'''Co(η^5-P_3C_2tBu$_2$)][pftb] (**5**) and the ring contraction product [Cp'''Co(η^3-PC_2tBu$_2$)][pftb] (**6**) were observed in the same reaction. The oxidation of the 1,3-diphosphete ring in **1** is a possible step to the combined ring expansion/ring contraction reaction towards the triphosphacobaltocenium **5** and the cobalt phosphirenylium complex **6**, which were isolated under mild conditions.

Since the first successful synthesis of the phosphaalkyne *t*BuC≡P in 1981,[1] a lot of chemistry has been conducted with this class of compounds with a carbon-phosphorus triple bond.[2] Especially cycloadditions have been in focus since the first [2+2] cycloadditions of two phosphaalkynes in the coordination sphere of a transition metal have been reported to yield complexes of the formula [Cp^{R}M(1,3-P_2C_2tBu$_2$)] (M = Co, Ir, Rh, Cp^R = Cp, Cp*).[3] The coordination chemical behaviour of these 1,3-diphosphacyclobutadiene (1,3-diphosphete) complexes is described in the literature for a variety of complexes.[3a,4] In all of these cases, a coordination of the phosphorus moiety on the diphosphete ring towards an unsaturated metal fragment takes place. But especially the use of group 11 metal salts leads to a variety of products, including dimeric and tetrameric complexes as well as one- and two dimensional supramolecular assemblies (cf. Figure 9-1).[5]

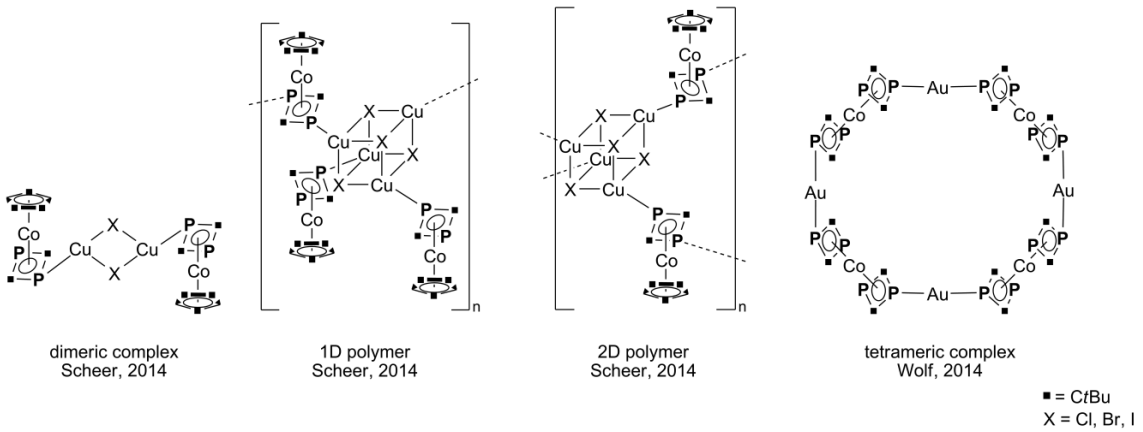

Figure 8-1 Cu(I) and Au(I) coordination of 1,3-diphosphete complexes.

Interestingly, although reactions with highly oxidative compounds like Ag^+ have already been conducted, only coordination products could be isolated.[5b,5c] Additionally, oxidation chemistry of 1,3-diphosphete complexes has not been thoroughly investigated so far with only two papers mentioning electrochemical processes: Driess *et al.* discussed the cyclovoltammogram of [(toluene)Fe(1,3-P_2C_2tBu$_2$)][6] and Lammertsma *et al*. were able to electrochemically and chemically oxidise their anionic homoleptic bis-diphosphete complexes $[Fe(P_2C_2t\text{Bu}_2)_2]^-$ and $[Co(P_2C_2t\text{Bu}_2)_2]^-$.[7] To closer investigate such processes is especially intriguing as the oxidation potential of Ag^+ is highly dependent on the solvent in which the reaction is carried out.[8] We were especially interested in investigating the potential of 1,3-diphosphete complexes to be oxidised by the silver(I) salt of the weakly coordinating anion (WCA) $Ag[Al\{OC(CF_3)_3\}_4]$ (Ag[pftb]). This salt has been chosen due to the ability to stabilise complexes with P_4 and As_4 as ligands[9] and oxidation products in its vicinity as well as its good solubility.[10]

The structural isomers of 1,3-diphosphete complexes, the 1,2-diphosphacyclobutadiene (1,2-diphosphete) complexes, should be the thermodynamically and kinetically favoured product of a [2+2] cycloaddition of any two phosphaalkynes.[11] Because of this it is interesting that the majority of reported diphosphete complexes are complexes of the 1,3-isomer.[i] To our knowledge, only one system is known in which the 1,2-isomer is formed exclusively: the tantalum complex [Cp*TaCl$_2$(η^4-1,2-P_2C_2tBu$_2$)].[12] The other two examples [Ti(COT)(η^4-1,2-P_2C_2tBu$_2$)] and [W(CO)$_4$(η^4-1,2-P_2C_2Me$_2$)] are co-formed with their 1,3-isomer counterparts.[4d,13] 1,2-Diphosphete complexes have not yet been used in comprehensive studies concerning their coordination abilities.

[i] Based on concept search in SciFinder: 1,2-diphosphete: mentioned in three publications; 1,3-diphosphete: mentioned in 45 publications (adjusted for duplicates and irrelevant results). As many publications feature several 1,3-diphosphete complexes, the real percentage of experimentally observed diphosphete complexes is even higher.

Herein we report on the stepwise formation of the one dimensional polymer [Ag{Cp'''Co(η^4:η^1:η^1-P_2C_2tBu$_2$)}]$_n$·n[pftb], and the isomerisation of the 1,3-diphosphete complex [Cp'''Co(η^4-1,3-P_2C_2tBu$_2$)] (**1**) to the 1,2-diphosphete coordination compound [Ag$_2${Cp'''Co(μ,η^4:η^1:η^1-1,2-P_2C_2tBu$_2$)}$_2${Cp'''Co(μ,η^4:η^1-1,2-P_2C_2tBu$_2$)}$_2$]·2[pftb]. Also the ring expansion product [Cp'''Co(η^5-P_3C_2tBu$_2$)][pftb] and the ring contraction product [Cp'''Co(η^3-PC_2tBu$_2$)][pftb], respectively, are formed in the reaction of **1** and Ag[pftb] by employing the correct reaction conditions.

8.2 Results and Discussion

Compound **1** has been synthesised according to literature procedure[5a] and cyclovoltammographic data has been collected (see SI, Figure 8-10). An irreversible oxidation step has been found at $E_{1/2}$ = +0.45 V, indicating that it should be possible to oxidise **1** using silver(I) salts. Furthermore, it should be also possible to isolate products of coordination below the potential of the first oxidation step of E = 0.45 V: the oxidation potential of silver(I) salts is dependent on the solvent used, and in coordinating solvents like THF or Et_2O ($E^{0\prime}$ = +0.41 V) the potential is considerably lower than in e.g. dichloromethane ($E^{0\prime}$= +0.65 V).[8]

Different reaction pathways have been employed which indeed led to coordination compounds as well as oxidation products (see Scheme 8-1).

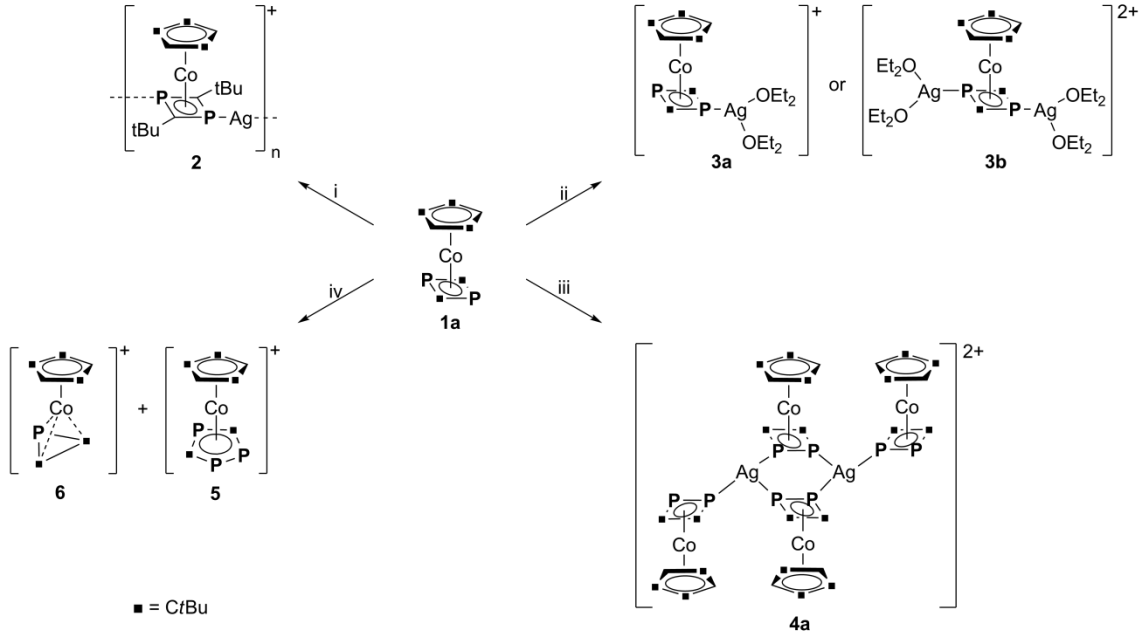

Scheme 8-1 Reaction and transformation pathways for [Cp'''Co(η^4-P_2C_2tBu$_2$)] (**1**): i) Ag[pftb] in CH_2Cl_2/Et_2O mixture, -80 °C → r.t.; ii) 2 Ag[pftb] in Et_2O, -80 °C → -60 °C (**3a**) or -80 °C → 0 °C (**3b**); iii) 2 Ag[pftb] in CH_2Cl_2, -80 °C → r.t., iv) 2 Ag[pftb] in CH_2Cl_2 layered with **1** in hexane at -30°.

First, **1** has been stirred in Et_2O/hexane together with Ag[pftb] in CH_2Cl_2 from -80 °C to r.t., which led to the formation of the 1D polymeric compound

[Ag{Cp'''Co(η^4:η^1:η^1-$P_2C_2tBu_2$)}]$_n$·n[pftb] (**2**). Dark red crystals could be grown by diffusion of hexane into a CH_2Cl_2 solution of **2** at -30 °C, however the weak diffraction power of the crystals (d_{min} ~ 1Å) made it impossible to establish structural details beyond the heavy atom framework. The preliminary structural model in monoclinic space group $P2_1/c$ contains four repeating units and thus four pftb anions in the asymmetric unit. The large independent part and the presence of the highly disordered pftb anions complicate structure refinement. A representation of the cationic strand is shown in Figure 8-2. However, the composition of the crystals could be verified by elemental analysis.

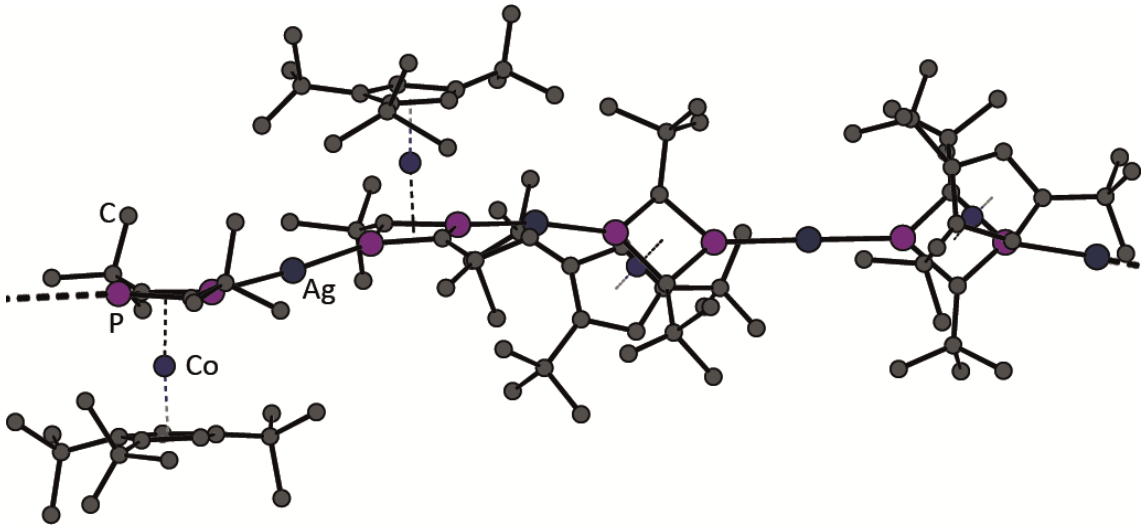

Figure 8-2 Schematic representation of the cationic repetition unit of **2** in the solid state. Hydrogen atoms are omitted for clarity.

Wolf *et al*. also proposed a one dimensional polymer of Ag(I) of the homoleptic 1,3-diphosphete [Co(η^4-$P_2C_2Ad_2$)$_2$] (Ad = adamantyl) complex: [Ag{Co($P_2C_2Ad_2$)$_2$}]$_n$. However, the crystal structure could not be determined and the authors were not able to dissolve the neutral polymer again in any common organic solvent to conduct further NMR spectroscopic and mass spectrometric investigations.[5b] The formation of a charged polymer and the use of the [pftb]$^-$ anion is of advantage here since the solubility of compounds with this anion is often increased in comparison to the salts of smaller anions or neutral compounds.[14] Mass spectrometric analysis of the polymer shows different fragments of **1** and Ag combined. Also, in the ^{31}P and ^{31}P{^{1}H} NMR spectra **2** shows only one broad signal for both magnetically and chemically equivalent phosphorus atoms, which is often the case for phosphorus containing polymeric compounds.[15]

In contrast, the reaction of **1** in pure Et_2O with Ag[pftb] in a CH_2Cl_2/Et_2O mixture is highly dependent on temperature. Stirring the reaction from -80 °C to reach -60 °C yields [(Et_2O)$_2$Ag{Cp'''Co(η^4:η^1-$P_2C_2tBu_2$)}][pftb] (**3a**), in which one silver ion is coordinated by the 1,3-diphosphete moiety and by the solvent molecules. Orange crystals of **3a** can be obtained

by layering the reaction mixture with pure hexane and subsequent storage at -30 °C. If the reaction temperature reaches 0 °C, however, the formation of a coordination compound is observed where both phosphorus moieties are coordinated to a silver atom. Both silver(I) cations are trigonally planar coordinated by altogether four additional ether molecules to form $[(Et_2O)_4Ag_2\{Cp'''Co(\mu,\eta^4{:}\eta^1{:}\eta^1\text{-}P_2C_2tBu_2)\}]\cdot 2[pftb]$ (**3b**). The orange compound **3b** crystallises in the space group *P*-1 with one formula unit in the asymmetric unit. A representation of the cations of **3a** and **3b** is shown in Figure 8-3.

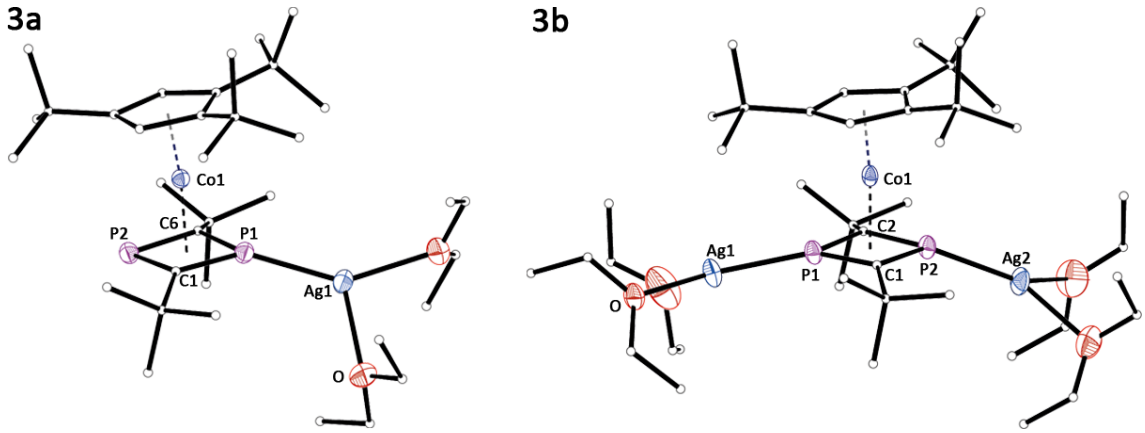

Figure 8-3 Molecular structures of the cations of **3a** and **3b** in the solid state. Hydrogen atoms are omitted and carbon atoms of the ligands are shown in a ball-and-stick representation for clarity. Thermal ellipsoids are shown at 50% probability level. Selected bond lengths [Å] and angles [°]: **3a**: P1-C1 1.774(2), P2-C1 1.792(2), P2-C6 1.795(2), P1-C6 1.777(2), P1-Ag1 2.3535(6), P1-C1-P2 96.99(10), C6-P2-C1 82.53(11); **3b**: P1-C1 1.777(4), P2-C1 1.783(4), P2-C6 1.778(4), P1-C6 1.777(4), P1-Ag1 2.3711(11), P2-Ag2 2.3487(11), P1-C1-P2 95.3(2), C6-P2-C1 84.47(19).

There is no structural conspicuous feature in the structures of **3a** or **3b** as bond lengths and angles within the 1,3-diphosphete moiety are similar to those of complex **1**.[5a] Interestingly, only the slight change of the reaction conditions (an excess of Et_2O) leads to the saturation of the silver atoms by ether molecules rather than the formation of a 1D polymer as is the case in **2**. As there is no evidence in the solution NMR spectrum for a possible breakage of the polymeric structure by addition of Et_2O to **2**, it is deducted that **2** and **3a/b** are only formed when the exact stoichiometry and solvent ratio is used. Depending on the temperature at which the reaction is stopped and left to crystallise, different molecular products could be formed.

Interestingly, the saturation of the Ag^+ centres by ether molecules seems to be reversible: drying crystal probes of **3a** and **3b** in order to obtain elemental analyses leads to their decomposition and loss of Et_2O in the molecules. Trying to recrystallise them in dichloromethane subsequently fails but leads to the formation to **4** and **5** (*vide infra*). Because of these problems it is difficult to collect further analytical data for **3a** and **3b**.

In contrast to the coordination reactions described above, the use of CH_2Cl_2 as the sole solvent in the reaction of **1** with Ag[pftb] increases the oxidation potential and leads to the oxidation of **1**. Starting the reaction at -80 °C and slowly reaching r.t. while stirring both reactants together leads to a rearrangement of the 1,3-diphosphete moiety to form the unprecedented 1,2-diphosphete coordination compound $[Ag_2\{Cp'''Co(\mu,\eta^4{:}\eta^1{-}1,2{-}P_2C_2tBu_2)\}_2\{Cp'''Co(\mu,\eta^4{:}\eta^1{-}1,2{-}P_2C_2tBu_2)\}_2]\cdot 2[pftb]$ (**4**) in addition to a silver mirror. Compound **4** can be recrystallised by diffusion of hexane into a CH_2Cl_2 solution of **4** and crystallises in the orthorhombic space group *Pbca* (see Figure 8-4). Only half of the dication as well as one $[pftb]^-$ anion can be found in the asymmetric unit.

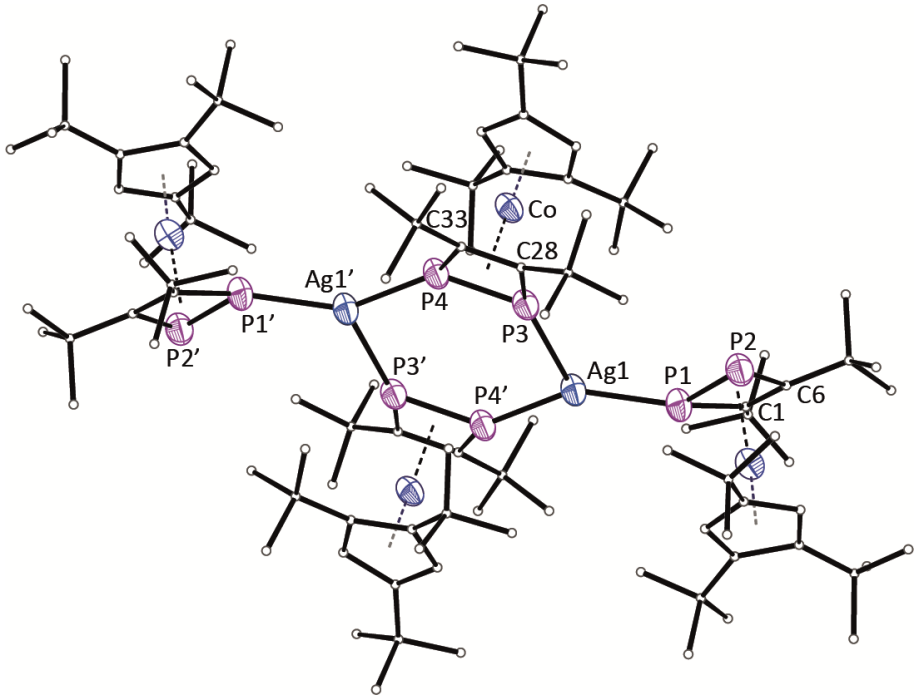

Figure 8-4 Molecular structure of the cation of **4** in the solid state. Hydrogen atoms are omitted, carbon atoms are shown in ball-and-stick representation for clarity. Thermal ellipsoids are shown at 50% probability level. Selected bond lengths [Å] and angles [°]: P1-P2 2.153(3), P1-C1 1.813(8), P2-C6 1.817(8), C1-C6 1.443(11), P3-P4 2.151(3), P3-C28 1.807(8), P4-C33 1.803(8), P4-Ag1' 2.560(2), P1-Ag1-P3 144.74(7), P1-Ag1-P4' 118.86(7), P3-Ag1-P4' 96.38(7), P2-P1-Ag1 129.86(11), C1-P1-P2 80.3(3), C6-P2-P1 77.0(3), C6-C1 P1 99.0(5), C1-C6-P2 103.5(5).

In **4**, all bonds lengths within the planar P_2C_2 four-membered rings are between a single and a double bond distance which underlines the anti-aromatic character of the 1,2-diphosphete ligand. Four 1,2-diphosphete complexes of cobalt and two silver(I) cations come together to form a coordination compound in which the silver is trigonally planar coordinated. The six-membered Ag_2P_4 ring is reminiscent of structures obtained by silver(I) salts and P_2 ligand containing compounds like $[\{CpMo(CO)_2\}_2(\mu,\eta^2{:}\eta^2{-}P_2)]$.[16]

The obvious structural feature of **4** is the 1,2-diphosphete moiety which has so far only been observed in very few compounds (see introduction): $[Ti(COT)(\eta^4{-}1,2{-}P_2C_2tBu_2)]$ (COT = cyclooctatetraene),[13] $[W(CO)_4(\eta^4{-}1,2{-}P_2C_2Me_2)]$[4d] and $[Cp^*TaCl_2\{\sigma,\sigma,\pi{-}1,2{-}P_2C_2tBu_2\}]$.[12] The

bond parameters of **4** are comparable to those of the known 1,2-diphosphete complexes. Additionally, in our own group a rearrangement of the triphosphaferrocene [Cp'''Fe(η^5-1,2,4-P_3C_2tBu$_2$)] could be observed in the reaction with CuBr to form [{Cp'''Fe(η^4:η^1:η^1-P_2C_2tBu$_2$)}(μ-CuBr)]$_2$.[17] Here, the stoichiometry of CuX (X = Cl, Br) used has a direct influence on the isolated products of a fragmentation. It is notable that if triphosphaferrocene [Cp'''Fe(η^5-1,2,4-P_3C_2tBu$_2$)] was treated with Ag[pftb], only a coordination compound could be isolated.

The coordination compound **4** is soluble in CH_2Cl_2. In the $^{31}P\{^1H\}$ NMR spectrum at r.t. three broad signals at δ [ppm] = 4.8 (s, 2P), 1.7 (s, 1P) and -1.6 (s, 1P) are observed, which reveal dynamic processes in solution. VT NMR studies have been conducted to further investigate the origin of these dynamic behaviour. Upon cooling to -80 °C, the two small singlets split into a doublet shifting to low field while the singlet at δ = 4.8 ppm sharpens significantly and displays a highfield shift, so both signal groups change their respective places (cf. Figure 8-5).

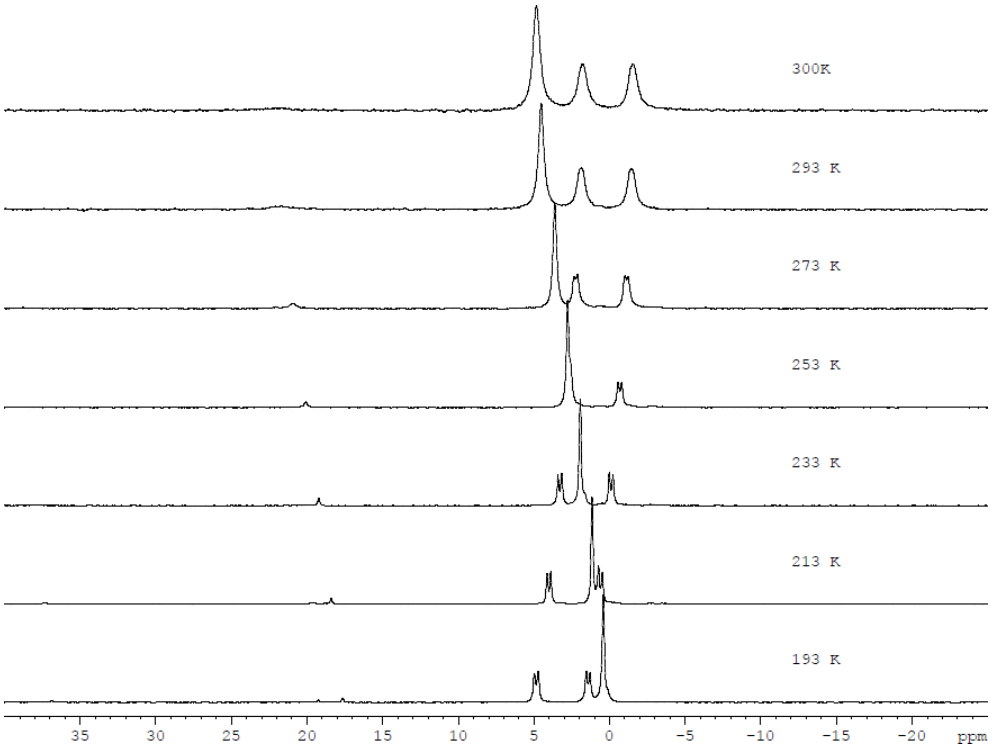

Figure 8-5 $^{31}P\{^1H\}$ VT NMR spectrum of **4**. The solution has been cooled in steps of 20 K from 293 K to 193 K.

Also, the formation process of **4** was investigated by monitoring the reaction progress by ^{31}P NMR spectroscopy from -80 °C to r.t. (cf. SI, Figure 8-16). However, in the NMR time scale no additional signals could be found which prevented a better understanding of the formation mechanism.

As there is only a limited amount of known 1,2-diphosphete complexes in literature (*vide supra*), we wanted to try and extract [Cp'''Co(η^4-1,2-P_2C_2tBu$_2$)] (**I-1**) from coordination compound **4**. For that purpose **4** has been dissolved in pure pyridine, which is a suitable and strong donor ligand for Ag(I) and could thus replace the 1,2-diphosphete complex within the coordination sphere of silver. After removal of the solvent *in vacuo* and subsequent addition of hexane to the resulting oil, a red solution was obtained which could be filtered from some oily residue. The $^{31}P\{^1H\}$ NMR spectrum of the solution shows a singlet at δ = -83.8 ppm, which could be assigned to the two magnetically and chemically equivalent phosphorus atoms in **I-1**. A comparison between the phosphorus NMR shifts of 1,2-diphosphete and 1,3-diphosphete ligands is shown in Table 8-1.

Table 8-1 Comparison of NMR data of similar 1,3- and 1,2-diphosphete complexes.

Compound	**$^{31}P\{^1H\}$ NMR, δ [ppm]**	**difference[i] [ppm]**	**literature**
[Ti(COT)(η^4-1,3-P_2C_2tBu$_2$)]	214.5 (s)	80.9	[12]
[Ti(COT)(η^4-1,2-P_2C_2tBu$_2$)]	133.6 (s)		
[W(CO)$_4$(η^4-1,3-P_2C_2Me$_2$)]	-4.0	70.8	[1e]
[W(CO)$_4$(η^4-1,2-P_2C_2Me$_2$)]	-74.8		
[Cp'''Co(η^4-1,3-P_2C_2tBu$_2$)] (**1**)	23.4 (s), 42.3 (s)[ii]	116.6	[2a]
[Cp'''Co(η^4-1,2-P_2C_2tBu$_2$)] (**I-1**)	-83.8		this work

[i] difference calculated from midpoint of signals if phosphorus atoms are not equivalent

[ii] due to the steric demand of the Cp''' ligand and the *t*Bu substituents on the diphosphete moiety, the two phosphorus atoms of **1** are magnetically not equivalent.

From the literature it can be seen that $^{31}P\{^1H\}$ NMR signals for 1,2-diphosphete complexes are always significantly high field shifted in comparison to those of their 1,3-diposphete isomers, a series which is continued by **I-1**. It was possible to crystallise **I-1** from the resulting orange-red solution as orange blocks. Compound **I-1** crystallises in orthorhombic space group *Pbca*. A representation of the structure can be found in Figure 8-6.

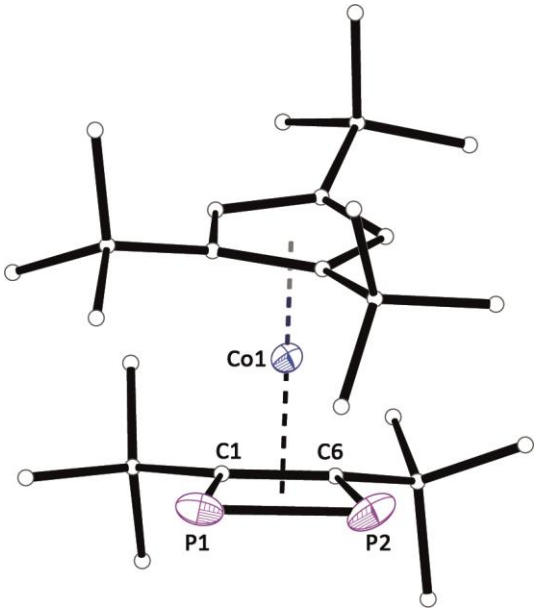

Figure 8-6 Molecular structure of **I-1** in the solid state. Hydrogen atoms are omitted for clarity. Thermal ellipsoids are shown at 50% probability level. Selected bond lengths [Å] and angles [°]: P1-P2 2.1818(7), P1-C1 1.8158(18), P2-C6 1.8077(18), C1-C6 1.443(2), C1-P1-P2 78.16(6), C6-C1-P1 101.56(11).

All bond lengths in the 1,2-diphosphete ligand in **I-1** are in the range between single bonds and double bonds (P-P: 2.1818(7), P-C: 1.8077(18)-1.8158(18), C-C: 1.443(2)). In addition, the dihedral angle within the P1-C1-C6-P2 ring is only 0.14°. It can be concluded that the four-membered ring in the 1,2-diphosphete complex **I-1** has a similar delocalised character as the 1,3-diphosphete ring in **1**. The geometric parameters of the DFT optimised geometry of **I-1** are in very good agreement with the experimental data (c.f. SI).

The observed ^{31}P NMR shift of δ = -83.3 ppm for **I-1** can also be found in VT NMR studies for **1** which our group published earlier.[5a] However, as no reference substance has been available at that time, the peak at high field was simply viewed as a decomposition product. With the new information in mind, **1** has been refluxed in toluene for three days to convert it to **I-1** (Figure 8-7). After this, 70% of **1** are converted to **I-1**. This is also in agreement with the 1,2-diphosphete being the thermodynamically favoured product as mentioned above. Longer refluxing times or higher temperatures[ii] are not favourable as they do not change the ratio significantly. After six days, still only 75% have been converted to **I-1**, but a new singlet at δ = 91.8 ppm arises in both the ^{31}P and ^{31}P{^{1}H} spectra which could not be assigned to any known species so far.[iii] As **1** and **I-1** have quite similar properties, separation via column chromatography has not been possible. DFT calculations at the B3LYP/def2-TZVP level show that **I-1** is thermodynamically more stable by 1.89 kJ·mol^{-1} in comparison to **1**. The relatively

[ii] The thermolysis has also been conducted in 1,3-diisopropylbenzene, b.p. 203 °C.
[iii] Binger et al. possibly observed a mixture of [Ti(COT)(η^4-1,2-P$_2$C$_2$*t*Bu$_2$)] (45%) and [Ti(COT)(η^4-1,3-P$_2$C$_2$*t*Bu$_2$)] (55%) also because of the reaction conditions used: To form the diphosphete complexes, [Ti(COT)$_2$] has been refluxed with *t*BuC≡P in toluene for five days.[13]

harsh conditions for the isomerisation of **1** to **I-1** are probably due to the high activation barrier for this process.

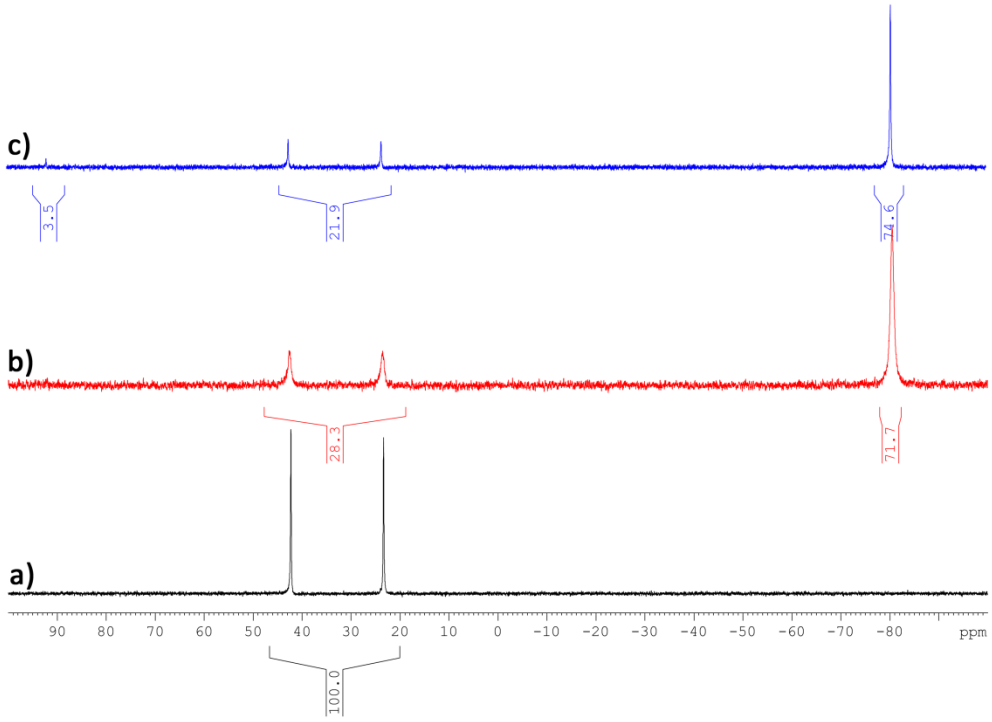

Figure 8-7 **a)** ^{31}P NMR spectra of a solution of **1** in C_6D_6. **b)** The same solution after three days of refluxing in toluene. During this time, roughly 70% of **1** have been converted to **I-1**. **c)** The same solution after six days of refluxing in toluene. The ratio did not change much, however a new signal at 91.8 ppm arises.

The ^{31}P NMR signal for **I-1** is also found after an extended storage of the coordination compound **4** in solution. This together with the formation of a black precipitate hints towards the decomposing of **4** over time. Solutions show a decrease of the signal sets of **4** and the appearance two new sets of signals: one singlet at -90 ppm (**I-1**) and a set of a doublet at 118.8 ppm and a triplet at 114.0 ppm with coupling constants of $^2J_{PP}$ = 39.7 Hz (cf. SI, Figure 8-18). In order to isolate this compound, another approach was chosen to investigate this reaction thoroughly. Upon diffusion of a solution of **1** in hexane layered onto a solution of Ag[pftb] in CH_2Cl_2 at -30°, two different compounds could be isolated: The triphosphacobaltocenium [Cp‘‘‘Co(η^5-1,2,4-P_3C_2tBu$_2$)][pftb] (**5**) with a five-membered C_2P_3 ring and the counterpart [Cp‘‘‘Co(η^3-PC_2tBu$_2$)][pftb] (**6**) with a three-membered C_2P ring (cf eq. (8-1)).

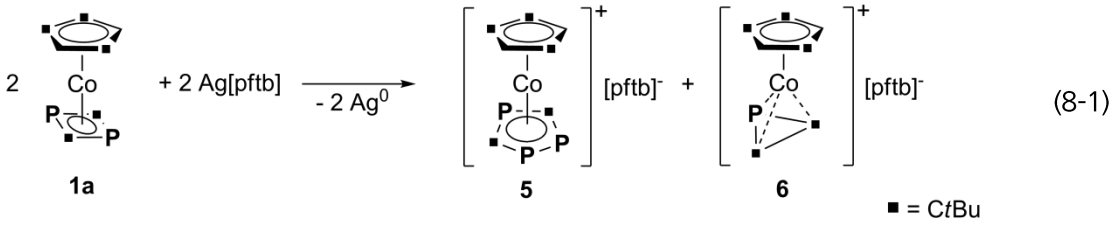

(8-1)

A dilution of reaction mixtures of **5** and **6** with CH_2Cl_2 and subsequent layering of hexane leads to the crystallisation of red crystals of **5**. After further dilution, a second fraction of crystals of **5** can be obtained together with green block-shaped crystals of **6**. Compound **5** and **6** both crystallise in the orthorhombic space group *Pbca*. A structural representation is shown in Figure 8-8.

The bond distances in the C_2P_3 five membered ring are all between single and double bonds, indicating a planar, delocalised $6e^-$ aromatic ring system. The bond lengths of the five-membered ring in **5** can be compared with those of other triphospholyl rings.[17-18]

In compound **6**, large differences in the bond distances and angles within the three membered C_2P ring and between the cobalt atom and the three members of the ring lead to the conclusion a formal C_2P^+ ring is present with a carbocation (C1) which has a trigonally planar surrounding and a formally negatively charged carbon atom (C6) which has a distorted tetrahedral coordination geometry. To balance the charge of the 16 VE complex, also a positively charged phosphorus atom needs to be present, which leads to the conclusion a cyclopropenylium (phosphirenylium) cation is present in compound **6**. This could also be confirmed by DFT calculations (vide infra).

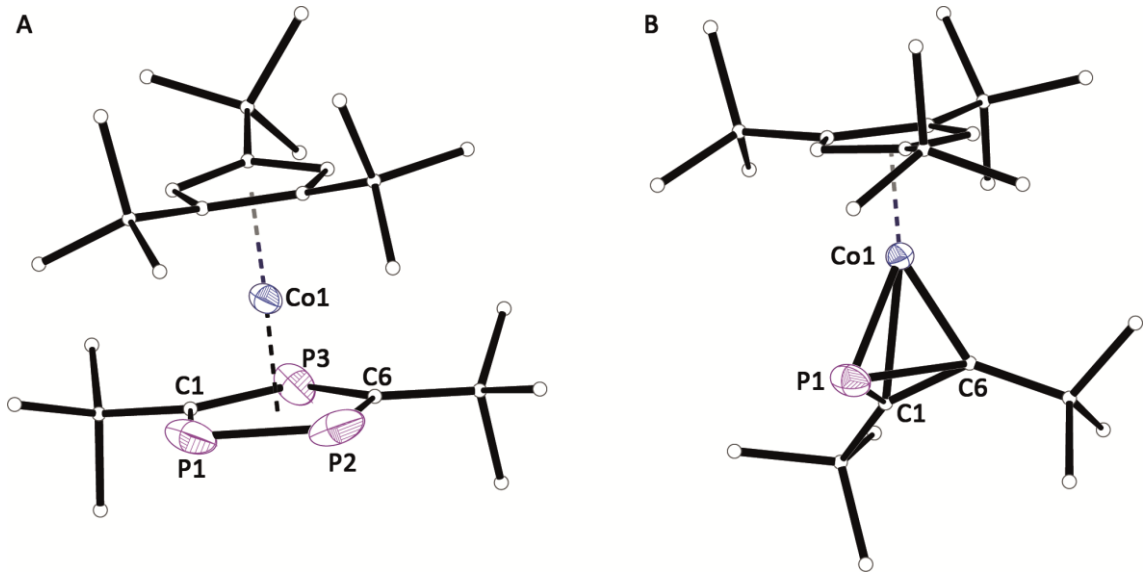

Figure 8-8 **A**) Molecular structure of the cation of **5** in the solid state. Hydrogen atoms are omitted, carbon atoms are shown in ball-and-stick representation for clarity. Thermal ellipsoids are shown at 50% probability level. Selected bond lengths [Å] and angles [°]: P1-P2 2.127(3), P1-C1 1.779(7), P2-C6 1.815(13), P3-C1 1.758(6), P3-C6 1.775(14), C1-P1-P2 98.9(2), C6-P2-P1 100.0(4), C1-P3-C6 100.5(5), P3-C1-P1 121.6(4). **B**) Molecular structure of the cation of **6** in the solid state. Hydrogen atoms are omitted, carbon atoms are shown in ball-and-stick representation for clarity. Thermal ellipsoids are shown at 50% probability level. Selected bond lengths [Å] and angles [°]: P1-C1 1.762(3), C1-C6 1.376(4), P1-C6 2.163(3), Co1-P1 2.1018(9), Co1-C1 2.254(3), Co1-C6 1.879(3), C1-P1-C6 39.40(12), C6-C1-P1 86.21(19), C1-C6-P1 54.40(15).

A relevant reaction in regards to the formation of **5** and **6** has been published by the group of Zenneck. Their complex $[Mo(\eta^4\text{-}1,3\text{-}P_2C_2t\text{Bu}_2)_3]$ shows a temperature-dependent topotactic bond formation between two neighbouring P_2C_2 ligands in X-ray studies at 100 K

while at 293 K no such interaction could be observed. This topotactic reaction is fully reversible in the solid state.[19] The discussed bond formation between two neighbouring diphosphete rings could be a possible starting point to the formation of compounds **5** and **6** when oxidising **1** with Ag(I). Our own group could observe a rearrangement and elimination of one phosphorus atom out of the triphosphaferrocene [Cp'''Fe(η^5-1,2,4-$P_3C_2t\mathrm{Bu}_2$)] in the reaction with CuBr to form [{Cp'''Fe(η^4:η^1:η^1-$P_2C_2t\mathrm{Bu}_2$)}(μ-CuBr)]$_2$.[17] However, it was not possible to react **5** with another equivalent of Ag[pftb] to yield a similar elimination leading to the formation of coordination compound **4** or a similar complex.

DFT calculations show that the disproportionation of the hypothetical, oxidised complex [Cp'''Co(η^4-1,3-$P_2C_2t\mathrm{Bu}_2$)]$^+$ (**1**$^+$) to [Cp'''Co(η^5-1,2,4-$P_3C_2t\mathrm{Bu}_2$)]$^+$ and [Cp'''Co(η^3-$PC_2t\mathrm{Bu}_2$)]$^+$ is thermodynamically favoured in the gas phase by –88.19 kJ·mol^{-1}. In the doublet spin state, the spin density in [Cp'''Co(η^4-1,3-$P_2C_2t\mathrm{Bu}_2$)]$^+$ is mainly localised on cobalt with minor contribution of the C_2P_2 ring. The consequence of the oxidation of **1** to **1**$^+$ is the weakening of the Co-$PC_2t\mathrm{Bu}_2$ bonding as it is reflected in the Wiberg Bond Indices (WBI; **1**: Co-P 0.85, Co-C 0.44; **1**$^+$: Co-P 0.74, Co-C 0.39). This might explain the rearrangement of **1** and fragmentation to **5** and **6** upon oxidation. The oxidation of **1** to **1**$^+$ is accompanied by the increase of the NPA charge on cobalt from +0.38 to +0.85, respectively, indicating formal oxidation states of +1 and +2, respectively. The NPA charges on Co in **5** and **6** are with +0.41 and +0.45, respectively, very similar to the one found in **1**, showing the presence of Co(I). Accordingly, the $t\mathrm{Bu}_2C_2P$ ligand in **6** can be best described as a phosphacyclopropenylium cation, which coordinates in an asymmetric fashion to the cobalt centre. The lengthened C-P bond in the $t\mathrm{Bu}_2C_2P$ ligand is due to the involvement of the C-P σ-bond into the coordination to the cobalt atom (Figure 8-9). The distortion of the C_2P ring is also reflected in the Wiberg Bond Indicies. The WBI of the C1-C6 and P1-C1 bonds (labelling according to Figure 8-8 **B**) are very close to unity (0.98 and 0.99 respectively) while the WBI of the C6-P1 bond is considerably lower (0.61). The same trend is also observed for the Co-C and Co-P WBIs. The localised molecular orbitals representing the Co-PC_2 bonding is depicted in Figure 8-9.

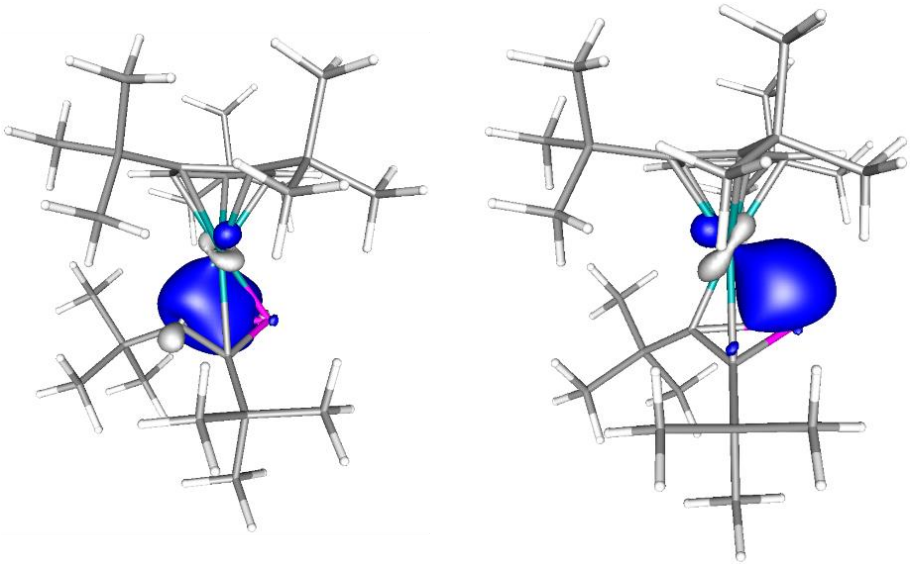

Figure 8-9 Localised molecular orbitals in **6** representing the Co-PC_2 bonding.

The 19 VE complex 1,2,4-triphosphacobaltocene is unknown in the literature so far. Only the heteroleptic 18 VE complex [Co(η^5-1,2,4-P_3C_2tBu$_2$)(η^4-P_2C_2tBu$_2$)] is known from the co-condensation reaction of Co and *t*BuC≡P.[20] Cyclovoltammographic measurements show that no reduction of **5** is possible in CH_2Cl_2, but two irreversible oxidations are taking place at $E_{1/2}$ = 100 mV and 400 mV (for CV see SI, Figure 8-11). These are likely connected to a further change of structure as after a few cycles the first half-wave potential is declining while the second is rising slightly.

Both substances are diamagnetic, and NMR spectra could be collected. In the ^{31}P and ^{31}P{^{1}H} NMR spectra, **5** shows the typical doublet and triplet pattern for the 1,2,4-triphospholyl ring at δ [ppm] = 114.0 (t) and 118.8 (d). This is in accordance with the [AB_2] spin system of the phosphorus nuclei. Slightly low field shifted, **6** shows a singlet at 442.3 ppm. Mass spectrometry also confirms the composition of **5** and **6**. As crystals of **5** are always co-crystallising with **6** and both compounds are insoluble in hexane but poorly soluble in toluene, a separation has been impossible to present.

8.3 Conclusions

We could show that the reaction between Ag[pftb] and the 1,3-diphosphete complex [Cp'''Co(η^4-P_2C_2tBu$_2$)] (**1**) yields interesting new coordination compounds or oxidised species depending on the reaction conditions. These could be thoroughly characterised because of the use of the [pftb]$^-$ anion, which promotes solubility and stabilises reactive species. The stepwise coordination of the phosphorus lone pairs of **1** could be observed by stopping the reaction between **1** and Ag[pftb] in CH_2Cl_2/Et_2O mixtures at different temperatures. The two related molecular species [$(Et_2O)_2$Ag{Cp'''Co(μ,η^4:η^1:η^1-P_2C_2tBu$_2$)}]·[pftb] (**3a**) and

$[(Et_2O)_4Ag_2\{Cp'''Co(\mu,\eta^4:\eta^1:\eta^1\text{-}P_2C_2tBu_2)\}]\cdot 2[pftb]$ (**3b**) could be isolated when stopping the reaction at the appropriate temperature, and the 1D polymeric compound $[Ag\{Cp'''Co(\eta^4:\eta^1:\eta^1\text{-}P_2C_2tBu_2)\}]_n\cdot n[pftb]$ (**2**) was obtained when leaving the reaction to reach room temperature as well as using the right stoichiometry. The first group 11 coordination complex of 1,2-diphosphete complexes, $[Ag_2\{Cp'''Co(\mu,\eta^4:\eta^1:\eta^1\text{-}1,2\text{-}P_2C_2tBu_2)\}_2\{Cp'''Co(\mu,\eta^4:\eta^1\text{-}1,2\text{-}P_2C_2tBu_2)\}_2]\cdot 2[pftb]$ (**4**) was obtained after an interesting isomerisation took place. This kind of complex has not been known in the literature so far. Isolation of the novel 1,2-diphosphete $[Cp'''Co(\eta^4\text{-}1,2\text{-}P_2C_2tBu_2)]$ (**I-1**) was possible by the complexation of the silver cation with a stronger donor, and by characterising the NMR shifts of **I-1** this substance could also be obtained by thermolysis of **1** in 70% conversion. Also the novel ring expansion product, the triphosphacobaltocenium $[Cp'''Co(\eta^5\text{-}P_3C_2tBu_2)][pftb]$ (**5**) and the ring contraction product, the phosphirenylium complex $[Cp'''Co(\eta^3\text{-}PC_2tBu_2)][pftb]$ (**6**), which are formed by a formal reaction between two diphosphete complexes **1** promoted by Ag^+, could be isolated and characterised.

8.4 Supporting Information

8.4.1 Experimental

All steps were performed under an atmosphere of dry argon with standard Schlenk techniques. All solvents were freshly collected from a Solvent Purification System by M. Braun and were degassed prior to use. All NMR spectra have been recorded using CD_2Cl_2, which was dried over CaH_2, or C_6D_6, which was dried over Na/K alloy; both were refluxed for three hours and then distilled under an inert atmosphere. [Cp'''Co(η^4-$P_2C_2tBu_2$)] **1** was synthesised according to literature procedure,[5a] as was Ag[Al{OC(CF_3)$_3$}$_4$] (shortened Ag[pftb] in the following).[21]

Synthesis of I-1

a) via extraction from 4

A residue (oil or crystals) of **4** *(vide infra)* is dissolved in pure pyridine. After stirring for four hours, the solvent is removed *in vacuo*. The resulting oil is then extracted with pentane to yield an orange solution over a brownish residue. The solution is filtered and the solvent is removed almost completely. At room temperature, small orange crystals of **I-1** suitable for X-ray analysis are forming over a few days.

b) via high temperature conversion from 1

50 mg of **1** are dissolved in 10 ml toluene and refluxed at 120 °C for three days at which point ^{31}P-NMR spectra show a 72% conversion to **I-1**. The solution is dried *in vacuo*, taken up in 2 ml of fresh hexane, filtered and left to crystallise at -30 °C.

Analytical data for **I-1**:

^{1}H-NMR (C_6D_6)	δ [ppm] = 1.14 (s, 9H, $C_5H_2tBu_3$), 1.17 (s, 18H, $C_5H_2tBu_3$), 1.29 (s, 18 H, $P_2C_2tBu_2$), 4.90 (s, 2H, $C_5H_2tBu_3$)
^{31}P-NMR (C_6D_6)	δ [ppm] = -83.3 (s)
^{31}P{^{1}H}-NMR (C_6D_6)	δ [ppm] = -83.3 (s)
Elemental analysis	calculated for $C_{27}H_{47}CoP_2$ (492.25 g·mol^{-1}): C 65.82, H 9.62; found: C 65.4, H 9.3
LIFDI-MS (Toluene)	*m/z* [%] = 492.5 (100) [**M**$^+$], 816.4 (12) [(Cp'''Co)$_2$(PC*t*Bu)$_2$O$_2$]

Synthesis of 2

A solution of $1.02 \cdot 10^{-4}$ mol (50 mg) **1** in 20 ml Et_2O is cooled to -80 °C. To this solution, $2.03 \cdot 10^{-4}$ mol (235 mg) Ag[pftb] in 5 ml CH_2Cl_2 are added at -80 °C and the reaction mixture is stirred over night to reach room temperature. After this, the formation of a black precipitate can be observed. The solvent is removed under reduced pressure and the residue is taken up in 5 ml CH_2Cl_2. The solution is filtered and layered with 20 ml of hexane and stored at +5 °C. After some time, orange crystals of **2** are formed at the solvent boundary.

Yield: 210 mg (72 %)

^{1}H-NMR (CD_2Cl_2)	δ [ppm] = 1.1 (s, 18 H, $P_2C_2tBu_2$), 1.44 (s, 9H, $C_5H_2tBu_3$), 1.55 (s, 18H, $C_5H_2tBu_3$), 5.04 (s, 2H, $C_5H_2tBu_3$)
^{31}P-NMR (CD_2Cl_2)	δ [ppm] = -0.3 (br, $\omega_{1/2}$ = 888 Hz)
^{31}P{^{1}H}-NMR (CD_2Cl_2)	δ [ppm] = -0.3 (br, $\omega_{1/2}$ = 888 Hz)
^{19}F-NMR (CD_2Cl_2)	δ [ppm] = -75.5 (s)
^{19}F{^{1}H}-NMR (CD_2Cl_2)	δ [ppm] = -75.5 (s)
Elemental analysis	calculated for $C_{43}H_{47}CoP_2AgAlO_4F_{36} \cdot 2CH_2Cl_2$ (1733.9 g·mol^{-1}): C 31.14, H 2.96; found: C 30.47, H 2.91
Cation ESI-MS (CH_2Cl_2)	*m/z* [%] = 393.1 (1) [Cp'''CoP*C*tBu]$^+$, 599.2 (100) [**L**Ag]$^+$, 1093.6 (60) [**L**$_2$Ag]$^+$,
Anion ESI-MS (CH_2Cl_2)	*m/z* [%] = 967.1 (100) [pftb]$^-$

L = **1** = Cp'''Co(η^4-$P_2C_2tBu_2$)

Synthesis of 3a

A solution of $1.02 \cdot 10^{-4}$ mol (50 mg) **1** in 10 ml Et_2O is cooled to -80 °C. To this solution, $2.03 \cdot 10^{-4}$ mol (235 mg) Ag[pftb] in 5 ml CH_2Cl_2 are added at -80 °C and the reaction mixture is stirred for 10 minutes to reach -60. The solution is filtered via cannula, layered under 20 ml of hexane and stored at -30 °C. Two days later, orange crystals of **3a** can be found at the solvent boundary as well as stray green needle-shaped crystals of $[(Cp'''Co)_2O_2]$[pftb].

^{1}H-NMR (CD_2Cl_2)	δ [ppm] = 1.09 (s, 18H, $P_2C_2tBu_2$), 1.21 (t, $^3J_{HH}$ = 7.01 Hz, 12H, $O(CH_2CH_3)_2$), 1.42 (s, 9H, $C_5H_2tBu_3$), 1.55 (s, 18H, $C_5H_2tBu_3$), 3.52 (q, $^3J_{HH}$ = 7.01 Hz, 8H, $O(CH_2CH_3)_2$), 4.99(s, 2H, $C_5H_2tBu_3$)
^{31}P-NMR (CD_2Cl_2)	δ [ppm] = 0 ppm (br, $\omega_{1/2}$ = 451 Hz)
^{31}P{^{1}H}-NMR (CD_2Cl_2)	δ [ppm] = 0 ppm (br, $\omega_{1/2}$ = 451 Hz)
^{19}F-NMR (CD_2Cl_2)	δ [ppm] = -75.6 (s)
^{19}F{^{1}H}-NMR (CD_2Cl_2)	δ [ppm] = -75.6 (s)
Elemental analysis	calculated for $C_{43}H_{47}CoP_2AgAlO_4F_{36}$ (1566.1 g·mol^{-1}): C 32.9, H 3.02 found: C, 33.58, H, 3.33;

L = **1** = Cp'''Co(η^4-$P_2C_2tBu_2$)

Synthesis of 3b

A solution of $3.22 \cdot 10^{-4}$ mol (374 mg) Ag[pftb] in 5 ml CH_2Cl_2 is cooled to -80 °C. To this solution, $2.84 \cdot 10^{-4}$ mol (140 mg) **1** in 5 ml Et_2O are added at -80 °C and the reaction mixture is stirred for one hour to reach 0 °C. The solution is filtered via cannula, layered under 10 ml of hexane and stored at -30 °C. After some time, orange crystals of **3b** can be found at the solvent boundary.

Cation ESI-MS (CH_2Cl_2) *m/z* [%] = 1093.6 (100) $[\mathbf{L}_2Ag]^+$
Anion ESI-MS (CH_2Cl_2) *m/z* [%] = 967.0 (100) $[pftb^-]$
L = **1** = Cp'''Co(η^4-P_2C_2tBu$_2$)

Synthesis of 4

A solution of $2.84 \cdot 10^{-4}$ mol (140 mg) **1** in 5 ml CH_2Cl_2 is cooled to -80 °C. To this solution, $2.84 \cdot 10^{-4}$ mol (330 mg) Ag[pftb] in 5 ml CH_2Cl_2 are added at -80 °C and the reaction mixture is stirred over night to reach room temperature. After this, the formation of a black precipitate can be observed. The solvent is removed under reduced pressure and the residue is taken up in 3 ml CH_2Cl_2. The solution is filtered, layered under 10 ml of hexane and stored at -30 °C. After some time, red crystals of **4** can be found at the solvent boundary.

^{1}H-NMR (CD_2Cl_2) δ [ppm] = 1.08 (s, 18 H, P_2C_2tBu$_2$), 1.41 (s, 9H, C_5H_2tBu$_3$), 1.55 (s, 18H, C_5H_2tBu$_3$), 4.97 (s, 2H, C_5H_2tBu$_3$)
^{31}P-NMR (CD_2Cl_2) δ [ppm] = 4.8 (s, 2P), 1.7 (s, 1P), -1.6 (s, 1P)
^{31}P{^{1}H}-NMR (CD_2Cl_2) δ [ppm] = 4.8 (s, 2P), 1.7 (s, 1P), -1.6 (s, 1P)
^{19}F-NMR (CD_2Cl_2) δ [ppm] = -75.6 (s)
^{19}F{^{1}H}-NMR (CD_2Cl_2) δ [ppm] = -75.6 (s)
Elemental analysis calculated for $C_{140}H_{188}Co_4P_8Ag_2Al_2O_8F_{72}$ (4116.61 g·mol^{-1}): C 40.81, H 4.60; found: C 40.46, H 4.63
Cation ESI-MS (CH_2Cl_2) *m/z* [%] = 492.2 (4) $[\mathbf{L}H]^+$ 599.0 (8) $[\mathbf{L}Ag]^+$, 847.4 (10) $[\mathbf{L}_3Ag_2]^{2+}$, 1093.6 (100) $[\mathbf{L}_2Ag]^+$
Anion ESI-MS (CH_2Cl_2) *m/z* [%] = 967.1 (100) $[pftb^-]$
L = **1** = Cp'''Co(η^4-P_2C_2tBu$_2$)

Synthesis of 5 and 6

A solution of $8.6 \cdot 10^{-5}$ mol (42 mg) **1** in 10 ml Hexane is layered over a solution of $1.72 \cdot 10^{-4}$ mol (200 mg) Ag[pftb] in 5 ml CH_2Cl_2. The Schlenk is stored in the freezer at -30 °C until diffusion is completed. After this, the formation of a black precipitate and a silver mirror on the wall of the Schlenk can be observed. The solvent is removed under reduced pressure and the residue is taken up in 3 ml CH_2Cl_2. The solution is filtered, layered under 10 ml of hexane and stored at -30 °C. After some time, orange needles of **5** can be found at the solvent boundary. Further crystallisation of the mother liquor eventually leads to the crystallisation of green plates of **6** next to orange **5**.

Yield (total): 135 mg (53%)

Analytical data for **5**:

^{1}H-NMR (CD_2Cl_2)	δ [ppm] = 1.46 (s, 9H, $C_5H_2tBu_3$) 1.53 (s, 18H, $C_5H_2tBu_3$), 1.54 (s, 18H, $P_3C_2tBu_2$), 5.2 (s, 2H, $C_5H_2tBu_3$)
^{31}P-NMR (CD_2Cl_2)	δ [ppm] = 114.0 (t, $^2J_{PP}$ = 39.7 Hz, 1P), 118.8 (d, $^2J_{PP}$ = 39.7 Hz, 2P)
^{31}P{^{1}H}-NMR (CD_2Cl_2)	δ [ppm] = 114.0 (t, $^2J_{PP}$ = 39.7 Hz, 1P), 118.8 (d, $^2J_{PP}$ = 39.7 Hz, 2P)
^{19}F-NMR (CD_2Cl_2)	δ [ppm] = -75.6 (s)
^{19}F{^{1}H}-NMR (CD_2Cl_2)	δ [ppm] = -75.6 (s)
Elemental analysis	calculated for $C_{43}H_{47}CoP_3AlO_4F_{36} \cdot CH_2Cl_2$ (1574.08 g·mol^{-1}): C 33.54, H 3.13; found: C 33.28, H 3.32
Cation ESI-MS (CH_2Cl_2)	*m/z* [%] = 523.1 (100) [**M**]$^+$, 541.2 (15) [**M**·H_2O]$^+$, 555.22 (10) [**M**·O_2]$^+$, 599.1 (20) [(Cp‘‘‘Co)$_2$O]$^+$
Anion ESI-MS (CH_2Cl_2)	*m/z* [%] = 967.1 (100) [pftb$^-$]

Analytical data for **6**:

^{31}P-NMR (CD_2Cl_2)	δ [ppm] = 442.3 (s)
^{31}P{^{1}H}-NMR (CD_2Cl_2)	δ [ppm] = 442.3 (s)
^{19}F-NMR (CD_2Cl_2)	δ [ppm] = -75.6 (s)
^{19}F{^{1}H}-NMR (CD_2Cl_2)	δ [ppm] = -75.6 (s)
Cation ESI-MS (CH_2Cl_2)	*m/z* [%] = 309.14 (40) [(Cp‘‘‘CoO)$_2$]$^{2+}$, 460.99 (15) [**M**]$^+$, 523.2 (10) [**5**]$^+$, 599.0 (8) [**L**Ag]$^+$, 617.2 (100) [**L**Ag·H_2O]$^+$, 1093.4 (8) [**L**$_2$Ag]$^+$
Anion ESI-MS (CH_2Cl_2)	*m/z* [%] = 966.9 (100) [pftb$^-$]

L = **1** = Cp‘‘‘Co(η^4-$P_2C_2tBu_2$)

8.4.2 Cyclovoltammogramms

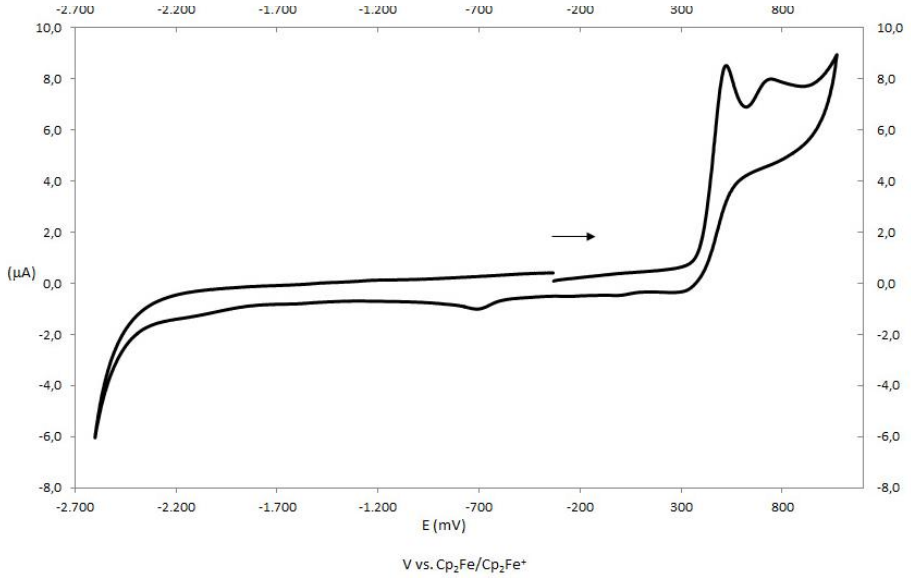

Figure 8-10 Cyclovoltammogram of **1** recorded at a platinum disc electrode in CH_2Cl_2 at 100 mV/s, referenced against Cp_2Fe/Cp_2Fe^+. Supporting electrolyte $[Bu_4N][PF_6]$ (0.1 mol/L). An irreversible oxidation at $E_{1/2}$ = 0.45 V with a subsequent decomposition of the complex can be observed.

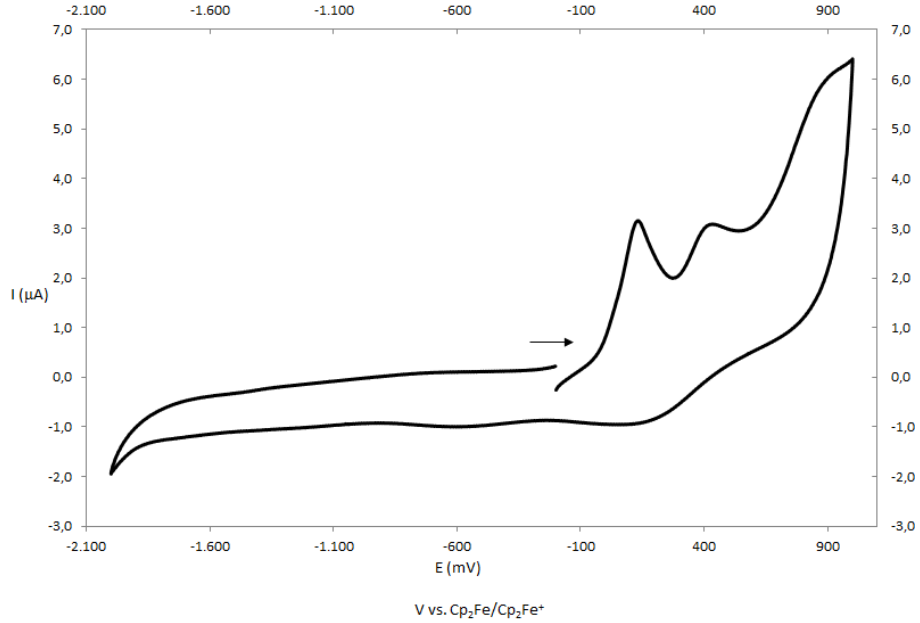

Figure 8-11 Cyclovoltammogram of **5** recorded at a platinum disc electrode in CH_2Cl_2 at 100 mV/s, referenced against Cp_2Fe/Cp_2Fe^+. Supporting electrolyte $[Bu_4N][PF_6]$ (0.1 mol/L). Two irreversible oxidations at $E_{1/2}$ = 0.1 V and 0.4 V with a subsequent decomposition of the complex can be observed.

8.4.3 NMR Spectra

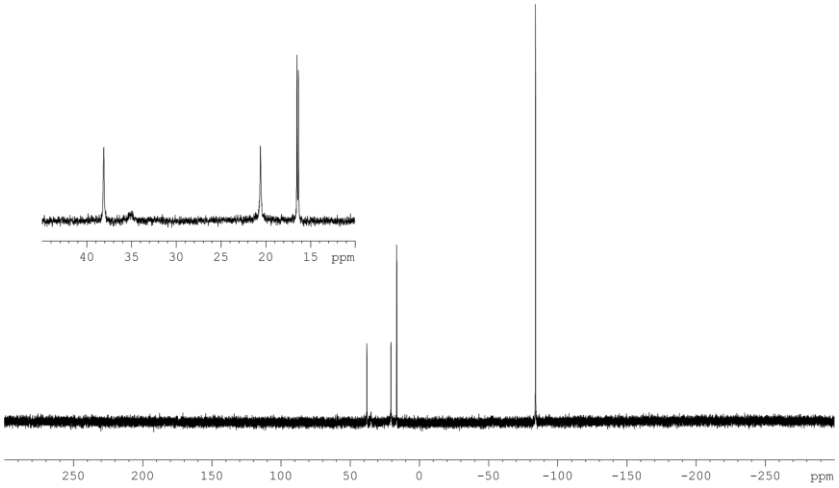

Figure 8-12 $^{31}P\{^{1}H\}$ NMR spectrum of pyridine-extracted **I-1** at 300 K in pyr-d5. Signals at 38 and 21 ppm belong to residual **1**. Signal at 16 ppm could not be assigned properly.

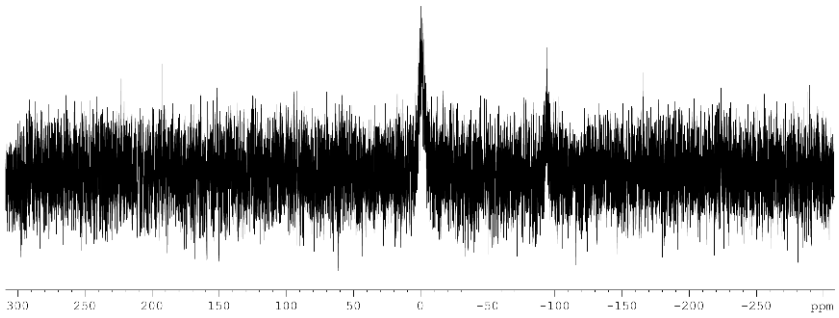

Figure 8-13 $^{31}P\{^{1}H\}$ NMR spectrum of **2** at 300 K in CD_2Cl_2.

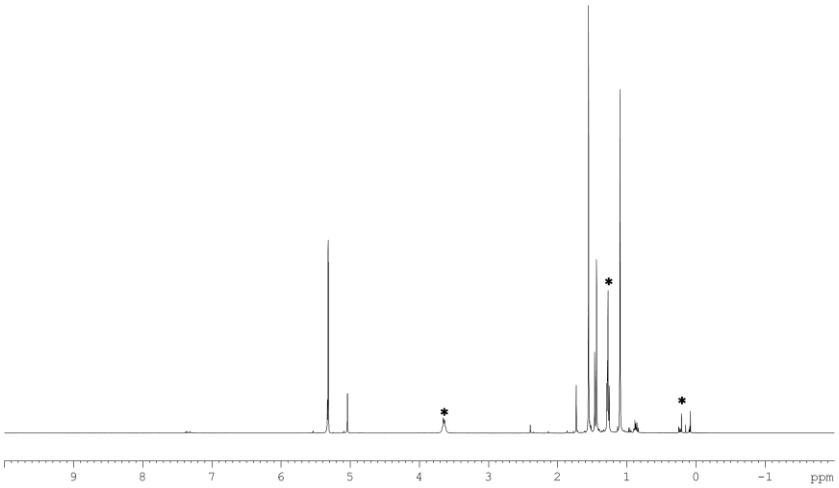

Figure 8-14 ^{1}H NMR spectrum of **2** at 300 K in CD_2Cl_2. Signals marked with an asterisk are residual ether and an impurity from silicon grease.

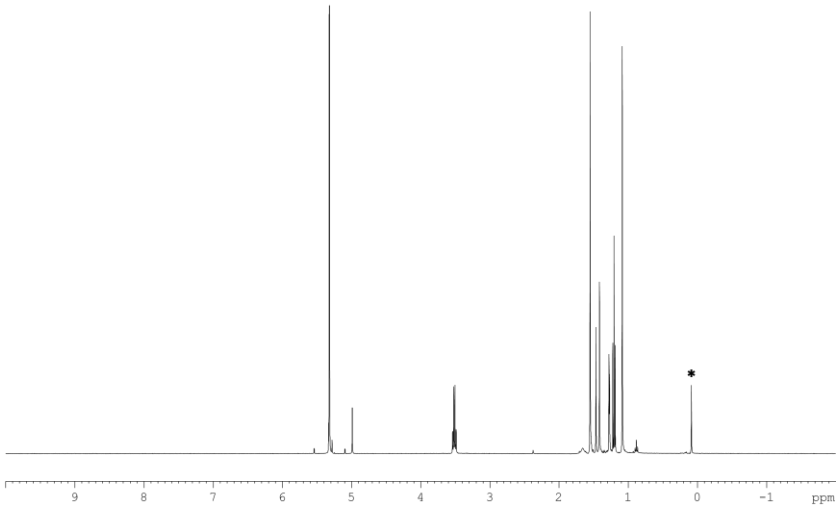

Figure 8-15 ^{1}H NMR spectrum of **3a** at 300 K in CD_2Cl_2. Signal marked with an asterisk is silicon grease.

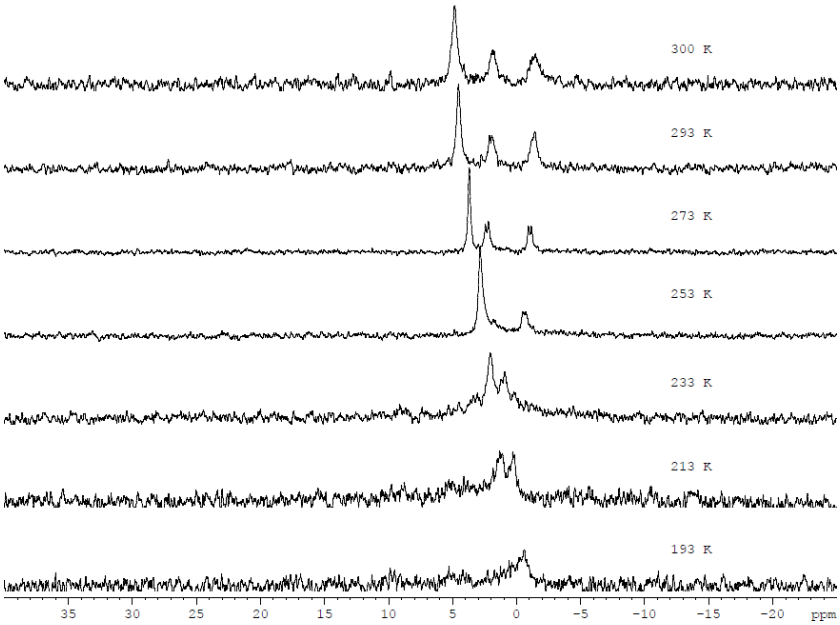

Figure 8-16 $^{31}P\{^{1}H\}$ VT NMR spectra showing the formation of **4** starting at 193 K and heated to r.t. in steps of 20 K.

1 and Ag[pftb] have been frozen in a NMR tube at -80 °C and slowly heated to r.t. in steps of 20 K. The formation of the coordination compound can be seen instantly as no signal for pure **1** can be observed (δ [ppm] = 42 (s), 23 (s)). No signals could be observed outside the section shown above in Figure 8-16.

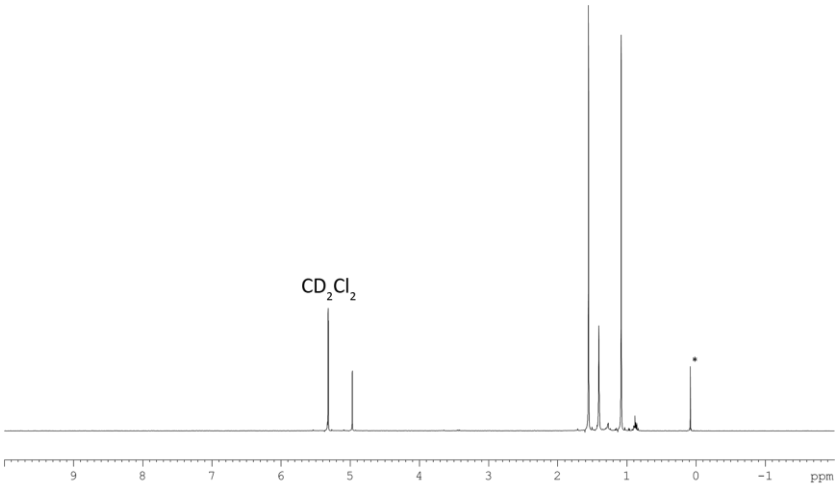

Figure 8-17 ^{1}H NMR spectrum of **4** at 300 K in CD_2Cl_2. Signal marked with an asterisk is an impurity from silicon grease.

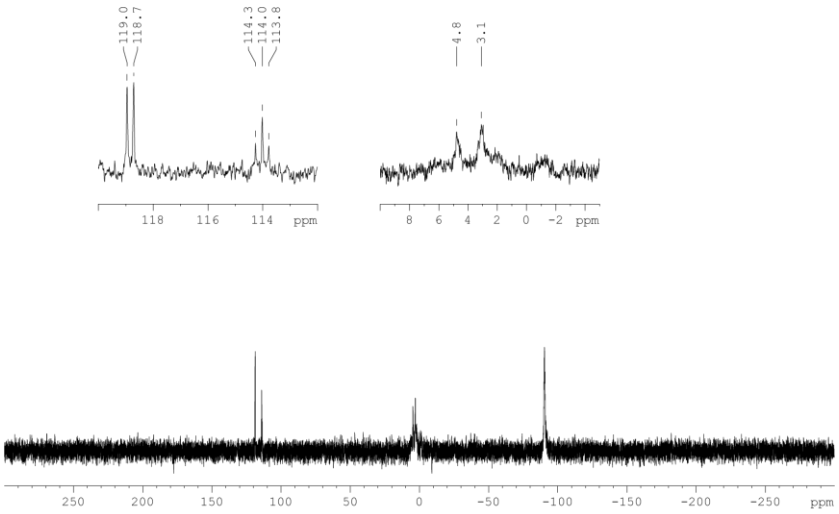

Figure 8-18 $^{31}P\{^{1}H\}$ NMR spectrum of **4** after two months. The building of **5** could be observed as well as an additional singlet at -90 ppm (**I-1**) while coordination compound **4** at around 0 ppm is decreasing.

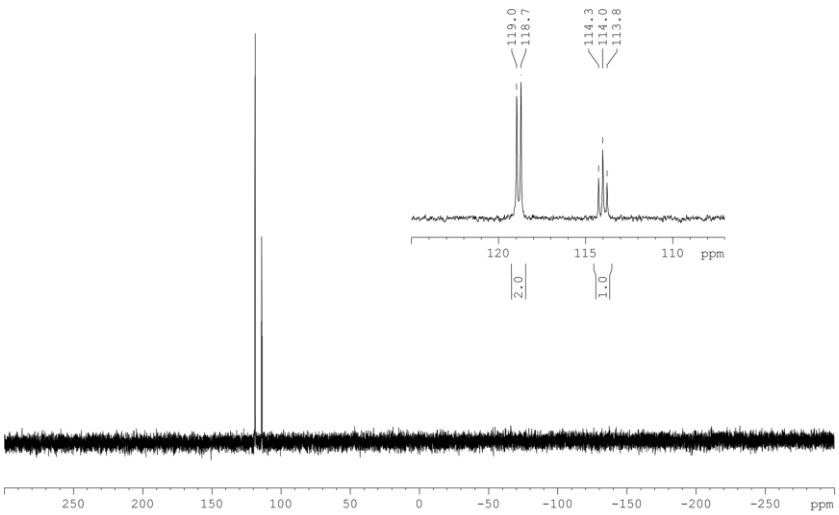

Figure 8-19 $^{31}P\{^{1}H\}$ NMR spectrum of **5** at 300 K in CD_2Cl_2.

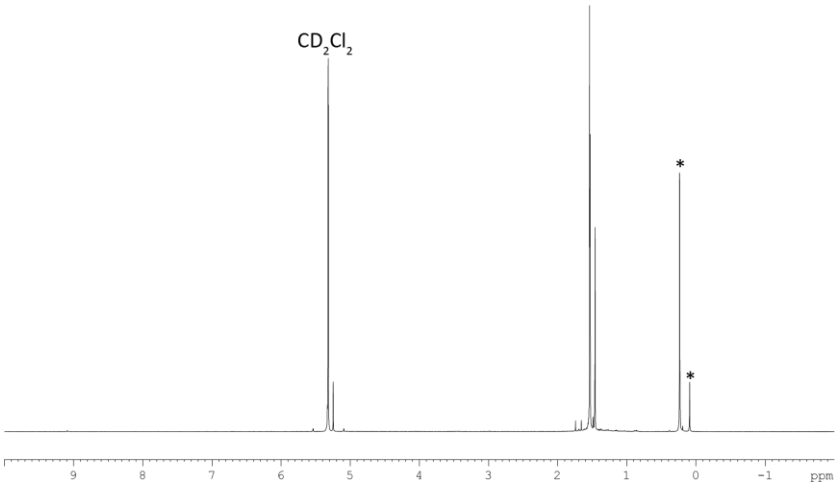

Figure 8-20 ^{1}H NMR spectrum of **5** at 300 K in CD_2Cl_2. Signal marked with an asterisk are impurities.

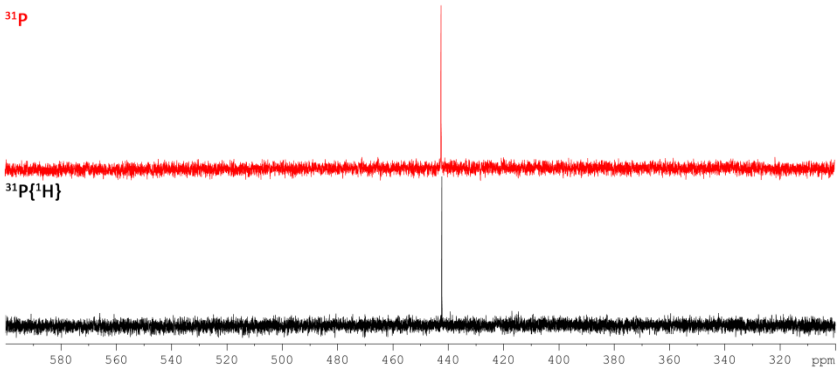

Figure 8-21 ^{31}P and ^{31}P{^{1}H} NMR spectra of **6** at 300 K in CD_2Cl_2.

8.4.4 Crystallographic Data

All structures have been processed using Olex2,[22] the structures were solved with the ShelXT[23] structure solution program, using the Direct Methods solution method. The models were refined with version 2014/6 of ShelXL[24] using Least Squares minimisation. Experimental and crystal data created by ReportPlus in Olex2.

8.4.4.1 Compound I-1

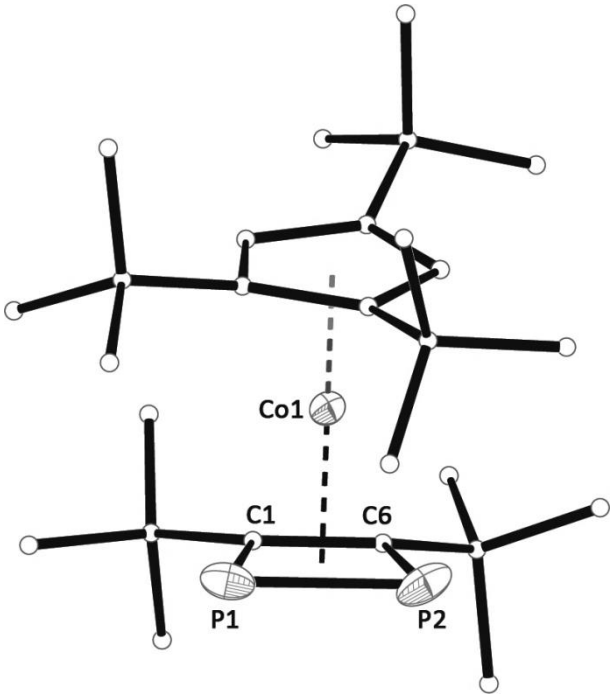

Figure 8-22 Molecular structure of **I-1** in the solid state. Hydrogen atoms are omitted for clarity. Thermal ellipsoids are shown at 50% occupation level. Selected bond lengths [Å] and angles [°]: P1-P2 2.1818(7), P1-C1 1.8158(18), P2-C6 1.8077(18), C1-C6 1.443(2), C1-P1-P2 78.16(6), C6-C1-P1 101.56(11).

Single clear light orange plate-shaped crystals of **I-1** were recrystallised from pentane by slow evaporation of the solvent. A suitable crystal (0.36×0.15×0.12) was selected and mounted on a mylar loop in perfluoroether oil on a Xcalibur, Atlas^{S2}, Gemini ultra diffractometer. The crystal was kept at T = 123.00(14) K during data collection.

Crystal Data for **I-1**. $C_{27}H_{47}P_2Co$, M_r = 492.51, orthorhombic, *Pbca* (No. 61), a = 17.1327(2) Å, b = 17.3967(3) Å, c = 18.2653(3) Å, V = 5444.02(16) Å^3, T = 123.00(14) K, Z = 8, Z' = 1, μ(CuK$_\alpha$) = 6.116, 25284 reflections measured, 4777 unique (R_{int} = 0.0300) which were used in all calculations. The final wR_2 was 0.0594 (all data) and R_1 was 0.0251 (I > 2σ(I)).

8.4.4.2 Compound 3a

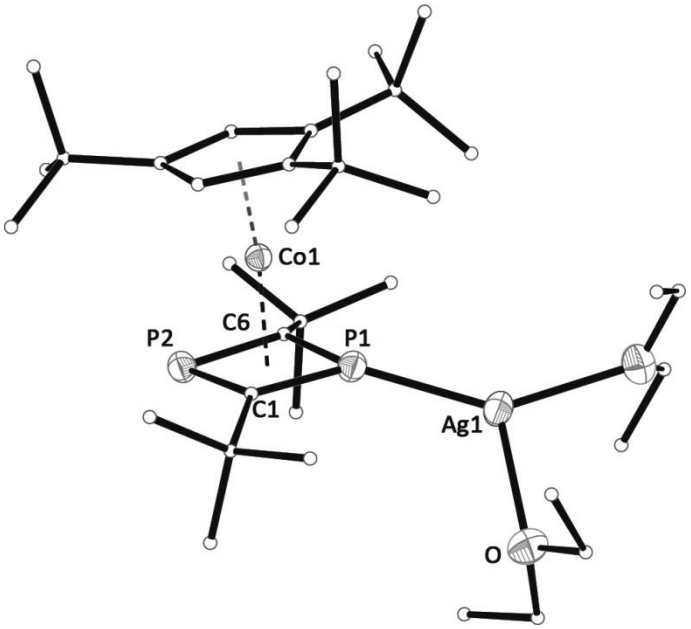

Figure 8-23 Molecular structure of the cation of **3a** in the solid state. Hydrogen atoms are omitted, carbon atoms are shown in ball-and-stick representation for clarity. Thermal ellipsoids are shown at 50% probability level. Selected bond lengths [Å] and angles [°]: P1-C1 1.774(2), P2-C1 1.792(2), P2-C6 1.795(2), P1-C6 1.777(2), P1-Ag1 2.3535(6), P1-C1-P2 96.99(10), C6-P2-C1 82.53(11).

Single clear light orange plate-shaped crystals of **3a** were recrystallised from a mixture of hexane and CH_2Cl_2 by solvent layering. A suitable crystal (0.27×0.13×0.10) was selected and mounted on a mylar loop in perfluoroether oil on a SuperNova, Single source at offset, Atlas diffractometer. The crystal was kept at T = 122.98(10) K during data collection.

Crystal Data for **3a**. $C_{51}H_{67}AgAlCoF_{36}O_6P_2$, M_r = 1715.76, monoclinic, $P2_1/c$ (No. 14), a = 22.1433(4) Å, b = 15.5680(3) Å, c = 19.4491(4) Å, β = 90.7370(17)°, V = 6704.1(2) Å^3, T = 122.98(10) K, Z = 4, Z' = 1, μ(CuK_α) = 6.203, 43176 reflections measured, 13043 unique (R_{int} = 0.0404) which were used in all calculations. The final wR_2 was 0.1090 (all data) and R_1 was 0.0374 (I > 2σ(I)).

8.4.4.3 Compound 3b

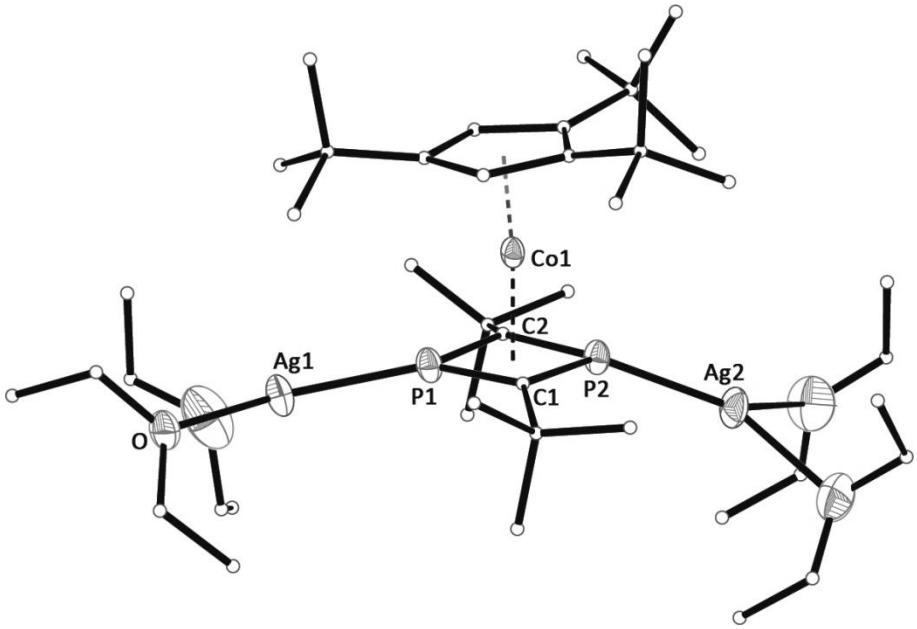

Figure 8-24 Molecular structure of the cation of **3b** in the solid state. Hydrogen atoms are omitted, carbon atoms are shown in ball-and-stick representation for clarity. Thermal ellipsoids are shown at 50% probability level. Selected bond lengths [Å] and angles [°]: P1-C1 1.777(4), P2-C1 1.783(4), P2-C6 1.778(4), P1-C6 1.777(4), P1-Ag1 2.3711(11), P2-Ag2 2.3487(11), P1-C1-P2 95.3(2), C6-P2-C1 84.47(19).

Single clear light orange block-shaped crystals of **3b** were obtained by crystallisation from diffusion of hexane into a CH_2Cl_2 solution of **3b**. A suitable crystal (0.82×0.44×0.17) was selected and mounted on a mylar loop on a Xcalibur, AtlasS2, Gemini ultra diffractometer. The crystal was kept at T = 122.9(2) K during data collection.

Crystal Data for **3b**: $C_{75}H_{86}Ag_2Al_2CoF_{72}O_{12}P_2$, M_r = 2938.00, triclinic, P-1 (No. 2), a = 11.7494(2) Å, b = 19.0466(3) Å, c = 25.4981(5) Å, α = 77.7260(15)°, β = 85.9901(15)°, γ = 78.4140(15)°, V = 5459.89(18) Å^3, T = 122.9(2) K, Z = 2, Z' = 1, μ(CuK_a) = 6.092 mm^{-1}, 67314 reflections measured, 19139 unique (R_{int} = 0.0473) which were used in all calculations. The final wR_2 was 0.1873 (all data) and R_1 was 0.0629 (I > 2σ(I)).

8.4.4.4 Compound 4

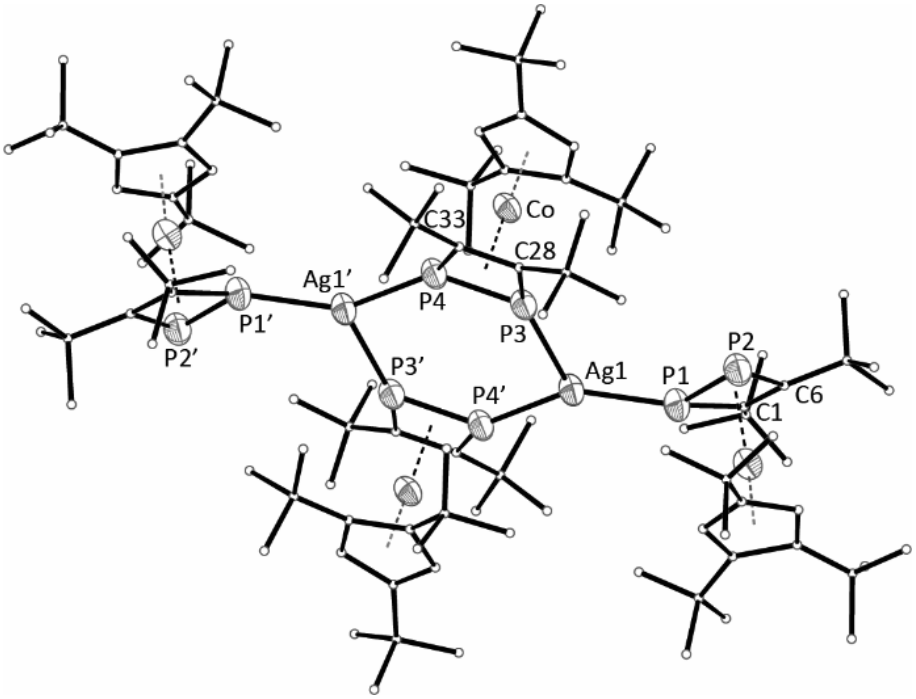

Figure 8-25 Molecular structure of the cation of **4** in the solid state. Hydrogen atoms are omitted, carbon atoms are shown in ball-and-stick representation for clarity. Thermal ellipsoids are shown at 50% probability level. Selected bond lengths [Å] and angles [°]: P1-P2 2.153(3), P1-C1 1.813(8), P2-C6 1.817(8), P3-P4 2.151(3), P3-C28 1.807(8), P4-Ag1' 2.560(2), P4-C33 1.803(8), C1-C2 1.522(12), C1-C6 1.443(11), P1-Ag1-P3 144.74(7), P1-Ag1-P4' 118.86(7), P3-Ag1-P4' 96.38(7), P2-P1-Ag1 129.86(11), C1-P1-P2 80.3(3), C6-P2-P1 77.0(3), C6-C1 P1 99.0(5), C1-C6-P2 103.5(5)

Single clear light red block-shaped crystals of **4** were obtained by recrystallisation from diffusion of hexane into a solution of **4** in CH_2Cl_2. A suitable crystal (0.26×0.11×0.10) was selected and mounted on a mylar loop on a Xcalibur, AtlasS2, Gemini ultra diffractometer. The crystal was kept at T = 123.00(14) K during data collection.

Crystal Data for **4**: $C_{70}H_{94}AgAlCo_2F_{36}O_4P_4$, M_r = 2060.04, orthorhombic, *Pbca* (No. 61), a = 26.9884(3) Å, b = 21.0726(3) Å, c = 31.2693(5) Å, V = 17783.4(4) Å^3, T = 123.00(14) K, Z = 8, Z' = 1, μ(CuK_a) = 6.489 mm^{-1}, 86069 reflections measured, 15741 unique (R_{int} = 0.0887) which were used in all calculations. The final wR_2 was 0.2788 (all data) and R_1 was 0.0915 (I > 2σ(I)).

8.4.4.5 Compound 5

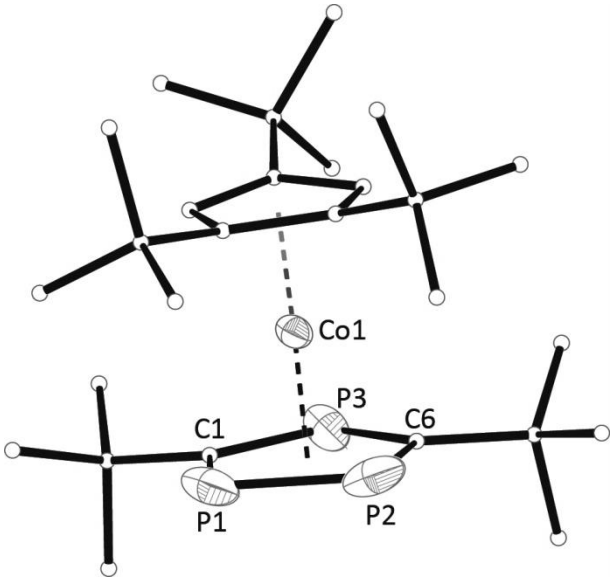

Figure 8-26 Molecular structure of the cation of **5** in the solid state. Hydrogen atoms are omitted, carbon atoms are shown in ball-and-stick representation for clarity. Thermal ellipsoids are shown at 50% probability level. Selected bond lengths [Å] and angles [°]: P1-P2 2.127(3), P1-C1 1.779(7), P2-C6 1.815(13), P3-C1 1.758(6), P3-C6 1.775(14), C1-P1-P2 98.9(2), C6-P2-P1 100.0(4), C1-P3-C6 100.5(5), P3-C1-P1 121.6(4).

Single red block-shaped crystals of (**5**) were obtained by recrystallisation from diffusion of hexane into a solution of **5** in CH_2Cl_2. A suitable crystal (0.34×0.24×0.11) was selected and mounted on a mylar loop on a Xcalibur, AtlasS2, Gemini ultra diffractometer. The crystal was kept at T = 123.1(6) K during data collection.

Crystal Data for **5**. $C_{43}H_{47}AlCoF_{36}O_4P_3$, M_r = 1490.62, orthorhombic, *Pbca* (No. 61), a = 17.03181(13) Å, b = 20.44691(16) Å, c = 33.2365(3) Å, V = 11574.54(16) Å^3, T = 123.1(6) K, Z = 8, Z' = 1, μ(CuK_a) = 4.721 mm^{-1}, 71404 reflections measured, 10168 unique (R_{int} = 0.0457) which were used in all calculations. The final wR_2 was 0.2872 (all data) and R_1 was 0.0917 (I > 2σ(I)).

8.4.4.6 Compound 6

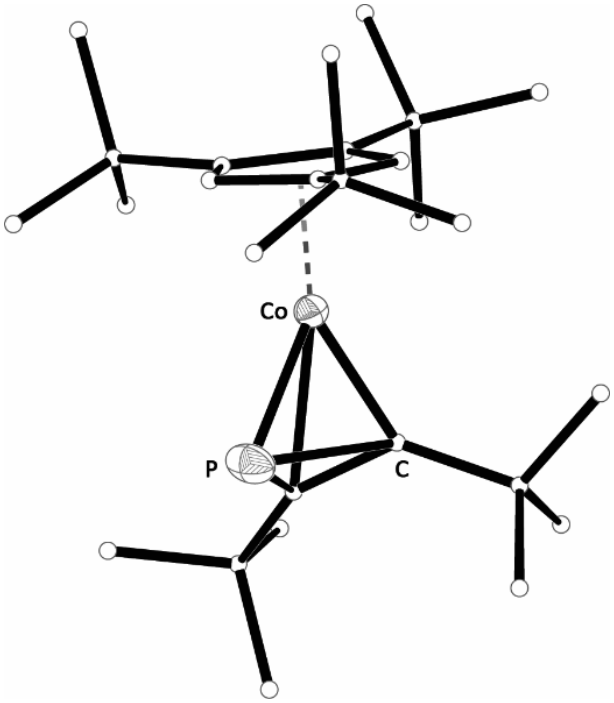

Figure 8-27 Molecular structure of the cation of **6** in the solid state Hydrogen atoms are omitted, carbon atoms are shown in ball-and-stick representation for clarity. Thermal ellipsoids are shown at 50% probability level. Selected bond lengths [Å] and angles [°]: P1-C1 1.762(3), C1-C6 1.376(4), P1-C6 2.163(3), Co1-P1 2.1018(9), Co1-C1 2.254(3), Co1-C6 1.879(3), C1-P1-C6 39.40(12), C6-C1-P1 86.21(19), C1-C6-P1 54.40(15).

Single dark green block-shaped crystals of (**6**) were obtained by recrystallisation from diffusion of hexane into a solution of **6** in CH_2Cl_2. A suitable crystal (0.26×0.18×0.14) was selected and mounted on a mylar loop on a Xcalibur, AtlasS2, Gemini ultra diffractometer. The crystal was kept at T = 123.00(14) K during data collection.

Crystal Data for **6**. $C_{43}H_{47}AlCoF_{36}O_4P$, M_r = 1428.68, orthorhombic, Pbca (No. 61), a = 16.37073(17) Å, b = 21.9800(2) Å, c = 30.6657(3) Å, V = 11034.4(2) Å^3, T = 123.00(14) K, Z = 8, Z' = 1, $\mu(CuK_\alpha)$ = 4.389 mm^{-1}, 32850 reflections measured, 9628 unique (R_{int} = 0.0256) which were used in all calculations. The final wR_2 was 0.1000 (all data) and R_1 was 0.0374 (I > 2 σ(I)).

8.4.5 DFT Calculations

All calculations have been performed with the TURBOMOLE program package[25] at the RI[26]-B3LYP[27]/def2-TZVP[26b, 28] level of theory. The Multipole Accelerated Resolution of Identity (MARI-J)[29] approximation was used in the geometry optimisation steps. The final energies and the Natural Population Analyses (NPA) have been obtained by single point calculations without using the RI approximation. For the relative energies, the total SCF energies have been used without corrections.

Numbering: [Cp‘‘‘Co(η^4-1,3-P_2C_2tBu$_2$)] (**1**)

[Cp‘‘‘Co(η^4-1,3-P_2C_2tBu$_2$)]$^+$ (**1**$^+$)

[Cp‘‘‘Co(η^5-1,2,4-P_3C_2tBu$_2$)]$^+$ (**5**$^+$)

[Cp‘‘‘Co(η^3-PC_2tBu$_2$)]$^+$ (**6**$^+$)

Table 8-2 Summed natural charges calculated at the B3LYP/def2-TZVP level of theory.

Fragment	1	1$^+$	5$^+$	6$^+$
Co	0.38	0.85	0.41	0.45
Cp'''	-0.18	0.00	0.33	0.21
tBu$_2$C$_2$P$_2$	-0.20	0.15	-	-
tBu$_2$C$_2$P	-	-	-	0.34
tBu$_2$C$_2$P$_3$	-	-	0.26	-

Table 8-3 Selected Wiberg Bond Indices calculated at the B3LYP/def2-TZVP level of theory. Labelling according to figure X.

1		1$^+$		5$^+$		6$^+$	
p2 - co1	0.86	p2 - co1	0.75	p2 - co1	0.54	p2 - co1	1.10
p3 - co1	0.84	p3 - co1	0.73	p3 - co1	0.54	p3 - co1	0.25
p3 - p2	0.12	p3 - p2	0.13	p3 – p2	1.24	p3 - p2	0.98
c4 - co1	0.42	c4 - co1	0.38	p4 - co1	0.57	c17 - co1	0.70
c4 - p2	1.03	c4 - p2	0.98	c5 - co1	0.31	c17 - p2	0.61
c4 - p3	1.04	c4 - p3	0.99	c5 - p2	1.13	c17 - c3	0.99
c5 - co1	0.46	c5 - co1	0.40	c5 - p4	1.14	c31 - co1	0.48
c5 - p2	1.07	c5 - p2	1.01	c6 - c5	0.93	c32 - co1	0.26
c5 - p3	1.08	c5 - p3	1.03	c7 - co1	0.31		
p2 - co1	0.86			c7 - p3	1.14		
p3 - co1	0.84			c7 - p4	1.08		
				c9 - co1	0.36		
				c10 - co1	0.34		
				c10 - c9	0.57		
				c11 - co1	0.62		
				c12 - co1	0.29		
				c13 - co1	0.58		

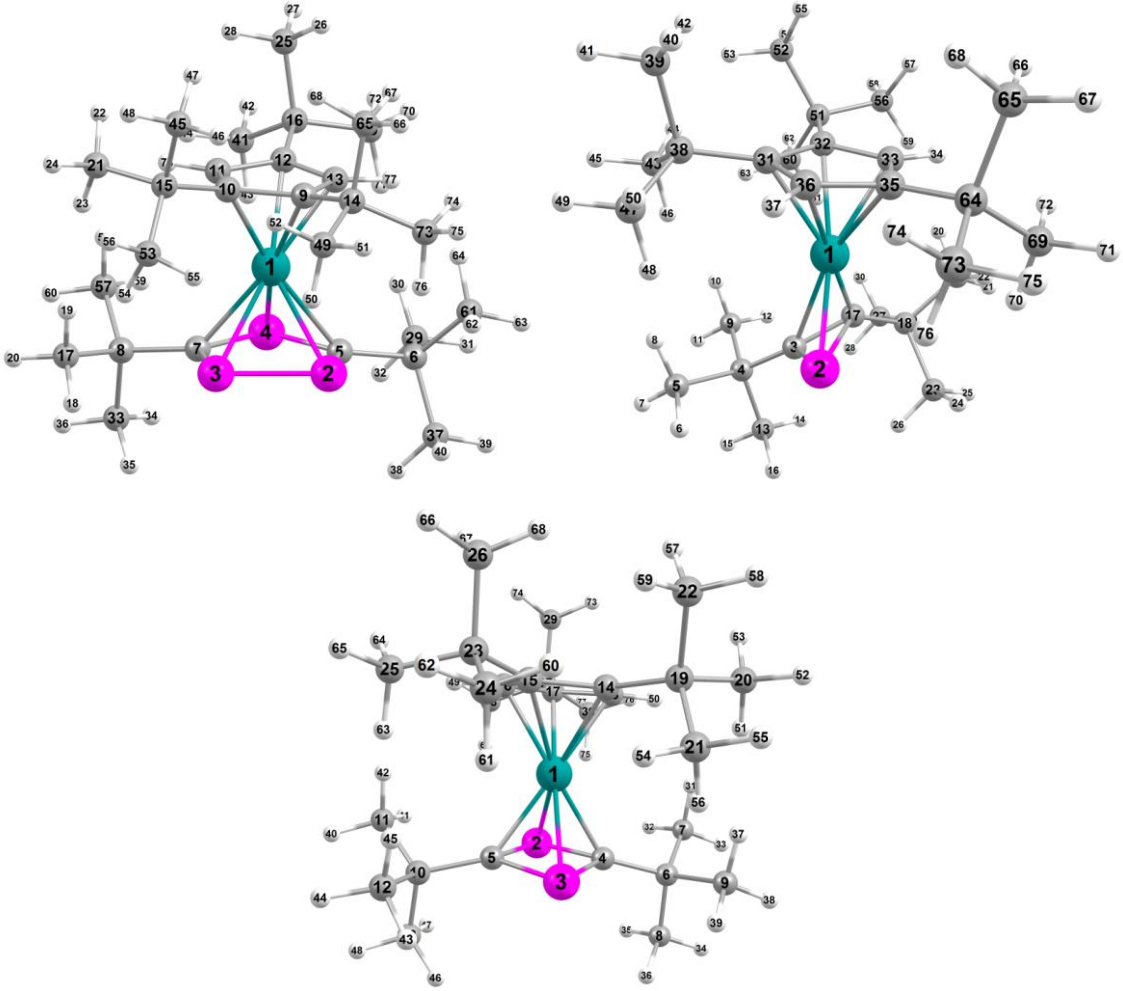

Figure 8-28 Labelling scheme used for the WBIs.

Geometry optimisation

Table 8-4 Cartesian coordinates of the optimised geometry of [Cp'''Co(η^4-1,3-P_2C_2tBu$_2$)] (**1**) at the B3LYP/def2-TZVP level of theory. Total Energy: −3122.17286280366 a.u.

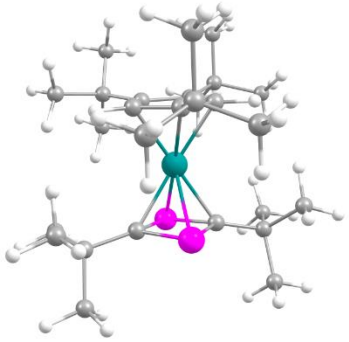

Atom	x	y	z
Co	0.1869483	0.0098576	-0.3906849
P	1.6804367	0.0979186	-2.0917838
P	-1.0012549	-0.1138737	-2.3352123
C	0.4253090	-1.1812432	-2.1334280
C	0.2452252	1.1615855	-2.1875504
C	0.6038727	-2.6567221	-2.4574027
C	1.7169122	-3.3074154	-1.6203311
C	1.0146243	-2.7404733	-3.9492191
C	-0.6980771	-3.4552442	-2.2907784
C	0.1785354	2.6351958	-2.5483938
C	1.0917429	3.4926218	-1.6554895
C	-1.2681172	3.1576204	-2.5103093
C	0.6806717	2.7724112	-4.0075440
C	-0.8239686	-0.7250522	1.3766497
C	-0.8174390	0.7355961	1.4030460
C	0.5546745	1.1303345	1.3453526
C	1.4137630	0.0016934	1.3376713
C	0.5505007	-1.1256465	1.3271126
C	-1.9446697	-1.7781185	1.5614784
C	-1.3326201	-3.1918955	1.6738173
C	-2.9634759	-1.8163936	0.4062949
C	-2.7020523	-1.5583628	2.8900219
C	-1.8887603	1.7913839	1.7519253
C	-3.2564067	1.5791132	1.0840405
C	-1.4196859	3.2107852	1.3681245
C	-2.0547032	1.8201244	3.2929375
C	2.9127385	0.0099015	1.6062999
C	3.5859095	1.2840834	1.0728171
C	3.0809653	-0.0286103	3.1451182
C	3.6197136	-1.2143048	1.0072643
H	1.4606376	-3.3250790	-0.5613823
H	2.6611757	-2.7706161	-1.7296684
H	1.8823351	-4.3376751	-1.9455577
H	1.1363626	-3.7846435	-4.2499220
H	1.9582145	-2.2217851	-4.1270156
H	0.2544944	-2.2880934	-4.5889214
H	-1.0155936	-3.4993298	-1.2513797
H	-0.5561103	-4.4818152	-2.6374106
H	-1.5099342	-3.0171810	-2.8757132
H	1.1002186	4.5287678	-2.0035527
H	2.1201964	3.1256222	-1.6830219
H	0.7627404	3.4867235	-0.6180957
H	-1.8842516	2.6439007	-3.2514248
H	-1.2939851	4.2258736	-2.7387743
H	-1.7349491	3.0107700	-1.5381996
H	0.0876218	2.1540529	-4.6839483
H	1.7241342	2.4646059	-4.0946492
H	0.6022043	3.8117419	-4.3383182
H	0.8951550	2.1494411	1.3515716

H	0.8877151	-2.1452727	1.3144922
H	-0.7497743	-3.4668745	0.7965543
H	-2.1385089	-3.9213581	1.7717448
H	-0.6929884	-3.2860479	2.5535620
H	-3.4372869	-0.8562319	0.2314847
H	-3.7477840	-2.5431009	0.6355783
H	-2.4889934	-2.1151554	-0.5249457
H	-2.0116086	-1.4527768	3.7291249
H	-3.3376307	-2.4245262	3.0879884
H	-3.3495803	-0.6864103	2.8652315
H	-3.7667351	0.6904586	1.4444829
H	-3.1597111	1.4996913	0.0003621
H	-3.9044074	2.4305342	1.3040478
H	-1.1838633	3.2947934	0.3117003
H	-0.5473437	3.5256005	1.9413230
H	-2.2186929	3.9206877	1.5892619
H	-2.7610632	2.6069698	3.5702737
H	-1.1005604	2.0419242	3.7750889
H	-2.4224215	0.8829405	3.6988879
H	3.4910874	1.3548720	-0.0108314
H	4.6497447	1.2712070	1.3206529
H	3.1596530	2.1858309	1.5161618
H	4.1412372	-0.0168681	3.4094242
H	2.6358037	-0.9315885	3.5677642
H	2.6043242	0.8338187	3.6153794
H	3.5568937	-1.2102634	-0.0803566
H	3.1944959	-2.1504792	1.3733001
H	4.6760196	-1.2045267	1.2858009

Table 8-5 Cartesian coordinates of the optimised geometry of [Cp'''Co(η^4-1,2-P_2C_2tBu$_2$)] (**I-1**) at the B3LYP/def2-TZVP level of theory. Total Energy: -3122.17358351987 a.u.

Atom	x	y	z
Co	-0.3776539	-0.2082436	-0.3591036
P	-1.7192708	0.5043515	-2.0552745
P	-1.0160289	-1.5612655	-2.0729469
C	0.5321999	-0.6379770	-2.2557997
C	0.0740000	0.7224289	-2.2388254
C	-0.0114429	0.8992812	1.4087896
H	0.3161511	1.9217754	1.4746446
C	0.8522777	-0.2224876	1.4582769
C	0.0087184	-1.3535571	1.3472783
H	0.3529549	-2.3712901	1.3281073
C	-1.3862232	0.4919484	1.3771855
C	-1.3751850	-0.9663759	1.3255356
C	2.2964480	-0.2197872	1.9497527
C	1.8758543	2.4999889	-1.6811769
H	1.5265060	2.6223344	-0.6565295
H	2.2806090	3.4592027	-2.0154286
H	2.6904638	1.7832782	-1.6766483
C	-2.4827196	-2.0374030	1.4634959
C	-2.1108481	2.9167523	1.0643452
H	-1.1479915	3.2988355	1.4012466
H	-2.8653039	3.6498575	1.3570545

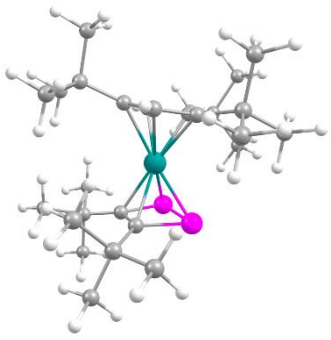

H	-2.1039249	2.8601751	-0.0226586
C	3.0547600	-1.4991248	1.5685330
H	2.5521694	-2.3939311	1.9396997
H	4.0539171	-1.4808169	2.0095540
H	3.1697410	-1.5964210	0.4908411
C	-3.5688057	-2.0042104	0.3703515
H	-4.0074972	-1.0250218	0.2236896
H	-4.3730034	-2.6949061	0.6377555
H	-3.1564227	-2.3333815	-0.5832815
C	0.7169466	2.0789906	-2.5994752
C	1.8173311	-1.3703608	-2.6792957
C	3.0895330	1.0028271	1.4681051
H	3.2090486	1.0054010	0.3868883
H	4.0851954	0.9982010	1.9175904
H	2.6070878	1.9384605	1.7557486
C	-1.8737147	-3.4556575	1.4050074
H	-1.3459051	-3.6293130	0.4666479
H	-2.6802500	-4.1883580	1.4710300
H	-1.1915494	-3.6465828	2.2353487
C	3.1406222	-0.6484758	-2.3858177
H	3.2588016	0.2584226	-2.9746568
H	3.9755794	-1.3066036	-2.6387569
H	3.2330178	-0.3880476	-1.3329289
C	2.2127119	-0.1593646	3.4966106
H	1.7052795	0.7479520	3.8288838
H	3.2170310	-0.1652236	3.9277512
H	1.6662749	-1.0162772	3.8948110
C	-2.4719081	1.5495496	1.6800785
C	-3.1323627	-1.9065902	2.8606573
H	-2.3735464	-1.9266472	3.6460574
H	-3.8124381	-2.7447610	3.0298344
H	-3.7077648	-0.9909873	2.9736672
C	-3.8949845	1.2416740	1.1924150
H	-3.9192178	1.1028433	0.1114636
H	-4.5389737	2.0911704	1.4314788
H	-4.3315225	0.3692087	1.6696848
C	-2.4989237	1.7267961	3.2195319
H	-2.7531710	0.8000571	3.7327361
H	-3.2411532	2.4801095	3.4950760
H	-1.5277206	2.0581554	3.5917104
C	1.8726265	-2.7528236	-1.9979842
H	1.9462810	-2.6651298	-0.9153454
H	2.7434272	-3.3061451	-2.3568548
H	0.9871252	-3.3486589	-2.2255739
C	1.2009470	2.0385016	-4.0655922
H	1.5260723	3.0352483	-4.3746241
H	0.3954200	1.7259188	-4.7331303
H	2.0400155	1.3609176	-4.2082587
C	-0.3388751	3.1988570	-2.5165050
H	-0.7369090	3.3026077	-1.5079832
H	-1.1733582	3.0231432	-3.1968872
H	0.1204243	4.1516021	-2.7894263
C	1.7249354	-1.6208445	-4.2055055
H	0.8432456	-2.2159581	-4.4480808
H	2.6084456	-2.1674868	-4.5459419
H	1.6663734	-0.6903280	-4.7686535

Table 8-6 Cartesian coordinates of the optimised geometry of [Cp'''Co(η^4-1,2-P_2C_2tBu$_2$)]$^+$ (**1**$^+$) (doublet spin state) at the B3LYP/def2-TZVP level of theory. Total Energy: −3121.94720814733 a.u.

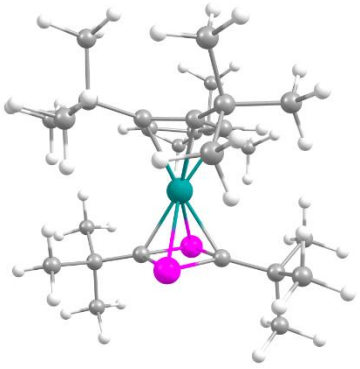

Atom	x	y	z
Co	0.2005690	0.0007925	-0.4305505
P	1.7274143	0.1001962	-2.1669930
P	-0.9742646	-0.1294310	-2.4450834
C	0.4696299	-1.1876453	-2.2435781
C	0.2741974	1.1527385	-2.3004259
C	0.6462091	-2.6608588	-2.5347553
C	1.7836553	-3.2845173	-1.7102807
C	1.0304535	-2.7403215	-4.0390363
C	-0.6527127	-3.4544734	-2.3305858
C	0.1911806	2.6250889	-2.6266788
C	1.1160720	3.4675174	-1.7313824
C	-1.2580271	3.1341545	-2.5586050
C	0.6807618	2.7621923	-4.0949282
C	-0.8460497	-0.7252092	1.4380042
C	-0.8348548	0.7437696	1.4799170
C	0.5318572	1.1337475	1.3859419
C	1.3957172	0.0005184	1.3621085
C	0.5239467	-1.1286832	1.3551445
C	-1.9667655	-1.7745213	1.6101669
C	-1.3596594	-3.1908198	1.7129208
C	-2.9707022	-1.7920094	0.4392006
C	-2.7285831	-1.5519297	2.9367075
C	-1.8994327	1.8030573	1.8223337
C	-3.2747288	1.5879804	1.1714531
C	-1.4269625	3.2171487	1.4214265
C	-2.0405191	1.8293846	3.3684074
C	2.8907276	0.0060413	1.6373809
C	3.5708156	1.2775798	1.1071619
C	3.0306815	-0.0245220	3.1824713
C	3.5959437	-1.2274422	1.0561006
H	1.5494011	-3.2912582	-0.6458227
H	2.7251636	-2.7499280	-1.8505874
H	1.9447581	-4.3171120	-2.0235382
H	1.1552466	-3.7869136	-4.3223966
H	1.9685999	-2.2209283	-4.2407863
H	0.2537365	-2.3090846	-4.6725563
H	-0.9506316	-3.4799102	-1.2839925
H	-0.5115637	-4.4856554	-2.6576237
H	-1.4772679	-3.0372180	-2.9128801
H	1.1129082	4.5056631	-2.0670698
H	2.1478061	3.1120442	-1.7760294
H	0.7941918	3.4509424	-0.6910476
H	-1.8930110	2.6177761	-3.2816952
H	-1.2925511	4.1987009	-2.7945723
H	-1.6967209	2.9986397	-1.5709346
H	0.0771494	2.1588635	-4.7748100
H	1.7241516	2.4599626	-4.1982392
H	0.5981567	3.8053285	-4.4054722
H	0.8738814	2.1523385	1.4067674

H	0.8564268	-2.1502212	1.3556037
H	-0.7867267	-3.4705391	0.8293417
H	-2.1694092	-3.9137419	1.8123435
H	-0.7179921	-3.2968047	2.5893841
H	-3.4296172	-0.8255937	0.2585027
H	-3.7675611	-2.5053073	0.6580156
H	-2.4888889	-2.1085810	-0.4845188
H	-2.0439892	-1.4686404	3.7824501
H	-3.3743261	-2.4123518	3.1181789
H	-3.3654057	-0.6729711	2.9177788
H	-3.7784688	0.6941650	1.5256387
H	-3.1993485	1.5318009	0.0840040
H	-3.9197311	2.4334351	1.4144755
H	-1.2072720	3.2957142	0.3591344
H	-0.5498293	3.5397610	1.9823340
H	-2.2215379	3.9288315	1.6456273
H	-2.7452155	2.6153468	3.6465728
H	-1.0835484	2.0572702	3.8409410
H	-2.4049084	0.8933740	3.7795554
H	3.5003085	1.3457017	0.0207224
H	4.6291438	1.2628038	1.3709834
H	3.1446162	2.1841138	1.5396715
H	4.0875218	-0.0158952	3.4541277
H	2.5805983	-0.9240417	3.6058437
H	2.5568745	0.8439360	3.6431571
H	3.5540347	-1.2342905	-0.0333514
H	3.1671188	-2.1603287	1.4254927
H	4.6471578	-1.2187207	1.3473124

Table 8-7 Cartesian coordinates of the optimised geometry of [Cp'''Co(η^3-PC$_2$*t*Bu$_2$)]$^+$ (**6**$^+$) at the B3LYP/def2-TZVP level of theory. Total Energy: −2780.61362723508 a.u.

Atom	x	y	z
Co	0.5078430	0.3288824	-0.2192738
P	1.5796215	0.2795581	-2.0474411
C	0.1602796	-0.7431101	-2.2636179
C	-0.0265145	-2.1032946	-2.9133550
C	1.2454680	-2.9423996	-2.7045143
H	2.1255652	-2.4474790	-3.1205451
H	1.1396925	-3.9047201	-3.2065098
H	1.4274749	-3.1371904	-1.6469067
C	-1.2325149	-2.8501479	-2.3200975
H	-1.1135566	-3.0077582	-1.2478592
H	-1.3159577	-3.8305442	-2.7916455
H	-2.1682603	-2.3201953	-2.4842468
C	-0.2252043	-1.8879574	-4.4324473
H	-1.1378022	-1.3377803	-4.6563612
H	-0.2968091	-2.8622622	-4.9184419
H	0.6186190	-1.3548303	-4.8732234
C	-0.5358347	0.3567831	-1.8241794
C	-1.6575402	1.2012702	-2.4134676
C	-2.0837741	2.3337356	-1.4724493
H	-2.5149657	1.9427971	-0.5521605
H	-2.8439738	2.9461458	-1.9596038

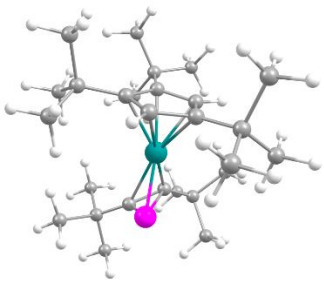

H	-1.2456064	2.9796901	-1.2185352
C	-1.1192266	1.8241278	-3.7227268
H	-0.2420565	2.4475149	-3.5371320
H	-1.8910137	2.4614116	-4.1571356
H	-0.8528707	1.0645744	-4.4571272
C	-2.8929175	0.3328205	-2.7279557
H	-2.6885698	-0.4179559	-3.4881920
H	-3.6871688	0.9777983	-3.1073282
H	-3.2717545	-0.1674145	-1.8361576
C	0.9514241	-0.5321311	1.6637431
C	-0.3655659	0.1210431	1.7623530
C	-0.1515206	1.4730879	1.4002222
H	-0.9194412	2.2227825	1.3522417
C	1.2389254	1.7284578	1.1467698
C	1.8922048	0.4888515	1.3236395
H	2.9475320	0.3304811	1.2003847
C	1.4821693	-1.9372342	2.0041852
C	1.8362650	-1.9336841	3.5138920
H	2.5748584	-1.1629816	3.7402593
H	2.2659114	-2.8997423	3.7857583
H	0.9673831	-1.7628408	4.1452604
C	0.5287507	-3.1025546	1.7006435
H	-0.3816417	-3.0786204	2.2902772
H	1.0336268	-4.0413788	1.9322007
H	0.2558769	-3.1322367	0.6448711
C	2.7916837	-2.2314356	1.2358772
H	2.6589023	-2.1573510	0.1558295
H	3.1118171	-3.2489297	1.4612607
H	3.6096645	-1.5741381	1.5283616
C	-1.7470758	-0.3640139	2.2498330
C	-1.6293700	-0.9827671	3.6602217
H	-1.0778126	-1.9176735	3.6730242
H	-2.6293657	-1.1911396	4.0438205
H	-1.1464243	-0.2915840	4.3534257
C	-2.7108923	0.8334611	2.3960908
H	-2.3365491	1.5762745	3.1024282
H	-3.6664641	0.4720062	2.7766936
H	-2.9124258	1.3272120	1.4454885
C	-2.4181592	-1.3574400	1.2816537
H	-2.6146329	-0.8803882	0.3207851
H	-3.3757989	-1.6793862	1.6951828
H	-1.8222197	-2.2460220	1.1005984
C	1.8976572	3.0828836	0.9622916
C	2.0090527	3.6918383	2.3843341
H	1.0265301	3.8314771	2.8382174
H	2.4953638	4.6671308	2.3264390
H	2.6025291	3.0562675	3.0435674
C	1.0625179	4.0273693	0.0844167
H	0.9857177	3.6564475	-0.9386659
H	1.5397887	5.0075821	0.0461275
H	0.0556021	4.1734200	0.4779877
C	3.3081940	2.9566887	0.3662143
H	3.9690580	2.3606001	0.9972830
H	3.7568489	3.9467351	0.2754930
H	3.2888334	2.5115057	-0.6303450

Table 8-8 Cartesian coordinates of the optimised geometry of [Cp'''Co(η^3-P_3C_2tBu$_2$)]$^+$ (**6**$^+$) at the B3LYP/def2-TZVP level of theory. Total Energy: −3463.31437982397 a.u.

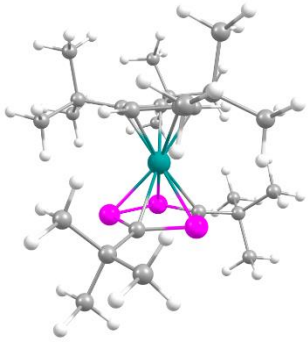

Atom	x	y	z
Co	-0.1111102	-0.0529840	-0.4565684
P	-1.2444430	-1.2542306	-2.1912869
P	-1.3337236	0.8816612	-2.2989318
P	1.5873272	-0.0649448	-2.1373894
C	0.5094460	-1.4602822	-2.1764070
C	1.0987455	-2.8863267	-2.3396528
C	0.3908434	1.2330711	-2.2524725
C	0.9015722	2.6759185	-2.4937568
C	-1.3097288	-0.5784828	1.2514017
C	-1.0982254	0.8696305	1.2363867
C	0.3239947	1.0583408	1.2445049
C	1.0122729	-0.1757618	1.3655599
C	-0.0012408	-1.1663495	1.2843962
C	-2.5389189	-1.4760125	1.4997451
C	-2.0371249	2.0799630	1.4670737
C	2.4537712	-0.3637518	1.8078554
C	-0.2116705	3.7301923	-2.3928456
H	-1.0070999	3.5565359	-3.1194509
H	-0.6604572	3.7621856	-1.4007249
H	0.2060764	4.7172606	-2.5967885
C	-1.2148330	3.3820158	1.5836118
H	-0.5410222	3.3689380	2.4420415
H	-0.6329404	3.5931490	0.6871405
H	-1.9019863	4.2165089	1.7239891
C	2.4426172	-0.0744586	3.3334631
H	1.7621247	-0.7436159	3.8629790
H	3.4452969	-0.2249638	3.7368612
H	2.1451594	0.9539549	3.5442663
C	2.6371810	-2.8973417	-2.3438602
H	3.0624427	-2.5321086	-1.4097536
H	2.9883210	-3.9206333	-2.4854770
H	3.0454566	-2.2959792	-3.1579894
C	1.4335867	2.6872507	-3.9497042
H	2.2835749	2.0139992	-4.0733920
H	0.6582400	2.3936670	-4.6593507
H	1.7626243	3.6956123	-4.2074732
C	0.6282004	-3.3746013	-3.7336834
H	0.9357843	-2.6860305	-4.5225346
H	1.0735461	-4.3485639	-3.9442038
H	-0.4566235	-3.4836107	-3.7776801
C	3.4207080	0.6182995	1.1308244
H	4.4157820	0.5043204	1.5632343
H	3.4962867	0.4308940	0.0600754
H	3.1215864	1.6568831	1.2787241
C	-2.7298965	1.9011145	2.8409132
H	-3.4922823	1.1281432	2.8321563
H	-2.0089423	1.6692347	3.6270665
H	-3.2206056	2.8380487	3.1084134
C	-3.8702453	-0.9639980	0.9322817

H	-3.8145787	-0.8133769	-0.1467345
H	-4.6410367	-1.7134955	1.1164160
H	-4.2085833	-0.0426713	1.3952813
C	-3.1013828	2.3241194	0.3809675
H	-2.6495432	2.7091926	-0.5309185
H	-3.6660021	1.4364596	0.1192216
H	-3.8074463	3.0744404	0.7416457
C	2.0498895	3.0697924	-1.5495024
H	1.7157545	3.1225452	-0.5132571
H	2.8869534	2.3732583	-1.6048350
H	2.4252177	4.0565657	-1.8252884
C	0.5929810	-3.8751010	-1.2776503
H	-0.4952473	-3.9211626	-1.2479621
H	0.9590981	-4.8764492	-1.5097929
H	0.9583361	-3.6141200	-0.2842703
C	-2.6498805	-1.6332232	3.0412557
H	-3.5005991	-2.2765228	3.2722043
H	-1.7550531	-2.1044496	3.4518487
H	-2.7970694	-0.6861845	3.5535820
C	2.9415585	-1.8022485	1.5944030
H	2.3355846	-2.5256544	2.1428118
H	2.9384668	-2.0768350	0.5410141
H	3.9654738	-1.8991597	1.9572237
C	-2.3407191	-2.8968333	0.9310882
H	-1.4727447	-3.4079180	1.3455687
H	-3.2120812	-3.4973551	1.1935049
H	-2.2615429	-2.8890452	-0.1542840
H	0.1800442	-2.2251160	1.3072872
H	0.8047041	2.0187870	1.2355838

8.5 References

[1] G. Becker, G. Gresser, W. Uhl, *Z. Naturforsch., Teil B* **1981**, *36B*, 16.

[2] a) J. F. Nixon, *Chem. Rev.* **1988**, *88*, 1327; b) M. Regitz, *Chem. Rev.* **1990**, *90*, 191; c) J. F. Nixon, *Endeavour* **1991**, *15*, 49; d) A. C. Gaumont, J. M. Denis, *Chem. Rev.* **1994**, *94*, 1413; e) J. F. Nixon, *Coord. Chem. Rev.* **1995**, *145*, 201; f) F. Mathey, *Angew. Chem. Int. Ed.* **2003**, *42*, 1578; g) A. Chirila, R. Wolf, J. C. Slootweg, K. Lammertsma, *Coord. Chem. Rev.* **2014**, *57*, 270.

[3] a) P. B. Hitchcock, M. J. Maah, J. F. Nixon, *Chem. Commun.* **1986**, 737; b) P. Binger, R. Milczarek, R. Mynott, M. Regitz, W. Rösch, *Angew. Chem. Int. Ed.* **1986**, *25*, 644; c) P. Binger, R. Milczarek, R. Mynott, M. Regitz, W. Rösch, *Angew. Chem.* **1986**, *98*, 645.

[4] a) P. Binger, R. Milczarek, R. Mynott, C. Krüger, Y.-H. Tsay, E. Raabe, M. Regitz, *Chem. Ber.* **1988**, 637; b) H. F. Dare, J. A. K. Howard, M. U. Pilotti, F. G. A. Stone, J. Szameitat, *Chem. Commun.* **1989**, 1409; c) P. B. Hitchcock, M. J. Maah, J. F. Nixon, *Heteroat. Chem.* **1991**, *2*, 253; d) C. Jones, C. Schulten, A. Stasch, *Dalton Trans.* **2006**, 3733; e) C. Rödl, R. Wolf, *Eur. J. Inorg. Chem.* **2015**, n/a.

[5] a) E.-M. Rummel, M. Eckhardt, M. Bodensteiner, E. V. Peresypkina, W. Kremer, C. Gröger, M. Scheer, *Eur. J. Inorg. Chem.* **2014**, 1625; b) J. Malberg, T. Wiegand, H. Eckert, M. Bodensteiner, R. Wolf, *Chem. Eur. J.* **2013**, *19*, 2356; c) J. Malberg, T. Wiegand, H. Eckert, M. Bodensteiner, R. Wolf, *Eur. J. Inorg. Chem.* **2014**, *2014*, 1638; d) J. Malberg, M. Bodensteiner, D. Paul, T. Wiegand, H. Eckert, R. Wolf, *Angew. Chem.* **2014**, *126*, 2812; e) J. Malberg, M. Bodensteiner, D. Paul, T. Wiegand, H. Eckert, R. Wolf, *Angew. Chem. Int. Ed.* **2014**, *53*, 2771.

[6] M. Driess, D. Hu, H. Pritzkow, H. Schäufele, U. Zenneck, M. Regitz, W. Rösch, *J. Organomet. Chem.* **1987**, *334*, C35.

[7] a) R. Wolf, J. C. Slootweg, A. W. Ehlers, F. Hartl, B. de Bruin, M. Lutz, A. L. Spek, K. Lammertsma, *Angew. Chem. Int. Ed.* **2009**, *48*, 3104; b) R. Wolf, J. C. Slootweg, A. W. Ehlers, F. Hartl, B. de Bruin, M. Lutz, A. L. Spek, K. Lammertsma, *Angew. Chem.* **2009**, *121*, 3150; c) R. Wolf, A. W. Ehlers, J. C. Slootweg, M. Lutz, D. Gudat, M. Hunger, A. L. Spek, K. Lammertsma, *Angew. Chem.* **2008**, *120*, 4660; d) R. Wolf, A. W. Ehlers, J. C. Slootweg, M. Lutz, D. Gudat, M. Hunger, A. L. Spek, K. Lammertsma, *Angew. Chem. Int. Ed.* **2008**, *47*, 4584; e) R. Wolf, A. W. Ehlers, M. M. Khusniyarov, F. Hartl, B. de Bruin, G. J. Long, F. Grandjean, F. M. Schappacher, R. Pöttgen, J. C. Slootweg, M. Lutz, A. L. Spek, K. Lammertsma, *Chem. Eur. J.* **2010**, *16*, 14322.

[8] N. G. Connelly, W. E. Geiger, *Chem. Rev.* **1996**, *96*, 877.

[9] a) I. Krossing, *J. Am. Chem. Soc.* **2001**, *123*, 4603; b) C. Schwarzmaier, M. Sierka, M. Scheer, *Angew. Chem. Int. Ed.* **2013**, *52*, 858; c) C. Schwarzmaier, M. Sierka, M. Scheer, *Angew. Chem.* **2013**, *125*, 891.

[10] M. Fleischmann, F. Dielmann, L. J. Gregoriades, E. V. Peresypkina, A. V. Virovets, S. Huber, A. Y. Timoshkin, G. Balázs, M. Scheer, *Angew. Chem.* **2015**, *127*, 13303.

[11] a) M. T. Nguyen, L. Landuyt, L. G. Vanquickenborne, *J. Org. Chem.* **1993**, *58*, 2817; b) S. Creve, M. T. Nguyen, L. G. Vanquickenborne, *Eur. J. Inorg. Chem.* **1999**, *1999*, 1281; c) T. Höltzl, D. Szieberth, M. T. Nguyen, T. Veszprémi, *Chem. Eur. J.* **2006**, *12*, 8044.

[12] a) A. D. Burrows, A. Dransfeld, M. Green, J. C. Jeffery, C. Jones, J. M. Lynam, M. T. Nguyen, *Angew. Chem.* **2001**, *113*, 3321; b) A. D. Burrows, A. Dransfeld, M. Green, J. C. Jeffery, C. Jones, J. M. Lynam, M. T. Nguyen, *Angew. Chem. Int. Ed.* **2001**, *40*, 3221.

[13] P. Binger, G. Glaser, S. Albus, C. Krüger, *Chem. Ber.* **1995**, 1261.

[14] a) I. Krossing, I. Raabe, *Angew. Chem. Int. Ed.* **2004**, *43*, 2066; b) I. Krossing, I. Raabe, *Angew. Chem.* **2004**, *116*, 2116.

[15] a) C. Heindl, S. Heinl, D. Lüdeker, G. Brunklaus, W. Kremer, M. Scheer, *Inorg. Chim. Acta* **2014**, *422*, 218; b) B. Attenberger, E. V. Peresypkina, M. Scheer, *Inorg. Chem.* **2015**, *54*, 7021.

[16] a) J. Bai, E. Leiner, M. Scheer, *Angew. Chem.* **2002**, *114*, 820; b) J. Bai, E. Leiner, M. Scheer, *Angew. Chem. Int. Ed.* **2002**, *41*, 783; c) M. Scheer, L. J. Gregoriades, M. Zabel, J. Bai, I. Krossing, G. Brunklaus, H. Eckert, *Chem. Eur. J.* **2008**, *14*, 282.

[17] S. Deng, C. Schwarzmaier, M. Zabel, J. F. Nixon, M. Bodensteiner, E. V. Peresypkina, G. Balázs, M. Scheer, *Eur. J. Inorg. Chem.* **2011**, *2011*, 2991.

[18] a) R. Bartsch, P. B. Hitchcock, J. F. Nixon, *Chem. Commun.* **1987**, 1146; b) R. Bartsch, P. B. Hitchcock, J. F. Nixon, *J. Organomet. Chem.* **1988**, *356*, C1; c) R. Bartsch, P. B. Hitchcock, J. F. Nixon, *J. Organomet. Chem.* **1989**, *375*, C31; d) A. Elvers, F. Heinemann, S. Kummer, B. Wrackmeyer, M. Zeller, U. Zenneck, *Phosphorus, Sulfur, and Silicon and the Related Elements* **1999**, *144*, 725; e) F. E. Hahn, D. L. Van, L. Wittenbecher, M. C. Moyes, T. V. Fehren, R. Fröhlich, E. U. Würthwein, *Phosphorus, Sulfur, and Silicon and the Related Elements* **2002**, *177*, 1863; f) C. Fish, M. Green, J. C. Jeffery, R. J. Kilby, J. M. Lynam, C. A. Russell, C. E. Willans, *Organometallics* **2005**, *24*, 5789; g) S. Deng, C. Schwarzmaier, U. Vogel, M. Zabel, J. F. Nixon, M. Scheer, *Eur.*

J. Inorg. Chem. **2008**, *2008*, 4870; h) A. Schindler, G. Balazs, M. Zabel, C. Groeger, R. Kalbitzer, M. Scheer, *C. R. Chim.* **2010**, *13*, 1241; i) C. Heindl, A. Schindler, M. Bodensteiner, E. V. Peresypkina, A. V. Virovets, M. Scheer, *Phosphorus, Sulfur, and Silicon and the Related Elements* **2014**, *190*, 397; j) C. Heindl, E. V. Peresypkina, A. V. Virovets, V. Y. Komarov, M. Scheer, *Dalton Trans.* **2015**, *44*, 10245.

[19] a) C. Topf, T. Clark, F. W. Heinemann, M. Hennemann, S. Kummer, H. Pritzkow, U. Zenneck, *Angew. Chem.* **2002**, *114*, 4221; b) C. Topf, T. Clark, F. W. Heinemann, M. Hennemann, S. Kummer, H. Pritzkow, U. Zenneck, *Angew. Chem. Int. Ed.* **2002**, *41*, 4047.

[20] F. G. N. Cloke, P. B. Hitchcock, J. F. Nixon, D. M. Vickers, *J. Organomet. Chem.* **2001**, *635*, 212.

[21] I. Krossing, *Chem. Eur. J.* **2001**, *7*, 490.

[22] O. V. Dolomanov, L. J. Bourhis, R. J. Gildea, J. A. K. Howard, H. Puschmann, *J. Appl. Crystallogr.* **2009**, *42*, 339.

[23] G. M. Sheldrick, *Acta Cryst.* **2015**, *A71*, 3.

[24] G. M. Sheldrick, *Acta Cryst.* **2015**, *C71*, 3.

[25] a) F. Furche, R. Ahlrichs, C. Hättig, W. Klopper, M. Sierka, F. Weigend, *WIREs Comput. Mol. Sci.* **2014**, *4*, 91; b) R. Ahlrichs, M. Bär, M. Häser, H. Horn, C. Kölmel, *Chem. Phys. Lett.* **1989**, *162*, 165; c) O. Treutler, R. Ahlrichs, *J. Chem. Phys.* **1995**, *102*, 346

[26] a) K. Eichkorn, O. Treutler, H. Öhm, M. Häser, R. Ahlrichs, *Chem. Phys. Lett.* **1995**, *242*, 652; b) K. Eichkorn, F. Weigend, O. Treutler, R. Ahlrichs, *Theor. Chem. Acc.* **1997**, *97*, 119.

[27] a) P. A. M. Dirac, *Proc. Royal Soc. A* **1929**, 714; b) J. C. Slater, *Phys. Rev.* **1951**, 385; c) S. H. Vosko, L. Wilk, M. Nusair, *Can. J. Phys.* **1980**, 1200; d) A. D. Becke, *Phys. Rev. A* **1988**, 3098; e) C. Lee, W. Yang, R. G. Parr, *Phys. Rev. B* **1988**, 785; f) A. D. Becke, *J. Chem. Phys.* **1993**, 5648.

[28] A. Schäfer, C. Huber, R. Ahlrichs, *J. Chem. Phys. Lett.* **1994**, 5829.

[29] M. Sierka, A. Hogekamp, R. Ahlrichs, *J. Chem. Phys.* **2003**, *118*, 9136.

9 Thesis Treasury: The use of 1,3-Diphosphete complexes in coordination chemistry with group 11 metal salts

≡ Syntheses and characterisations were performed by Eva-Maria Rummel

≡ Figures and schemes were made by Eva-Maria Rummel

≡ X-ray measurements, structure solution and refinement were done by Eva-Maria Rummel

≡ Manuscript was written by Eva-Maria Rummel

Preface

The contents of this chapter are preliminary results obtained during the process of this thesis. However, as some analyses or further investigations still remain open or ongoing, they do not yet qualify for a publication on their own. As a comprehensive introduction is given at the beginning of this thesis, this subchapter will only be brushing the body of literature. All results given here are entry points to possible future research.

9.1 Introduction

Cyclodimerizations of phosphaalkynes have first been reported by the groups of Nixon[1] and Binger[2] in 1986, in which phosphaalkynes and $[Cp^RM(C_2H_4)_2]$ (M = Co, Rh, Ir) are reacted to yield 1,3-diphosphacyclobutadiene (1,3-diphosphete) complexes with the general formula $[Cp^RM(\eta^4\text{-}P_2C_2R_2)]$.[1] As we have shown previously, we have also been able to react both *tert*-butyl and *iso*-proyl phosphaalkyne with $[(Cp'''Co)_2(tol)]$ to yield the 1,3-diphosphete complexes $[Cp'''Co(\eta^4\text{-}P_2C_2tBu_2)]$ (**1a**) and $[Cp'''Co(\eta^4\text{-}P_2C_2iPr_2)]$ (**1b**), respectively. In the reaction of **1a** and **1b** with Cu(I) halides, products of different composition could be obtained depending on the stoichiometry used (cf. Figure 9-1).[3]

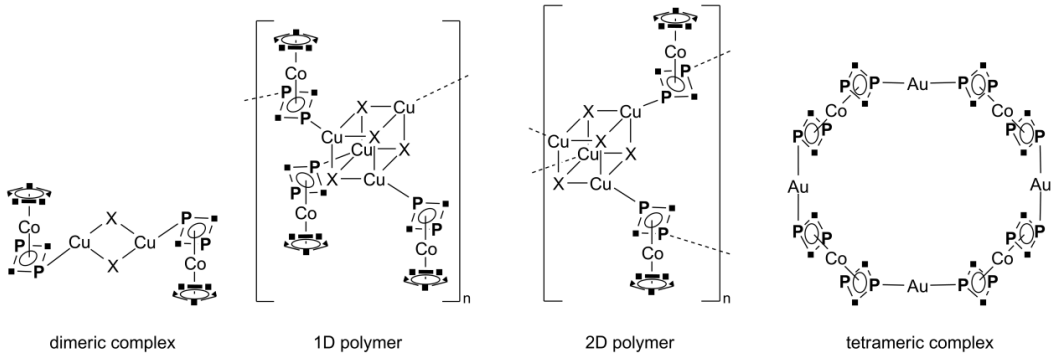

Figure 9-1 Possible Cu(I) and Au(I) coordination of 1,3-diphosphete complexes.

In a previous chapter, it has been discussed how **1a** reacts with $Ag[Al\{OC(CF_3)_3\}_4]$ (Ag[pftb]) to yield both coordination products and oxidation products depending on stoichiometry and solvent. Here, in the reaction of Ag[pftb] and **1a** in CH_2Cl_2 a 1,2-diphosphete coordination complex of Ag^+, $[Ag_2\{Cp'''Co(\mu,\eta^4\text{:}\eta^1\text{-}1,2\text{-}P_2C_2tBu_2)\}_2\{Cp'''Co(\mu,\eta^4\text{:}\eta^1\text{-}1,2\text{-}P_2C_2tBu_2)\}_2]\cdot 2[pftb]$, could be isolated. In this complex, the former 1,3-diphosphete isomerised to a 1,2-diphosphete complex $[Cp'''Co(\eta^4\text{-}1,2\text{-}P_2C_2tBu_2)]$, which could subsequently be extracted from its coordination compound. 1,2-Diphosphete complexes with a four-membered anti aromatic ring and a direct P-P bond are scarcely known in the literature[4] although calculations show that the 1,2-diphosphete complexes are thermodynamically and kinetically more stable than their 1,3-diphosphete isomers.[5] Recently, also coordination compounds containing homoleptic 1,3-diphosphete complexes and Au(I) salts have been reported (Figure 9-1).[6]

In the following, the reactivity of **1b** with Ag[pftb] will be discussed as well as a further studies concerning the formation of 1,2-diphosphete complexes. Additionally, the reactions of **1a** with $AgBF_4$ and WCA salts of Au^+ will be reviewed.

9.2 Results and Discussion

The reaction between **1a** and Ag[pftb] in CH_2Cl_2 starting at low temperatures and reaching r.t. leads to the formation of a coordination complex where four molecules of **1a** isomerised to [Cp‘‘‘Co(η^4-1,2-P_2C_2tBu$_2$)] (**I-1a**) and are linked via two Ag(I) centres to yield [Ag_2{Cp‘‘‘Co(μ,η^4:η^1-1,2-P_2C_2tBu$_2$)}$_2${Cp‘‘‘Co(μ,η^4:η^1-1,2-P_2C_2tBu$_2$)}$_2$]·2[pftb] (**2a**). The same reaction can be carried out with **1b** and leads to a similar result: Here, also a rearrangement of the 1,3-diphosphete ring to form a 1,2-diphosphete ring was observed to give [Ag_2{Cp‘‘‘Co(μ,η^4:η^1-1,2-P_2C_2iPr$_2$)}$_2$(η^2-tol)$_2$]·2[pftb] (**2b**) (see eq. (9-1))

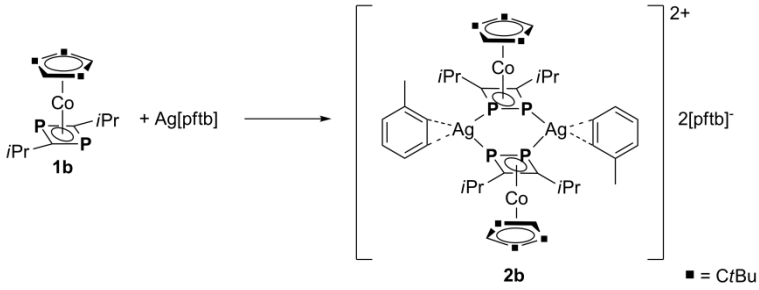

(9-1)

The compound can be crystallised by diffusion of toluene into a CH_2Cl_2 solution of **2b**. This product shows a similar structural motif of a Ag_2P_4 six-membered ring like **2a**, although the coordination sites of Ag(I) cations are saturated by the solvent molecule here (cf. Figure 9-2).

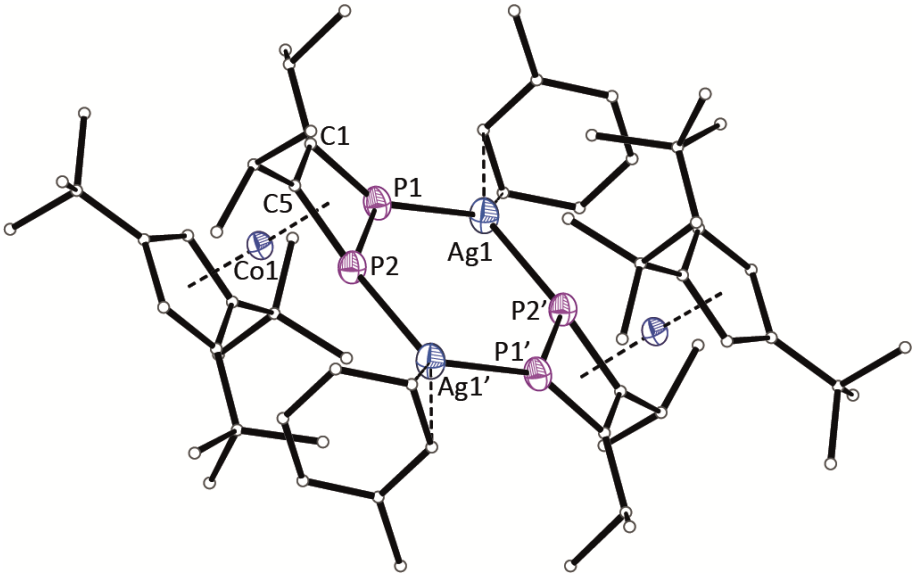

Figure 9-2 Molecular structure of the cation of **2b** in the solid state. Hydrogen atoms are omitted, carbon atoms are shown in ball-and-stick representation for clarity. Thermal ellipsoids are shown at 50% probability level. Selected bond lengths [Å] and angles [°]: P2-P1 2.160(2), P1-C1 1.800(6), P2-C5 1.803(6), C1-C5 1.412(8), P1-Ag1-P21 101.86(5), P1-P2-Ag1‘ 129.54(8) C5-P2-Ag1‘ 148.9(2), C5-P2-P1 77.8(2), C1-P1-P2 78.20(19), C5-C1-P1 101.8(4), C1-C5-P2 102.1(4).

Bond lengths and angles within the 1,2-diphosphete ring are in the same range as for known 1,2-diphosphete complexes.[4,7]

In an unrelated side reaction, single crystals of a combined hydrolysis/decomposition product could once be obtained: [Cp'''Co(η^3-{(POOH)(C*i*Pr)}$_2${Cp'''}] (**1b-Ox**). Here, the four-membered diphosphete ring is no longer planar and both phosphorus atoms are oxidised. Of the four oxygen atoms in the molecule, one is bearing an excess Cp''' ligand while two are OH groups. Only one has a short P=O double bond distance.

Attempts to reproduce this species by oxidation on air with the addition of Cp'''H naturally failed due to the air sensitivity of the product. Oxidation agents like S_8 and Se_{red} did not lead to the analogue products. However, a clear insight is gained on what possibly happens during oxidation processes to the diphosphete moiety by reviewing the crystal structure of the isolated **1b-Ox** (Figure 9-3).

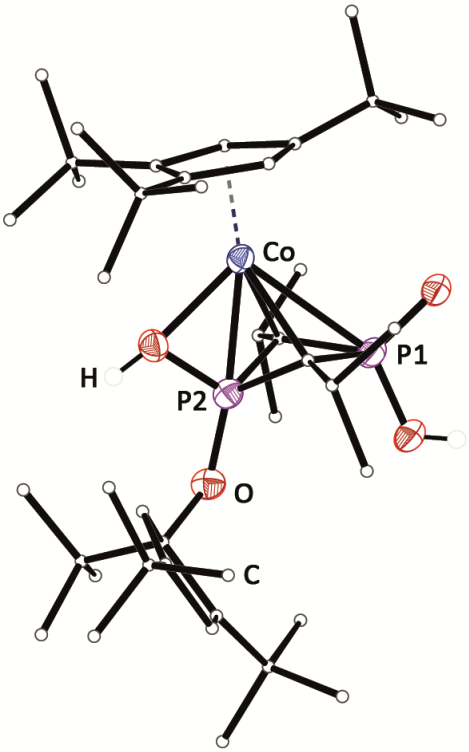

Figure 9-3 Molecular structure of **1b-Ox** in the solid state. Hydrogen atoms on the ligands are omitted and carbon framework is shown in ball-and-stick representation for clarity. Thermal ellipsoids are shown at 50% probability level. Selected bond lengths [Å] and angles [°]: Co1-P1 2.7848(7), Co1-O4 2.0474(15), Co1-P2 2.2800(6), Co1-C1 2.147(2), Co1-C5 2.170(2), P1-C1 1.792(2), P1-C5 1.781(2), P2-C1 1.781(2), P2-C5 1.765(2), C5-P1-C1 83.22(10), C5-P2-C1 83.99(10), P2-C1-P1 89.59(10), P2-C5-P1 90.42(10).

The P-C bond lengths of **1b-Ox** within the four-membered ring are between 1.765(2) (P2-C5) and 1.792(2) (P1-C1). However, it can clearly be seen that an oxidation leads the P1 atom of the former 1,3-diphosphete ring to be bent out of the plane by 37°. Additionally, the bond length between Co1 and P1 is elongated in comparison to the other three atoms of the four-membered ring. The non-planar four-membered ring now shows a η^3 coordination mode. Clearly a future intention is to reproduce this species to gain further insight to the building process of oxidised diphosphete species.

So far, investigations have been conducted with Lewis acidic copper(I) halides and weakly coordinating silver(I) salts. Cu(I) coordination can lead to molecular and polymeric structural motifs because of the variability of geometries possible on a Cu(I) centre (linear, trigonal planar and tetrahedral). For Au(I), this flexibility is mostly limited to a coordination number of 2 (linear coordination). In the following, different coordination polymers and oligomers will be discussed. All are derived from weakly coordinating anions of Au(I) as well as the coordinating silver(I) salt $AgBF_4$ in the reaction with the diphosphete complex [Cp'''Co(η^4-$P_2C_2t Bu_2$)] (**1a**). The reaction of **1a** with $AgBF_4$ and [$(tht)_2$Au][pftb] leads to the formation of the one dimensional polymers [Ag{Cp'''Co(η^4:η^1:η^1-$P_2C_2t Bu_2$)}AgF{Cp'''Co(η^4:η^1:η^1-$P_2C_2t Bu_2$)}]$_n$·2n[BF_4] (**3**) and [Au{Cp'''Co(η^4:η^1:η^1-$P_2C_2t Bu_2$)}]$_n$·n[pftb] (**4**) (cf Scheme 9-1).

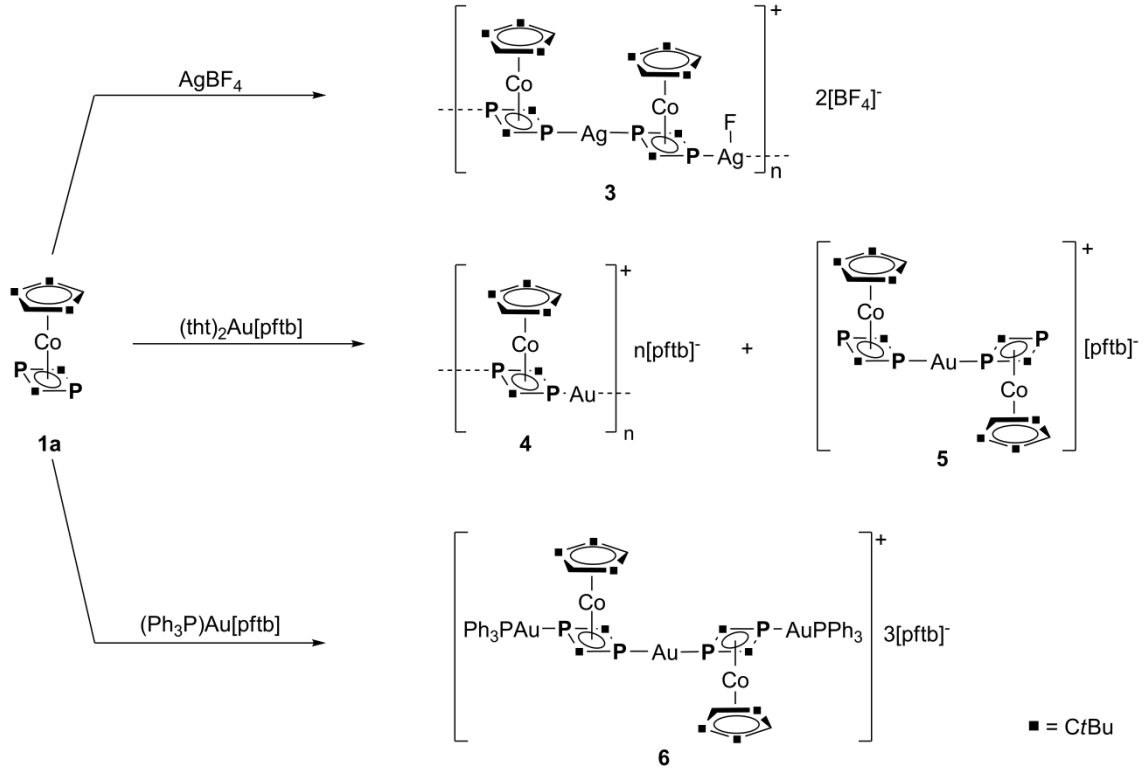

Scheme 9-1 Reaction pathways of **1a** with coordinating and weakly coordinating group 11 salts.

Both compounds have in common the η^1-coordination mode of the diphosphete moiety which is coordinating to the group 11 metal centre. However, the use of BF_4^- shows its relatively easy decomposition in comparison to the WCA $pftb^-$ anion. In compound **3**, every second silver centre is coordinated in a distorted tetrahedral fashion by two diphosphete complexes **1a**, the anion BF_4^- and an additional fluorine atom which has been abstracted from BF_4^-. Residual BF_3 has most likely been removed by the workup. Compound **4**, in comparison, is a straight forward one dimensional polymer in which the repeat units consist of one formula unit of **1a** and one Au^+ metal centre. As a second product in the reaction of [(tht)Au][pftb] and **1a**, the coordination compound [Au{Cp'''Co(η^4:η^1-$P_2C_2t Bu_2$)}$_2$][pftb] (**5**)

could be obtained. Compounds **4** and **5** can be separated by fractionalised crystallisation: **4** is the first compound to crystallise, while the mother liquor almost exclusively contains **5**.

By using a gold salt with PPh_3 as a capping group the formation of the oligomeric compound $[(\eta^1\text{-}PPh_3)_2Au_3\{Cp'''Co(\eta^4\text{:}\eta^1\text{:}\eta^1\text{-}P_2C_2t\text{Bu}_2)\}_2]\cdot 3[pftb]$ (**5**) is observed exclusively. Here, two diphosphete complexes **1a** are coordinating in an η^1 fashion with both of their phosphorus lone pairs to the gold centres. One gold(I) centre in the middle of the molecule is only coordinated by **1a** while the two outside Au(I) centres are coordinatively saturated by PPh_3 (cf Scheme 9-1).

X-ray structure analysis could be conducted for all four compounds. The molecular structure of **3** (Figure 9-4) shows two different coordination geometries for the Ag(I) atoms: As the BF_4^- anions are not separated from the cations in the polymeric strand, half of the anions reacted with half of the Ag(I) centres to lose one Fluorine atom. A trigonally planar coordination mode is observed for the silver atoms only coordinated by **1a** and BF_4^-, and a distorted tetrahedral coordination mode is observed for the silver atoms additionally coordinated by a fluorine atom.

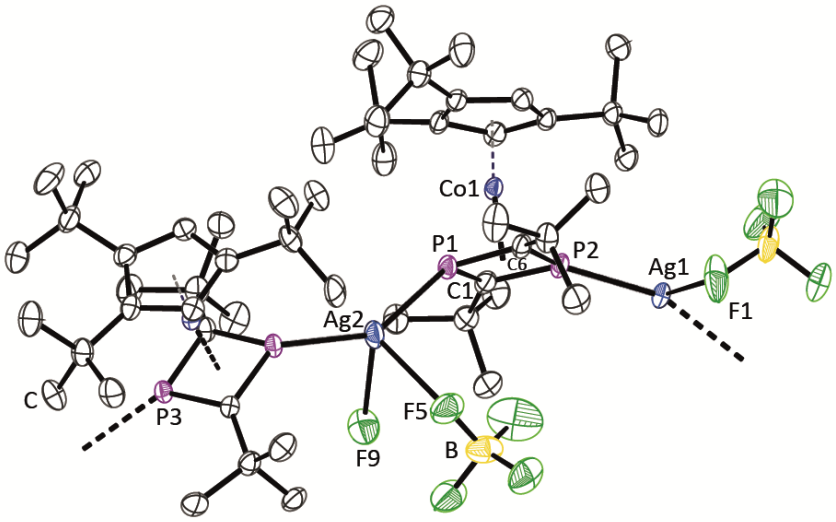

Figure 9-4 Molecular structure of **3** in the solid state. Hydrogen atoms are omitted for clarity. Thermal ellipsoids are shown at 50% probability level Selected bond lengths [Å] and angles [°]: Ag1-P2 2.3829(10), Ag1-P3 2.4007(10), Ag2-F9 2.458(4), Ag2-F5 2.557(3), Co1-P1 2.2419(12), Co1-P2 2.2261(12), Co1-C6 2.141(4), Co1-C1 2.117(4), P1-C1 1.782(4), P1-C6 1.784(4), P2-C6-P1 95.1(2), P2-C1-P1 95.1(2), C1-P1-C6 84.6(2), C6-P2-Ag1 135.51(14), C1-P2-Ag1 135.06(15), F9-Ag2-F5 78.58(11).

The bond lengths in the 1,3-diphosphete moiety do not change much in comparison to free **1a**. As the silver atoms clearly have a different chemical environment, the 1D polymeric strand is not straight but twisted, with the diphosphete complexes **1a** rotating around the axis in a small turn (over the trigonal planar Ag(I) centre) and a large turn (over the tetrahedral Ag(I) centre). This turn could not be observed for the linearly coordinated Au(I) centres in **4** (Figure 9-5) and **5** (Figure 9-6), where the two neighbouring diphosphete complexes are

taking a trans configuration towards each other. Unfortunately, the quality of single crystals for compounds **4** and **6** (Figure 9-7) together with more than one independent $pftb^-$ anion in the unit cell made it hard to assert anything beyond the heavy atom framework, so analysis is still on-going.

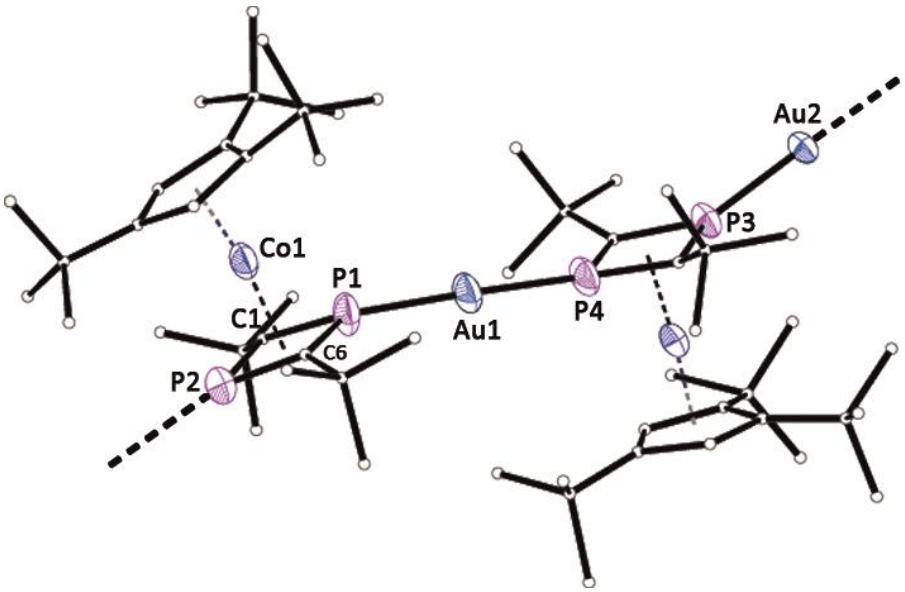

Figure 9-5 Molecular structure of the cationic repetition unit of **4** in the solid state. Hydrogen atoms are omitted, carbon atoms are shown in ball-and-stick representation for clarity. Thermal ellipsoids are shown at 50% probability level. Selected bond lengths [Å] and angles [°]: Au1-P1 2.286(3), Au2-P3 2.275(3), Au2-P2 2.275(3), P1-C1 1.757(12), P1-C6 1.781(15), P3-C16 1.751(14), P2-C1 1.743(14), P2-C6 1.775(15), P3-Au2-P2 174.94(13), C1-P2-C6 86.8(6), P2-C1-P1 94.4(7), P2-C6-P1 92.5(8), C1-P2-C6 86.8(6).

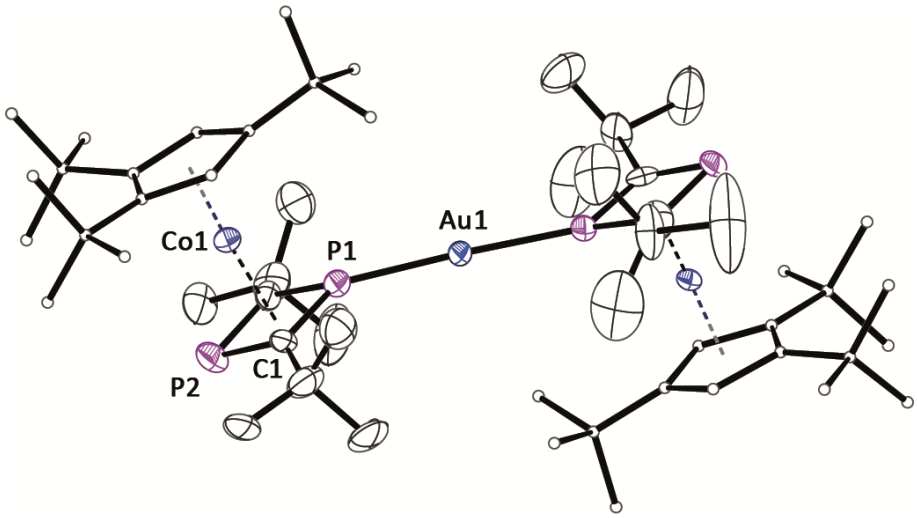

Figure 9-6 Molecular structure of the cation of **5** in the solid state. Hydrogen atoms are omitted, carbon atoms are shown in ball-and-stick representation for clarity. Thermal ellipsoids are shown at 50% probability level. Selected bond lengths [Å] and angles [°]: Au1-P1 2.286(4), Au1-P3 2.281(4), P1-C1 1.750(13), P2-C1 1.797(14), P3-C6 1.775(13), P4-C6 1.768(15), C1-P1-C1' 85.6(9), C1-P2 C1' 82.9(9), P1-C1-P2 95.7(7), P3-Au1-P1 177.54(15).

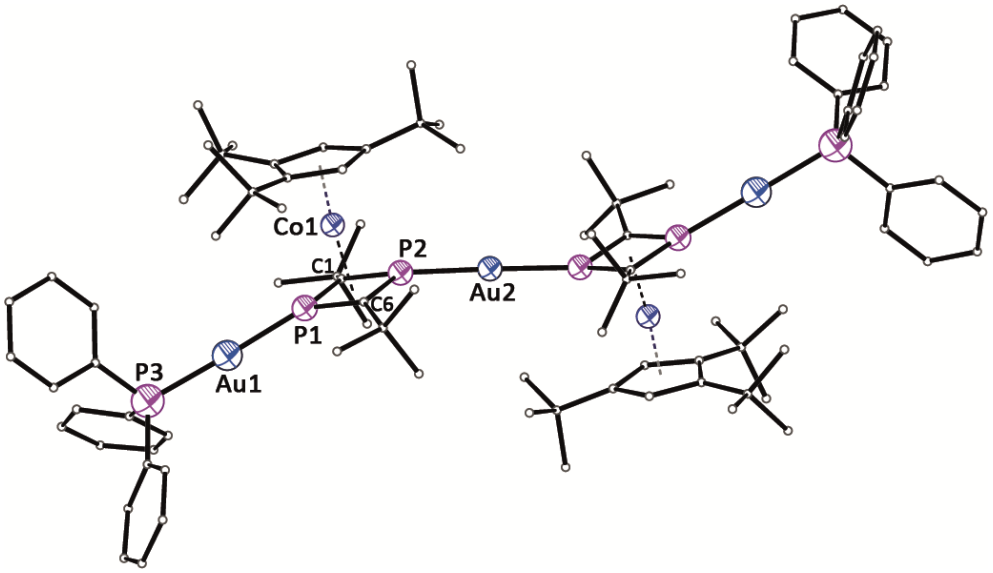

Figure 9-7 Molecular structure of the cation of **6** in the solid state. Hydrogen atoms are omitted, carbon atoms are shown in ball-and-stick representation for clarity. Thermal ellipsoids are shown at 50% probability level. Selected bond lengths [Å] and angles [°]: P1-C1 1.761(10), P1-C6 1.794(9), P1-Au1 2.268(3), P2-C 1.758(9), P2-C6 1.774(9), Au2-P2 2.278(2), Au1-P3 2.346(3), P2-Au2-P2' 175.79(12), C1-P1-C6 86.7(4), C1-P2-C6 87.4(4), P2-C6-P1 92.1(4).

The coordination compound **5** shows no structural conspicuousness and is related to the published tungsten complex $[(CO)_4W\{Cp'''Co(\eta^4{:}\eta^1\text{-}P_2C_2iPr_2)\}_2]$ (**1b-W**).[3] Here, also two diphosphete moieties are coordinating to the metal centre in a η^1 fashion. The bond lengths in the four-membered ring resemble those in complex **1a** and coordination compounds derived from **1a**.

Elemental analysis and mass spectroscopic results confirm the constitution of **3**; however no clean phosphorus NMR spectra could be obtained for this species due to low yields (10% crystalline). In the $^{31}P\{^1H\}$ NMR spectra, ca. 10% by-products could be seen in addition to the signals for the diphosphete phosphorus atoms in **3**. The different environment of the phosphorus atoms leads to two signals: A singlet can be found for the phosphorus atoms coordinating to the trigonal planar silver atoms, and a doublet which arises from a $^2J_{PF}$ coupling between the phosphorus and fluorine atoms bound to the tetrahedrally coordinated silver atoms. Due to both signals being very broad, no reliable statement can be made in regard to the coupling constants. As compounds **5** and **4** can be isolated next to each other from CH_2Cl_2 solutions, NMR shifts for both compounds can be found in the crude ^{31}P NMR spectra of the reaction between $[(tht)_2Au][pftb]$ and **1a**. Compound **4** shows a broad peak around 0 ppm in the $^{31}P\{^1H\}$ NMR. Compound **5** shows the two signals at δ = 48.4 and -15.0 ppm, of which the high field shifted signal can be assigned to the phosphorus atom coordinated to the gold centre. Similar shifts can also be observed in the crude ^{31}P NMR spectrum of compound **3**, so it seems natural that a similar coordination compound is also formed in the reaction of $AgBF_4$ with **1a**. However, no such compound could be isolated.

9.3 Conclusions

The coordination behaviour of [Cp'''Co(η^4-P_2C_2tBu$_2$)] (**1a**) and [Cp'''Co(η^4-P_2C_2iPr$_2$)] (**1b**) towards group 11 metal salts of weakly coordinating anions has been investigated. In the reaction between **1a** and Ag[pftb] previously an isomerisation of **1a** from a 1,3-diphosphete complex to a 1,2-diphosphete complex coordinated to silver(I) could be obtained (this dissertation, vide supra). The same was now observed for the reaction of **1b** and Ag[pftb], in which compound [Ag_2{Cp'''Co(μ,η^4:η^1-1,2-P_2C_2iPr$_2$)}$_2$(η^2-tol)$_2$]·2[pftb] (**2b**) could be obtained in moderate yields. In an unrelated side reaction once the oxidation/hydrolysis product [Cp'''Co(η^3-{(POOH)(C*i*Pr)}$_2${Cp'''}] (**1b-Ox**) could be obtained, giving hints to the possible structural changes when oxidising the 1,3-diphosphete moiety. The difference between the anion BF_4^- and the WCA [pftb]$^-$ can be seen in the formation of one dimensional polymers of **1a** with Ag and Au. While BF_4^- is partially decomposing into BF_3 and F^-, which in return is coordinating to half of the silver atoms in [Ag{Cp'''Co(η^4:η^1:η^1-P_2C_2tBu$_2$)}AgF{Cp'''Co(η^4:η^1:η^1-P_2C_2tBu$_2$)}]$_n$·2n[BF_4] (**3**), the [pftb] anion is neither decomposing nor coordinating to the cationic polymeric strand in [Au{Cp'''Co(η^4:η^1:η^1-P_2C_2tBu$_2$)}]$_n$·n[pftb] (**4**). Additionally, in the reaction of **1a** with [(tht)$_2$Au][pftb], the coordination compound [Au{Cp'''Co(η^4:η^1-P_2C_2tBu$_2$)}$_2$][pftb] (**5**) could be obtained. **4** and **5** can be separated by fractionalised crystallisation. Another interesting result could be obtained in the reaction between **1a** and [(PPh_3)Au][pftb], where the PPh_3 groups are capping end groups to form the oligomeric compound [(η^1-PPh_3)$_2$$Au_3${Cp'''Co($\eta^4$:$\eta^1$:$\eta^1$-$P_2C_2tBu_2$)}$_2$]·3[pftb] (**6**).

9.4 Experimental

All steps were performed under an atmosphere of dry argon with standard Schlenk techniques. All solvents were freshly collected from a Solvent Purification System by M. Braun and were degassed prior to use. All NMR spectra have been recorded using CD_2Cl_2, which was dried over CaH_2. It was refluxed for three hours, distilled under inert atmosphere and degassed prior to use. **1a** and **1b**,[3] Ag[pftb],[8] and Tl[pftb][9] have been synthesised according to literature procedures. [(tht)AuCl] has been kindly donated by Jens Braese, University of Regensburg. $AgBF_4$ has been purchased and handled as received in a dry glove box.

Synthesis of 2b

A solution of $4.3 \cdot 10^{-5}$ (20 mg) mol **1b** in 4 ml CH_2Cl_2 is cooled to -80 °C. To this solution, $8.6 \cdot 10^{-5}$ mol (100 mg) Ag[pftb] in 3 ml CH_2Cl_2 is added at -80 °C and the reaction mixture is stirred over night to reach room temperature. The formation of a black precipitate can be observed. Subsequently the solvent is removed under reduced pressure and the residue is taken up in 5 ml dichloromethane. The solution is filtered, layered under 10 ml of toluene and stored at -30 °C. After some time, a few orange crystals of **2b** can be found at the solvent boundary.

$^{19}F\{^1H\}$-NMR (CD_2Cl_2)	δ [ppm] = -75.6 (s)
^{19}F-NMR (CD_2Cl_2)	δ [ppm] = -75.6 (s)
Cation ESI-MS (CH_2Cl_2)	*m/z* [%] = 379.2 (15) [Cp‘‘‘CoP*C*iPr]$^+$, 1037.5 (100) [**1b**$_2$Ag]$^+$,
Anion ESI-MS (CH_2Cl_2)	*m/z* [%] = 967.2 (100) [pftb$^-$]

1b = [Cp‘‘‘Co(η^4-$P_2C_2i Pr_2$)]

Synthesis of 3

To a solution of $1.02 \cdot 10^{-4}$ mol (20 mg) $AgBF_4$ in 3 ml CH_2Cl_2 are added $1.02 \cdot 10^{-4}$ mol (50 mg) **1a** in 3 ml CH_2Cl_2 at -80 °C. After the solution reaches room temperature a black precipitate of Ag^0 is formed. The solvent is removed *in vacuo*. 3 ml dichloromethane are added, layered under 20 ml of hexane and stored at -30 °C. After some time, red crystals of **3** are forming at the solvent boundary.

Yield: 7 mg (10 %)

^1H-NMR (CD_2Cl_2)	δ [ppm] = 1.08 (s, 18 H, $P_2C_2t Bu_2$), 1.40 (s, 9H, $C_5H_2t Bu_3$), 1.55 (s, 18H, $C_5H_2t Bu_3$), 4.96 (s, 2H, $C_5H_2t Bu_3$)
^{31}P-NMR (CD_2Cl_2)	δ [ppm] = 4.5 (br, $\omega_{1/2}$ = 163 Hz), 0.1 (d, br, $\omega_{1/2}$ = 160.4, $^2J_{PF}$) plus 5% impurities each at 54.9 (s) and -15.7 (s)
$^{31}P\{^1H\}$-NMR (CD_2Cl_2)	δ [ppm] =4.5 (br, $\omega_{1/2}$ = 163 Hz), 0.1 (d, br, $\omega_{1/2}$ = 160.4, $^2J_{PF}$) plus 5% impurities each at 54.9 (s) and -15.7 (s)
Cation ESI-MS (CH_2Cl_2)	*m/z* [%] = 640.2 (100) [**1a**Ag+MeCN]$^+$, 1093.6 (80) [**1a**$_2$Ag]$^+$, 1728.0 (0.2) [**1a**$_3$Ag$_2$F$_2$]$^+$, 1871.7 (0.2) [**1a**$_3$Ag$_3$F$_4$]$^+$

Anion ESI-MS (CH_2Cl_2)	*m/z* [%] = 86.7 (100) $[BF_4]^-$
Elemental analysis	calculated for $C_{54}H_{94}Co_2P_4Ag_2B_2F_9 \cdot 0.5CH_2Cl_2$ (1433.28 g·mol^{-1}): C 45.3, H 6.6; found: C 45.89, H 6.94

1a = [Cp‘‘‘Co(η^4-P_2C_2tBu$_2$)]

Synthesis of 4 and 5

To a solution of $5.07 \cdot 10^{-5}$ mol (16 mg) [(tht)AuCl] in 2 ml CH_2Cl_2 are added $5.07 \cdot 10^{-5}$ mol (60 mg) Tl[pftb] and 0.5 ml tht. After half an hour of stirring, TlCl solidifies as a colourless precipitate. The colourless solution is filtered and added to a solution of $1.01 \cdot 10^{-4}$ mol (50 mg) **1a** in 2 ml CH_2Cl_2 at -80 °C. After the solution reaches room temperature the solvent is removed *in vacuo*. 4 ml dichloromethane are added, layered under 10 ml of hexane and stored at -30 °C. After some time, dark red crystals of **4** are forming at the solvent boundary. Filtration of the mother liquor and subsequent layering of hexane led to crystals of **5**.

Yield: **4**: 10 mg (11 %), **5**: 28 mg (25 %)

Analytical data for **4**:

^{1}H-NMR (CD_2Cl_2)	δ [ppm] = 1.11 (s, 18 H, P_2C_2tBu$_2$), 1.40 (s, 9H, C_5H_2tBu$_3$), 1.55 (s, 18H, C_5H_2tBu$_3$), 4.98 (s, 2H, C_5H_2tBu$_3$)
^{31}P-NMR (CD_2Cl_2)	δ [ppm] = 2.13 (br)
^{31}P{^{1}H}-NMR (CD_2Cl_2)	δ [ppm] = 2.13 (br)
^{19}F{^{1}H}-NMR (CD_2Cl_2)	δ [ppm] = -75.6 (s)
^{19}F-NMR (CD_2Cl_2)	δ [ppm] = -75.6 (s)
Cation ESI-MS (CH_2Cl_2)	*m/z* [%] = 393.16 (10) [Cp‘‘‘CoP*C*t*Bu*]$^+$, 1181.3 (100) [**1a**$_2$Au]$^+$
Anion ESI-MS (CH_2Cl_2)	*m/z* [%] = 966.7 (100) [pftb]$^-$
Elemental analysis	calculated for $C_{43}H_{47}CoP_2AuAlO_4F_{36} \cdot (C_4H_8S)$ (1744.15 g·mol^{-1}): C 32.33, H 3.17; found: C 32.6, H 3.65

1a = [Cp‘‘‘Co(η^4-P_2C_2tBu$_2$)]

Analytical data for **5**:

^{1}H-NMR (CD_2Cl_2)	δ [ppm] = 1.11 (s, 18 H, P_2C_2tBu$_2$), 1.40 (s, 9H, C_5H_2tBu$_3$), 1.55 (s, 18H, C_5H_2tBu$_3$), 4.98 (s, 2H, C_5H_2tBu$_3$)
^{31}P-NMR (CD_2Cl_2)	δ [ppm] = 48.6 (s), -15.0 (s)
^{31}P{^{1}H}-NMR (CD_2Cl_2)	δ [ppm] = 48.6 (s), -15.0 (s)
^{19}F{^{1}H}-NMR (CD_2Cl_2)	δ [ppm] = -75.6 (s)
^{19}F-NMR (CD_2Cl_2)	δ [ppm] = -75.6 (s)
Cation ESI-MS (CH_2Cl_2)	*m/z* [%] = 1181.3 (100) [**1a**$_2$Au]$^+$
Anion ESI-MS (CH_2Cl_2)	*m/z* [%] = 966.7 (100) [pftb]$^-$
Elemental analysis	calculated for $C_{70}H_{94}Co_2P_4AuAlO_4F_{36} \cdot 0.5(CH_2Cl_2)$ (2190.34 g·mol^{-1}): C 38.62, H 4.37; found: C 38.53, H 4.37

Synthesis of 6

A solution of $7.75 \cdot 10^{-5}$ mol **1a** in 5 ml Et_2O is added to a solution of $1.16 \cdot 10^{-4}$ mol (175 mg) [(tht)Au(PPh_3)][pftb] in 5 ml CH_2Cl_2 and the reaction mixture is stirred overnight. The solvent is removed under reduced pressure and the residue is taken up in 3 ml fresh dichloromethane. The solution is filtered, layered under 7 ml of hexane and stored at -30 °C. After some time, dark red crystals of **6** can be found at the solvent boundary.

$^{31}P\{^1H\}$-NMR (CD_2Cl_2)	δ [ppm] =-15.9 (s, 1P, PPh_3), 45.6 (s, 2P, (tBuC)$_2P_2$), 53.3 (s), 50.3 (s), 48.3 (s), 32.4 (s), 23.7 (s), -15.2 (s)
^{19}F-NMR (CD_2Cl_2)	δ [ppm] = -75.6 (s)
$^{19}F\{^1H\}$-NMR (CD_2Cl_2)	δ [ppm] = -75.6 (s)

9.5 Crystallographic Details

All compounds have been solved using Olex2.[10] The models were solved using ShelXT[11] and refined with version 2015-6 of ShelXL[12] using Least Squares minimisation. As crystal structure refinement on compounds **2b**, **4** and **5** is still on-going, only preliminary models of those compounds are given.

9.5.1.1 Compound 2b

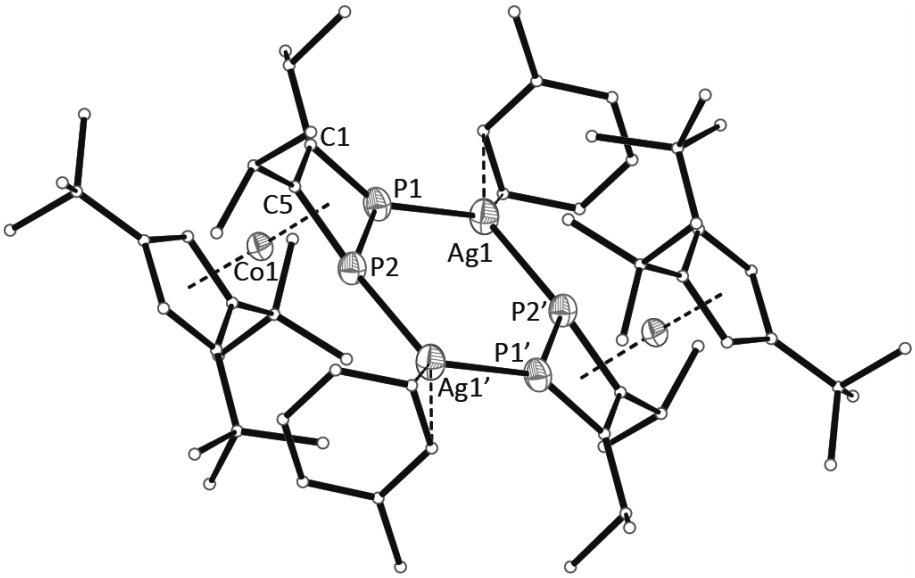

Figure 9-8 Molecular structure of the cation of **2b** in the solid state. Hydrogen atoms are omitted, carbon atoms are shown in ball-and-stick representation for clarity. Thermal ellipsoids are shown at 50% probability level. Selected bond lengths [Å] and angles [°]: P2-P1 2.160(2), P1-C1 1.800(6), P2-C5 1.803(6), C1-C5 1.412(8), P1-Ag1-P21 101.86(5), P1-P2-Ag1' 129.54(8) C5-P2-Ag1' 148.9(2), C5-P2-P1 77.8(2), C1-P1-P2 78.20(19), C5-C1-P1 101.8(4), C1-C5-P2 102.1(4).

Single clear light orange block-shaped crystals of **2b** were obtained by recrystallisation from diffusion of toluene into a solution of **2b** in CH_2Cl_2. A suitable crystal (0.42×0.22×0.08) was selected and mounted on a mylar loop on a Xcalibur, AtlasS2, Gemini ultra diffractometer. The crystal was kept at T = 122.7(10) K during data collection.

Crystal Data for **2b**: $C_{49}H_{53}AgAlCl_2CoF_{36}O_4P_2$, M_r = 1716.53, monoclinic, $P2_1/c$ (No. 14), a = 14.43705(15) Å, b = 30.4164(3) Å, c = 14.82498(14) Å, β = 102.9580(10)°, V = 6344.21(12) Å^3, T = 122.7(10) K, Z = 4, Z' = 1, μ(CuK_α) = 7.291 mm^{-1}, 70162 reflections measured, 11206 unique (R_{int} = 0.0422) which were used in all calculations. The final wR_2 was 0.2284 (all data) and R_1 was 0.0757 (I > 2σ(I)).

9.5.1.2 Compound 1b-Ox

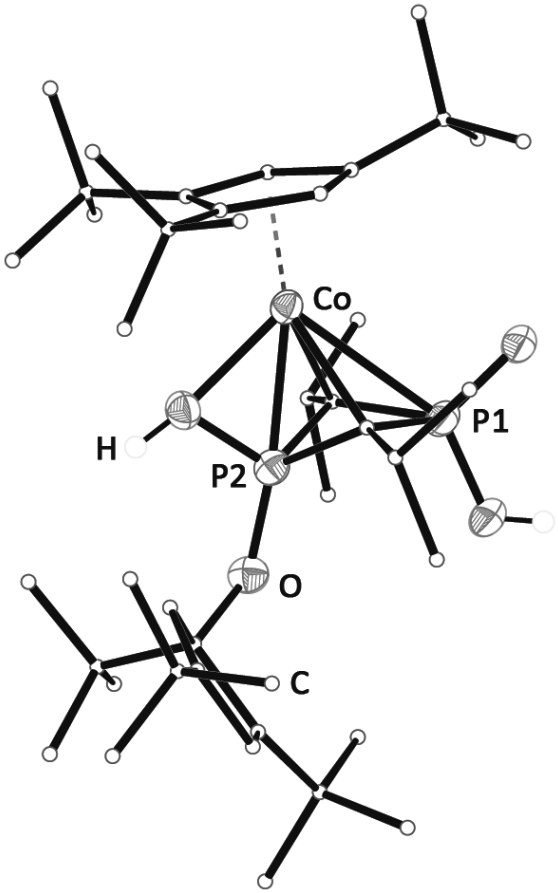

Figure 9-9 Molecular structure of **1b-Ox**. Hydrogen atoms on the ligands are omitted and carbon framework is shown as ball-and-stick model for clarity. Thermal ellipsoids are shown at 50% probability level. Selected bond lengths [Å] and angles [°]: Co1-P1 2.7848(7), Co1-O4 2.0474(15), Co1-P2 2.2800(6), Co1-C1 2.147(2), Co1-C5 2.170(2), P1-C1 1.792(2), P1-C5 1.781(2), P2-C1 1.781(2), P2-C5 1.765(2), C5-P1-C1 83.22(10), C5-P2-C1 83.99(10), P2-C1-P1 89.59(10), P2-C5-P1 90.42(10).

Single clear dark green block-shaped crystals of **1b-Ox** were obtained by recrystallisation from hexane. A suitable crystal (0.11×0.08×0.04) was selected and mounted on a mylar loop on a SuperNova, Single source at offset, Atlas diffractometer. The crystal was kept at T = 123.01(10) K during data collection.

Crystal Data for **1b-Ox**: $C_{42}H_{74}Co_1O_4P_2$, M_r = 762.98, monoclinic, $P2_1/n$ (No. 14), a = 11.6116(3) Å, b = 26.9359(7) Å, c = 13.6372(3) Å, β = 91.248(2)°, V = 4264.29(19) Å^3, T = 123.01(10) K, Z = 8, Z' = 2, μ(CuK_α) = 4.146 mm^{-1}, 26675 reflections measured, 8293 unique (R_{int} = 0.0420) which were used in all calculations. The final wR_2 was 0.1058 (all data) and R_1 was 0.0409 (I > 2σ(I)).

9.5.1.3 Compound 3

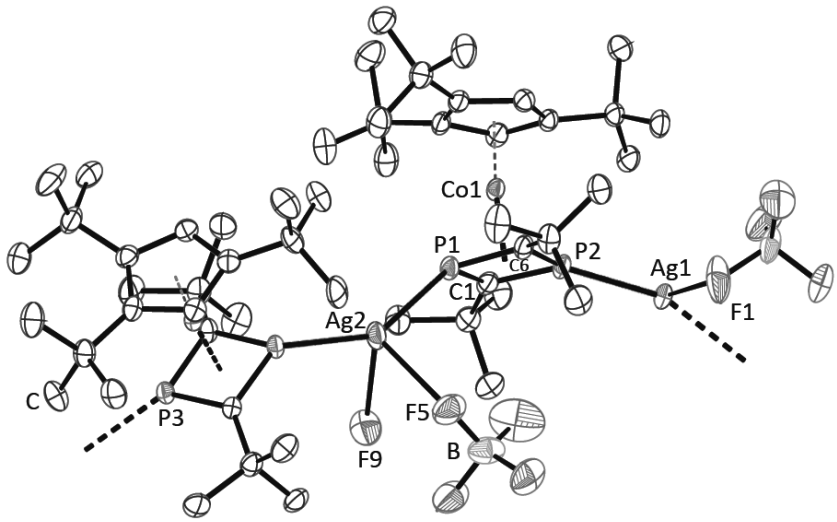

Figure 9-10 Molecular structure of **3** in the solid state. Hydrogen atoms are omitted for clarity. Thermal ellipsoids are shown at 50% probability level. Selected bond lengths [Å] and angles [°]: Ag1-P2 2.3829(10), Ag1-P3 2.4007(10), Ag2-F9 2.458(4), Ag2-F5 2.557(3), Co1-P1 2.2419(12), Co1-P2 2.2261(12), Co1-C6 2.141(4), Co1-C1 2.117(4), P1-C1 1.782(4), P1-C6 1.784(4), P2-C6-P1 95.1(2), P2-C1-P1 95.1(2), C1-P1-C6 84.6(2), C6-P2-Ag1 135.51(14), C1-P2-Ag1 135.06(15), F9-Ag2-F5 78.58(11).

Single clear light red block-shaped crystals of **3** were obtained by recrystallisation from diffusion of hexane into a solution of **3** in CH_2Cl_2. A suitable crystal (0.17×0.14×0.11) was selected and mounted on a mylar loop on a Xcalibur, AtlasS2, Gemini ultra diffractometer. The crystal was kept at T = 125(3) K during data collection.

Crystal Data for **3**: $C_{57}H_{100}Ag_2B_2Cl_{5.5}Co_2F_9P_4$, M_r = 1630.44, monoclinic, *C2/c* (No. 15), a = 33.8906(9) Å, b = 24.51316(19) Å, c = 25.4884(7) Å, β = 137.688(5)°, V = 14254.3(11) Å^3, T = 125(3) K, Z = 8, Z' = 1, μ(CuK$_\alpha$) = 11.157 mm^{-1}, 36844 reflections measured, 12419 unique (R_{int} = 0.0309) which were used in all calculations. The final wR_2 was 0.1393 (all data) and R_1 was 0.0446 (I > 2σ(I)).

9.5.1.4 Compound 4

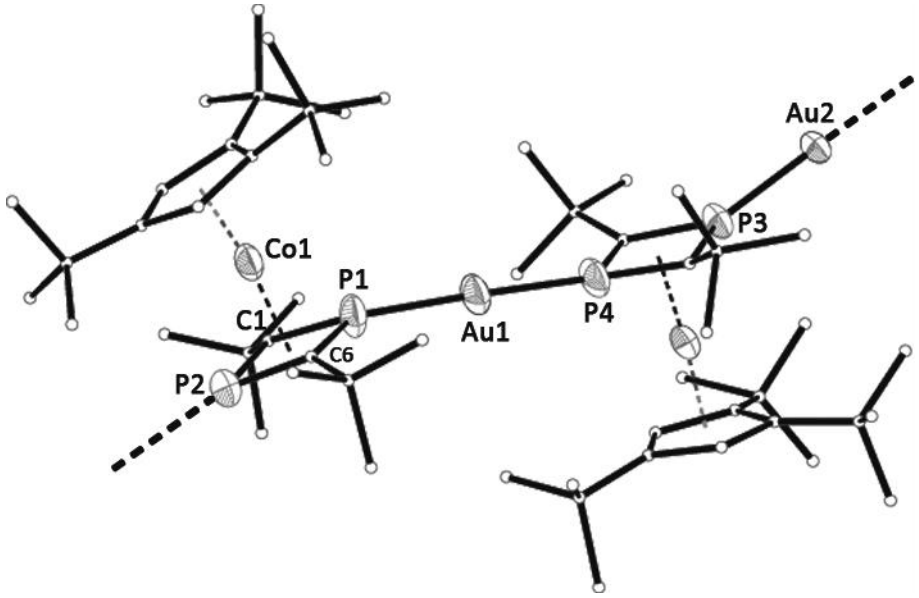

Figure 9-11 Molecular structure of the cationic repetition unit of **4** in the solid state. Hydrogen atoms are omitted, carbon atoms are shown in ball-and-stick representation for clarity. Thermal ellipsoids are shown at 50% probability level. Selected bond lengths [Å] and angles [°]: Au1-P1 2.286(3), Au2-P3 2.275(3), Au2-P2 2.275(3), P1-C1 1.757(12), P1-C6 1.781(15), P2-C1 1.743(14), P2-C6 1.775(15), P3-Au2-P2 174.94(13), C1-P2-C6 86.8(6), P2-C1-P1 94.4(7), P2-C6-P1 92.5(8), C1-P2-C6 86.8(6).

Single clear dark red block-shaped crystals of **4** were obtained by recrystallisation from a solution of **4** in CH_2Cl_2 by solvent layering with hexane. A suitable crystal (0.46×0.26×0.16) was selected and mounted on a mitogen holder on a Xcalibur, AtlasS2, Gemini ultra diffractometer. The crystal was kept at T = 122.8(6) K during data collection.

Crystal Data for **4**: $C_{76.1}H_{92.7}Al_{1.5}Au_{1.5}Cl_{1.7}Co_2F_{46.5}O_{5.5}P_4$, M_r = 2615.41, orthorhombic, *Fdd*2 (No. 43), a = 62.3021(7) Å, b = 33.9351(4) Å, c = 20.8643(2) Å, V = 44111.9(8) Å^3, T = 122.8(6) K, Z = 16, Z' = 1, μ(CuK$_\alpha$) = 8.130 mm^{-1}, 62401 reflections measured, 17023 unique (R_{int} = 0.0246) which were used in all calculations. The final wR_2 was 0.1759 (all data) and R_1 was 0.0628 (I > 2σ(I)).

9.5.1.5 Compound 5

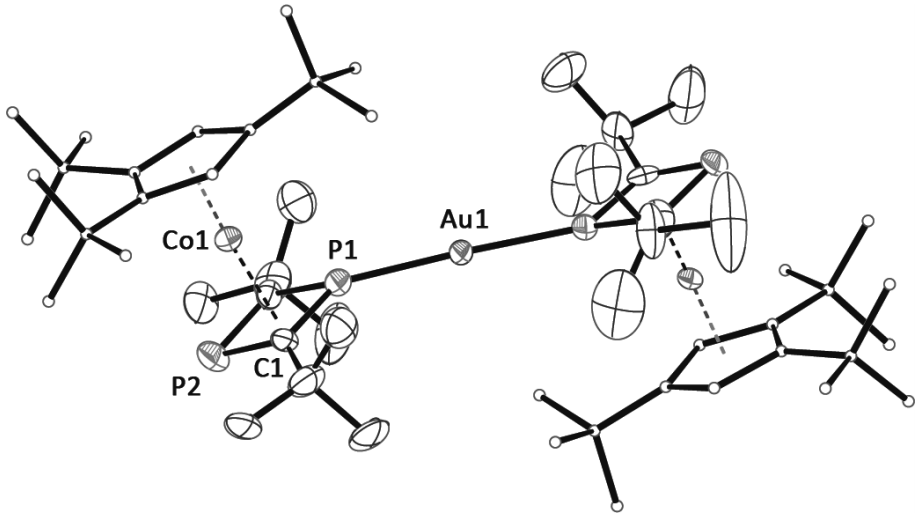

Figure 9-12 Molecular structure of the cation of **5** in the solid state. Hydrogen atoms are omitted, carbon atoms are shown in ball-and-stick representation for clarity. Thermal ellipsoids are shown at 50% probability level. Selected bond lengths [Å] and angles [°]: Au1-P1 2.286(4), Au1-P3 2.281(4), P1-C1 1.750(13), P2-C1 1.797(14), P3-C6 1.775(13), P4-C6 1.768(15), C1-P1-C1' 85.6(9), C1-P2 C1' 82.9(9), P1-C1-P2 95.7(7), P3-Au1-P1 177.54(15).

Single red block shaped crystals of **5** were obtained by recrystallisation from diffusion of hexane into a solution of **5** in CH_2Cl_2. A suitable crystal (0.28×0.16×0.13) was selected and mounted on a mitogen holder on a Xcalibur, AtlasS2, Gemini ultra diffractometer. The crystal was kept at T = 122.95(10) K during data collection.

Crystal Data for **5**. $C_{36.25}H_{47}Al_{0.5}Au_{0.5}CoF_{20}O_{2.5}P_2$, M_r = 1135.58, monoclinic, *C*2/*m* (No. 12), a = 26.3634(9) Å, b = 16.5505(8) Å, c = 19.7299(10) Å, β = 99.758(4)°, V = 8484.2(6) Å^3, T = 122.95(10) K, Z = 8, Z' = 1, μ(CuK$_\alpha$) = 8.272 mm^{-1}, 27264 reflections measured, 7720 unique (R_{int} = 0.0461) which were used in all calculations. The final wR_2 was 0.2558 (all data) and R_1 was 0.1023 (I > 2σ(I)).

9.5.1.6 Compound 6

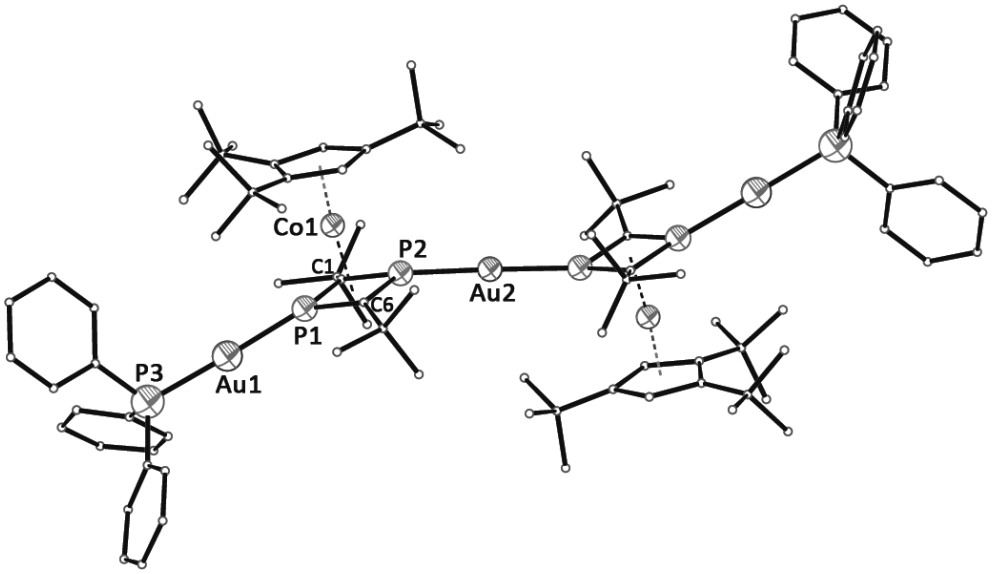

Figure 9-13 Molecular structure of the cation of **6** in the solid state. Hydrogen atoms are omitted, carbon atoms are shown in ball-and-stick representation for clarity. Thermal ellipsoids are shown at 50% probability level. Selected bond lengths [Å] and angles [°]: P1-C1 1.761(10), P1-C6 1.794(9), P1-Au1 2.268(3), P2-C1 1.758(9), P2-C6 1.774(9), Au2-P2 2.278(2), Au1-P3 2.346(3), P2-Au2-P2' 175.79(12), C1-P1-C6 86.7(4), C1-P2-C6 87.4(4), P2-C6-P1 92.1(4).

Single red block-shaped crystals of **6** were obtained by recrystallisation from diffusion of hexane into a layer of **6** in Ch_2Cl_2. A suitable crystal (0.22×0.14×0.09) was selected and mounted on a mitogen holder on a Xcalibur, AtlasS2, Gemini ultra diffractometer. The crystal was kept at T = 122.8(6) K during data collection.

Crystal data for **6**. $C_{69}H_{62}Al_{1.5}Au_{1.5}CoF_{54}O_6P_3$, M_r = 2500.94, monoclinic, $C2/c$ (No. 15), a = 26.1658(3) Å, b = 16.1441(3) Å, c = 44.8707(6) Å, β = 94.0895(12)°, V = 18906.2(5) Å^3, T = 122.8(6) K, Z = 8, Z' = 1, μ(CuK$_\alpha$) = 7.688 mm^{-1}, 41918 reflections measured, 16361 unique (R_{int} = 0.0288) which were used in all calculations. The final wR_2 was 0.2380 (all data) and R_1 was 0.0830 (I > 2σ(I)).

9.6 References

[1] P. B. Hitchcock, M. J. Maah, J. F. Nixon, *Chem. Commun.* **1986**, 737.

[2] a) P. Binger, R. Milczarek, R. Mynott, M. Regitz, W. Rösch, *Angew. Chem. Int. Ed.* **1986**, *25*, 644; b) P. Binger, R. Milczarek, R. Mynott, M. Regitz, W. Rösch, *Angew. Chem.* **1986**, *98*, 645.

[3] E.-M. Rummel, M. Eckhardt, M. Bodensteiner, E. V. Peresypkina, W. Kremer, C. Gröger, M. Scheer, *Eur. J. Inorg. Chem.* **2014**, 1625.

[4] a) A. D. Burrows, A. Dransfeld, M. Green, J. C. Jeffery, C. Jones, J. M. Lynam, M. T. Nguyen, *Angew. Chem.* **2001**, *113*, 3321; b) A. D. Burrows, A. Dransfeld, M. Green, J. C. Jeffery, C. Jones, J. M. Lynam, M. T. Nguyen, *Angew. Chem. Int. Ed.* **2001**, *40*, 3221; c) C. Jones, C. Schulten, A. Stasch, *Dalton Trans.* **2006**, 3733; d) P. Binger, G. Glaser, S. Albus, C. Krüger, *Chem. Ber.* **1995**, 1261.

[5] a) M. T. Nguyen, L. Landuyt, L. G. Vanquickenborne, *J. Org. Chem.* **1993**, *58*, 2817; b) S. Creve, M. T. Nguyen, L. G. Vanquickenborne, *Eur. J. Inorg. Chem.* **1999**, *1999*, 1281; c) T. Höltzl, D. Szieberth, M. T. Nguyen, T. Veszprémi, *Chem. Eur. J.* **2006**, *12*, 8044.

[6] a) J. Malberg, T. Wiegand, H. Eckert, M. Bodensteiner, R. Wolf, *Chem. Eur. J.* **2013**, *19*, 2356; b) J. Malberg, T. Wiegand, H. Eckert, M. Bodensteiner, R. Wolf, *Eur. J. Inorg. Chem.* **2014**, *2014*, 1638; c) J. Malberg, M. Bodensteiner, D. Paul, T. Wiegand, H. Eckert, R. Wolf, *Angew. Chem.* **2014**, *126*, 2812; d) J. Malberg, M. Bodensteiner, D. Paul, T. Wiegand, H. Eckert, R. Wolf, *Angew. Chem. Int. Ed.* **2014**, *53*, 2771.

[7] this dissertation, vide supra

[8] I. Krossing, *Chem. Eur. J.* **2001**, *7*, 490.

[9] M. Gonsior, I. Krossing, N. Mitzel, *Z. Anorg. Allg. Chem.* **2002**, *628*, 1821.

[10] O. V. Dolomanov, L. J. Bourhis, R. J. Gildea, J. A. K. Howard, H. Puschmann, *J. Appl. Crystallogr.* **2009**, *42*, 339.

[11] G. M. Sheldrick, *Acta Cryst.* **2015**, *A71*, 3.

[12] G. M. Sheldrick, *Acta Cryst.* **2015**, *C71*, 3.

10 Summary

Phosphaalkynes are a vast research subject. Since their discovery and their first laboratory scale synthesis, many efforts were made in determining the properties and reactivity of this class of substances. This is apparent from the state of the literature, which was presented in the introductory chapter. Although coordination and cyclodimerisation of phosphaalkynes has been known for some time, some questions concerning the processes taking place and products being formed are still pending. From this, one minor and two major aspects for our own research could be deducted (chapter 2). In the following, the major aspects of coordination forms of phosphaalkynes and cyclodimerisation will be summarised as well as the minor aspect of reactivity of phosphaalkynes leading to non-stoichiometric phospholide compounds. The results will be given in the same order as discussed in the main body of this thesis.

10.1 Coordination of Phosphaalkynes

The first part of this thesis deals with the coordination chemistry of phosphaalkynes. As has been discussed in the introductory chapter, five coordination forms are known for phosphaalkynes in the literature (Figure 10-1).

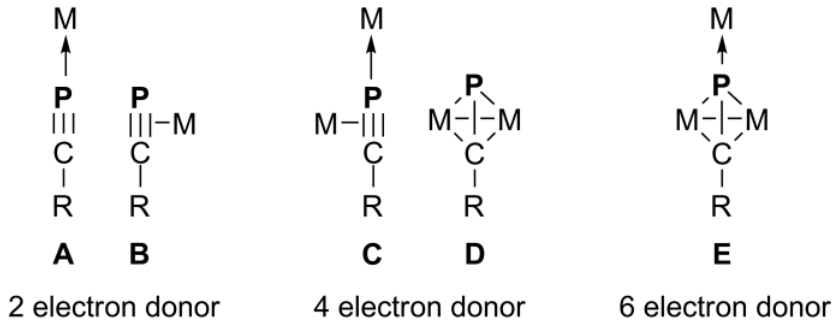

Figure 10-1 Coordination forms of phosphaalkynes

As the HOMO of phosphaalkyne molecules represents the triple bond between phosphorus and carbon, side-on coordination (type **B**) is far more common than end-on coordination (type **A**). However, both types could be obtained during the course of this thesis. An interesting question was solved in whether homoleptic complexes of phosphaalkynes are possible. Until now, no such complex has been reported in the literature, while homoleptic alkyne complexes have already been known for years. To stabilise the highly reactive phosphaalkyne in such an environment, the group 11 weakly coordinating anion compounds $Ag[Al\{OC(CF_3)_3\}_4]$ (Ag[pftb]) and $Ag[FAl\{OC_{12}F_{15}\}_3]$ (Ag[fal]) have been chosen as likely

candidates. And indeed, in the reaction with *tert*-butyl phosphaalkyne at low temperatures, the first homoleptic complexes of phosphaalkynes, $[Ag(P{\equiv}C\mathit{t}Bu)_2]^+[pftb]^-$ (**1**) and $[Ag(P{\equiv}C\mathit{t}Bu)_2]^+[fal]^-$ (**2**), could be isolated (cf. Scheme 10-1).

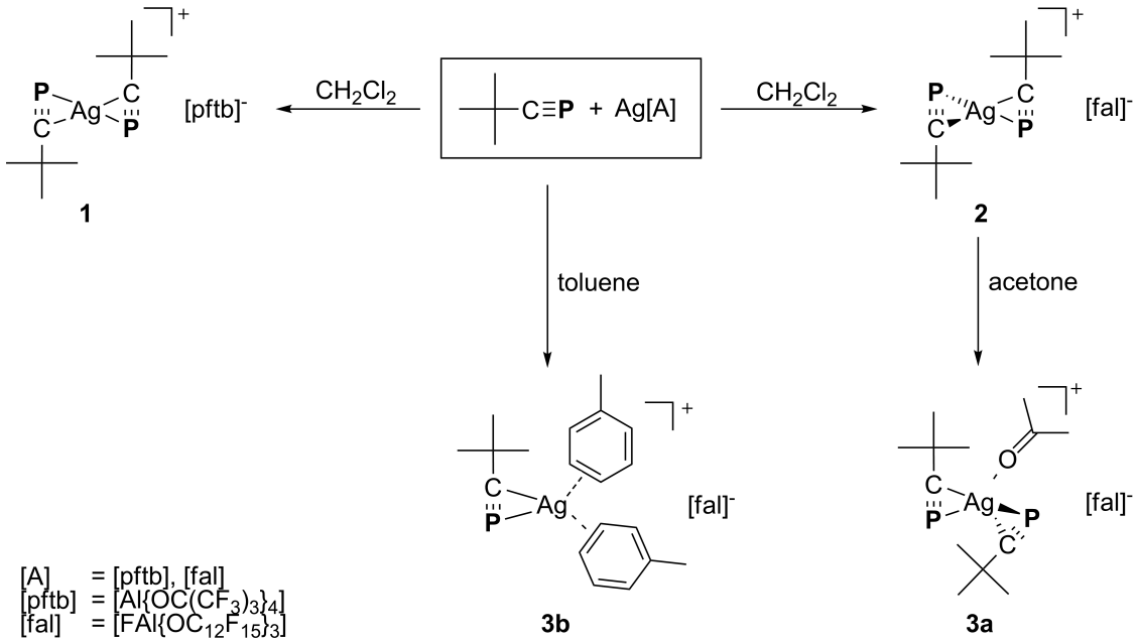

Scheme 10-1 Reaction pathway towards homoleptic phosphaalkyne complexes **1** and **2**, with additional change of geometry as σ- or π-donor ligands are added to form **3a** and **3b**.

The different geometries on compounds **1**, where the phosphaalkynes are planar to each other and **2**, where the silver atom is tetrahedrally coordinated by the phosphaalkynes, most likely arise from the different size of the anions. While the [pftb] anion in **1** is spherical and leaves only enough space for the *t*BuC≡P ligands to coordinate the silver cation squarely planar, the [fal] anion in **2** is more squarely shaped and leaves enough open space for a tetrahedral coordination of the phosphaalkynes between the anions in the solid state. The calculated minimum structure is the perpendicular arrangement in **2**. In solution, a certain dynamic is observed in the ^{31}P NMR spectra which point to a rotation of the ligands around the $(PC)_{cent}Ag(PC)_{cent}$ axis as well as a concentration dependent intermolecular exchange mechanism. Calculations show that the trigonally planar complex $[Ag(\mathit{t}BuC{\equiv}P)_3]^+$ should be stable, but it could not be observed in NMR studies or in the solid state. However, addition of the σ-donor ligand acetone to **2** leads to the addition of one solvent molecule to the cation to form the trigonally planar complex $[((CH_3)_2CO)Ag(P{\equiv}C\mathit{t}Bu)_2]^+[fal]^-$ (**3a**). Furthermore, conducting the reaction in toluene leads to the trigonally planar complex $[(C_7H_8)_2Ag(P{\equiv}C\mathit{t}Bu)]^+[fal]^-$ (**3b**), which shows that trigonally planar coordination on the silver cation with similarly sized ligands is indeed possible.

The use of the WCAs [pftb] and [fal] is crucial as only decomposition took place when using smaller anions. These big anions are able to separate the cations effectively and thus stabilise the coordination of the P≡C triple bond towards the silver atoms. This can be clearly seen on the P-C bond lengths of all four compounds, which retain their triple bond character.

The use of the [pftb] anion also improves the crystallisation process of other compounds as the next chapter showed: Here, the end-on coordination products of *tert*-butyl phosphaalkyne and acetonitrile to an unsaturated ruthenium complex $[Cp^*Ru(dppe)]^+[A]^-$ (A = pftb: **4a**; A = PF_6: **4b**) could only be structurally characterised for the complexes which were charge balanced by the bigger [pftb] anion (Scheme 10-2).

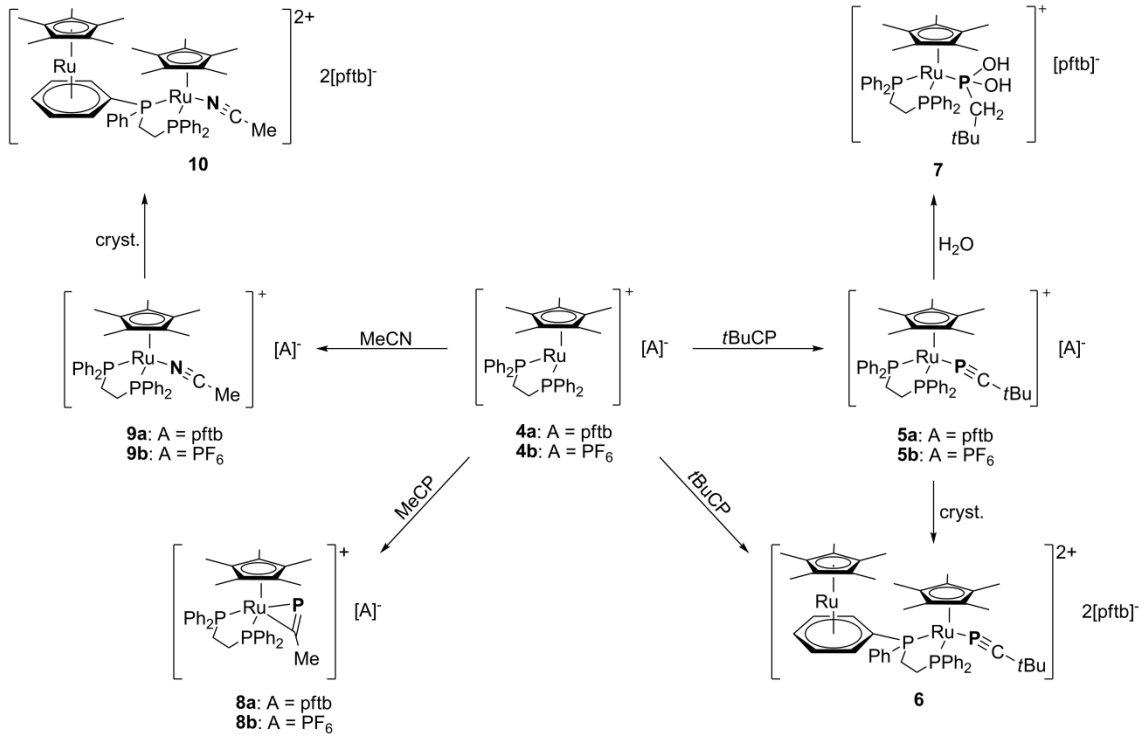

Scheme 10-2 Reaction pathways for the addition of phosphaalkynes and nitriles to the unsaturated ruthenium complexes **4a** and **4b**.

As stated earlier, as the HOMO of the phosphaalkyne molecules is the triple bond, side-on coordination is always favoured. However, choosing the right geometry on a Lewis acid (like in **4a** and **4b**) can promote end-on coordination. Trying to achieve this coordination form for methyl phosphaalkyne, we first conducted experiments with the kinetically stabilised *t*BuC≡P. Here, as $^{31}P\{^1H\}$ VT NMR investigations suggest, at low temperatures exclusively the compounds $[Cp^*Ru(dppe)(\eta^1\text{-}t\text{BuC}{\equiv}P)]^+[A]^-$ (A = pftb: **5a**; A = PF_6: **5b**) are formed, while crystallisation processes as well as the reaction at ambient temperatures led to the formation of $[\{Cp^*Ru(dppe)\}\{Cp^*Ru\}(\eta^1\text{-}t\text{BuC}{\equiv}P)]^{2+}\cdot 2[pftb]^-$ (**6**). Furthermore, hydrolysis of **5a** could be observed to form the novel phosphine product $[Cp^*Ru(dppe)(\eta^1\text{-}P(OH)_2CH_2t\text{Bu})][pftb]$ (**7**). The hydrolysis of the phosphaalkyne in a complex of this kind has not been detected so far to our

knowledge. As expected, CH_3CN coordinates in an end-on mode to form $[Cp^*Ru(dppe)(\eta^1\text{-}MeC{\equiv}N)]^+[A]^-$ (A = pftb: **9a**; A = PF_6: **9b**). Again only the complex with an additional [Cp*Ru] fragment $[\{Cp^*Ru(dppe)\}\{Cp^*Ru\}(\eta^1\text{-}MeC{\equiv}N)]^+[pftb]^-$ (**10**) could be structurally characterised. The comparison of the ^{31}P NMR shifts of both end-on phosphaalkyne complexes with products of the reaction between **4a**/**4b** and MeC≡P however lead to the conclusion that in this case rather a side-on complex is formed. Here, the resonance of the phosphorus atom is shifted to very low field. The compounds $[Cp^*Ru(dppe)(\eta^2\text{-}MeC{=}P)]^+[A]^-$ (A = pftb: **8a**; A = PF_6: **8b**) could unfortunately not be structurally characterised. Efforts to obtain crystals of those compounds are on-going.

10.2 Polyphospholide rings derived from Phosphaalkynes and Zintl ions

The reduction of phosphaalkynes leads to the formation of five-membered phosphorus containing rings. These heterocycles could also be obtained from the reaction of *tert*-butyl phosphaalkyne and the zintl ions K_4Ge_9 and Li_3P_7. In both cases, mixtures of products have been obtained which contained different five membered rings (Ge_9^{4-}: **B**; P_7^{3-}: **A-C**) in addition to uncharacterised products.

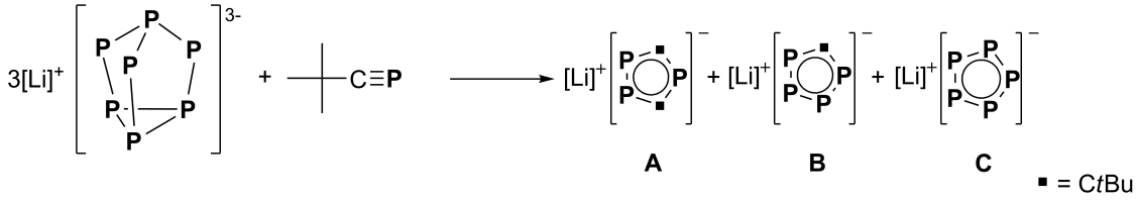

Scheme 10-3 Reaction of Li_3P_7 and *t*BuC≡P to form five membered heterocycles **A**, **B**, and **C**.

As the reactions with K_4Ge_9 are limited by the choice of the solvent, the reactions with Li_3P_7 have been intensively studied by ^{31}P NMR spectroscopy.

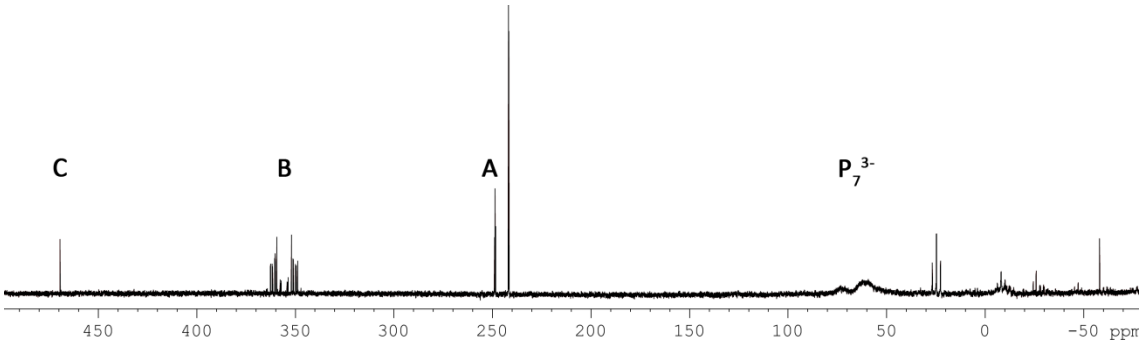

Figure 10-2 Assignment of the different $[P_n(CtBu)_{5-n}]^-$ (n=3-5) rings in the ^{31}P NMR spectrum.

Further research will be conducted to see whether a separation is possible after complexation of the phospholyl rings **A-C**. A special focus will be directed to the isolation of complexes of the tetraphospholide ring **B**, which could be characterised by simulation of the $^{31}P\{^1H\}$ NMR signal at δ =348-368 ppm.

10.3 1,3-Diphosphete complexes: Coordination modes and Isomerisation processes

Until now, in reactions of phosphaalkynes with complexes with metal-metal multiple bonds always a side-on reactivity could be observed. Starting from complex LCr^{5}CrL (L=Ar=$N_2C_{25}H_{29}$, **11**) with a Cr^{5}Cr quintuple bond, we were able to isolate the first complex in which two equivalents of *tert*-butyl phosphaalkyne underwent a [2+2] head-to-tail cycloaddition to yield a 1,3-diphosphacyclobutadiene (1,3-diphosphete) complex on top of a Cr-Cr multiple bond moiety: [$L_2Cr_2(\mu,\eta^{1:1:2:2}$-$P_2C_2tBu_2)$] (**12**) (Scheme 10-4). Repeating the reaction with a phosphaalkyne with a sterically more demanding substituent (here: adamantyl) however still leads to the side-on coordination complex [$L_2Cr_2(\mu,\eta^{2:2}$-P=CAd)] (**14**).

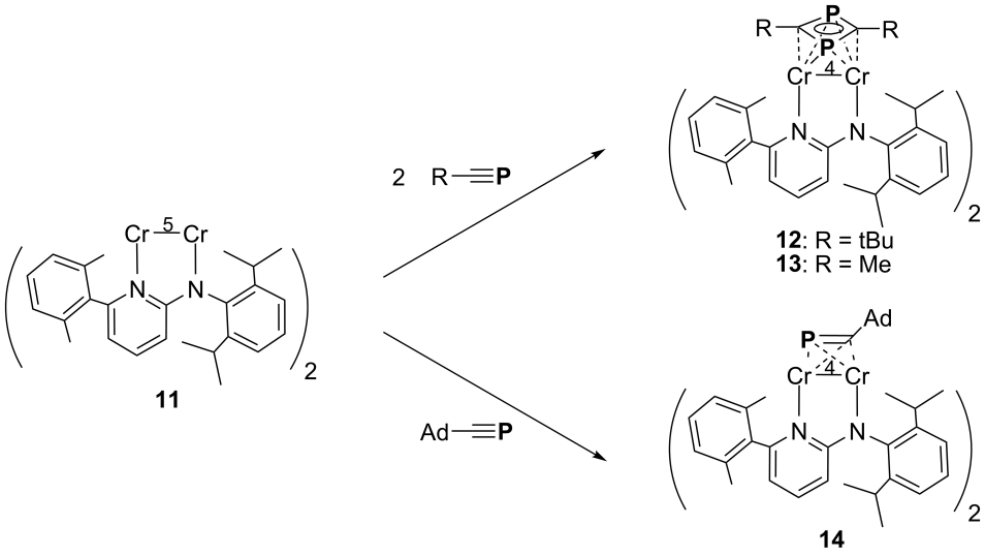

Scheme 10-4 Reaction of **11** and different phosphaalkynes yielding the respective 1,3-diphosphete complexes **12** and **13** or the side-on complex **14**.

In both the 1,3-diphosphete complex **12** and the side-on coordination complex **14** the bond length between the chromium atoms is elongated to a quadruple bond. For reasons of size comparison, it has also been attempted to isolate the product of the reaction between L_2Cr_2 and MeC≡P. NMR spectroscopic and mass spectrometric evidence point towards a [2+2] cycloaddition product like in **12**, but the presumed compound [$L_2Cr_2(\mu,\eta^{1:1:2:2}$-$P_2C_2Me_2)$] (**13**) could not be isolated due to the fast decomposition of the complex.

Another unusual coordination mode for 1,3-diphosphete ligands could be observed in the reaction of the triple decker complex [$(Cp'''Co)_2(\mu,\eta^4$:η^4-$C_7H_8)$] with methyl phosphaalkyne: Here, the triple decker complex [$\{Cp'''Co\}_2(\mu,\eta^4$:η^4-$P_2C_2Me_2)$] (**15**) could be obtained (first synthesised by Maria Eckhardt) in addition to the 1,3-diphosphete sandwich compound [$Cp'''Co(\eta^4$-$P_2C_2Me_2)$] (**16**), which is only the second known 1,3-diphosphete sandwich complex for methyl phosphaalkyne (Scheme 10-5).

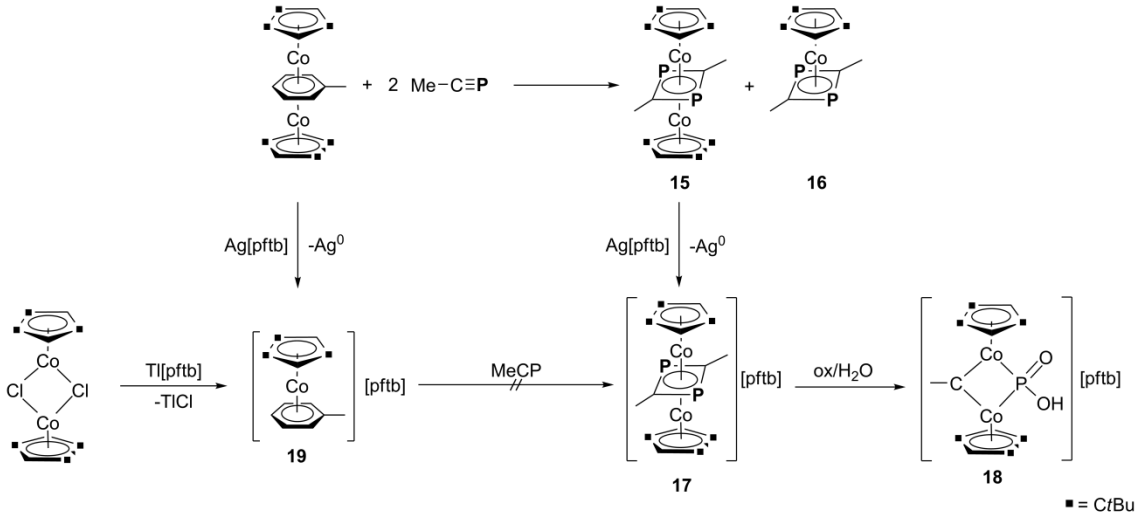

Scheme 10-5 Reaction pathways for the formation of 1,3-diphosphete complexes of methyl phosphaalkyne and their subsequent oxidation and decomposition upon hydrolysis. An alternative synthesis to **17** via **19** has been proposed but did not lead to the wanted product.

An oxidation by the WCA salt Ag[pftb] was possible for **15**, which led to the formation of the paramagnetic 1 e^- oxidation product [{Cp'''Co}$_2$(μ,η^4:η^4-$P_2C_2Me_2$)][pftb] (**17**). The EPR spectrum at 77 K of **17** showed the coupling of both cobalt centres. Further oxidation/hydrolysis of **17** with subsequent loss of one formula unit of MeC≡P led to the fragmentation product [{Cp'''Co}$_2$(μ-CCH_3)(μ-POOH)][pftb] (**18**). All attempts to form **17** in the reaction of the 19 VE complex [Cp'''Co_2(η^6-C_7H_8)][pftb] (**19**) with methyl phosphaalkyne, however, failed.

Also the previously synthesised and published compounds [Cp'''Co(η^4-1,3-P_2C_2tBu$_2$)] (**20a**, diploma thesis of Maria Eckhardt) and [Cp'''Co(η^4-1,3-P_2C_2iPr$_2$)] (**20b**, own master thesis) have been used in the reactions with Ag[pftb] (Scheme 10-6). A variety of adducts, 1D polymers, isomerisation and ring expansion/contraction products could be obtained for this system.

At lower temperatures and in a solvent mixture of CH_2Cl_2/Et_2O, the adduct species [(Et_2O)$_2$Ag{Cp'''Co(μ,η^4:η^1:η^1-P_2C_2tBu$_2$)}]·[pftb] (**22a**) and toluene-saturated [(Et_2O)$_4$$Ag_2$Cp'''Co(μ,η^4:η^1:η^1-$P_2C_2tBu_2$)}]·2[pftb] (**22b**) could be isolated when impeding the same reaction at the appropriate temperature (-60 °C: **22a**, -30 °C: **22b**). Leaving the solution to reach room temperature leads to the formation of the 1D polymer [Ag{Cp'''Co(η^4:η^1:η^1-P_2C_2tBu$_2$)}]$_n$[pftb]$_n$ (**21**).

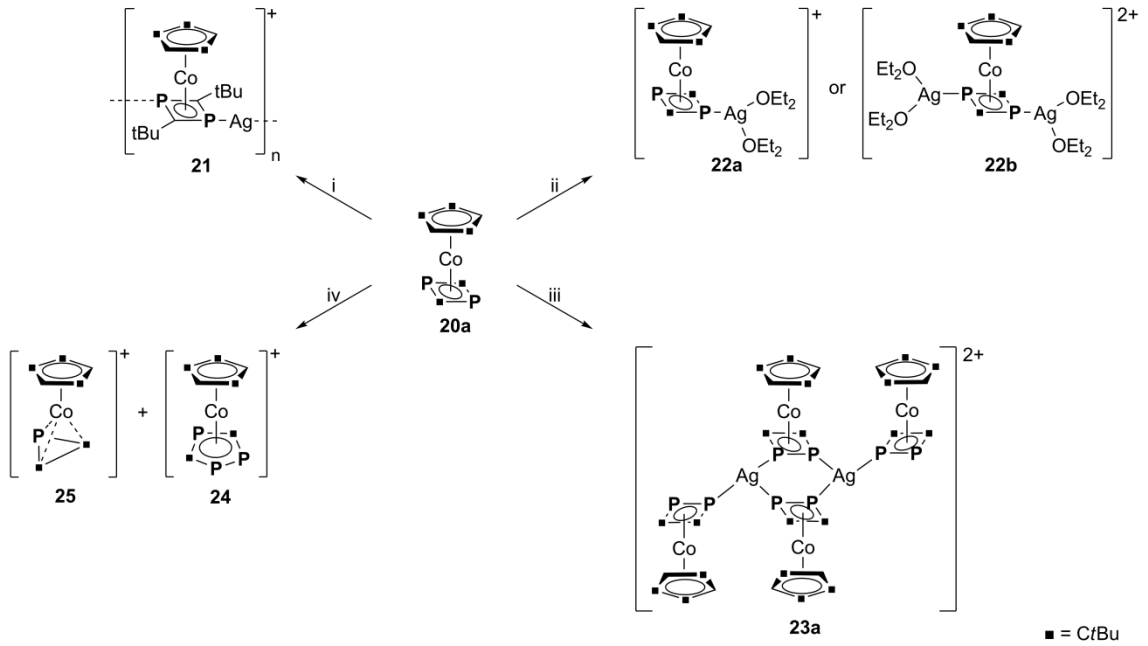

Scheme 10-6 Reaction and transformation pathways for **20a**: i) Ag[pftb] in CH_2Cl_2/Et_2O mixture, -80 °C → r.t.; ii) 2 Ag[pftb] in Et_2O, -80 °C → -60 °C (**22a**) or -80 °C → 0 °C (**22b**); iii) 2 Ag[pftb] in CH_2Cl_2, -80 °C → r.t., iv) 2 Ag[pftb] in CH_2Cl_2 layered with **20a** in hexane at -30°.

After longer storage time of **22b** in CH_2Cl_2 at -30 °C or when conducting the reaction in CH_2Cl_2 as the sole solvent, an isomerisation between the 1,3-diphosphete complex **20a** and the 1,2-diphosphete complex [Cp'''Co(η^4-1,2-P_2C_2tBu$_2$)] (**I-20a**) can be observed and a coordination compound with silver(I): [Ag_2{Cp'''Co(μ,η^4:η^1:η^1-1,2-P_2C_2tBu$_2$)}$_2${Cp'''Co(μ,η^4:η^1-1,2-P_2C_2tBu$_2$)}$_2$]·2[pftb] (**23a**) could be isolated. A similar product could be obtained in the reaction of **20b** with Ag[pftb], in which the silver atoms are saturated by toluene molecules: [Ag_2{Cp'''Co(μ,η^4:η^1:η^1-1,2-P_2C_2iPr$_2$)}$_2$(η^2-tol)$_2$]·2[pftb] (**23b**) (eq. (10-1)).

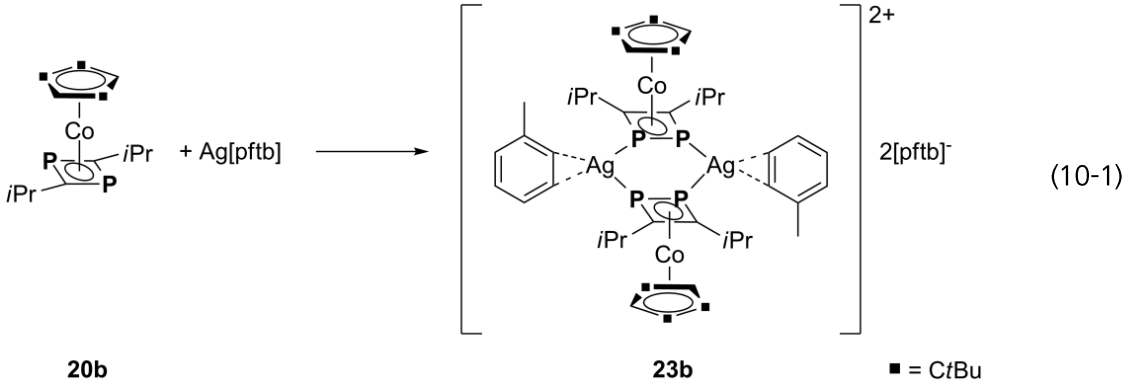

(10-1)

The 1,2-diphosphete complex **I-20a** could be extracted at the addition of strong σ-donors like pyridine to **23a**. This leads the silver atoms to be complexated and the neutral **I-20a** can be isolated by washing with hexane. Compound **I-20a** can also be formed when refluxing solutions of **20a** at 110 °C for three to five days. In this way, **I-20a** could be obtained in

yields of up to 70% as seen in the ^{31}P NMR spectra. A separation of both compounds has not been possible due to the similar solubility and properties of the neutral diphosphete complexes.

Changing the reaction conditions further by conducting layering experiments at low temperatures (-30 °C), **20a** disappears completely and gives rise to the ring expansion product [Cp'''Co(η^5-$P_3C_2tBu_2$)][pftb] (**24**) and the ring contraction product [Cp'''Co(η^3-PC_2tBu_2)][pftb] (**25**). DFT calculations show that oxidised **20a**$^+$ shows a doublet spin state and that disproportionation to **24** and **25** is thermodynamically favoured. Two unprecedented complexes are forming with the triphosphacobaltocenium **24** and the phosphacyclopropenylium ligand complex **25**.

In addition to these findings, first reactions between **20a** and gold(I) WCA salts have been conducted as well as comparative reactions with $AgBF_4$ (Scheme 10-7).

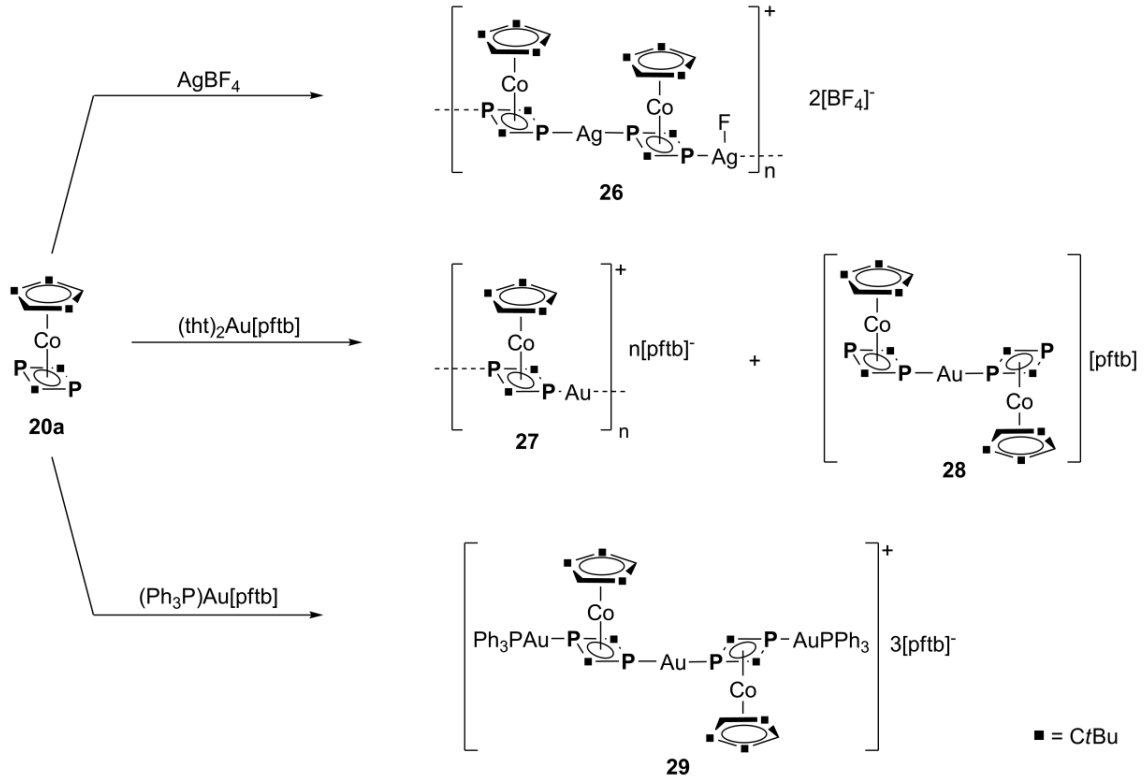

Scheme 10-7 Reaction pathways between **20a** and WCA salts of Ag(I) and Au(I).

In these reactions, 1D polymeric compounds like [Ag{Cp'''Co(η^4:η^1:η^1-$P_2C_2tBu_2$)}AgF{Cp'''Co(η^4:η^1:η^1-$P_2C_2tBu_2$)}]$_n$·2n[BF_4] (**26**) and [Au{Cp'''Co(η^4:η^1:η^1-$P_2C_2tBu_2$)}]$_n$·n[pftb] (**27**) are obtained. Again the presence of the WCA [pftb] is vital to the products formed, as the coordinating BF_4^- anion decomposes into BF_3 and F^-, which adds to the polymeric structure. In the reaction with [(tht)$_2$Au][pftb], additionally a 1:2 coordination compound [Au{Cp'''Co(η^4:η^1-$P_2C_2tBu_2$)}$_2$][pftb] (**28**) could be isolated. Using

another Au(I) salt with PPh_3 as capping groups leads to the formation of an oligomer of the formula $[(\eta^1\text{-}PPh_3)_2Au_3\{Cp'''Co(\eta^4{:}\eta^1{:}\eta^1\text{-}P_2C_2t\text{Bu}_2)\}_2]\cdot 3[pftb]$ (**29**). It will be interesting to future research whether other molecular products leading to 1D polymers can be isolated at lower temperatures from these reactions like it was possible for the system **20a**/Ag[pftb].

11 Appendices

11.1 Thematic List of Abbreviations

NMR abbreviations

NMR	nuclear magnetic resonance
δ	chemical shift
ppm	parts per million
s(NMR)	singlet
d(NMR)	doublet
t(NMR)	triplet
q(NMR)	quartet
sept(NMR)	septet
br(NMR)	broad
J(NMR)	coupling constant
Hz	Hertz, s^{-1}
COSY	correlation spectroscopy
$\omega_{1/2}$	half width
VT	Various Temperature

Solvents

Et_2O	Diethylether, $(C_2H_5)_2O$
HMDSO	hexamethyldisiloxane, $((CH_3)_3Si)_2O$
THF	tetrahydrofurane, C_4H_8O
TMS	tetramethylsilane, $Si(CH_3)_4$

Weakly coordinating anions

WCA	weakly coordinating anions
pftb	$[Al\{OC(CF_3)_3\}_4]$
fal	$[FAl\{O(C_{12}F_{15})\}_3]$

Mass and IR abbreviations

MS	mass spectrometry
EI	electron impact
ESI	electron spray ionization
FD	field desorption ionization
m/z	mass to charge ratio
IR	infrared spectroscopy
w(IR)	weak
m(IR)	medium
s(IR)	strong
sh(IR)	shoulder
$\tilde{\nu}$	frequency/wavenumber

Theoretical Expressions

DFT	density functional theory
$E°_0$	reaction energy
$H°_{298}$	standard reaction enthalpy
$G°_{298}$	standard Gibbs reaction energy
HOMO	highest occupied molecular orbital
LUMO	lowest unoccupied molecular orbital
IP	Ionization potential
ΔE_N	Difference in electronegativity
MO	molecular orbital
PE	Photoelectron spectra
VE	valence electron
vdW	van der Waals
VGSE	Vacuum Gas-Solid Evaporation
WBI	Wiberg Bond Indices

Ligands

Ad	Adamantyl, -$C_{10}H_{15}$
butterfly	*bicyclo*[1.1.0]butane
Cp	cyclopentadienyl, η^5-C_5H_5
Cp''	1,3-di-*tert*-butylcyclopentadienyl, η^5-$C_5H_3tBu_2$
Cp'''	1,2,4-tris-*tert*-butylcyclopentadienyl, η^5-$C_5H_2tBu_3$
Cp*	pentametyhlcyclopentadienyl, η^5-C_5Me_5
Cp^{BIG}	pentakis-4-*n*butylphenylcyclopentadienyl, η^5-$C_5(4\text{-}nBuC_6H_4)_5$
Cp^{Bn}	pentabenzylcyclopentadienyl, η^5-$C_5(CH_2Ph)_5$
Cp^R	substituted cyclopentadienyl ligand
COD	Cyclooctadiene
COT	Cyclooctatetraene
Dipp	2,6-diisopropylphenyl
dme	1,2-dimethoxyethane
dppe	$C_2H_4(PPh_2)_2$
L	ligand (specified in text)
Me	Methyl
*t*Bu	*tert*-Butyl, -C_4H_9
tht	tetrahydrothiophene, C_4H_8S
triphos	1,1,1-tris(diphenylphosphanylmethyl)ethane, $CH_3C(CH_2PPh_2)_3$
Ts^{tol}	tris(N-(4-MeC_6H_4)amidodimethylsilyl)methane)
R	organic substituent (specified in text)

Other

1D	one dimensional
2D	two dimensional
Å	Angstrøm, 1 Å = $1 \cdot 10^{-10}$ m
°C	degree Celsius
CV	cyclovoltammography
d	distance
e^-	electron
E	element of the 15th group (except nitrogen), specified in text
M	metal
r.t.	room temperature

11.2 List of numbered compounds

No.	Chapter	No. in Chapter	Formula
1		**1**	$[Ag(P{\equiv}C\textit{t}Bu)_2]^+[pftb]^-$
2	**3**	**2**	$[Ag(P{\equiv}C\textit{t}Bu)_2]^+[fal]^-$
3a		**3a**	$[((CH_3)_2CO)Ag(P{\equiv}C\textit{t}Bu)_2]^+[fal]^-$
3b		**3b**	$[(C_7H_8)_2Ag(P{\equiv}C\textit{t}Bu)]^+[fal]^-$
4a		**1a**	[Cp*Ru(dppe)][pftb]
4b		**1b**	$[Cp^*Ru(dppe)][PF_6]$
5a		**2a**	$[Cp^*Ru(dppe)(\eta^1\text{-}\textit{t}BuC{\equiv}P)][pftb]$
5b		**2b**	$[Cp^*Ru(dppe)(\eta^1\text{-}\textit{t}BuC{\equiv}P)][PF_6]$
6		**3**	$[\{Cp^*Ru(dppe)\}\{Cp^*Ru\}(\eta^1\text{-}\textit{t}BuC{\equiv}P)]^{2+}\cdot 2[pftb]^-$
7	**4**	**4**	$[Cp^*Ru(dppe)(\eta^1\text{-}P(OH)_2CH_2\textit{t}Bu)][pftb]$
8a		**5a**	$[Cp^*Ru(dppe)(\eta^2\text{-}MeC{=}P)][pftb]$
8b		**5b**	$[Cp^*Ru(dppe)(\eta^2\text{-}MeC{=}P)][PF_6]$
9a		**6a**	$[Cp^*Ru(dppe)(\eta^1\text{-}MeC{\equiv}N)][pftb]$
9b		**6b**	$[Cp^*Ru(dppe)(\eta^1\text{-}MeC{\equiv}N)][PF_6]$
10		**7**	$[\{Cp^*Ru(dppe)\}\{Cp^*Ru\}(\eta^1\text{-}MeC{\equiv}N)][pftb]$
11		**1**	$LCr^{5}CrL$ (L=Ar=$N_2C_{25}H_{29}$)
12	**5**	**2**	$[L_2Cr_2(\mu,\eta^1{:}\eta^1{:}\eta^2{:}\eta^2\text{-}P_2C_2\textit{t}Bu_2)]$
13		**3**	$[L_2Cr_2(\mu,\eta^1{:}\eta^1{:}\eta^2{:}\eta^2\text{-}P_2C_2Me_2)]$
14		**4**	$[L_2Cr_2(\mu,\eta^2{:}\eta^2\text{-}PCAd)]$
15		**1**	$[\{Cp'''Co\}_2(\mu,\eta^4{:}\eta^4\text{-}P_2C_2Me_2)]$
16		**2**	$[Cp'''Co(\eta^4\text{-}P_2C_2Me_2)]$
17	**6**	**[1][pftb]**	$[\{Cp'''Co\}_2(\mu,\eta^4{:}\eta^4\text{-}P_2C_2Me_2)][pftb]$
18		**3**	$[\{Cp'''Co\}_2(\mu\text{-}CCH_3)(\mu\text{-}POOH)][pftb]$
19		**5**	$[Cp'''Co_2(\eta^6\text{-}C_7H_8)][pftb]$
20a		**1 (1a)**	$[Cp'''Co(\eta^4\text{-}1,3\text{-}P_2C_2\textit{t}Bu_2)]$
20b		**(1b)**	$[Cp'''Co(\eta^4\text{-}1,3\text{-}P_2C_2\textit{i}Pr_2)]$
I-20a		**I-1**	$[Cp'''Co(\eta^4\text{-}1,2\text{-}P_2C_2\textit{t}Bu_2)]$
21		**2**	$[Ag\{Cp'''Co(\eta^4{:}\eta^1{:}\eta^1\text{-}P_2C_2\textit{t}Bu_2)\}]_n\cdot n[pftb]$
22a		**3a**	$[(Et_2O)_2Ag\{Cp'''Co(\mu,\eta^4{:}\eta^1{:}\eta^1\text{-}P_2C_2\textit{t}Bu_2)\}][pftb]$
22b	**7 (8)**	**3b**	$[(Et_2O)_4Ag_2\{Cp'''Co(\mu,\eta^4{:}\eta^1{:}\eta^1\text{-}P_2C_2\textit{t}Bu_2)\}]\cdot 2[pftb]$
23a		**4 (2a)**	$[Ag_2\{Cp'''Co(\mu,\eta^4{:}\eta^1{:}\eta^1\text{-}1,2\text{-}P_2C_2\textit{t}Bu_2)\}_2\{Cp'''Co(\mu,\eta^4{:}\eta^1\text{-}1,2\text{-}P_2C_2\textit{t}Bu_2)\}_2]\cdot 2[pftb]$
23b		**(2b)**	$[Ag_2\{Cp'''Co(\mu,\eta^4{:}\eta^1{:}\eta^1\text{-}1,2\text{-}P_2C_2\textit{i}Pr_2)\}_2(\eta^2\text{-}tol)_2]\cdot 2[pftb]$
24		**5**	$Cp'''Co(\eta^5\text{-}P_3C_2\textit{t}Bu_2)][pftb]$
25		**6**	$[Cp'''Co(\eta^3\text{-}PC_2\textit{t}Bu_2)][pftb]$
26		**3**	$[Ag\{Cp'''Co(\eta^4{:}\eta^1{:}\eta^1\text{-}P_2C_2\textit{t}Bu_2)\}AgF\{Cp'''Co(\eta^4{:}\eta^1{:}\eta^1\text{-}P_2C_2\textit{t}Bu_2)\}]_n\cdot 2n[BF_4]$
27	**8**	**4**	$[Au\{Cp'''Co(\eta^4{:}\eta^1{:}\eta^1\text{-}P_2C_2\textit{t}Bu_2)\}]_n\cdot n[pftb]$
28		**5**	$[Au\{Cp'''Co(\eta^4{:}\eta^1\text{-}P_2C_2\textit{t}Bu_2)\}_2][pftb]$
29		**6**	$[(\eta^1\text{-}PPh_3)_2Au_3\{Cp'''Co(\eta^4{:}\eta^1{:}\eta^1\text{-}P_2C_2\textit{t}Bu_2)\}_2]\cdot 3[pftb]$
-		**1b-Ox**	$[Cp'''Co(\eta^3\text{-}\{(POOH)(C\textit{i}Pr)\}_2\{Cp'''\}]$

11.3 Acknowledgments

While carrying out the works and writings of this thesis, many different people have helped in many different ways for which I am indefinitely grateful. First and foremost I am exceedingly thankful to my supervisor Mr. Scheer for having me in his working group and giving me free rein in my research choices, with only one condition: they had to be connected to phosphaalkynes. In the end, this was a very gripping topic to be researching in and the reassurance and trust I have been given along the way (also in my jobs as "Bestelltante" and in helping organize IRIS-14) leave me appreciative of my time here. The same can be said about Gábor Balázs, who started out as a kind of semi-supervisor but ended up being more helpful than simply that. Gábor not only helped in making DFT calculations for my crazy molecules but also proof-read parts of this thesis and helped in ordering my thoughts by painting countless reaction pathways and ideas onto a collection of sheets (which I still have).

Of course I would also like to thank the people that helped me out in other ways: Eugenia Peresypkina tried their best to help me solve "problem teflonate x-ray structures" and guided me when I was at a loss, and Alexander Virovets helped in refining a crazy cation. Michael B. also had a look on some of my structures and Michi S. helped with every question I had.

Conducting experiments is one thing, but without the proper analysis they're useless. With great appreciation of their technical knowledge I thank Anette Schramm, Georgine Stühler and Fritz Kastner for conducting countless NMR experiments (actually, I can count: they made well over 300). Josef Kiermaier did ESI MS and Wolfgang Söllner performed EI and FD experiments, although we did not always agree on the solvents. Luis also helped me out in measuring some more substances with ESI-MS. Moritz collected EPR data of my paramagnetic substances. The team of the Microelemental lab (Helmut Schüller, Barbara Baumann and Wilhelmina Krutina) have been so kind to always measure my elemental analyses, no matter how high the fluorine content has been.

I have also been lucky in regards to my lab colleagues. Most of my time here I spent with Walter and Andi, and I had a blast with both of them singing and enjoying the occasional drink (of course ONLY in our free time). Martin joined us when I started writing this thesis and Mia left when she got pregnant. I also had diligent bachelor students: Marcella and Andreas.

Some of my time has been going into the extra work I did with the JCF Regensburg. I had a real blast (and not only with fireworks). I want to say particular thanks to Michi, Christoph and Sabine for countless hours of crafting and mixing the perfect mixture for crackers; Fabi, Andi, Fidi and Marcella for taking over, and Rebecca for holding the cookie monster in high esteem.

Thanks to the staff: Karin (who always lent a helping hand), Barbara (best lab supervisor ever), Petra (for "tratsching"), Martina (for Cp'''), Matthias (all the calmness), Musch for being Musch, and Muschine and Schotti for helping the JCF out.

The Scheer working group is a big one. That being said, there are some with which I formed special friendships: Because they've always been there for me when I was frustrated in the lab, Claudi and Sebi. Because she told me I can do it, Sabine (and Bernd and Pünktchen). Because I've known them since they've started their studies, Fabi and Andi. Because they know their liquor, Moni and sμ. Because of all the videos and his rage, Eric.

All the others I want to mention: The ones that joined the group the same time I did: Hias (countless cups of coffee) and Martin (Simpsons!); the in-betweeners: Jens (for all the drunken compliments) and Moritz (still waters run deep), Barbara (I'd climb every mountain with you, hands down), Felix (for being random most of the time, but on spot when he needs to be), Oli (for being a good sport), Reini and Dani, Rudi and Luigi; Helena (with the most infectious laughter!), Julian (who, legends say, has been filtering stuff since 2014), Valentin, Luis, Andrea (sorry again for making you a chemist) and Tobi; Robert, Tobias, Michi, Claudia, and all the "old ones": Thomsi and Conny, Wast, Wurzel, Michi, Miriam, Bianca, Susanne and Christian, Fabi, Oime, Welschi and everybody I missed.

I want to thank my friends Christina (for all the talks, walks, coffes, dinners, and 'appreciating' organic chemistry just like I did), Ali (for all the days in the library), Andrea (for being a friend and family), Oli (for all the suite evenings), Steffi (for updates), Gero (for hiking and helping in TC), Alex (for being the best bride) and Sve (for fencing with me) and their little Mats and baby to come – thank you all for enduring my temper and keeping in touch.

Sincere love goes to my family for supporting me however abstract my troubles were. Although you didn't always understand my problems, I appreciate every second you spent listening to them nonetheless. Thank you for all of your advice. I am indefinitely grateful for that. And for all the food you make, cakes you bake, and things you fix.

And finally, I want to thank Martin because he is everything to me. Without your support and love I would not have made it through the undergrad studies and certainly would have lost my mind several times during the PhD program. I would not want to miss any second we spent together. This work is dedicated to you.